

## Durham E-Theses

---

### *Modelling tidal changes within the wash and Morecambe bay during the Holocene*

Hinton, A.C.

#### How to cite:

---

Hinton, A.C. (1992) *Modelling tidal changes within the wash and Morecambe bay during the Holocene*, Durham theses, Durham University. Available at Durham E-Theses Online:  
<http://etheses.dur.ac.uk/6130/>

#### Use policy

---

The full-text may be used and/or reproduced, and given to third parties in any format or medium, without prior permission or charge, for personal research or study, educational, or not-for-profit purposes provided that:

- a full bibliographic reference is made to the original source
- a [link](#) is made to the metadata record in Durham E-Theses
- the full-text is not changed in any way

The full-text must not be sold in any format or medium without the formal permission of the copyright holders.

Please consult the [full Durham E-Theses policy](#) for further details.

The copyright of this thesis rests with the author.  
No quotation from it should be published without  
his prior written consent and information derived  
from it should be acknowledged.

# **Modelling Tidal Changes Within The Wash and Morecambe Bay During The Holocene**

**Volume 1**

by

**A.C. Hinton**

**A Thesis submitted in partial fulfilment  
of the requirements for the degree of  
Doctor of Philosophy**

**Geography Department**

**The University of Durham  
1992**



**27 APR 1993**

**Addendum to Ph.D. thesis 'Modelling tidal changes within The Wash and Morecambe Bay during the Holocene' by A.C. Hinton, 1992.**

Subsequent to the examination and acceptance of the thesis for the degree of Ph.D., the author discovered that the adjustment to the water depths made for the palaeogeographic simulations for the EC3, WASH, LBM and MBM models was incorrect. This affects the accuracy of the figures in chapter 4, results in chapter 6 and data in the appendices. The reader is referred to Hinton (1995) for corrected results for The Wash.

Hinton, A.C. (1995) Holocene tides of The Wash, U.K.: The influence of water-depth and coastline-shape changes on the record of sea-level movements. *Marine Geology*, **124**, 87-111.

A.C. Hinton, 21st April 1997

The results contained in this thesis are all my own work. Information derived from other sources is acknowledged at the appropriate point in the text. Work presented here has not been published elsewhere.

Signed

Anne C. Hinton

Copyright © 1992 by A.C. Hinton

The copyright of this thesis rests with the author. No quotation from it should be published without A.C. Hinton's prior written consent and information derived from it should be acknowledged.

The copyright of the bathymetric and label data for the Liverpool Bay and Morecambe Bay tidal models for present sea-level conditions, presented in Appendix 6.1, is held by the Proudman Oceanographic Laboratory, Birkenhead.

## ABSTRACT

Palaeotidal changes are one of the least known factors of the sea-level record variation at the local scale (Shennan, 1986a; Devoy, 1987). This thesis extends knowledge of tidal alterations with sea-level change by means of an approach integrating numerical tidal models with geological stratigraphic data recording former tidal heights.

The last 10,000 years (the Holocene period) were chosen for study due to the sedimentary sequence available recording sea-level changes. Two macro-tidal embayments, the Wash and Morecambe Bay, are examined for palaeotidal changes by running a series of seven numerical tidal models from the scale of the north-east Atlantic to that of the bays. In order to obtain results to the required resolution to carry out the work, two new tidal models were developed for the Wash.

Tidal model simulations for lowering of sea depths from current bathymetric values without coastline shape changes showed reductions of a maximum of 10% of the sea-level reductions in the bays. Changes to tidal altitudes were not so great for alterations to coastal shape alone, where no modification of present sea depth values was included. A combination of sea depth and coastline changes used in the reconstruction of former tidal height patterns within the embayments showed differences corresponding broadly to the variations in altitude of sea-level index points within the Wash Fenlands, although altitudinal differences are within the model error band for tidal predictions. For Morecambe Bay, however, tidal inundation does not occur to altitudes predicted by sea-level index points and it is suggested, following Tooley (1978, 1987), that neotectonic movements may well have influenced the Holocene sea-level record in this area. Better palaeogeographic data are required for more accurate palaeotidal simulations in embayments. Sediment compaction is also identified as an area requiring further research in the attempt to explain altitudinal variation of sea-level index points within local areas and so enable regional comparisons of sea-level change to be made.

## ACKNOWLEDGEMENTS

The receipt of a Natural Environment Research Council Studentship held at the University of Durham for a period of three years is gratefully acknowledged. The Studentship was based in the Department of Geography at Durham University and the work presented in this thesis was carried out during that time under the supervision of Dr. Ian Shennan and Dr. Michael Tooley. Use of the facilities in the Geography Department and Computer Centre at Durham and the help of staff from both Departments is much appreciated.

This work would not have been possible without the assistance of Dr. Roger Flather and other staff at the Proudman Oceanographic Laboratory, Birkenhead, who provided the tidal model program used in the study. The assistance of staff at the University of London Computer Centre in permitting use of the Cray supercomputer at London for obtaining results from the tidal models employed is also acknowledged with gratitude.

Dr. Martyn Waller provided access to Fenland radiocarbon dates and stratigraphic data currently in press and colleagues at Durham, Dr. D. Donoghue and Dr. Y. Zong, provided access to unpublished stratigraphic data for the Wash Fenland and Morecambe Bay respectively. Staff at the British Geological Survey in Keyworth and Edinburgh also assisted with useful discussions.

Earlier drafts of parts of this thesis were read and commented on by Dr. Shennan, Dr. Flather, Dr. Williams, Dr. Proctor and Dr. Tooley to whom I express my thanks. Dr. W.R. Williams, Mr. P. Dodds and Miss M. Pringle provided assistance with computerised graphics and statistics packages.

## SYMBOLS USED IN THE TEXT

Symbol	Meaning (units)
$a, b$	Real and imaginary parts of a complex time-varying coefficient
$c$	Speed of progression of the tidal wave (metres per second)
$c_g$	Phase speed (radians)
$C_D$	Dimensionless drag coefficient
$D$	Total water depth ( $h + \zeta$ )
$E$	Matrix consisting of values of elements predicted from the model
$f$	Nodal factor - adjustment of tidal amplitude made for the 18.61 year nodal cycle of lunar declination
$f_c$	Coriolis parameter
$f_e$	Nodal factor of the Equilibrium Tide at time zero
$F$	Stress in the $x$ direction
$F_B$	Bottom stress in the $x$ direction
$g$	Gravitational constant ( $6.67 \times 10^{-11} \text{Nm}^2 \text{kg}^{-2}$ )
$G_e$	Phase lag of the Equilibrium Tide at Greenwich (radians)
$G_y$	Stress in the $y$ direction
$G_B$	Bottom stress in the $y$ direction
$h$	Mean water depth
$h_{max}$	Maximum bathymetric value in model (metres)
$h_{ws}$	Smallest model grid width
$h_w$	Model grid width
$H$	Tidal amplitude
$H_e$	Tidal amplitude of harmonic constituent $e$
$HO$	Matrix consisting of values of amplitude and phase of harmonic constituents
$i, m$	Number of points at which calculations are made in the latitudinal and longitudinal directions respectively
$I$	An unspecified harmonic constituent
$j, k$	Constants
$l$	Tidal wavelength
$L$	Length of bay from sea mouth to head
$m_e$	Mass of the earth ( $5.97 \times 10^{24} \text{kg}$ )
$m_l$	Mass of the moon ( $7.35 \times 10^{22} \text{kg}$ )
$M$	A point at the centre of the moon
$n$	Nodal angle - adjustment of tidal phase made for the 18.61 year nodal cycle of lunar declination
$n_e$	Nodal angle of the Equilibrium Tide at time zero
$O$	A point at the centre of the earth
$P$	Hydrostatic pressure
$P_A$	Atmospheric pressure on the water surface
$P_{Z_d}$	Hydrostatic pressure at a point at depth $z_d$ metres below the water surface

Symbol	Meaning (units)
$\mathbf{q}$	Depth-mean current vector
$R$	Equatorial radius of the earth (6,378 kilometres)
$R_l$	Distance from the centre of the earth to the centre of the moon (384,400 kilometres)
$s$	Coefficient of bottom friction
$s'$	An element of space
$t$	Time
$T(t)$	Tidal level at time $t$
$u$	Latitudinal velocity
$u_q$	Component of the depth-mean current in the direction of increasing $\chi$
$U$	A constant
$v$	Longitudinal velocity
$v_q$	Component of the depth-mean current in the direction of increasing $\phi$
$V_e$	Phase angle of the Equilibrium Tide at time zero (radians)
$x$	Latitudinal distance
$X, Y, Z$	Points at the surface of the earth
$y$	Longitudinal distance
$z$	Sea surface elevation
$z_d$	Distance below water surface
$z_0, Z_0$	Mean sea-level
$\Delta S$	Grid width
$\Delta t, \Delta T$	Timestep (seconds)
$\zeta$	Displacement of water level from mean value
$\theta$	North co-latitude ( $90^\circ - \text{latitude}$ )
$\lambda$	Wavelength of the progressive wave
$\rho$	Water density ( $1025\text{kg/m}^3$ )
$\sigma$	Angular frequency (of a tidal constituent)
$\sigma_e$	Angular frequency at time zero of a tidal constituent $e$
$\tau_b$	Bottom stress
$\phi$	Angle of latitude
$\chi$	East longitude
$\omega$	Angular frequency of the earth's rotation
$\Omega$	Gravitational potential at the surface of the earth
$\Omega_Y$	Gravitational potential at a point $Y$ on the surface of the earth



## Harmonic Constituents

Constituent	Speed	Meaning
$M_2$	28.9841	lunar semi-diurnal tidal constituent
$M_3$	43.4761	lunar third-diurnal tidal constituent
$M_4$	57.9682	lunar quarter-diurnal tidal constituent
$M_6$	86.9523	lunar sixth-diurnal tidal constituent
$MS_4$	58.9841	generated by the interaction of $M_2$ and $S_2$
$2MS_2$ (or $Meu_2$ )	27.9682	in shallow water
$S_2$	30.0000	solar semi-diurnal tidal constituent

# CONTENTS

## Volume 1

### Chapter 1. Introduction

1.1. Subject of the thesis	1
1.2. Sea-level indicators	2
1.3. Past work on tidal changes	8
1.3.1. Sedimentary analysis	8
1.3.2. Modelling	9
1.3.3. Unanswered questions	11
1.4. Aims of the project	11
1.4.1. What is the magnitude of tidal variations within embayments?	11
1.4.2. What effect does the shape of the coastline of an embayment have on tidal variations?	12
1.4.3. What effect does the sea-bed morphology have on tidal variations?	12
1.4.4. What is the contribution of neotectonics and sediment compaction to altitudinal variations of sea-level index points within the chosen embayments?	12
1.4.5. What are the implications of answers to 1.4.1 to 1.4.4 above for a rise of sea-level?	13
1.5. Study areas	13

### Chapter 2. The Geological Development of the Field Areas

2.1. Geology and pre-Quaternary history of the Fenland and Morecambe Bay	17
2.1.1. Pre-Quaternary geology and structural history of the Fenland area	17
2.1.2. Pre-Quaternary solid geology and structure of Morecambe Bay	19
2.1.3. Comparison of the geological history of the Fenland and Morecambe Bay	21

2.2. Pre-Holocene Quaternary geology of the field areas	22
2.2.1. Quaternary geology of the Fenland before 10,000 years B.P.	22
2.2.2. Quaternary geology of Morecambe Bay before 10,000 years B.P.	28
2.2.3. Comparison of the pre-10,000 years B.P. Quaternary history of the two areas	32
2.3. The Holocene development of the Wash Fenlands and Morecambe Bay	33
2.3.1. The Wash Fenlands	33
2.3.2. Morecambe Bay	41
2.3.3. Comparison of the development of the Fenland and Morecambe Bay during the Holocene	46

## **Chapter 3. Tidal Theory and Tidal Models**

3.1. Tidal theory	50
3.1.1. Tidal generation	50
3.1.2. Shallow water effects	55
3.1.3. Resonance	58
3.1.4. Kelvin waves	59
3.1.5. Residual flow	59
3.1.6. Tidal analysis	64
3.1.6.1. Harmonic analysis of tides	64
3.1.6.2. Response analysis of tides	66
3.2. Tidal modelling	68
3.2.1. Methods of tidal modelling	68
3.2.1.1. Criteria for consideration in the development of a numerical model	69
3.2.1.2. Numerical modelling	71
3.2.1.2.1. Finite difference models	73
3.2.1.2.1.1. Implicit schemes	74
3.2.1.2.1.2. Explicit schemes	74
3.2.1.2.1.3. Criteria to be satisfied by numerical models	75

## **Chapter 4. Palaeogeographic Maps**

4.1. Stratigraphic record	77
4.1.1. The Wash Fenlands	78
4.1.2. Morecambe Bay	83
4.2. Chronostratigraphic record	83
4.2.1. The Wash Fenlands	85
4.2.2. Morecambe Bay	90
4.3. Construction of palaeogeographic maps	90
4.3.1. The Wash Fenlands	92
4.3.2. Morecambe Bay	93

## **Chapter 5. Tidal Model Methodology**

5.1. Tidal models used	104
5.1.1. North-east Atlantic Model	108
5.1.2. Models for The Wash	108
5.1.3. Models for Morecambe Bay	112
5.2. Input data	112
5.2.1. Bathymetric data	112
5.2.1.1. Labels	118
5.2.2. Tidal input	118
5.3. Model program	124
5.4. Harmonic analysis	130
5.4.1. Constituents used	131

## **Chapter 6. Tidal Changes within The Wash and Morecambe Bay**

6.1. Procedure adopted to obtain results	134
6.2. Limitations of the analysis	137

6.2.1. Ocean/ shelf boundary tidal changes	137
6.2.2. Sea bed friction	138
6.2.3. Eustatic sea-level changes	139
6.2.4. Isostatic bathymetry changes	139
6.2.5. Sediment movements	140
6.3. Presentation of results	141
6.4. Accuracy of model results	146
6.4.1. The Wash	146
6.4.2. Morecambe Bay	154
6.4.3. Comparison of The Wash and Morecambe Bay	160
6.5. Robustness of the tidal models	160
6.5.1. Modification 1 - Introduction of a spit	162
6.5.1.1. The Wash	162
6.5.1.2. Morecambe Bay	163
6.5.2. Modification 2 - Depth changes within the embayments	164
6.5.2.1. The Wash	164
6.5.2.2. Morecambe Bay	165
6.5.3. Comparison of results	166
6.6. Reduced sea depth simulations	168
6.6.1. The Wash	169
6.6.2. Morecambe Bay	175
6.6.3. Comparison of The Wash and Morecambe Bay	182
6.7. Coastline modifications	183
6.7.1. The Wash	183
6.7.2. Morecambe Bay	187
6.7.3. Comparison of The Wash and Morecambe Bay	189
6.8. Palaeogeographic reconstructions	190
6.8.1. The Wash	191

6.8.2. Morecambe Bay	196
6.8.3. Comparison of The Wash and Morecambe Bay	200
6.9. Discussion	203
6.9.1. The Wash	204
6.9.2. Morecambe Bay	206
6.9.3. Comparison of The Wash and Morecambe Bay	208
<b>Chapter 7. Neotectonics and Sediment Compaction</b>	
7.1. Neotectonic movements	209
7.2. Sediment compaction	212
7.3. Other factors	214
<b>Chapter 8. Conclusions</b>	
8.1. The magnitude of tidal variations within embayments	215
8.2. The effect of the shape of the coastline of an embayment on tidal variations	216
8.3. The effect of sea-bed morphology on tidal variations	216
8.4. The contribution of neotectonics and sediment compaction to the altitudinal variations of sea-level index points within the chosen embayments	216
8.5. The implications of the results of this study for a rise of sea-level	217
8.6. Recommendations for further research	218
8.7. Conclusions of the research with regard to sea-level change studies	218
<b>References</b>	220
Admiralty Chart References	244
<b>Appendices relating to Chapter 4</b>	
Appendix 4.1. Stratigraphic data sources for The Wash Fenlands	245
Appendix 4.2. Stratigraphic data sources for Morecambe Bay	246

Appendix 4.3. Wash Fenland radiocarbon dates	247
Appendix 4.4. Radiocarbon dates from the Morecambe Bay area	251

**Appendices relating to Chapter 6: Data on diskettes**

Appendix 6.1. Bathymetric and label data for model simulations	254
Appendix 6.2. Tidal input for model simulations	257
Appendix 6.3. Maximum sea-level elevations from model simulations	260

**Volume 2**

<b>Figures relating to Chapter 6</b>	<b>1</b>
--------------------------------------	----------

## CHAPTER 1

### INTRODUCTION

#### 1.1. Subject of the thesis

Sea-level, or the relationship of the altitude of the land to that of the sea, is modified by a number of factors. This is due to changes to both the land and sea, such as tectonic movements, which may cause the level of the land relative to the sea to rise or fall, and eustatic factors, which may, for example, reduce the volume of water in the sea during a glacial or cold period when there is an increase in the proportion of water stored on land (in the form of ice) compared with that in the oceans. These work on a variety of temporal and spatial scales and it is their interaction which causes the altitude of the sea relative to the land to change.

The sea-level change factor with the highest frequency is that due to tidal movements, excluding the effects of wave action. In most parts of the world, sea-level rises and falls twice daily due to tides, for reasons which will be examined in Chapter 3, although in some areas, such as Karumba in Australia (Pugh, 1987), the rise and fall may be diurnal and in other parts of the world very complicated rise and fall patterns exist.

Few attempts have been made to assess the significance of tidal changes on the sea-level history of areas. Most sea-level studies have assumed that tidal regimes have remained constant over time. A study of former tidal patterns might offer an explanation of the variation within an embayment in the altitude of sea-level index points, which are locations in a stratigraphic section identified as having a particular relationship to a level of the sea, such as the mean high water of spring tides. Inclusion of tidal variations in the sea-level



history of an area would give a clearer picture of local sea-level change, and not just the history of movement of mean high water of spring tides, for example. It would also enable the amount of sea-level change recorded due to other factors, such as sediment compaction and hydrological changes, to be assessed. A broader estimate of the order of magnitude of change of tidal patterns with time allows sea-level curves to be reduced to the same baseline. The paucity of studies on this topic has led to the study of palaeo-tidal changes in this thesis. To elucidate this problem numerical models for tidal prediction are linked with geological evidence of altitudes reached by the sea to simulate the tidal regimes at former sea-levels.

Together with the factors which determine the amount of sea-level change in any place, the indicators of sea-level from the geological record and their accuracy must be assessed in order to obtain a full determination of past sea-level change. Features used as sea-level indicators in obtaining the record of former sea-levels and their accuracy are discussed in the next section.

## **1.2. Sea-level indicators**

In a stratigraphic section the sequence of organic and clastic sediments is used as an indicator of sea-level changes. However, it cannot be assumed that the presence of a peat layer overlying sand or silt, for example, represents a decrease in the marine influence, suggesting a lowering of sea-level, from lithostratigraphic evidence alone. Furthermore, it is possible that local morphological changes within an estuary may give rise to a sediment sequence suggesting a sea-level regression, for example (Carter *et al.*, 1990). Analysis of the micro- and macro-fossil content of the sequence is also required to establish the presence or absence of marine indicators. These may be pollen from plants tolerant to inundation by salt water or marine or brackish water diatoms. A large number of indicators of sea-level have been used by different researchers. It is not intended to give a detailed account here. A good summary of features used as indicators of sea-level may be found in van de Plassche (1986). Discussion in this section will concentrate on the criteria

used to establish a former sea-level.

Van de Plassche (1977) recognised that to establish any single observation on a former sea-level, three criteria are required, namely

- (a) an indicative meaning (*i.e.* the relationship of the phenomenon to a water level)
- (b) an altitude
- (c) an age.

Shennan (1980) produced an assessment of the indicative meaning in relation to sea-level of a number of commonly used materials. These are shown in Table 1.1 below. Shennan (1986a) notes that the reference tide level given to assess the relationship of a phenomenon to sea-level may not be constant. For example, basis peat, has a varying indicative range (Shennan, 1980, suggests approximately 0.8 metre from work in the Fenland) depending on factors such as the tidal range at the time of deposition in the area in which it is found. Basis peat is a bed of organic material which has been formed on pre-Holocene deposits and in which a causal relation can be proved between formation of the peat and sea-level rise (Lange and Menke, 1967), as distinct from basal peat, which is the term used when a causal relation between peat formation and sea-level rise cannot be proved (Behre *et al.*, 1979). Furthermore, there is a lack of information on the contemporary relationships between tide-levels, soil conditions and the succession of coastal plant communities which lead to the formation of transgressive or regressive overlaps of organic or clastic beds (Tooley, 1978) as most have been altered by man. A further problem is that ecosystems which exist naturally today may not be the same as those which existed under different climatic conditions or under the same climatic conditions a few thousand years ago (Huntley, 1990) so that it may be extremely difficult to obtain any indicative meaning.

With reference to the indicative range of samples from the Fenland shown in Table 1.1, Shennan (1986a) stresses that the indicative meaning depends on the nature of the stratigraphic overlap (*e.g.* whether it was formed during a rising or during a falling sea-level).

Table 1.1. Indicative Range and Reference Water Level for some Commonly Dated Materials (after Shennan, 1980).

Default values, IGCP Project 61 (Streif, pers. comm.)

	Indicative Range	Reference Water Level
<i>Phragmites</i> peat	70cm	Mean High Tide + 18cm
Sedge peat	40cm	(b) Mean High Tide + 20cm (est.)
Fenwood peat	80cm	(a) Mean High Tide + 40cm
Moss peat (not in raised bog)	10cm	(b) Mean High Tide + 20cm
<i>Puccinella</i> grasses	40cm	Mean High Tide ± 0cm
<i>Spartina</i> grasses	30cm	Mean High Tide - 30cm

(a) only in coastal fen and level backswamps, otherwise groundwater table

(b) decreases with distance from open coast, approaches Mean Sea Level in lagoons and coastal backswamp

(est.) estimate only

Proposed values (inferred from Godwin, 1940; Kidson and Heyworth, 1979; van de Plassche, 1979; Tooley, 1979)

	Indicative Range	Reference Water Level
<i>Phragmites</i> or monocotyledonous peat:		
- directly above saltmarsh deposit	20cm	$((\text{MHWST} + \text{HAT})/2) - 20\text{cm}$
- directly below saltmarsh deposit	20cm	MHWST - 20cm
- directly above fen wood deposit	20cm	MHWST - 10cm
- directly below fen wood deposit	20cm	$((\text{MHWST} + \text{HAT})/2) - 10\text{cm}$
- middle of layer	70cm	infer from stratigraphy
Fen wood peat:		
- directly above <i>Phragmites</i> or salt marsh	20cm	$(\text{MHWST} + \text{HAT})/2$
- directly below <i>Phragmites</i> or salt marsh	20cm	MHWST
Basis peat:	?80cm	Mean Tide Level to MHWST

MHWST Mean High Water of Spring Tides

HAT Highest Astronomical Tide

Shennan (1986a) suggests that the reference water level for each type of indicator should be given as a mathematical expression of tidal parameters (such as the mid-point between mean high water of spring tides and highest astronomical tide) rather than a single tide level  $\pm$  a constant factor as the constant will indicate very different inundation characteristics for areas of different tidal range. He also stresses the importance of assessment of the accuracy of reference tide levels. This latter point is very important as sites used to indicate sea-level are rarely near tide gauges. The length of the inundation period is the most important factor determining the growth of plants of different species. A seasonal change in tidal patterns may be important here too. The shape of the tidal curve, which may be very complicated (as discussed in Chapter 3), determines the length of inundation at a particular altitude. The magnitude and frequency of occurrence of storms raising sea-level is therefore a further influence. Storms may result in standing water in an area for an indefinite length of time. The shape of the tidal curve and storm incidence need to be carefully assessed, especially in macrotidal areas, to obtain the correct indicative meaning for a sample. Palaeo-tidal changes must also be assessed as they determine how all the factors mentioned above have changed over time.

The second of van de Plassche's (1977) points concerning indicative meaning, that of sample altitude, is divided into two parts by Shennan (1986a); errors affecting the measured altitude of stratigraphic boundaries and errors associated with estimating the original altitude of stratigraphic boundaries. Errors of measurement may arise during measurement of depth in a borehole (see Chapter 4), during levelling of the site to an Ordnance Survey benchmark and finally with the assessment of the benchmark's accuracy to Ordnance Datum Newlyn (Shennan, 1986a). A high sampling density (Shennan, 1986a, suggests a thirty metre grid) will help to reduce errors of depth measurement in a borehole as a large number of records from a small area, over which the stratigraphy may be assumed to be reasonably uniform, will allow for a borer sampling the sediment having been sunk into the ground at slightly different angles in different places. The accuracy of levelling depends on the length of the survey line from Newlyn. Benchmarks are locally

accurate to  $\pm 0.01$  metre relative to each other, but inter-regional comparisons within England may only be accurate to  $\pm 0.15$  metre (Shennan, 1986a).

Errors affecting the original altitude of stratigraphic boundaries in regions not recently tectonically active (*i.e.* for the period during and since the sediments were deposited) are largely due to sediment compaction. Changes in local groundwater levels and river discharge, together with tidal effects, may also be important. Jelgersma (1961) stated that amounts of compaction may vary from 0% to 90%, depending on the nature of the sediments involved. Coarse-grained sediments suffer less compaction than organic materials. The difference between these two sediment types may lead to changes in altitude of the order of metres since sediment deposition (Streif, 1979). The depositional history of an area is also important in determining amounts of compaction as variations in the weight of overlying materials will alter amounts of compaction. Similarly where local pore water pressure is high due to poor drainage the sediment will be unable to undergo great amounts of compaction as it will be nearly impossible to decrease the void space. Desiccation, however, which may be due to a fall of sea-level or a lowering of the water table, will lead to overconsolidation of sediments (Greensmith and Tucker, 1971).

Streif (1979) suggests that the formation of intercalated peat layers is possible with a relatively slow rate of sea-level rise, which may include minor oscillations, associated with a slightly greater bog growth rate. The transgressive overlap forms when the rate of sea-level rise outstrips the rate of bog growth and, from this time, normal compaction of the peat increases with the increasing sediment overburden. However, Behre *et al.* (1979) explain cyclic peat formation as a result of either a rising ground surface or a lowering of mean high water and groundwater levels.

Behre *et al.* (1979) noted that peat layers resting on incompressible material eliminate altitudinal errors related to compaction. However, this leaves the possibility that peat growth unrelated to sea-level may occur. The alternative method is to correct altitudes for sediment compaction. A reduction in thickness of the sediments amounting to a halving of

their original altitudinal range at deposition is often assumed to have occurred (*cf.* Firth and Haggart, 1989), with no test to determine the actual amount of compaction. Smith (1985) used a soil mechanics technique, the oedometer test, on Holocene sediments in the Nar Valley, Norfolk, to obtain values for the reduction of void ratio with increasing applied load. This technique provides potentially useful quantitative estimates of compaction, but needs to be applied to sediments with different stress histories to give a better appreciation of the relationship between compressibility and lithostratigraphy which it provides (Smith, 1985).

The age of the sample used to indicate a former sea-level is also subject to error. In most cases organic layers, adjacent to clastic marine sediments, are dated by the radiocarbon method. Dates for rises and falls of the water table or sea-level are thus obtained. This method is better developed than, for example, luminescence techniques of dating clastic sediments (Bailiff, personal communication). The limitations of the radiocarbon method, as summarised by Bradley (1985), must, however, be borne in mind when assessing the accuracy of the given age of the organic material. Micro- and macrofossil analysis of the content of sediments in the sequence is also necessary to distinguish between a rise or fall in groundwater level and that of sea-level.

A further problem with the radiocarbon dating of organic sediments is the size of the sample required for dating. Where the organic content is low a sample covering a large vertical range may be required to obtain a date. This reduces the accuracy of the date obtained as an indication of water level movement.

An assessment is made below (in Chapter 1.3) of the work which has been carried out so far on the topic of palaeo-tidal changes. This falls broadly into two categories; that of analysis of sediments and that of (largely numerical) modelling.

### 1.3. Past work on tidal changes

#### 1.3.1. Sedimentary analysis

Roep *et al.* (1975) believed that fossil floodmarks (characterised by concentrations of light material, such as shells, driftwood and peat, and stratigraphic boundaries curving steeply upwards inland), evidence of marine bioturbation and eolian excavation could be used as indicators of palaeo mean high water. They estimated the palaeotidal range by comparison of the thickness of units in the sedimentary sequence with those formed under present day tidal conditions. Roep and Beets (1988) analysed sedimentary structures in coastal barrier deposits and deduced that the tidal range in the Netherlands was about 4 metres around 4,000 to 5,000 years B.P. and was reduced to approximately 3 metres by 2,000 years B.P., at which level it has remained to the present day.

The problem with analysis of sediments, as in the work outlined above, concerns the origin of the deposits and structures. The coastal barrier sediments may be just the effect of a temporary change of sea-level or a storm surge, or may, indeed, be indicative of sea-level over decades or centuries. The altitude of peat growth in relation to sea-level is still under discussion (see, for example, Shennan, 1986a; Firth and Haggart, 1989). Shells may be found over the whole width of the beach and both above high water mark and below low water mark. Driftwood and other items of flotsam and jetsam may mark the highest level reached by the sea or that of the maximum altitude attained at the last high tide level. Such items cannot be used to indicate a mean high water level of the sea. Roep *et al.* (1975) point out in their paper (page 13) that marine bioturbation must occur in areas frequently covered by the sea, so denying the possibility that evidence of this can be used as an indication of mean high water. Evidence of eolian excavation in a marine environment, not subsequently modified by the action of the sea, must occur above the highest level reached by wave action, ruling out its use as an indication of mean high water level. Estimation of tidal range from the thickness of sedimentary units is, at best, an elementary method. It does not allow, for example, for the possibility of a sea-level

rise or fall during sediment deposition or an increase or decrease in the rate or amount of sediment supply.

### 1.3.2. Modelling

One of the first attempts at modelling former tidal patterns was that by Jardine (1975). Jardine considered methods of calculating former tidal regimes within gulfs and estuaries. He simplified the shapes of gulfs and estuaries. Gulfs are represented as embayments with approximately parallel sides and approximately constant depth, while estuaries both decrease in depth and have sides which converge towards the head. Jardine used these models in combination with the equation for the wavelength of the tidal wave

$$\text{wavelength} = \text{period of tidal wave} \times \text{velocity of tidal wave} \quad (1.1)$$

$$L = T(gh)^{0.5} \quad (1.2)$$

to obtain firstly, for gulfs, the relationship of the distance of a site from the entrance to the gulf to tidal range and, secondly, for estuaries, comparison of mean depth, breadth and cross-sectional area of channels within the estuary to these values at the seaward entrance to the estuary. The equations produced allow calculation of the tidal range at any point within the gulf or estuary by comparison with the tidal range at its seaward entrance. Either tidal range at the mouth of the gulf or estuary may be altered or the shape of the gulf or estuary may be changed to represent its shape at a former sea-level.

Jardine's (1975) argument is only valid for changes of sea-level which produce a known change to tidal range at the mouth of the gulf or estuary (which is a circular argument) or for changes of sea-level within a gulf or estuary (for example, due to different sedimentation patterns). The applicability of the model is further limited by the simplifying assumptions made about the shape of gulfs and estuaries.

A different approach was used by Scott and Greenberg (1983) who considered the



tidal development in the Bay of Fundy, Canada, over the last 7,000 years. They used a numerical tidal model with input of the bathymetry of the area and tide-generating forces to reconstruct tidal patterns. To obtain former tidal heights, Scott and Greenberg used, as a basis, five sea-level curves from around the Bay produced by analysis of marsh foraminifera. Changes in relative sea-level were applied in the model as a plane surface, without taking account of the palaeogeography of the area. No additional changes in shoreline configuration were included in the model. A further problem was that the foraminifera used to obtain the sea-level curve are higher high water indicators (approximately equivalent to mean high water of spring tides). They therefore include the combined effect of a change in mean sea-level and change of magnitude of the tidal range, so that the amount of change of sea-level cannot be directly deduced.

Scott and Greenberg's (1983) results gave tidal ranges up to 75% lower than the present approximately 12 metre tidal range in the Bay of Fundy at 7,000 years B.P., with 75% of the present tidal range reached by 4,000 years B.P. However, in view of the assumptions made, these figures cannot be directly related to any former configuration of the Bay.

More recent examples of the approach to changes of tidal patterns using numerical tidal models include those of Franken (1987) and Austin (1988, 1991). Both authors lowered sea-level as a plane surface over the extent of the models of the north-west European continental shelf taking sea-levels from published sea-level curves. Franken (1987) suggested from his work that a lowering of sea-level by 20 metres corresponded to a one to one-and-a-half metre tidal range along the Netherlands coast at 7,700 years B.P. This is contrary to the work of Roep and Beets (1988), who suggested that tidal ranges were greater than present in the early Holocene along the Dutch coast. Austin (1988, 1991) also concluded that tidal ranges had generally been lower than present at lower sea-levels although his work was limited to the use of one tidal constituent. Neither author included any palaeogeographic data in his tidal model, again limiting the usefulness of the results.

Proctor and Carter (1989) studied the tidal and sedimentary regime of Cook Strait, New Zealand, over the post-glacial period. They used palaeogeographic information relating to former sea-levels to assess the response of the lunar semi-diurnal tidal constituent ( $M_2$ ) to the closure and opening of Cook Strait. The primary aim of the study was to explain the distribution of sediments on the floor of Cook Strait and, although assessment was made of the variation of amplitude of the  $M_2$  tide, no overall change to tidal ranges could be obtained as only the one tidal constituent was examined.

### **1.3.3. Unanswered questions**

The approaches to palaeo-tidal change outlined in Chapter 1.3.1 and Chapter 1.3.2 above make assumptions of varying quality and have been used for different purposes. The study of tidal changes at different sea-levels on the local scale, which was identified above (Chapter 1.2) as an area for research, requires a different approach. Sedimentary structures alone have been shown to be insufficient to reconstruct tidal patterns and numerical tidal models require modification to reflect the shape of coastlines and sea depths at former sea-levels. With these facts in mind, Chapter 1.4 outlines the aims of the work in this thesis.

## **1.4. Aims of the project**

### **1.4.1. What is the magnitude of tidal variations within embayments?**

Tidal changes at the local scale have not been considered in detail. The work of Jardine (1975) comes closest to this, but involves simplistic models. Shennan (1986b) argued that it is important to establish an accurate chronology of sea-level change (and therefore assess any tidal effects) on a local scale before regional comparisons may be made. In order to attempt this analysis, establishment of the present day variation of tidal range within the chosen embayments is necessary, followed by an assessment of how this has changed in the past. This will permit an answer to the question as to whether variations in the altitude of sea-level index points within the embayments may be explained by tidal changes.

#### **1.4.2. What effect does the shape of the coastline of an embayment have on tidal variations?**

The effect of a change in shape of the coastline of an embayment on the tidal regime has not been studied for former sea-levels. This work needs to be carried out to assess the accuracy of reconstructions which lower sea-level as a plane surface, making no further alteration for former coastline shapes. The availability of sufficient stratigraphic data to permit palaeogeographic reconstructions of coastal areas will enable this work to be carried out with the use of numerical tidal models.

#### **1.4.3. What effect does the sea-bed morphology have on tidal variations?**

Changes in the distribution of sea bed sediment accumulations over time may have an effect on tidal regimes. No data are available for offshore palaeo-sea depths, but modification of the bathymetry at former sea-levels using figures for isostatic movement of the land from Shennan (1989) permits some attempt to model this. The importance of this factor may be assessed by modifying sea depths for the present shoreline for comparison with tide gauge records. These tests will allow assessment of the relative importance of changes to sea-bed morphology, sea-level and coastal configuration.

#### **1.4.4. What is the contribution of neotectonics and sediment compaction to altitudinal variations of sea-level index points within the chosen embayments?**

The results from work outlined above will permit assessment of the amount of explanation of the variation within the embayments of the altitude of sea-level index points due to tidal changes. An assessment of remaining variation due to sediment compaction and neotectonic movements will be made. The relative contribution of each factor to the altitudinal variation of sea-level index points may then be obtained. Assessment of the influence of neotectonic movement will be by taking a map of faults of the area and determining whether a group of sea-level index points on one side is significantly higher than those on the other side of a fault at a given time. It is recognised that neotectonic movement does not necessarily occur along pre-existing fault lines, but the presence of existing

fault lines may be used to relieve stress. This method covers, therefore, a likely means of neotectonic movement. Analysis of possible effects of compaction around the embayment may be carried out by assessing the loading effects over time from the stratigraphic record, obtaining figures to apply from the literature. Isostatic movements of the land will be excluded from this analysis due to their inclusion in the sea depth modifications of the tidal models.

#### **1.4.5. What are the implications of answers to 1.4.1 to 1.4.4 above for a future rise of sea-level?**

An assessment of the possible implications of the research into present and former tidal patterns will be made for a sea-level rise. It has been predicted that sea-level will rise due to combinations of gases warming the earth's atmosphere, as a result of man's actions, causing ice from ice caps and glaciers to melt (see, for example, Houghton *et al.*, 1990). The importance of bathymetric changes *vis-á-vis* coastline changes will be considered.

### **1.5. Study areas**

The Holocene (the last 10,000 years) sedimentary record offers a greater possibility for a detailed study of sea-level change than for a period further back in time. There is often a good sequence of sediments preserved from this period which has not been destroyed by, for example, glacial action. Sediments are best preserved in depositional environments, such as embayments in the coastline, and this has influenced the choice of field areas for study in the thesis. Shennan (1986a) also notes that study of tidal changes will be more important for macrotidal, than meso- or microtidal, areas, although areas which have macrotidal ranges now may have had microtidal ranges a few thousand years ago and *vice versa*. For these reasons this study focusses on an assessment of the influence of tidal changes within two macrotidal embayments in the U.K. during the Holocene post-glacial period in which there is sedimentary evidence which records sea-level changes. Radiocarbon dating of sediments permits construction of palaeogeographic maps for the embayments during

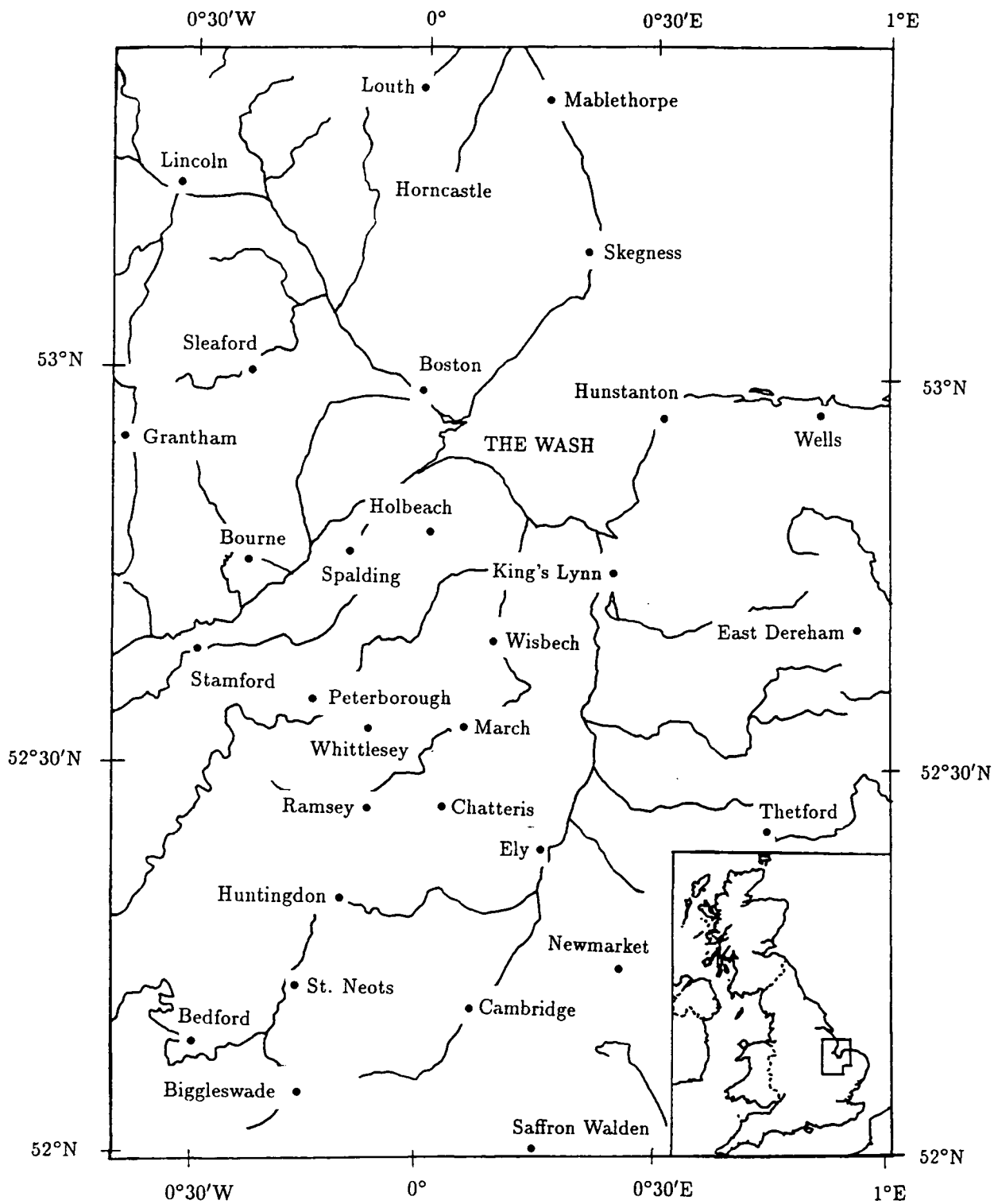


Figure 1.1. Map to Show the Location of the Wash Fenlands Field Area within Britain.

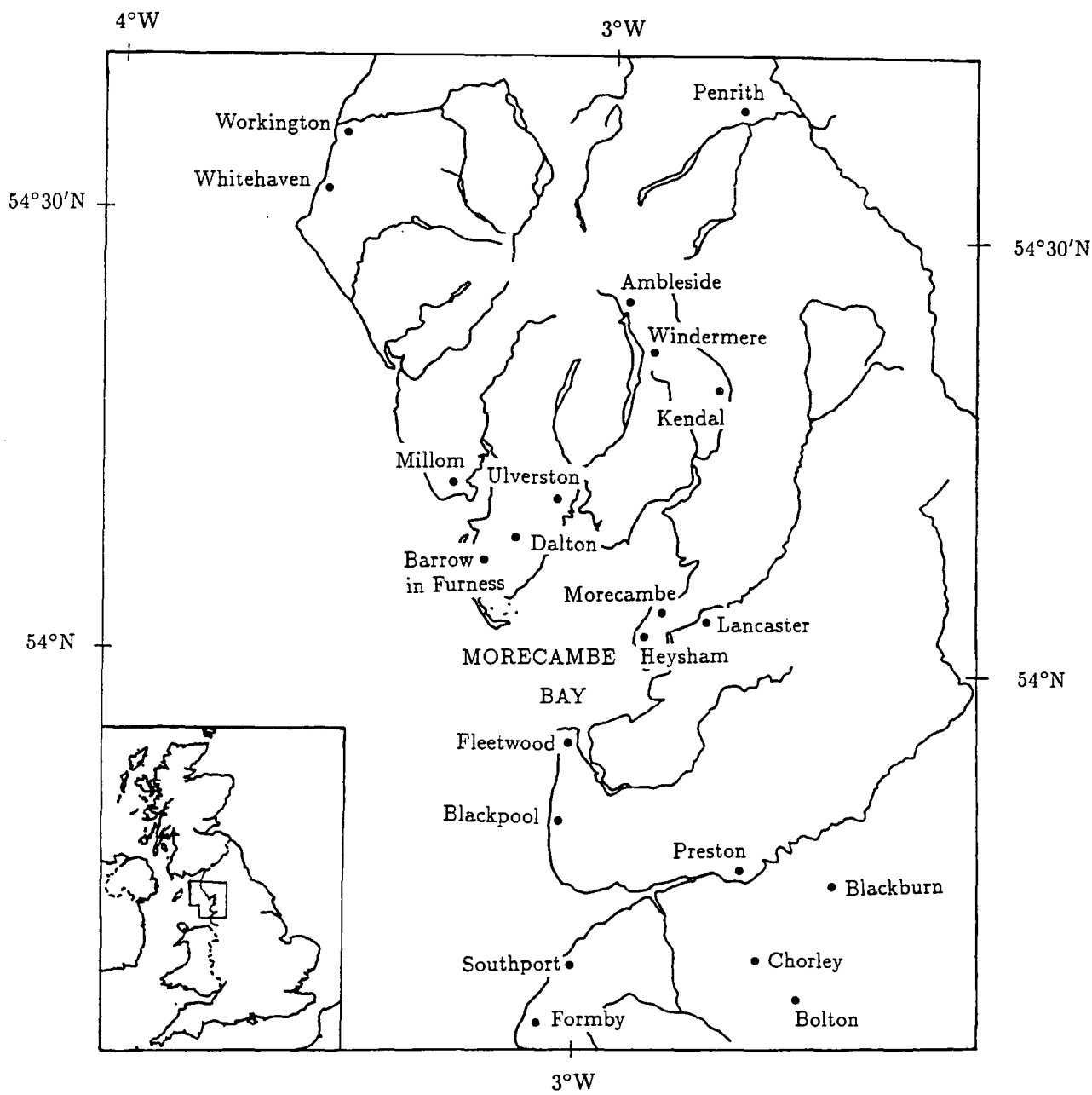


Figure 1.2. Map to Show the Location of the Morecambe Bay Field Area within Britain.

the Holocene. Numerical tidal models, which accurately predict present-day tides, are used with the palaeo-data to reconstruct former tidal patterns. The embayments chosen for study, The Wash and Morecambe Bay, have different histories during the Holocene in terms of isostatic movement. In addition the shape of their coastlines has altered in different ways during the Holocene as Morecambe Bay is surrounded by much higher land than The Wash. A greater area of low-lying land has therefore been open to marine inundation in the area of The Wash compared with Morecambe Bay, where inundation has only been possible up river valleys. Therefore the potentially different palaeogeographies of the two areas may have allowed different tidal responses between the two embayments, giving the possibility of a good comparative study. In the case of both embayments there is a good stratigraphic record covering the Holocene period linked to a number of radiocarbon dates (271 in The Wash Fenlands and 48 in Morecambe Bay), providing sea-level index points. The locations of the field areas are shown in Figures 1.1 and 1.2.

The geological development of each of the chosen field areas in relation to sea-level change is discussed in the next chapter. This is followed by an outline of tidal theory and tidal modelling. The implementation of the stratigraphic data from the field areas into the form of palaeogeographic maps and their use in the tidal models is the subject of Chapters 4 and 5. Results and analysis of data are presented in Chapter 6. In Chapter 7 the possible influence of factors other than tidal changes on the altitude of sea-level index points within the embayments under study is examined. The conclusions are presented in Chapter 8 together with suggestions for further research.

## CHAPTER 2

### THE GEOLOGICAL DEVELOPMENT OF THE FIELD AREAS

This chapter is divided into sections of different temporal periods to outline the geological background of the Fenland and Morecambe Bay and provide a comparison of the two areas in terms of their development. First, the solid geology and structural histories of the areas are outlined and contrasted. Next, more detailed attention is paid to their Pleistocene development. Finally, the evolution of the Fenland and Morecambe Bay during the Holocene is discussed with particular attention to the palaeogeography of the areas and the interaction of this with sea-level change.

#### **2.1. Geology and pre-Quaternary history of the Fenland and Morecambe Bay**

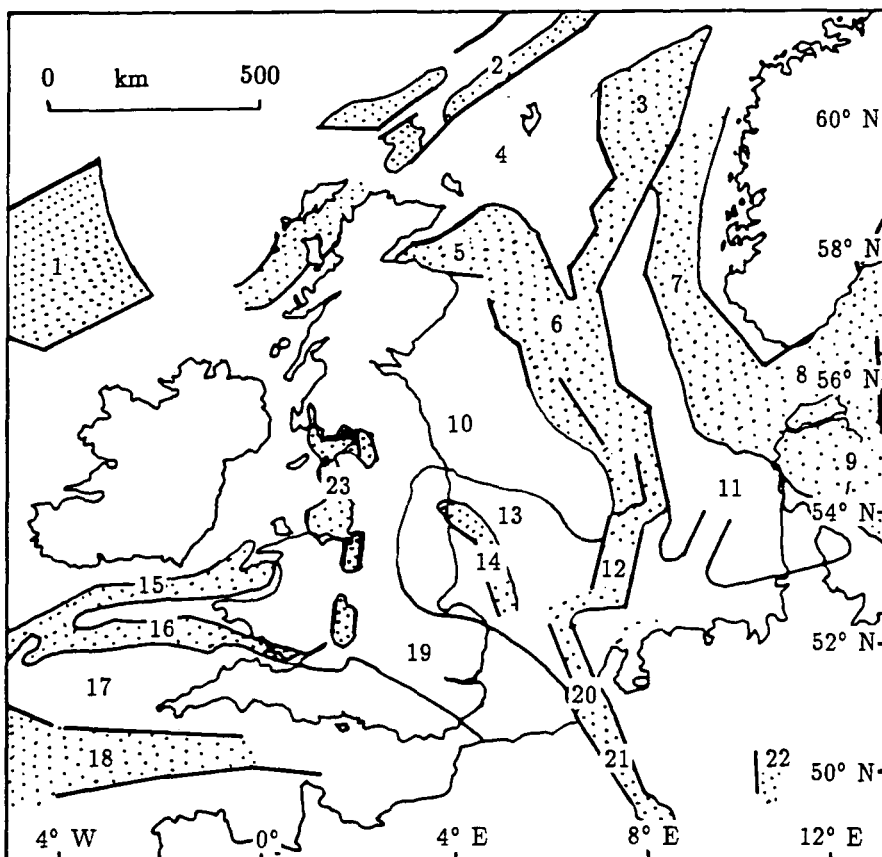
##### **2.1.1. Pre-Quaternary geology and structural history of the Fenland area**

The solid geology of the Wash Fenlands is composed of Jurassic and Cretaceous strata of primarily clays and limestones. The area lies on the western edge of the North Sea basin. This factor has affected its geological history, as is described below.

Depression of the North Sea basin probably commenced in the late Carboniferous (Kent, 1975). Deposition in this complex north-south graben system during the Mesozoic era was largely controlled by epeirogenic movements. The troughs formed in the area of the Wash are shown in Figure 2.1. A consequence of this was that the basin was opened to the ocean at times to the north and at others to the south. The alternating marine transgressive and regressive sequences recognised from the Holocene Fenland deposits are thus also characteristic of the Jurassic and Cretaceous strata. Both the Jurassic and Cretaceous strata were deposited sub-aqueously, but there was a long period of relative land uplift and denudation



Figure 2.1. The Main Structural Features Influencing the British Isles (after Naylor and Mounteney, 1975).



— Major sub-sea faults

▤ Rifts and troughs

- |                             |                             |                            |
|-----------------------------|-----------------------------|----------------------------|
| 1 Rockall Trough            | 9 Danish-Polish Trough      | 17 Cornubian Platform      |
| 2 West Shetland Basin       | 10 Mid North Sea High       | 18 Western Approaches      |
| 3 Northern North Sea Trough | 11 Danish High              | - English Channel          |
| 4 Shetland Platform         | 12 North Netherlands Trough | 19 Anglo-Brabant Massif    |
| 5 Moray Firth Trough        | 13 Southern North Sea Basin | 20 West Netherlands Trough |
| 6 Forties Trough            | 14 West Sole Trough         | 21 Lower Rhine Graben      |
| 7 West Norway Trough        | 15 North Celtic Sea Trough  | 22 Hessen Graben           |
| 8 Skagerrak Trough          | 16 South Celtic Sea Trough  | 23 Manx-Furness Basin      |

between these two phases (Chatwin, 1961; Swinnerton and Kent, 1976). At the transition from the Jurassic to the Cretaceous, the late Kimmerian phase of rifting affected the entire North Sea area (Ziegler and Louwerens, 1979). Rapid subsidence occurred in the Viking graben, but strong diapirism of the Zechstein salts partly obscured this tectonic phase in the central graben. A number of minor rifting phases interrupted the progressive subsidence of the central North Sea rift dome during the Cretaceous.

Subsidence was concentrated along the central axis of the North Sea basin and the strata of eastern England have a consequent low easterly dip. At the end of the Cretaceous, a number of inversion troughs were formed as a consequence of the Laramide tectonic phase in the North Sea, including the Sole Pit Trough near The Wash (Pegrum *et al.*, 1975). In this period, the North Sea area was slightly uplifted, causing the Cretaceous sea to retreat. There was continuous sedimentation in the North Sea during the Tertiary era, with considerably less disturbance associated with the major structural features, although subsidence occurred over the whole area and salt dome intrusion continued.

The second important structural feature of the area is the concealed Anglo-Brabant massif, which reaches as far north as The Wash (Figure 2.1). It is an area folded and compacted by Caledonian movements which has been substantially unaffected by tectonic movements since this time. The massif comprises a plateau-like surface over pre-Mesozoic rocks. This is a high block above which the Upper Cretaceous strata truncate the Jurassic and rest directly on Palaeozoic rocks. This area was one of relative stability between the surrounding troughs throughout the whole of Permian and Mesozoic times (Kent, 1975). The massif has remained close to sea-level throughout the Mesozoic and has undergone oscillation of only around 100 metres with little erosion or deposition.

### **2.1.2. Pre-Quaternary solid geology and structure of Morecambe Bay**

The solid geology of the catchment area of Morecambe Bay consists of rocks from Ingletonian (late Caledonian or early Ordovician) to Permo-Triassic in age, although those in the immediate neighbourhood of the Bay are Silurian and younger. The origin of the rocks

in this area is related to the position of north-west England on the edge of the Ordovician Iapetus Ocean which, at that time, divided northern England from Scotland. It is thought that the Iapetus Ocean was shrinking during the Ordovician by subduction of ocean crust on both sides of the Ocean (Broadhurst, 1985). The Ordovician volcanic rocks were probably produced as a consequence of this subduction and may have been part of a volcanic island arc system. Upper Ordovician and Silurian rocks indicate a return to marine sedimentation (Moseley, 1978; Broadhurst, 1985).

The Iapetus Ocean closed by the end of the Silurian and, with phases of compression, the resultant north-east/south-west trending Caledonian folds and thrusts were formed. No sediments of the subsequent Devonian period are found in north-west England. The Carboniferous, however, is well represented in the area. The Lower Carboniferous limestones were deposited in a marine environment in which the sea progressively flooded the area and subsequently fluctuated over it. In the Upper Carboniferous, the area was in a deltaic environment and there was a progressive decrease in the marine influence. At the very end of this period, faulting and folding occurred. This deformation is believed to have been the result of the collision of plates south of Britain which caused the formation of the Hercynian structures across central Europe.

The Permo-Triassic in north-west England is represented by rocks which the sedimentary structures suggest were deposited in fluvial, lacustrine and aeolian continental environments (Broadhurst, 1985). The Permian was characterised by normal faulting, associated with crustal extension as a precursor to the opening of the Atlantic Ocean during the Triassic. There are no representatives of subsequent geological periods around Morecambe Bay until the Pleistocene is reached.

Morecambe Bay lies on the north-eastern edge of the Manx-Furness basin which is one of a series of basins extending from the Celtic Sea through the Irish Sea to western Scotland. These basins have a general north-east / south-west trend and are dominated partly by the trend of the Caledonian mountain chains of Wales and Scotland and partly by the north-

north-east / south-south-west fractures, believed to be associated with the breakup of the European - North American continent (Naylor and Mounteney, 1975).

The structure of the southern part of Morecambe Bay and the offshore area is, however, not well known. The evidence suggests that the floor of the Bay comprises a synclinal structure (Bott, 1978), trending north-east/south-west, with simple faulting on its western flank and more complicated folding on the eastern side. The main syncline is thought to be cut by an extension of the Cumbrian Coast Boundary Fault and other associated faults (Patrick, 1987).

In more detail, the oldest rocks are at the headwaters of the catchments draining into Morecambe Bay (Patrick, 1987) and become younger seawards. The outcropping rocks also become younger from north to south clockwise around the Bay. The north-western part of the Bay is characterised by north-west/south-east trending normal faults cutting slightly folded Carboniferous beds which dip east and south-east at low angles. The Carboniferous rocks along the east coast of Morecambe Bay are folded into anticlines and synclines which trend generally north-east/south-west, cut by some normal faults trending approximately north-west/south-east. The regional trend of folding and faulting is north-south dominant with periodic phases of reactivation of movement in this direction (Moseley, 1972).

### **2.1.3. Comparison of the geological history of the Fenland and Morecambe Bay**

Morecambe Bay and the Wash Fenland belong to different structural units and factors which have influenced the evolution of one have had very little or no effect on the geological development of the other area. The structural background of the Fenland is largely related to the evolution of the North Sea graben system, whereas Morecambe Bay, on the other side of the country, owes its structural history to the plate movements prior to the opening of the Atlantic Ocean. The differences are mainly due to the influence of more recent geological deposition in the formation of the Fenland area, compared with the much greater age of the rocks around Morecambe Bay. The structural features of the Fenland are, therefore, far simpler than those of Morecambe Bay, where a considerably greater number of fault lines

and folded rocks are found, reflecting the former position of the area on a plate margin.

## **2.2. Pre-Holocene Quaternary geology of the field areas**

### **2.2.1. Quaternary geology of the Fenland before 10,000 years B.P.**

In the Pleistocene epoch of the Quaternary period (*i.e.* 2 million to 10,000 years B.P.) (Mangerud *et al.*, 1974), a combination of warm and cold episodes, isostatic and tectonic movements and alterations in the configuration of the geoid resulted in fluctuations of sea-level. The number of glacial - interglacial cycles in the Pleistocene has not yet been determined in many areas of the world. Initially, four glacial - interglacial cycles were recognised by Penck and Brückner (1909) in the Alps. More recent work in other areas of the world, such as that on oxygen isotope ratios from oceanic foraminifera (*e.g.* Shackleton and Opdyke, 1973, 1976, 1977) and on loess (*e.g.* Kukla, 1975), has led to the recognition of at least seventeen glacial - interglacial cycles in the Pleistocene. The number and cause of climatic fluctuations within the Pleistocene is still the subject of considerable discussion (see, for example, *Transactions of the Royal Society of Edinburgh* ser.C vol.18(4), 1990). The pattern of events in the Fenland during the Pleistocene is, therefore, by no means certain, but an attempt will be made below to outline the most important factors in the geological record.

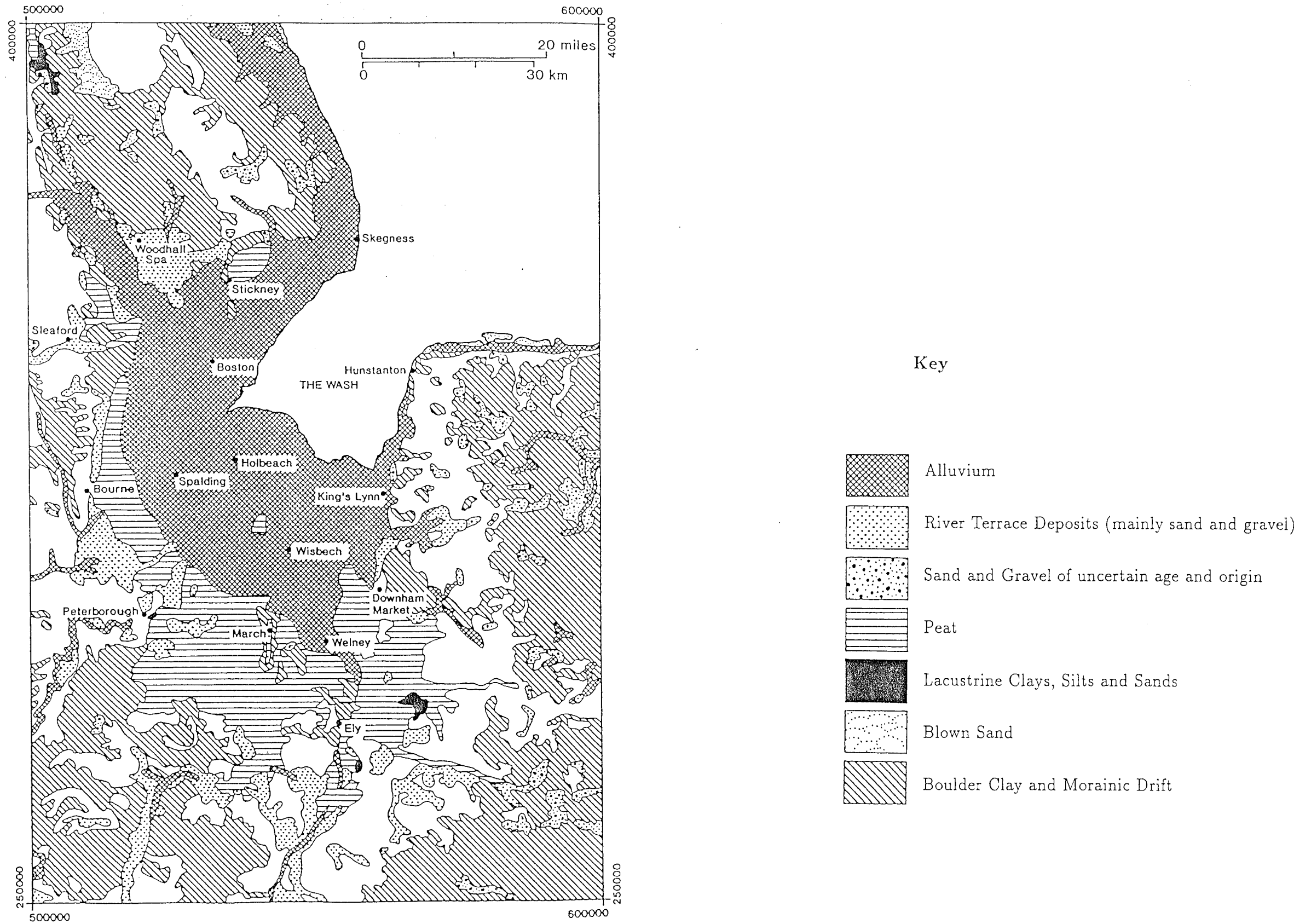
The recognition of three glacial (Anglian, Wolstonian and Devensian) and two interglacial (Hoxnian and Ipswichian) phases in Britain from field evidence has since been questioned. Bristow and Cox (1973), from stratigraphical work in East Anglia, found evidence to suggest that the Anglian and Wolstonian were two separate glacial phases within one cold stage. Summaries of the arguments both for and against the presence of a Wolstonian glaciation have been presented, most recently, in Shotton (1986) and Straw (1983). Rose (1987) proposed, based on lithological evidence, that the term "Wolstonian" should be abandoned for the stage between the Hoxnian and Ipswichian interglacial stages as the type Wolstonian glacial sediments were deposited before and during the Anglian stage and not subsequent to it. Gibbard and Turner (1988), however, argued for the retention of the Wolstonian stage as representative of a cold stage between the Hoxnian and Ipswichian interglacials.

The main recorded evidence of glaciation from the Fenland area comprises the Stickney moraine in Lincolnshire and a chalky boulder clay underlying much of the Holocene deposits. The chalky boulder clay is exposed in the cliffs at Hunstanton and outcrops to form the Fenland “islands”, at places such as Apes Hall, Butcher’s Hill, Manea and Stonea in the Ely district (Gallois, 1989). The Stickney moraine represents the southern limit of ice during the Devensian, whilst the chalky boulder clay, which predates it, is believed to have been deposited by an ice sheet from northern England, based on its geological composition, which comprises rocks almost exclusively from Lincolnshire, Cambridgeshire and Norfolk. Quaternary deposits in the Fenland are shown in Figure 2.2.

Perrin *et al.* (1979) attribute the formation of the Wash-Fens basin to erosion by ice that deposited the Lowestoft Till. They suggest that the main source of the ice passed through the mouth of the Wash and then spread out over eastern England in a fan shape. Gallois (1979) suggests that the Fenland valleys have a fluvio-glacial origin, as the valleys beneath the glacial deposits appear to be broad, structurally-controlled and form a dendritic pattern draining towards the Wash. Subglacial tunnel valleys would have steeper sides and be narrower than those found from seismic profiling. Thus the direction of the main drainage system was pre-glacial and has only been modified and partly filled with deposits during glacial episodes. A number of rivers which used to run west and then north from the pre-glacial chalk escarpment in Norfolk, such as the Nar (Gallois, 1979), have been altered to run in a more northerly direction. Buried valleys are cut to about  $-70$  metres O.D. in the Terrington and Denver area, with a deeper valley at the mouth of the Wash, cut down to about  $-100 \pm 15$  metres O.D. (Wingfield *et al.*, 1978). This gives an indication of the fall of relative sea-level during the glacial periods in the Quaternary and of the nature of the surface over which marine transgression occurred.

The Nar Valley beds in Norfolk comprise over thirty metres of fluvial sands and marine clays rising to 30 metres above present sea-level (Gallois, 1989) of Hoxnian age (Ventris, 1986). The Nar Valley beds have been correlated with the Third terrace of the River Cam (West, 1972), on the basis of incorporated fauna which suggested deposition in

Figure 2.2. The Quaternary Geology of the Fenland (from Woodland, 1977).



a cool temperate marine environment (Baden-Powell, 1934) and a maximum high tide level of twelve to thirteen metres O.D. (West, 1972). They also correlate (Davey, 1991) with the Woodston Beds in the western Fenland, which are a series of fluvial and estuarine sediments, comprising silty clays and fine sands, overlying a basal gravel of probable fluvial origin (Horton *et al.*, 1991).

The chalky boulder clay, in central parts of the Fenland, is unconformably overlain by up to six metres of shelly sand and flint gravel that Baden-Powell (1934) termed the March Gravels. Gallois (1989) suggested that the March Gravels were deposited in a low energy marine environment, comparable with the southern part of the Wash today. In common with Skertchly (1877), Gallois suggests that the sources of the March Gravels are the river terrace gravels of the Great Ouse and the Cam at their seaward limit (from evidence of their bedding dipping northwards towards the Wash), although this requires a higher sea-level than present, in a cooler climate. A raised beach at Hunstanton is thought to have been formed at the same time as the deposition of the March Gravels, from faunal evidence (Gallois, 1989), although the two features have differing lithologies. However, Bridgland *et al.* (1991) have recently questioned the age of the March Gravels. The March Gravels have been correlated by Castleden (1980) with the Second terrace of the River Cam. Ipswichian sediments occur within the First terrace deposits, so the March Gravels may be of intra-Saalian age (Bridgland *et al.*, 1991) and not represent the Ipswichian high sea-level.

Subsequent to the glaciation which deposited the chalky boulder clay there was a temperate phase during which the sea presumably covered at least part of the Fenland area (Gallois, 1989). A peat bed at Tattershall has been identified as of Ipswichian age on the basis of its pollen assemblage (Catt, 1977) and is interpreted as of fluvial origin by Holyoak and Preece (1985). At Tattershall Castle, Holyoak and Preece (1985) identify the peat as representative of riverside mud inundated only by spring tides on the basis of its macrofossil content. The peat at Tattershall Thorpe, however, is higher above sea-level and contains no evidence of brackish conditions (Holyoak and Preece, 1985). Thus the incorporated flora and fauna indicate that it is of supra-tidal origin, although the peat lies a few metres below



present mean sea-level.

Straw and Clayton (1979) remark that Ipswichian deposits at Tattershall and Wretton are overlain by Devensian gravels, whereas in the southern and south-western parts of the Fenland, Ipswichian deposits were converted into terraces before the Devensian gravels accumulated at a lower altitude beneath them. From this, they suggest slight relative subsidence of the north-eastern part of the Fenland before the middle Devensian, as a consequence of an early Devensian ice advance into the Wash gap. West (1972) also suggested that differential land movements may have occurred in addition to changes of sea-level, as lower Pleistocene marine deposits have been recorded at 183 metres O.D. at Netley Heath in Surrey, whereas the Crag deposits, which mark the Plio-Pleistocene boundary, are found at approximately O.D. in south-east Suffolk.

Following a fall of sea-level to just below the present altitude, as indicated by the First and Second terraces of the rivers Cam, Lark and Great Ouse, amongst others, sea level fell to much lower levels during the Devensian glaciation. In Lincolnshire, the Stickney moraine is matched closely across the Wash by the Heacham moraine, which passes into drift banked up against a former sea cliff at Hunstanton (Straw and Clayton, 1979). A till, lithologically similar to that at Hunstanton, is also found in patches beneath the Wash, although not in such large quantities as that of the chalky boulder clay. The Fenland was largely a lake area to the south and west of this ice limit (Straw, 1963).

The Fenland "islands", isolated low hills standing on an almost flat plain, of solid and Pleistocene deposits, are thought to have been formed at the end of the Pleistocene period (Gallois, 1989), within a lake or shallow sea. Gravel deposits of differing origin surround the "islands", but in the Ely district (Gallois, 1989) all are characterised by a marked change of slope on their sides beneath the Holocene deposits, from five to seven degrees above to less than one degree below the Holocene deposits. Gallois mentions that formation of the break of slope on the "islands" cannot readily be linked to the deposition of Holocene deposits as the peats and salt marsh clays which form the base of the Holocene sequence do not have

erosional contacts with the surface beneath. West (1991a, 1991b) has identified thermokarst activity in the area in the Devensian so it is possible that the “islands” were surrounded by alases, or thaw lakes, which resulted in their steep sides.

West (1980), from a study of pre-glacial Pleistocene sequences in East Anglia, found evidence of only a small (2-3 metre) deformation of land within the area in the Cromerian, though he did not take compaction of sediments into account in his work. West (1980) also found an altitudinal variation of 5-6 metres in Pastonian sediments in the same area which he suggests may indicate deformation in pre-Beestonian times. The amount of post-Cromerian deformation in East Anglia is not known, but West (1980) suggests that little variation in altitudes implies either that there has been little movement or that it has occurred parallel to the coast.

Jelgersma (1979) compared the altitude of Ipswichian (Eemian) sea-levels from south-east England with those found on the continent. Sea-levels from Belgium to Denmark have been recorded from present values to about eight metres below, whereas those along the North Sea coast of south-east England have been reported from one metre below to fifteen metres above present sea-level. Jelgersma suggests that these altitudinal differences may be due to differences in tectonic downwarping in and around the North Sea basin.

Eden *et al.* (1978) noted that the maximum average rate of Tertiary subsidence in the North Sea was around five millimetres per 100 years, compared with an average subsidence of approximately thirty millimetres per 100 years in the northern part of the North Sea during the Quaternary. Caston (1979) suggested that average Quaternary sedimentation rates may have been as high as 0.3 to 0.5 metres per 1,000 years, which is up to ten times as high as the comparable rate for the Tertiary. His work, based primarily on data from 188 wells, showed that Quaternary sediments are up to ten kilometres thick in parts of the North Sea. Stoker *et al.* (1985) note that stratigraphic evidence shows an extensive Lower Pleistocene sequence in the U.K. sector of the southern and central North Sea which thickens eastwards to the centre of the basin where up to 500 metres of sediment are found.

Eden *et al.* (1978) suggest that the increasingly rapid subsidence rate has resulted in sediments of the later part of the Quaternary comprising a disproportionate amount of those deposited since the beginning of the Tertiary. Clarke (1973) also drew attention to increasing average rates of subsidence in the central North Sea since the Cretaceous, although his data points were not well distributed temporally and water depths may not have been accurately assessed (Eden *et al.*, 1978). Eden *et al.* (1978) calculated the maximum tectonic subsidence for the North Sea for the late Pleistocene using Mörner's (1972) late- and post-glacial sea-level curve, extended to 130,000 years B.P. using estimates of temperature variations based on the work of Coope (1974) and by the use of polar ice front positions from analysis by McIntyre *et al.* (1972). From this, they concluded that average subsidence rates for the late Pleistocene are not due to tectonic subsidence alone and suggested that glacial sediment loading might also be responsible.

More recently, Preece *et al.* (1990) have shown that there was uplift in the area of the Isle of Wight before, during and after the Ipswichian. The differences in elevation of marine deposits of this age in north-west Europe had previously been attributed to subsidence of the southern North Sea (West, 1972; Zagwijn, 1983). The evidence of Preece *et al.* (1990) suggests that the English Channel area has not been tectonically stable since the Ipswichian, as assumed by Zagwijn in calculating the rate of downwarping of The Netherlands from that time to the present as 142 millimetres per 1,000 years. It is now thought probable that part of the difference in elevation of Ipswichian deposits across the Channel is the result of uplift in the Channel area.

### **2.2.2. Quaternary geology of Morecambe Bay before 10,000 years B.P.**

Sediments of Quaternary age predominate around the coastline of Morecambe Bay and offshore within the Bay. Buried valleys cut in solid rock beneath the Bay have altitudes of -60 to -80 metres O.D., suggesting that Morecambe Bay probably existed as an embayment of the Irish Sea during each interglacial, when sea-level reached approximately present levels (Tooley, 1987).

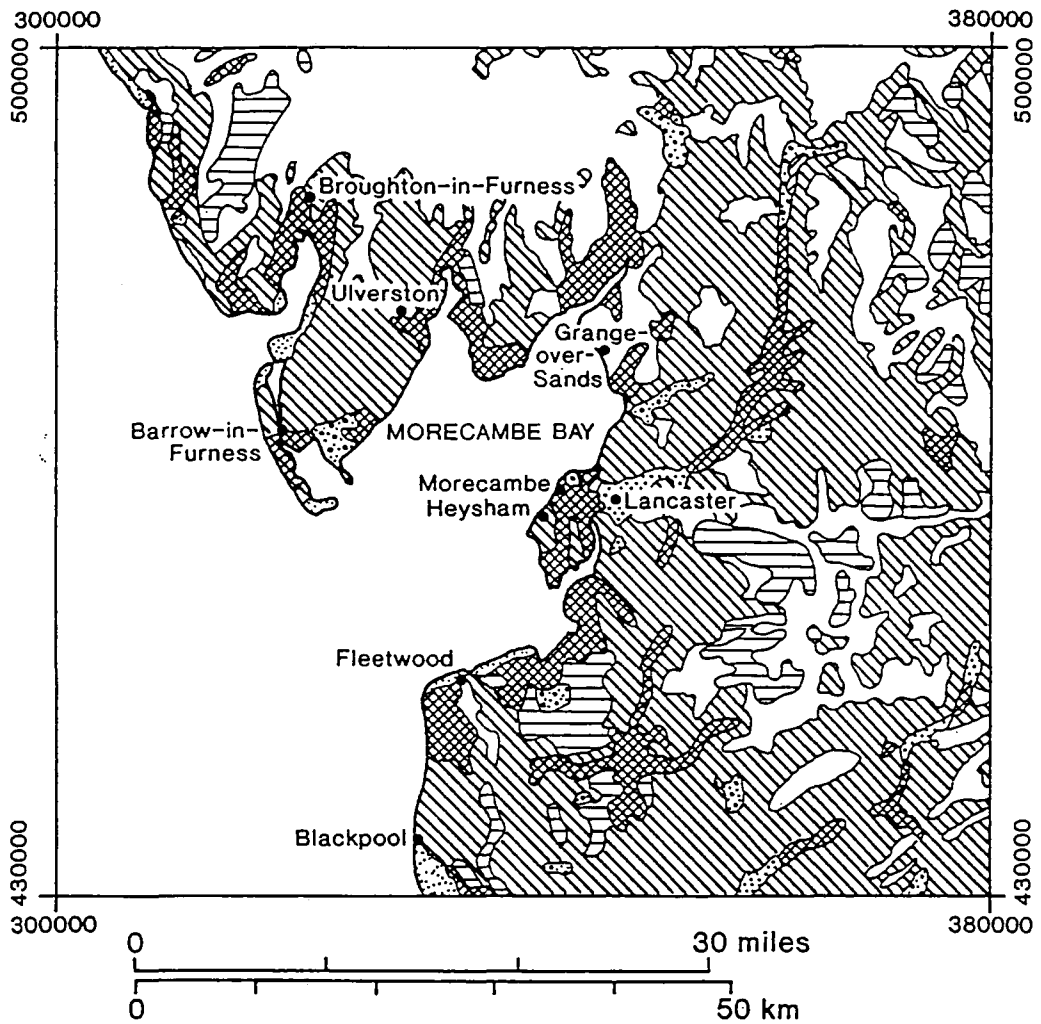
In the north-eastern part of the Irish Sea, Permo-Triassic rock is overlain, over most of the area, by boulder clay a few metres thick (Pantin, 1977). Pinger profiles, vibrocores and boreholes show that the boulder clay is overlain by well-bedded proglacial water-laid sediments over much of the area. These are, in turn, overlain by marine and estuarine sediments which are less well-bedded due to the effects of bioturbation. The proglacial water-laid sediments are thought to be Devensian in age, deposited during deglaciation. Erosion of boulder clay from the surrounding land by meltwater streams would have produced an abundant supply of material for these deposits (Pantin, 1978). It is suggested that a sea-level rise resulted in the deposition of the marine beds, which may be glacio-marine in origin (Pantin, 1977). The surficial Quaternary deposits surrounding Morecambe Bay are shown in Fig. 2.3.

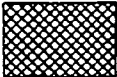
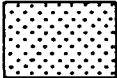
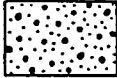
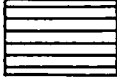
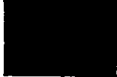


There is no unequivocal evidence for pre-Devensian Quaternary deposits or landforms within the Morecambe Bay area (Pennington, 1978; Tooley, 1987). Ashmead (1974) and Tooley (1987) have reviewed the available evidence from the Carboniferous limestone caves around the Bay. A peat of possible Ipswichian age was recorded between two tills in the north-western part of the Bay (Kendall, 1881). However, no record of a peat layer was found by the Institute of Geological Sciences (Anon., 1972) when a bore was put down in the area, although the top 26 metres, which may have contained the peat layer, were not sampled.

Erosive features around Morecambe Bay have been proposed as indicators of Quaternary sea levels (Ashmead, 1974; Tooley, 1987). Ashmead (1974) assigned a Devensian age, from archaeological evidence, to some possible sea caves and notches at +12 to +30 metres O.D., although Tooley (1985) linked marine features of this altitude to the Hoxnian, on the basis of a Hoxnian sea level of +23 metres O.D. recognised by West (1972). It is possible, though, that the limestone features are of phreatic origin (Gale, 1981) and do not indicate a former level of the sea.

Tooley (1987) suggests that, during the Devensian, ice from the Irish Sea affected the western part of Morecambe Bay, whilst ice from a Lake District ice cap influenced the rest

Figure 2.3. The Quaternary Geology of Morecambe Bay (from Woodland, 1977).



-  Alluvium
-  River Terrace Deposits (mainly sand and gravel)
-  Sand and Gravel of uncertain age and origin
-  Peat
-  Lacustrine Clays, Silts and Sands
-  Blown Sand
-  Boulder Clay and Morainic Drift

of the Bay. A tripartite sequence of glacial deposits has been recognised widely across Lancashire (Hull, 1864, cited in Mitchell *et al.*, 1973; King, 1976), consisting of a Lower Till, above which are the Middle Sands and an Upper Till. It is widely believed (King, 1976; Johnson, 1985; Huddart *et al.*, 1977; Vincent, 1985; Tooley, 1987) that the till and sand sequence of Lancashire represents one glaciation with an oscillating ice front. The lithology of the two tills is similar and both contain shells derived from the floor of the Irish Sea (King, 1976). In places, the Middle Sands are missing and it is impossible to separate the tills. On the floor of the northern part of Morecambe Bay, Knight (1977) found one till unit, up to 55 metres thick, overlaid by varved clays, silts and sands, which Vincent and Lee (1981) interpreted as sedimentation in a proglacial lake on an outwash plain. Eyles and McCabe (1989) believe that the glacial lacustrine deposits were deposited up to 40 metres above present sea-level.

Vincent (1985) summarises Huddart's (1971) sedimentological work on the tills of north-west England and concludes that soon after 26,000 years B.P. glaciers from the Lake District deposited a till over fluvio-glacial sediments. These valley glaciers were then overrun by a combined Scottish - north Lake District ice sheet which deposited a further till and formed extensive drumlin fields. This ice decayed *in situ* and left sequences of meltwater channels and fluvio-glacial deposits on the fells around Black Coombe, north-west of the Duddon estuary (Smith 1967, 1977). The upper of the two tills found in the region from Walney Island to the mainland is thought to have been deposited by a readvance of the Irish Sea ice, from the origin of erratics contained in the till. A second readvance of the Irish Sea ice north of Black Coombe left till deposits at altitudes below 60 metres.

Numerous landforms indicative of glaciation, such as drumlins, eskers and kettleholes, are found around Morecambe Bay. The varved sediments, found on the floor of the Bay (Knight, 1977), indicate sedimentation during deglaciation in a freshwater proglacial lake (Tooley, 1987). These varved clays are overlaid by slightly overconsolidated clays, silts and sands, interpreted by Knight (1977) as alluvial fan deposits, but reinterpreted by Vincent and Lee (1981) as outwash plain sediments. The slightly overconsolidated nature of the

sediments is attributed to a period of desiccation, which allowed the outwash plain deposits to form the loessic sediments found around Morecambe Bay.

The pattern of deglaciation of the Morecambe Bay area is not well supported by dates. Organic material, subsequent to deglaciation, has been dated to about 12,000 years B.P. in kettleholes near Morecambe Bay (Tooley, 1987). Tooley mentions, though, that evidence from the Windermere Basin gives dates of  $14,330 \pm 230$  years B.P. and  $14,623 \pm 360$  years B.P. in the Windermere Interstadial soon after the deglaciation of this area (Coope and Pennington, 1977), with plant evidence suggesting alpine conditions. At this time, silts and clays not trapped in the lake basins were swept into Morecambe Bay (Vincent, 1985). Sediments in the Windermere area indicate an interstadial of cool temperate conditions around 11,000 to 14,000 years B.P. There is no available evidence relating to these changing environmental conditions from sediments in Morecambe Bay (Tooley, 1987).

### **2.2.3. Comparison of the pre-10,000 years B.P. Quaternary history of the two areas**

Differences between the Pleistocene history of the Fenland and Morecambe Bay, as with the earlier geological development of the areas, again predominate over their similarities. Morecambe Bay was much closer to centres of ice accumulation, such as the Lake District, than the Fenland and has therefore experienced erosion during glacial episodes, whereas the Fenland has been at the outer margin of ice advance and consequently has many features of glacial deposition. Glacial deposits from Morecambe Bay relate, probably exclusively, to the last period of glaciation during the Devensian as any deposits from previous glaciations appear to have been eroded away. Beyond the fact that two tills are recognised as present in the Fenland and only the later, Devensian, is recorded by two tills of this age in Morecambe Bay, it is difficult to make further comparison of the Pleistocene deposits of the areas, as no features which can be ascribed with certainty to a particular interglacial have been recorded in the Morecambe Bay area. Buried valleys are, however, present in both areas. These indicate that sea-level fell to a minimum of about  $-80$  metres O.D. in both Morecambe Bay

and the Fenland during periods of low sea-level in glacial stages.

### **2.3. The Holocene development of the Wash Fenlands and Morecambe Bay**

In this section, the existing theories as to the development of the field areas during the last 10,000 years are discussed and compared. Factors influencing the accuracy of the proposed schemes are mentioned, but further clarification of these is given in Chapter 7. In Chapter 4, the palaeogeographies of the field areas, which have been reconstructed at selected times, are presented.

#### **2.3.1. The Wash Fenlands**

Stratigraphic evidence of sea-level change in the Fenland has been recorded for well over a hundred years (*e.g.* Wheeler, 1868; Skertchly, 1877). With the exception of that of Skertchly, though, the accounts were very descriptive. Skertchly, however, attempted to correlate the changes between different parts of the Fenland and assign causes to the variations in the deposits which he found. He divided the Fenland deposits into three types: gravel lands, silt lands and peat lands, and discussed the development of each in relation to the other. Skertchly recognised that peat beds occur both above and below a layer of clastic sediments in the Fenland, with surface peat beds occurring in the western part and silt at the surface in the east. He acknowledged that this illustrated an interplay between salt and freshwater influences in the development of the Fenland: "The marks which the sea put upon the land were ... beds of light flocculent silt ... The cognisance of the fresh-water was peat. Whenever fresh-water stagnated, peat grew. And, as the sea was continually damming itself back, by piling up its silt beds, the peat followed its retreating footsteps until the changing climate had so altered as to have become unfavourable to its growth" (Skertchly, 1877, p.129). Skertchly also recognised the existence of gravels underlying much of the Holocene deposits of the Fenland, but overlying the boulder clay. He suggested that the gravels were probably of different origin in different parts of the Fenland and proposed that they were either of fluvial or of marine origin. The origin of the Fenland gravels is still under discussion (see, for example, Gallois, 1989).



Subsequent work on the Fenland commenced with that of Godwin and the Fenland Research Committee in the 1930s, based heavily on stratigraphic and pollen analytical work, with some radiocarbon dates added in the 1960s. Godwin and Clifford (1938) established the four-fold division of the Fenland deposits into the upper silt, upper peat, fen clay and lower peat. Godwin (1978) revised his earlier work (*e.g.* Godwin, 1940) and produced a new relative sea-level curve for the Fenland. In this, he proposed time periods for the deposition of the peats and silty clays. Godwin suggested that, following the growth of the lower peat on the pre-Flandrian surface, the fen clay was deposited from the first marine transgression into the area in the Holocene, after  $8,422 \pm 170$  years B.P., the date of a moorlog trawled up from the Leman and Ower Banks (Godwin and Willis, 1959). The upper peat formed subsequent to this at around 3,000 to 3,500 years B.P. (Godwin, 1978), associated with a standstill or lowering of the level of the sea. Around 2,500 years B.P. a relative sea-level rise occurred in the Fenland which led to deposition of the upper silt associated with extensive coastal salt marshes. Freshwater was ponded back as the silt was deposited at the tidal limit of the rivers. This led to the development of the Fenland meres, such as Whittlesey Mere, most of which persisted until the drainage of the Fenland commenced in the seventeenth century.

Gallois (1979) applied the names lower peat, Barroway Drove Beds, Nordelph Peat and Terrington Beds to the four-fold sequence of deposits which he found in the Wisbech and King's Lynn areas, corresponding to Godwin's lower peat, fen clay, upper peat and upper silt. Gallois (1989) extended this new terminology, based on the names of sites where these beds are found, to cover the Ely district. The dates given to the phases of deposition in the Ely district by Gallois (1989) accord well with those of Godwin (1978). The oldest peats in the Ely area formed in river channels and poorly drained hollows between 9,000 and 7,000 years B.P. and were overlain by a freshwater peat which formed as the Fenland basin became flooded as a result of the rising sea-level. Subsequent to this, Gallois (1989) suggested that a marine transgression occurred about 4,700 years B.P. which deposited intertidal clay and silt. A relative fall of sea-level between about 4,000 and 2,050 years B.P. produced a

second widespread peat which was, itself, inundated by a relative sea-level rise during which intertidal deposits were laid down.

Radiocarbon dating of deposits was not possible until the 1960s (Willis, 1961). A number of Godwin's sites were revisited and samples were taken for dating. Prior to this, Godwin's classificatory scheme was entirely lithostratigraphic and its application to different areas of the Fenland could, therefore, give no indication of whether the deposits found were of comparable ages. Gallois' (1979, 1989) use of site names to describe the stratigraphy is, similarly, not of great chronostratigraphic value. His scheme was only intended to be of lithostratigraphic use. In both cases, the authors have worked largely in the southern Fenland and subsequent work has shown that the tendencies of sea-level were not necessarily synchronous or of equal magnitude in different parts of the Fenland (Godwin and Vishnu-Mittre, 1975; Shennan, 1986a; Waller, 1988).

Shennan (1986b) presented evidence based on stratigraphic and micropaleontological studies combined with radiocarbon dating, updating his former work (Shennan, 1980, 1981, 1982), which led him to conclude (Shennan, 1986a) that at least seven separate periods of positive sea-level tendency (which he termed 'Wash') could be found within the Fenland, the most recent of which were identified with the aid of archaeological evidence (*e.g.* Churchill, 1970). In addition, Shennan (1986a) makes the point that between *c.* 4,500 and 4,200 years B.P., during which the upper peat of the southern Fenland began to form in the Denver - Flaggrass - Wood Fen - Shippea Hill area, the fen clay had not yet reached its major period of deposition in other sedimentary basins to the north and west. Deposition of the fen clay continued in these basins until about 3,300 years B.P.

Shennan (1986a) drew a curve of sea-level change over the last 7,000 years in the Fenland (Figure 2.4) with an error band for altitudinal variation of the mean high water spring tide level. The results are shown for this tidal level as this is taken to be the sea-level recorded by most sea-level indicators. The curve shows that the level of mean high water of spring tides has risen from about -8.5 metres O.D. at 6,600 years B.P. to its present value of +3.8

metres O.D. with periods of positive and negative tendency, as noted above.

Shennan (1986a) noted differential crustal movements along the east coast of England during the Holocene. He refers to significant differences for 5,200 to 5,300 years B.P. between Hartlepool and the Fenland, and for about 6,200 years B.P. between Spurn and the Fenland, allowing for present differences in mean high water of spring tides. The reality of these differences must be put into perspective in the light of results presented in Chapter 5 of this thesis. Shennan (1989) extended this work with 58 radiocarbon-dated sea-level index points from the Fenland. The results had a coefficient of determination, or explanatory value for land movement, of 58% and showed a trend of linear subsidence of the Fenland until 5,000 years B.P. of approximately minus one metre per 1,000 years (with 37 data points). For the period from the present to 6,500 years B.P., a linear solution was not such a good fit to the data set.

Shennan (1980, 1986a) also drew attention to the fact that the whole Fenland area cannot be simply divided up into a quadripartite sedimentary sequence as areas of more peat and silt / clay intercalations exist, especially near to the present coastline. In addition, Shennan (1986a) discussed the spatial variation in the sediments composing the "fen clay" and "upper silt" deposits. The sediments which make up the "fen clay" layer are composed, typically, of *c.*55% clay, *c.*45% silt and less than 5% of fine sand away from the creek systems. Seale (1975) showed that a finely laminated silt loam or sandy silt loam is more characteristic of the roddons (former river channels). The "upper silt" deposits are generally coarser than those of the "fen clay", but, similarly, become coarser in the major channels (Shennan, 1986a). In both cases, a low energy environment of deposition is suggested by the nature of the clastic sediments. Similar sedimentary environments existed in each period of positive tendency of sea-level movement with different parts of the Fenland undergoing their maximum extents of marine or estuarine inundation at different times (Shennan, 1986a).

Waller (1988), in a preliminary report of the Fenland Project (which is attempting to integrate palaeoenvironmental changes in the Fenland with archaeological evidence), has

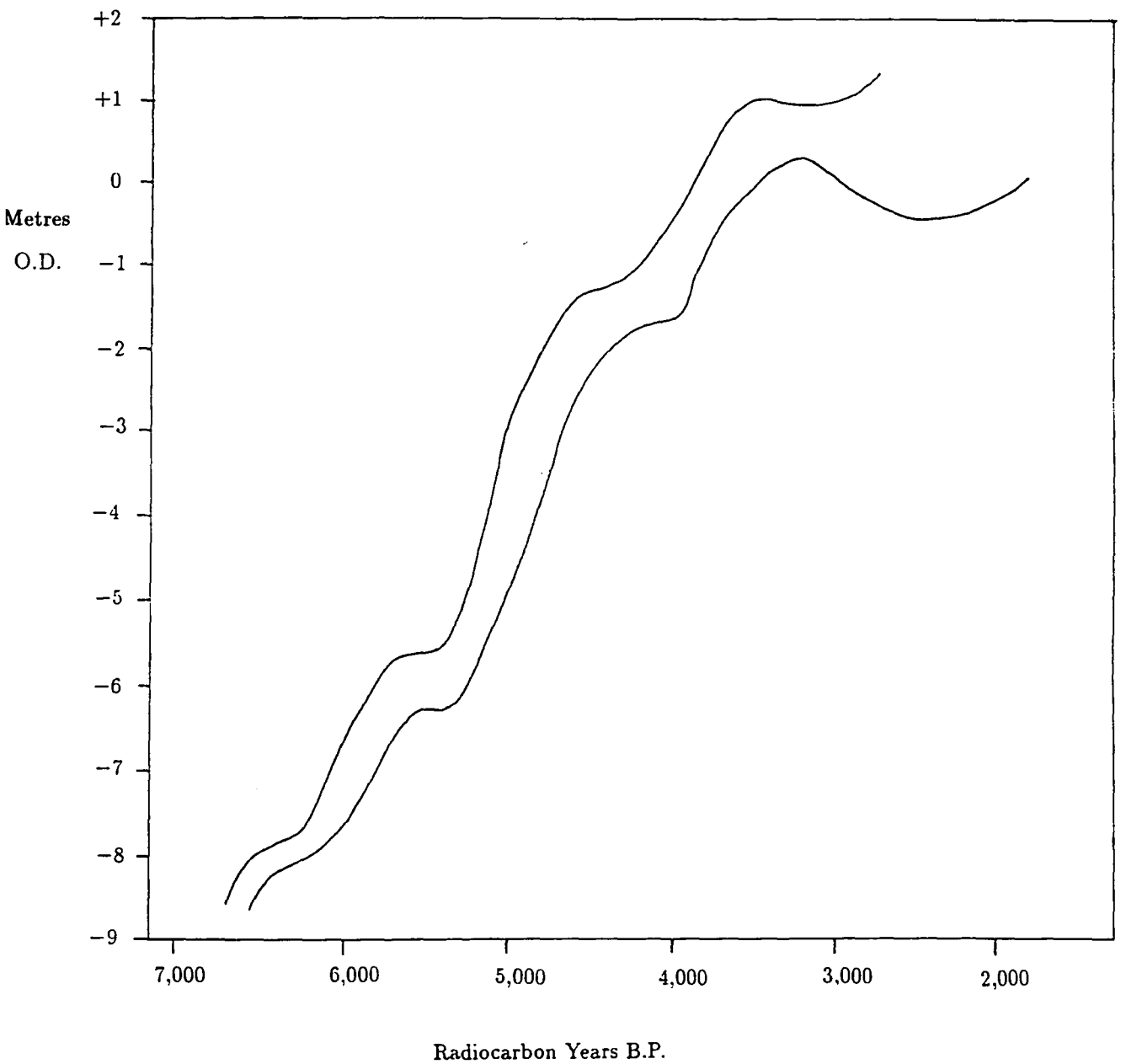


Figure 2.4. Sea-level curve for the Fenland with an error band for mean high water of spring tides (after Shennan, 1986).

considered the sedimentary evidence of each basin separately in terms of the tendencies of sea-level movement that have occurred. Within the south-eastern Fenland basin, to the north and east of Ely, dates of the deposition of the fen clay range from  $4,350 \pm 60$  years B.P. for the onset of marine conditions at Peacock's Farm to  $3,955 \pm 70$  years B.P. at Pymore. Waller mentions that this corresponds more closely to Godwin and Clifford's (1938) chronology, from archaeological evidence, than to that of Shennan (1986a), who suggests that fen clay deposition finished in this region at *c.*4,500 radiocarbon years before present Waller's (1988) dates and stratigraphic evidence from Farcet in the March - Chatteris - Ramsey - Whittlesey basin suggest that the marine deposits of this region may be equivalent to those at Bourne Fen (Shennan, 1986b), as suggested by Shennan (1986a). From work in East Fen in Lincolnshire and further south along the Wisbech bypass, Waller suggests that the marine phase which deposited the upper silts occurred at an earlier date in Lincolnshire than to the south, accounting for the differences in age ascribed to this phase between Godwin's chronology and that of Shennan (1986a).

Results of the Fenland Project suggest that in Roman times settlement was possible for the first time on a marine silt that had been deposited during the Iron Age (Hall, 1988). The date of commencement of this drier phase is not certain, however. Hallam (1970) pointed out that silting of drainage channels occurred from 200 A.D. onwards, but suggested that a small transgression also occurred in the third and fourth centuries. Potter (1981) attributed the flooding to freshwater rather than a marine incursion. Studies of salterns (Smith, 1970) suggest a transgressive period from around 1,550 to 1,150 years B.P. (Shennan, 1986a). It has been proposed that this was due to a lack of maintenance of Roman sea defences after the Romans had left the area (Salway, 1970). Subsequent to this, changes in the extent of the coastline were substantially affected by land reclamation works and periods of positive or negative sea-level tendency are difficult to separate from man's influence (Shennan, 1986a).

The different ideas concerning former sea-level tendencies in the Fenland, the major representatives of which have been described above, reflect the considerable differences in opinion as to the former coastal geography of the Wash Fenland area. The situation is

complicated by the fact that the present coastline is artificial as man has built sea defences to protect the Fenland from flooding. Therefore, no equivalent environments to those in which the intercalated clays, silts, sands and peats of the Fenland were deposited currently exist in the area. Shennan (1986b) mentions that there is a need to produce a model of the palaeogeographic environments in which fine particles of marine origin can become intercalated with organic deposits of terrestrial origin, thus combining the horizontal and vertical movements of the coastline. Three main hypotheses have been proposed in the literature and these are discussed below.

Shennan (1986b) has divided the models of coastal sequences into those proposing a static barrier across the Wash, those favouring a migrating barrier or barrier islands, or the alternative of an open coast. The hypothesis of a static barrier across the Wash was suggested by Swinnerton (1931), who proposed that some linear sand and gravel ridges currently found offshore to the north of the Wash are the eroded remnants of a barrier which formerly extended across the mouth of the Wash and northwards offshore from Lincolnshire. However, Robinson (1968) and Jeffrey (personal communication, 1989) have illustrated that the sand ridges are constantly being moved by tidal currents. By contrast, Eisma *et al.* (1979) and Jeffrey (personal communication, 1989) believe that the morainic ridges are relict features, which are undergoing little alteration at present. The advantage of the hypothesis was that it explained the formerly sheltered environment in which deposition occurred and the current eroding nature of the Lincolnshire coastline.

A modified version of Swinnerton's (1931) static barrier hypothesis was proposed by Godwin (1978). He claimed that the initial Flandrian rise of sea-level would have encountered a barrier of glacial drift, such as that related to the Hunstanton boulder clay, across the mouth of the Wash. Godwin suggested that, when this barrier was breached, the fen clay was deposited in a lagoonal environment behind it. Deposition of the fen clay in a lagoonal environment has, however, been questioned by Shennan (1986b) from evidence at Adventurer's Land. Further, there is no evidence that a continuous barrier of morainic material has ever existed across the mouth of the Wash. Godwin (1940) admits that no barrier has

been identified in relation to the fen clay formation.

A second hypothesis is that of a migrating barrier, moving progressively shorewards with a rise of sea-level. Such barriers have been identified in many areas, such as the south coast of the U.S.A. in the Gulf of Mexico (*e.g.* Leatherman, 1987) and the Netherlands coast (Jelgersma, 1966, 1979; Hageman, 1969). Similar features are found on the north Norfolk coast, although these, such as Scott Head Island and Blakeney Point, are largely the result of longshore drift. No irrefutable evidence of such barrier islands has been found, though. Evans and Mostyn (1979), from exploratory exposures made for a gas pipeline, describe sands with ripple marks which they ascribe to former sand bars. However, no further analysis of the sediments has been made.

A further point of interest concerning the barrier hypotheses is that of the tidal regime in which they would exist, as pointed out by Shennan (1986b). Barrier islands have been shown to be best developed in microtidal regimes (Hayes, 1975), with tidal ranges of 0 to 2 metres (Davies, 1964), and are not generally found in macrotidal regions (with a tidal range of over four metres), such as that of the Wash at the present day. The plausibility of this hypothesis can, therefore, be assessed in part with regard to the results shown in the current study.

The third hypothesis proposes an open coast with no more than local intertidal barriers (Shennan, 1980, 1981, 1986b). It is suggested that a low gradient shoreline would have existed from the Pre-Flandrian surface, giving low energy depositional environments with large intertidal flats. This concurs with the majority of evidence of deposits in the Fenland which were laid down in low energy conditions. The three hypotheses outlined above are considered further with the construction of palaeogeographic maps from stratigraphic evidence in Chapter 4.

Most Holocene sediments in the North Sea are derived from sediments already present in the area at the end of the Pleistocene period (Jelgersma, 1979; Johnson *et al.*, 1972) and there is little current input from fluvial sources (Wilmot and Collins, 1981; Veenstra, 1971).

By and large, the Holocene in this area has been characterised by reworking of Quaternary deposits. Sedimentation has occurred in some areas of the North Sea, such as on top of the Dogger Bank, where an additional fifteen metres of sediments have accumulated (Eisma *et al.*, 1979; Eisma, 1981). Scouring of the Outer Silver Pit immediately to the south-west of the Dogger Bank has also occurred (Jeffrey, personal communication, 1989). Other than this, some sediment has accumulated in the “deeps” in the northern part of the North Sea. Strong tidal currents in the south-western part of the North Sea have led to the development of linear sand ridges, parallel to current directions, and sand can be observed in motion on these ridges (Lees, 1980, 1981).

In a study of the Wash, Gallois (1979) found a basal peat overlying till and covered by sand in the intertidal zones. Wingfield *et al.* (1978) and Balson (personal communication, 1989) show that the present-day sediments of the Wash consist of gravels in the central and outer part of the estuary, derived from glacial tills, with increasingly finer material found shorewards onto the tidal flats. To the north of the Wash, off the Lincolnshire coast, de Serra (1799) reported inter-tidal islands of peat and clay, which are no longer present. Shennan (1986b) suggested that these may have been a seaward extension of the basal peat layer found by Swinnerton (1931).

### **2.3.2. Morecambe Bay**

Stratigraphic observations relevant to the Holocene history of Morecambe Bay have been reported from the late nineteenth century onwards (*e.g.* Kendall, 1900). The first major work dealing with sea-level changes in north-west England was, however, that of Gresswell (1953, 1957, 1958), who was primarily concerned with the search for raised beaches, which he identified geomorphologically as “areas of very flat ground” (Gresswell, 1958, p.80), comprising “an unconsolidated deposit (whether it be of shingle, sand, silt or clay, or heterogeneous) that has been laid down as the result of marine action on the open coast or in estuaries”.

Gresswell (1958) levelled much of the Greenodd and Kent estuaries and surrounding areas, where he found fine clayey silts in the upper parts of his boreholes, with coarser, fine



sandy silt at lower levels. He discovered that the average altitude of the 126 boreholes which he made was 15.25 feet (approximately 3.7 metres) above O.D., with a maximum variation of two feet (or 0.6 metre) on either side of this. Gresswell concluded that the "accordance of the levels in the different estuaries, which are entirely cut off from one another excepting by sea, appears to show conclusively that the deposits are of one origin, that is, that they are estuarine and cannot be of lake origin with ice dams at the estuary mouths" (Gresswell, 1958, p.88).

No techniques were used by Gresswell to determine under what conditions the silts and sands which he found had been deposited. Higher up the estuaries, peat layers were found in boreholes. Pollen analyses were carried out on peat layers from borings in the Duddon estuary, just west of Morecambe Bay, and peats found in borings in the Greenodd estuary. From the pollen found in the peat layers, Gresswell (1958) concluded that a transgressive period had occurred in Morecambe Bay between the deposition of the two peat layers.

Oldfield and Smith carried on the work around Morecambe Bay. Their interests were mainly in the post-glacial vegetational changes which had occurred (*e.g.* Oldfield, 1960a, 1963; Smith, 1959), but pollen spectra were also used to suggest dates of transgressive and regressive overlaps where sequences of clays intercalated with peats were found. Organic deposits of Ellerside Moss, in the Leven estuary (Oldfield and Statham, 1963), overlying the clay - silt transgression of around 3,800 B.C. (Gresswell, 1958) include the elm decline period, which has been dated between 5,435 to 4,810 radiocarbon years before present in the north-eastern part of Morecambe Bay (Smith *et al.*, 1971). Oldfield (1960b) also found evidence of a marine transgression in Silverdale Moss in the north-eastern part of Morecambe Bay from the same time. Smith (1959) dated a regressive overlap on Helsington Moss, north of the Kent estuary, to  $5,277 \pm 120$  years B.P. at +4.88 metres O.D. Oldfield (1963) suggested that pollen evidence of marked elm declines and "Landnam" ("land-taking") phases around Morecambe Bay indicates early Neolithic forest clearances by man. Tooley (1987) mentions that clearances over 600 or so years would result in soil erosion and an increased sediment supply to Morecambe Bay. He implies that the apparent relative fall of sea-level might be

partly due to major sediment input to the Bay.

The most recent work carried out concerning sea-level changes around Morecambe Bay is that by Tooley (*e.g.* Tooley, 1974, 1978, 1980, 1987). Tooley (1978) has summarised present knowledge of sea-level changes in Morecambe Bay (see Fig. 2.5). Tooley (1987) concurs with Oldfield (1963) to associate the end of marine sedimentation in Morecambe Bay with the elm decline around 5,000 years B.P., as mentioned above. He draws together evidence from around the Bay to suggest, as did Oldfield (1963) that there was a significant change in the shape of Morecambe Bay at this time as the sea did not progress as far up the estuaries and colonisation of former tidal flats occurred.

Tooley (1987) also reports more recent data concerning relative sea-level movements. At Arnside Moss, in the north-eastern part of Morecambe Bay, a saltmarsh soil overlies a peat at +5.7 metres O.D., dated to  $1,545 \pm 35$  years B.P., while further south, at Heysham Moss, a clayey silt was found overlaid by peat, dated at  $4,190 \pm 150$  years B.P. In addition, Tooley (unpublished) has recorded four periods of transgressive and regressive overlap from Skelwith Pool, by the eastern part of the Leven estuary, between about +2.7 and about +5.9 metres O.D.

Buried and intertidal peat beds have been recorded in the offshore part of the Bay between  $-17.6$  and  $-11.1$  metres O.D. (Knight, 1977), dating from  $9,270 \pm 200$  years B.P. to  $7,995 \pm 80$  years B.P., respectively. From their pollen assemblages, these organic deposits suggest that peat growth occurred as a result of the ponding back of water consequent upon a relative sea-level rise (Huddart *et al.*, 1977; Tooley, 1980). In many cases, there is a change to brackish water conditions in the peats, followed by minerogenic intertidal deposits.

Offshore the basal peat layer is very thin and not present in all boreholes. Above this, lying directly on the till where the peat is absent, is a clayey layer, between 5 and 45 metres thick, covered by silty sands with shells up to the present surface. These, together with the peats found in Heysham Harbour by Soil Mechanics Limited in 1967, at the site of the nuclear power station, and the cross-section of Heysham Harbour by Reade (1902) and the sections

from Barrow Harbour, described by Kendall (1900) in 1880, are the only offshore records from the Bay. The three boreholes by Soil Mechanics Limited show a sequence similar to that obtained for the barrage survey (Knight, 1977). A peat layer up to about a metre thick overlies clayey gravel and sand. Above the peat is a five metre thick sequence of clay on top of which sand with shells is found. Reade's cross-section is almost identical to this. In Barrow Harbour, Kendall (1900) found a silty clay overlying the peat.

Wingfield (personal communication, 1989) has shown, from a seismic profile, that Holocene sediments have accumulated in the Lune Deep, just west of the southern part of Morecambe Bay. Other "deeps" in the Irish Sea, particularly those off Dublin, Eire, have also seen accumulation of deposits during the Holocene (Whittington, 1977; Dobson, 1977b), but otherwise redistribution of sediments from the last glacial stage is all that has occurred on the floor of the Irish Sea during the Holocene.

In general, the radiocarbon dates from the offshore peats in Morecambe Bay (Knight, 1977) show younger ages at higher altitudes. A rapid rise of relative sea-level is suggested around 8,000 to 7,000 years B.P. as an onshore peat layer at Rusland Valley, north of the Leven estuary, gives a date of  $7,750 \pm 100$  years B.P. at  $-0.3$  metres O.D. (Tooley, 1987). Dickinson (1973) found a marine clay in this area at  $-0.75$  to  $+1.35$  metres O.D., deposited between about 7,000 and 8,000 years B.P. (Hibbert *et al.*, 1971). Tooley (1978, 1987) relates this to possible neotectonic movement associated with isostatic movements in Morecambe Bay. Isostatic movement would be expected to be greater nearer the former centre of ice accumulation to the north of Morecambe Bay. However, Tooley (1978) points out that the gradients on the, now buried, beaches were reversed in Morecambe Bay between 7,000 to 8,000 years B.P., dipping towards the former centre of ice loading at 11.9 metres per 100 kilometres, before assuming the expected southward dip north of Morecambe Bay at 11.7 metres per 100 kilometres.

Flemming (1982) analysed the radiocarbon-dated sea-level index points from the Morecambe Bay area and concluded that relative subsidence is characteristic of the area, but that

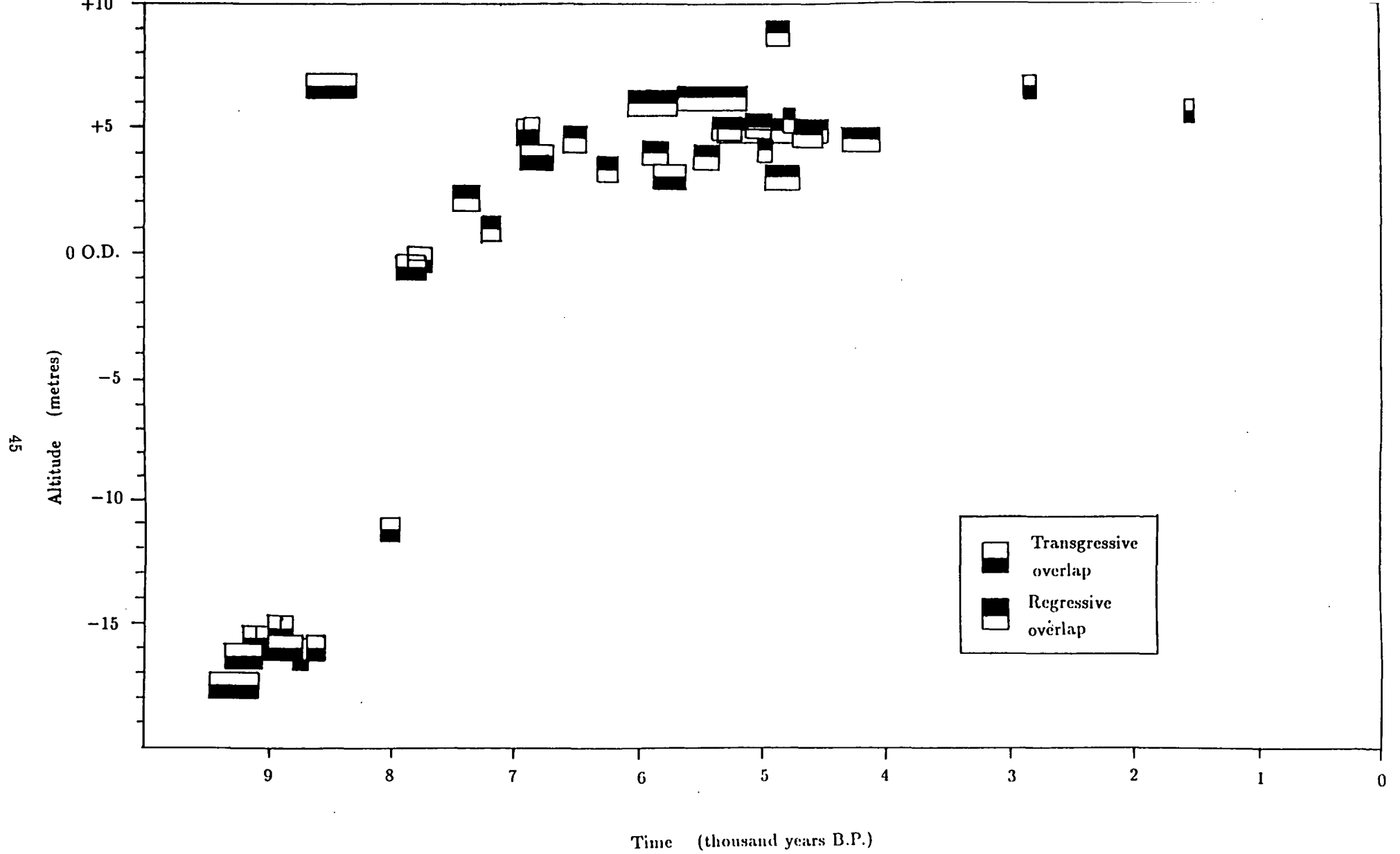


Figure 2.5. A time-altitude graph using data from Morecambe Bay and surrounding areas (after Tooley, 1987).

the subsidence was more rapid during the eighth to ninth millenium of radiocarbon years before present. This work was continued by Shennan (1987, 1989). Shennan (1987), working with data from north-west England, calculated a zero land uplift rate for the past 5,000 or 6,000 radiocarbon years with an exponential decrease before that. Compared with an exponential curve for isostatic uplift, the sea-level index point for 8,000 years B.P. in the dataset appears as a 6 metre residual. Shennan (1987) suggests that this can be partly explained by sediment consolidation and by using a sea-level band drawn through the error boxes of the data points. In his 1989 paper, Shennan recognises a clear distinction between the onshore and intertidal index points. The onshore points show an exponential decline in uplift which is approximately linear for the last 6,000 years ( $0.35 \pm 0.12$  millimetres *per annum*). He comments that the large error bands that may arise for the older intertidal index points are insufficient to reconcile these data with the onshore data and proposes that differential crustal movements are a possible explanation together with changes in palaeo-tidal range.

### **2.3.3. Comparison of the development of the Fenland and Morecambe Bay during the Holocene**

The extensive low-lying nature of the Fenland has attracted many research workers interested in ecological (particularly vegetation) and sea-level changes. Morecambe Bay, by contrast, is surrounded by a smaller area of lowland, despite the fact that half of its area dries out at low tide. Much more research has been carried out concerning the development of the Fenland during the Holocene than is the case for Morecambe Bay. In addition to research interests, the use of the Fenland as high grade farmland has led to a need to build roads and lay pipelines across the area, involving stratigraphic investigations (*e.g.* Monk, 1976; Evans and Mostyn, 1979). The greater relief around Morecambe Bay has meant that such investigations have been far fewer on the low-lying Holocene sediments here, which, including the estuary area, cover a far smaller area of land (*c.*600 km<sup>2</sup>) than in the Fenland (*c.*6,000 km<sup>2</sup>).

In addition to the far greater volume of work carried out in the Fenland, initially by

nineteenth century workers such as Skertchly (1877), followed by the Fenland Research Committee in the 1930s and carried on most recently by the Fenland Project, the spatial spread of stratigraphic investigations is also far better in the Fenland. In Morecambe Bay, most Holocene stratigraphic work has been carried out around the estuaries of the Kent and the Leven in the northern part of the Bay. Some work has also been carried out on the eastern and southern sides of the Bay, for example at Heysham and Pilling Moss, but the number of these investigations is far fewer than in the northern area. Much of the area of the Fenland, by contrast, has been covered in terms of its Holocene stratigraphy.

The accounts above illustrate that both the former and the current geographies of the two field areas are quite different. The Wash is, essentially, an open embayment from the North Sea and the evidence presented above suggests that it has taken on similar shapes, although sometimes of much greater extent, throughout the Holocene. Morecambe Bay, however, is an embayment with large river valleys entering it from surrounding areas of high relief, of the order of 100 metres, compared with the gently sloping land around the Fenland of *c.*25 metres. At various times during the Holocene, when relative sea-levels have risen, the river valleys have been flooded, rather than a larger bay area being opened up as in the case of later Holocene transgressions in The Wash. This is due to the geology of Morecambe Bay compared with The Wash; the former is surrounded by much higher land than the latter.

Work on isostatic movement (Shennan, 1987, 1989) has shown that whereas Morecambe Bay underwent uplift until *c.*6,000 years B.P. and has since been relatively stable, the Fenland, located further from former centres of ice accumulation, has undergone slight subsidence during the Holocene. However, Shennan *et al.* (1983) showed (Fig. 2.6) that between *c.*2,500 and 6,800 years B.P. there were a number of transgressive and regressive sea-level tendencies which coincide between the Fenland and north-west England (the latter of which includes an area beyond the extent of Morecambe Bay).

The record of sea-level changes goes back much further in Morecambe Bay than in the Fenland as the sea did not reach the Fenland until about 7,000 years B.P., whereas there is

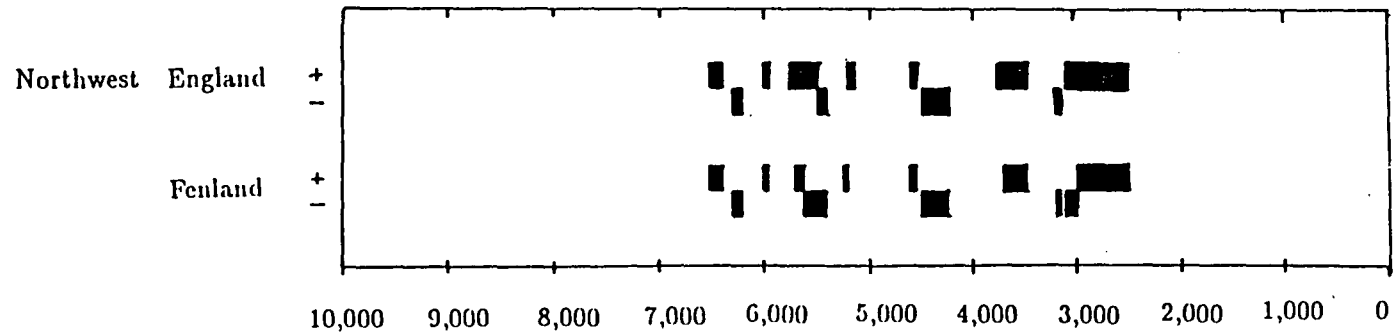


Figure 2.6. Chronologies of tendencies of sea-level movement from north-west England and the Fenland for tendencies of more than local significance (after Shennan *et al.*, 1983). The black bars represent periods for which a positive (+) or negative (-) tendency of sea-level change was in phase in both north-west England and the Fenland.

evidence of a transgression and then regression in Morecambe Bay before 8,000 years B.P. The major part of the dated records from Morecambe Bay relate to the time prior to 5,000 years B.P., while those for the Fenland are mostly between 5,500 and 2,500 years B.P. In addition, a far greater number of dated stratigraphic records are available for the Fenland. The dates used in this study to reconstruct the palaeogeographies of the Fenland and Morecambe Bay during the Holocene in Chapter 4 are given in Appendix 4.2. Reconstructions of the palaeogeography of the field areas in this study are limited to current sea depths modified by allowances for isostatic movement and sea-level altitude data obtained from sea-level curves in the surrounding areas. Further details are given in Chapter 4.



## CHAPTER 3

### TIDAL THEORY AND TIDAL MODELS

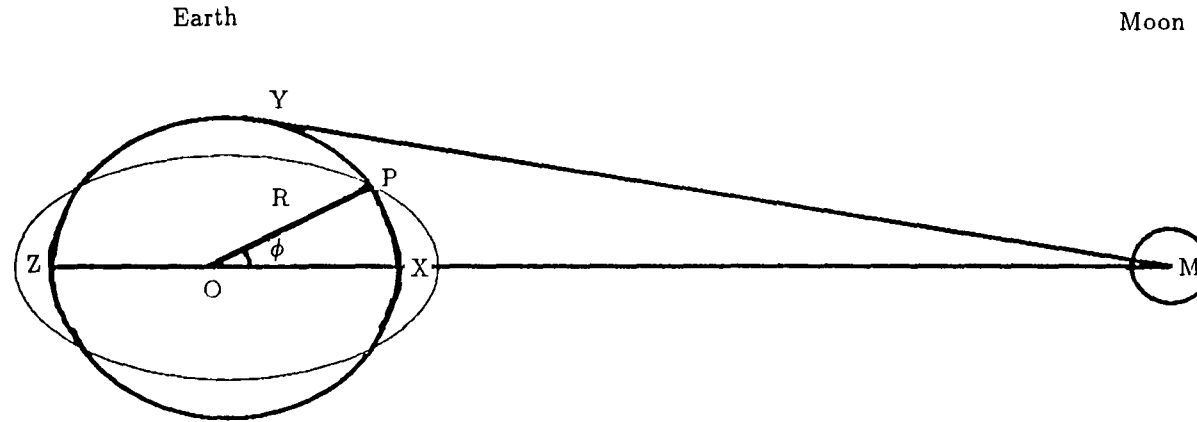
In this chapter an outline of tidal theory is given. Tidal theory is developed in the context of the present study to illustrate the factors important to tidal movements on the continental shelf and at the estuary scale. The ways in which changes to the tide may occur at different sea-levels are discussed, although they are not all identified in the present study. The last section of this chapter is devoted to an explanation of methods of modelling tidal movement and their relative advantages and disadvantages. The approach used in this study is examined briefly, but will be explained in greater detail in Chapter 5.

#### 3.1. Tidal theory

##### 3.1.1. Tidal generation.

A number of theories as to the motion of tides, or periodic movements of the sea, have been proposed. These were initially based on superstition (Pugh, 1987) rather than scientific fact. Sir Isaac Newton made a major advance in the understanding of the generation of tides. He applied the theory of gravitational attraction to illustrate the tidal response of a hypothetical completely water-covered earth. The resulting theoretical equilibrium tide could be explained by the fact that two bodies attract each other with a force proportional to the product of their masses and inversely proportional to the square of the distance between them. The equilibrium tide is the elevation of the sea surface that would be in equilibrium with the tidal forces if the earth were covered with water to such a depth that the response is instantaneous (Pugh, 1987). The equilibrium tide

Figure 3.1. Diagram to Show the Positions in the Earth - Moon System which are used to Derive the Tidal Forces (after Pugh, 1987). Not to scale.



Letters are referred to in text  
R Radius of the earth  
P,X,Y,Z Points on the earth's surface  
 $\phi$  Angle of latitude  
O Centre of the earth  
M Centre of the moon

accounts for the broad features of the observed tides, which are complicated, in detail, by the presence of land masses and non-uniform bathymetry of the oceans. Its importance lies in its use as a reference to which the observed phases and amplitudes of the harmonic constituents (discussed in Chapter 3.1.6.1) can be related. It also indicates the important harmonic constituents to be included in a correct tidal analysis model (Pugh, 1987).

Laplace formulated the equations of tidal movement on a rotating earth from the theoretical solution explained by Newton (Pugh, 1987). Laplace's equations have provided the basis of understanding tidal movement as a response to periodic forces. From the periodicities of the tidal forces, Lord Kelvin developed the first method of harmonic analysis of tides. He showed that the tidal forces could be analysed into astronomical components, each with its own frequency, related to the periodicities of movements of different heavenly bodies. The procedure involved is explained in more detail later in this Chapter.

The tide-generating force at a point X on the earth is defined as the difference in attractive force of the heavenly bodies (mainly the moon) experienced at X and that experienced at the centre of the earth (Doodson and Warburg, 1941). Considering only the influence of the moon, from Newton's Second Law of Motion, the force towards the moon at X is (Pugh, 1987)

$$\frac{gm_e m_l}{(R_l - R)^2} \quad (3.1)$$

(see Fig. 3.1), where  $g$  is the gravitational constant ( $6.67 \times 10^{-11} \text{ Nm}^2 \text{ kg}^{-2}$ ),  $m_e$  is the mass of the earth ( $5.97 \times 10^{24} \text{ kg}$ ),  $m_l$  is the mass of the moon ( $7.35 \times 10^{22} \text{ kg}$ ),  $R_l$  is the distance from the centre of the earth to the centre of the moon (384,400km) and  $R$  is the equatorial radius of the earth (6,378km). The force necessary to keep the earth in its orbit in relation to the moon is the same as for a particle at O (the centre of the earth):

$$\frac{gm_e m_l}{R_l^2} \quad (3.2)$$

where  $g$ ,  $m_e$ ,  $m_l$  and  $R_l$  are as defined in equation 3.1. The tide-generating force at X is the difference between these two forces:

$$gm_em_l \left[ \frac{1}{(R_l - R)^2} - \frac{1}{R_l^2} \right] = \frac{gm_em_l}{R_l^2} \left[ \frac{1}{\left(1 - \frac{R}{R_l}\right)^2} - 1 \right] \quad (3.3)$$

with  $R \approx 6,378$  kilometres and  $R_l \approx 384,400$  kilometres,

$$\frac{R}{R_l} \approx \frac{1}{60} \text{ so } \left( \frac{R}{R_l} \right)^2 \ll 1 \quad (3.4)$$

and

$$\left[ \frac{1}{\left(1 - \frac{R}{R_l}\right)^2} - 1 \right] \approx 1 + 2 \left( \frac{R}{R_l} \right) \text{ for small } \left( \frac{R}{R_l} \right) \quad (3.5)$$

Therefore the net force towards the moon is of magnitude

$$\frac{2gm_em_l R}{R_l^3} \quad (3.6)$$

at X directed along XM. Similar calculations at Z show that the gravitational attraction is too weak here to exert an influence and there is a net force away from the moon of the same magnitude. The net force at Y is towards the centre of the earth and is of magnitude

$$\frac{gm_em_l R}{R_l^3} \quad (3.7)$$

The fine line on the diagram (Fig. 3.1) illustrates the resulting shape of the ocean surface for the equilibrium tide. The solid earth rotates within the equilibrium ellipsoid. The tide is generated by the differences between the gravitational attractive forces on the earth's surface and the position of the earth's surface. The tide-generating effect of other heavenly bodies may be developed in a similar way, although their greater distance from the earth considerably reduces their tide-generating effects compared with that of

the moon. The influence of the sun is next in importance, although its effect is only 0.46 times that of the moon.

The amplitudes of the equilibrium tide are small. At the equator, amplitudes reach a maximum of *circa* 0.88 feet (0.267 metres) for the lunar semi-diurnal tide (Doodson and Warburg, 1941). Observed tides are generally much larger than the equilibrium tide because of the presence of land masses and variations in the bathymetry of the seas, but their oscillations occur at the same frequencies as those of the equilibrium tide.

Variations associated with the precession of the equinoxes, obliquity of the ecliptic and eccentricity of the orbit of astronomical bodies and the degree to which these are in or out of phase with each other affect the strength of the tide-generating force at any given location at any given time. The precession of the equinoxes is the cycle of movement of equal length of nights and days during the year, when the sun crosses the equator. These are currently in March and September, but vary in timing throughout the year on a 26,000 year cycle. The variation is caused by movement of the position of the earth's equator relative to the stellar background, so affecting the timing of maximum tide-generating potential. The variation of the plane of the earth's revolution around the sun is from  $23^{\circ}27'$  north to  $23^{\circ}27'$  south of the equator each year. This is known as the obliquity of the ecliptic and affects the location of maximum tide-generating potential. Finally, astronomical bodies orbit around each other in elliptical, rather than circular, paths, as shown by Newton and Kepler (Pugh, 1987). This means that the degree of proximity of one body to another, and hence the tide-generating potential, varies in magnitude with time. The most extreme tidal forces occur when the moon, sun and earth are in line and at their closest respective distances.

Maximum tidal amplitudes generally occur a few days after the astronomical maximum tide-producing force. This lag is due to the inability of the tidal wave on earth to keep up the speed of progression around the earth required by the astronomical forces, due to varying water depths. The time lag is less in the southern hemisphere, where there

are fewer land masses and the water is deep enough to allow a faster speed of progression of the tidal wave, the speed of which is given by

$$c = (gh)^{\frac{1}{2}} \quad (3.8)$$

where  $c$  is the speed of progression of the tidal wave (in metres per second),  $g$  is the gravitational constant and  $h$  is the water depth in metres.

In the wide and deep ocean basins, observed tides are generated by external gravitational forces, whereas in shelf seas, tides are driven by co-oscillation with the oceanic tides. Energy from the oceans is dissipated on continental shelves by bottom friction.

### 3.1.2. Shallow water effects

Three factors contribute to distort the tidal wave in shallow water on continental shelves and in estuaries (Pugh, 1987):

- (a) the amplitude of the tidal wave is a significant proportion of the total water depth in these areas
- (b) the stronger currents which develop in shallow water are resisted by drag due to bottom friction. This eventually removes much of the propagating energy and reduces amplitudes.
- (c) varying widths and depths cause complicated tidal patterns to develop with curvature of flow.

Components of the tidal wave may be written in terms of harmonic constituents, as is explained below. The main tide-generating forces in the oceans are the lunar and solar semi-diurnal (twice-daily) and diurnal (daily) constituents. The non-linear distortions to the tidal wave in shallow water may be expressed in terms of harmonic constituents which have angular frequencies that are multiples, sums or differences of the main diurnal and semi-diurnal tidal constituents. Higher harmonic constituents, which have at least two tidal cycles per day, are more generally of greater importance than low frequency compo-

nents, such as  $2MS_2$  which represents the difference  $S_2 - M_2$  and has a semi-diurnal period. The phase of the higher harmonics relative to the basic tidal wave constituents controls the shape of the tidal curve. The relative importance of higher harmonic constituents is greater near amphidromic systems of the semi-diurnal and diurnal tidal constituents, for example, around Southampton, Hampshire, where double high waters occur.

Bottom friction opposes flow and removes energy from the motion of the tidal wave, reducing its amplitude. Drag and current speeds have been shown to be related (Pugh, 1987) by:-

$$\tau_b = -C_D \rho \mathbf{q} |\mathbf{q}| \quad (3.9)$$

where  $\tau_b$  is the bottom stress,  $C_D$  is a dimensionless drag coefficient,  $\rho$  is the water density and  $\mathbf{q}$  is the current vector.

The value of  $C_D$  depends on the level above the sea bed at which the current is measured. For measurements at one metre above the sea bed,  $C_D$  is generally between 0.0015 and 0.0025. Taylor (1919) reported an average value of 0.0024 for the Irish Sea.

Higher harmonics are associated with the asymmetry of the tidal wave, which may be generated in shallow water. In general, wave speed ( $c$ ) is related to depth by the formula given in Eqn. 3.9, but where wave amplitude is comparable with total depth,

$$c = [g(h + \frac{3}{2}\zeta)]^{\frac{1}{2}} \quad (3.10)$$

where  $g$  is the gravitational constant,  $h$  is the water depth in metres and  $\zeta$  is the displacement of the water level from its mean value in metres, is a more accurate representation. This suggests that waves become asymmetrical in shallower waters.

Variations of bottom topography and coastal configuration affect tidal movements. Tidal currents tend to follow the contours of the coast (Pugh, 1987). Sea-levels are slightly

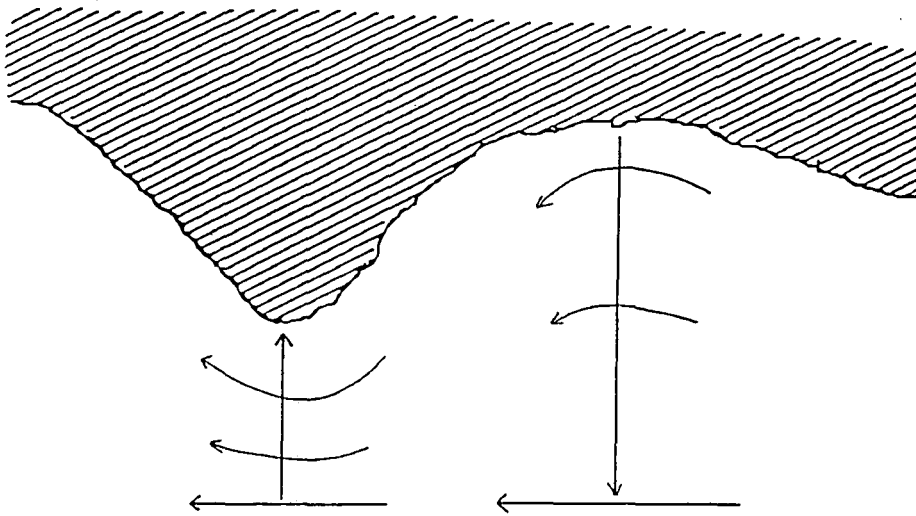


Figure 3.2. The Curvature of Streamlines for Tidal Flows near a Coast (after Pugh, 1987). The surface gradients which produce the curvature are represented by the arrows perpendicular to the coast which point down the slope. The situation is reversed half a tidal cycle later, but the surface gradients do not change direction.



lowered at headlands and raised in bays as a consequence when currents are strong (see Fig. 3.2), although this effect does not occur at slack water. The relative depression of sea-level twice in the tidal cycle (during both flood and ebb) leads to the apparent development of higher harmonic constituents near headlands.

Shallow water effects are important in a palaeotidal context as lower sea-levels at former times increased the extent of shallow water area over the north-west European continental shelf. This was especially the case in embayments and the Wash Fenlands area in particular was covered by a shallow water sea in the mid-Holocene.

### 3.1.3. Resonance

Tides undergo reflection at sudden changes of depth, such as the continental shelf edge and coastal boundaries. The combination of reflected and incident waves can produce a pattern of standing waves, which have alternate nodes of zero amplitude and antinodes of maximum amplitude, separated by a distance of  $\frac{\lambda}{4}$ , where  $\lambda$  is the wavelength of the progressive wave. For example, large amplitudes would be produced at the head of bays with lengths which correspond to a quarter of the tidal wavelength, *viz.*

$$\frac{4L}{(gh)^{\frac{1}{2}}} \quad (3.11)$$

where  $L$  is the distance from the sea to the head of the bay in kilometres,  $g$  is the gravitational constant and  $h$  is the water depth. For the  $M_2$  tide, quarter wave resonance would occur in a basin of 250 kilometres length and 50 metres water depth (Pugh, 1987). No energy is transmitted by standing waves, since they consist of two progressive waves of equal amplitude travelling in opposite directions.

Resonance effects may be important in a palaeotidal context. This has been shown to be the case in the Bay of Fundy (Scott and Greenberg, 1983). Scott and Greenberg (1983) traced the increase in tidal range in the Bay of Fundy during the Holocene as related, at least partly, to the change in shape and water depth in the Bay which has led to the

formation of standing waves, increasing tidal heights reached by resonance effects.

#### **3.1.4. Kelvin waves**

Kelvin waves are long-waves influenced by the earth's rotation. Tides on continental shelves may be regarded as Kelvin waves. Kelvin waves are discussed here as changes to the tidal wave on the continental shelf at different sea-levels are of direct relevance to the present study.

The rotation of the earth causes a deflection of currents towards the right in the northern hemisphere. Obstruction of such currents by a coastline results in changes in water level. This build-up of water gives rise to a pressure gradient across the path of wave movement. At equilibrium, this balances the Coriolis force due to water particle motion. A combination of Kelvin waves travelling in opposite directions results in the tidal wave rotating about a nodal point, called an amphidrome, instead of oscillating at a nodal line at a quarter of a wavelength from the head of the basin. If the reflected Kelvin wave is weaker than the ingoing Kelvin wave, the amphidrome is displaced from the centre of the channel to the left of the direction of the in-going tidal wave in the northern hemisphere. The strength of Kelvin waves may vary with changes of sea-level (Franken, 1987). Franken (1987) found, from a tidal model of the continental shelf with reductions of current sea depths, that a lower water depth gives lower propagating speeds of Kelvin waves and, by increasing friction, decreases the amplitude of Kelvin waves. With water depths below 30 metres in the southern North Sea, he found that tidal penetration (and therefore tidal amplitudes) were considerably reduced due to a large amount of energy dissipation.

#### **3.1.5. Residual flow**

In addition to the tidal movements related to movements of particular heavenly bodies, there are mean and residual currents. Residual movements may be driven by density gradients, wind stress or tidal motions. The speed of such currents is typically a few orders of magnitude less than tidal currents. Residual currents are important, though, because their persistence may allow them to dominate the distribution and movement of

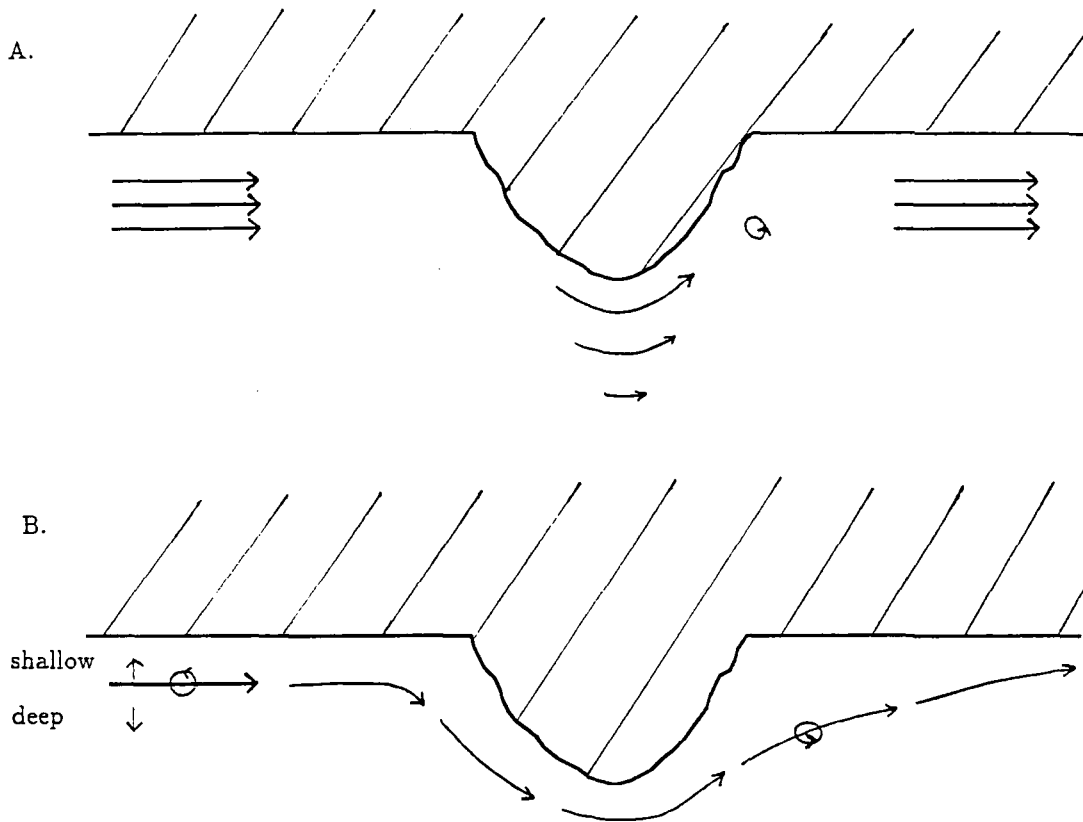
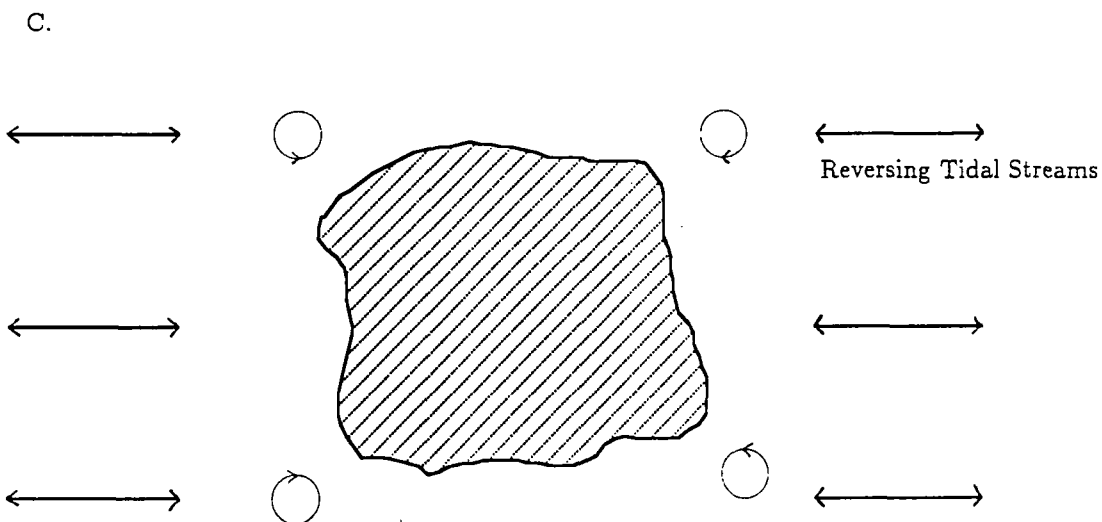


Figure 3.3. Eddies Produced by Headlands and Islands which impede tidal currents.

A. Residual eddy generated when the streamline 'overshoots' the headland (after Robinson, 1983).

B. Residual eddy generated by a headland, as a result of the torque induced by greater bottom friction inshore than offshore (after Robinson, 1983).

C. The pattern of four eddies generated by an island in a tidal stream (after Pugh, 1987).



water salinity levels and temperatures and affect the transport of sediment and pollutants (Robinson, 1983). Higher tidal harmonics accompany the generation of residual flows (Mardell and Pingree, 1981).

Mean currents are generated by the interaction of tidal currents with coastal features and bottom topography and are, therefore, very important in estuaries. Headland eddies have often been observed and they have been studied in some detail by Pingree and Maddock (1977a,b; 1979a), Pingree (1978) and Maddock and Pingree (1978). Bottom friction is more important in the shallower water near the coast than in deeper water further offshore. The difference in influence of bottom friction across the flow produces vorticity within the flow, which is equal and opposite when the flow reverses. At headlands, the tidal stream does not follow the coastline closely downstream from the headland, resulting in positive vorticity being carried offshore in this area, with negative vorticity on the upstream side (Figure 3.3a). This is not balanced completely by the return flow unless the headland is symmetrical.

An alternative explanation to the generation of headland eddies which explains the production of residual vorticity when the streamline pattern around the headland is almost the same for both tidal stream directions (Robinson, 1983). Bottom friction may be considered proportional to the second power of the tidal velocity, in which case, where a current shear occurs, the bottom friction exerts a net torque on the sea (Robinson, 1983). Thus, even in a case of constant water depth, the bottom friction resulting from increased velocities inshore around the headland would exert a torque to produce vorticity in the flow leaving the headland. Positive vorticity is carried to the east and negative vorticity to the west of the headland (Figure 3.3b). By this mechanism, the vorticity is generated only at the headland and so cannot be cancelled on the return flow, so two residual gyres remain. This explanation does not require flow separation at a headland creating eddies by the principle of continuity which requires a return flow or by tidal asymmetry and therefore has a more general application. However, once residual vorticity is present, tidal asymmetry is a consequence and vorticity is also produced within the flow where there

is sloping bottom topography. Four residual eddies (shown in Figure 3.3c) are generated as both mechanisms act as local vorticity sources around islands (Pingree and Maddock, 1979b).

Huthnance (1973) developed a two-dimensional representation of tidal currents which flow obliquely to sand bars which can account for the mean clockwise residual circulation around the parallel sand bars off the Norfolk coast. Provided there is a component of flow across (normal to) the linear sand bars, the flow is constricted vertically and the conservation of potential vorticity gives anticyclonic vorticity. This pattern is reversed as the flow moves into deeper water to the lee of the sand bars and cyclonic vorticity is created. The net effect over a tidal cycle is for negative vorticity over the shallow area and positive vorticity (Figure 3.4a) in the surrounding deep water. The resulting current pattern has residual flows parallel to the sand bars.

Bottom friction also generates vorticity as the stream is greater in shallower water than deeper water. Cyclonic vorticity is produced as the stream moves on to the sand bar and anticyclonic vorticity as the stream moves off it. This vorticity is advected with the stream flow so that cyclonic vorticity is found on the sand bar and anticyclonic in the surrounding deeper water. Thus with a tidal flow in one direction the effects of flow constriction and bottom friction oppose each other, whilst in the other direction they are reinforced (Figure 3.4b and c). The case where they are reinforced is the most common with parallel sand banks, such as those off the Norfolk coast (Robinson, 1983). In such cases the residual circulation appears to be reinforcing and is strengthened, although the sediment transport processes involved (beyond the scope of this thesis) have not yet been widely explored.

Friction effects may change at different sea-levels and with different palaeogeographies (*e.g.* due to an increase or decrease in shallow water areas), so giving alterations in residual flow. Sea-level changes may also alter residual flow patterns as the strength of the tidal current will be affected by both water depth and constriction (either laterally or vertically)

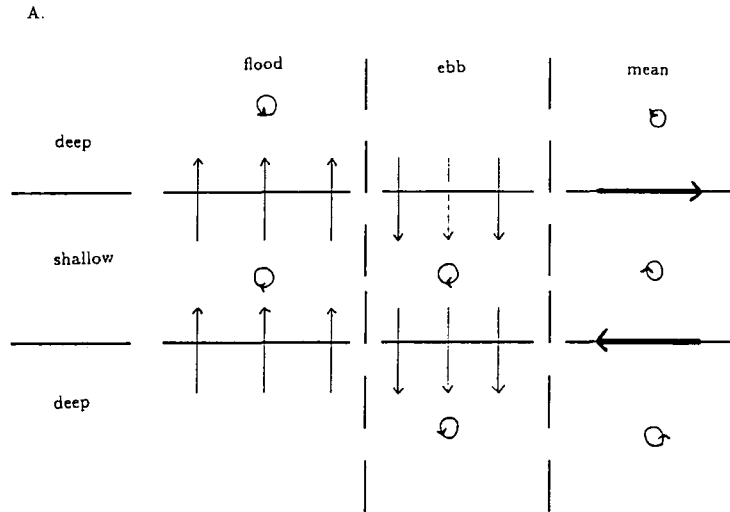
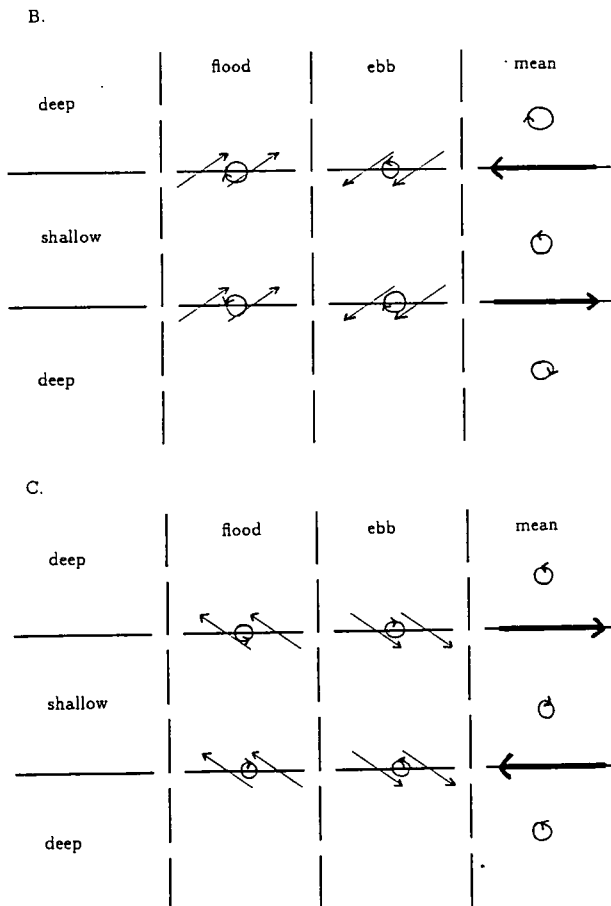


Figure 3.4. Residual eddies generated by stream flow over sand banks.

A. The vorticity generated by the stretching and squeezing of a water column passing over a ridge (after Robinson, 1983).

B. Vorticity generated by differential friction over a ridge (after Robinson, 1983).

C. Vorticity generated by differential friction over a ridge with current streams following a different direction from those shown in Figure 3.4b (after Robinson, 1983).



of flow as a result of the change to the geography of the area, altering the residual flow pattern. Changes to residual flow patterns at former sea-levels are not examined further in this thesis, but are discussed as they are of potential importance to sedimentation and current flow changes with sea-level and tidal change and, as such, provide an area for more detailed research into the changes to the tidal regime in bays and estuaries than is presented in this thesis.

### 3.1.6. Tidal analysis

#### 3.1.6.1. Harmonic analysis of tides

The basis of harmonic analysis is the representation of the tidal wave at a given point by a combination of harmonic constituents which represent the effects of the different heavenly bodies (Godin, 1972). The contributions of the various constituents to the tidal wave are represented by their amplitudes and phase values calculated according to their angular frequency, in the form

$$H_e \cos(\sigma_e t - g_e) \tag{3.12}$$

where  $H_e$  is the tidal amplitude of constituent  $e$ ,  $g_e$  is a phase lag of constituent  $e$  in radians relative to the high water of the equilibrium tide at Greenwich,  $t$  is time with  $t = 0$  at equilibrium high water and  $\sigma_e$  is the angular frequency of constituent  $e$ . The period of the  $e$  th constituent is given by

$$t_e = \frac{2\pi}{\sigma_e} \tag{3.13}$$

Shallow water terms may be expressed as higher harmonics of the main tidal constituents, as mentioned above. Shallow water terms in the fourth- and sixth- order (even order) bands (e.g.  $M_4$ ,  $M_6$ ,  $2MS_2$ ) are usually more important than those in the odd order bands (e.g.  $M_3$ ) (Doodson and Warburg, 1941). In addition, nodal modulation terms are often included in the harmonic analysis of tides. The nodal factors,  $f$  and  $n$ ,

are adjustments of amplitude and phase made for the 18.61 year nodal cycle of lunar declination. For the  $M_2$ , lunar semi-diurnal, tidal constituent, amplitudes vary by 4% over the cycle. For  $M_2$  the maximum value of  $f$  is 1.037 at maximum declination ( $28^\circ 36'$ ). For solar constituents, the nodal factor ( $f$ ) is 1.0 and the nodal angle ( $n$ ) is 0.0. If nodal modulation terms are included, the equation above is rewritten (Pugh, 1987) as

$$H_e f_e \cos[\sigma_e t - g_e + (V_e + n_e)] \quad (3.14)$$

where  $H_e$  is the tidal amplitude of constituent  $e$ ,  $V_e$  is the phase angle of constituent  $e$  of the equilibrium tide at time zero,  $f_e$  is the nodal factor and  $n_e$  is the nodal angle.

The tidal function (Pugh, 1987)

$$T(t) = Z_0 + \sum_e H_e f_e \cos[\sigma_e t - g_e + (V_e + n_e)] \quad (3.15)$$

is fitted to the observed tidal curve in harmonic analysis, where  $T(t)$  is the computed tide level in metres at time  $t$ , and  $Z_0$  is the mean sea-level in metres, so that the standard error (between observed and computed tide levels) is zero, or as near to this as possible. The choice of tidal constituents to include in the analysis depends on their amplitudes relative to each other in the expansion of the astronomical forcing for any given position on the earth. Least squares fitting is performed by matrix inversion methods. The length of observed data determines the number of constituents which may be separated in an analysis. For example, to determine  $M_2$  and  $S_2$  independently requires

$$\frac{360}{(30.00 - 28.98)} \text{ hours} = 14.77 \text{ days} \quad (3.16)$$

as the angular frequency of  $S_2$  is  $30.00^\circ$  per hour and that of  $M_2$  is  $28.98^\circ$  per hour. It therefore takes the time given in equation 3.15 for  $M_2$  and  $S_2$  to come into phase with each other.



Non-harmonic terms, such as mean spring range, may be expressed in terms of harmonic constituents. In a semi-diurnal dominated tidal area, such as the north-west European continental shelf, at syzygy, when the moon, earth and sun are in line, the gravitational forcing reaches its maximum value, resulting in spring tides. The combined values of the  $M_2$  and  $S_2$  amplitudes, together with the mean sea-level, then approximate to the level of mean high water of spring tides (Doodson and Warburg, 1941), in the absence of shallow water effects. Higher harmonic tidal constituents, especially  $M_4$  and  $MS_4$ , modify the values in shallow water areas.

### 3.1.6.2. Response analysis of tides

An alternative to the harmonic analysis of tides involves the use of response analysis techniques. In the discussion below, use is made of the concept of gravitational potential in a more general development of the tidal forces than that described in Chapter 3.1.1. Gravitational potential is the work which must be done against the force of attraction to remove a particle of unit mass to an infinite distance from the body (Pugh, 1987). The gravitational potential at a point  $Y$  on the surface of the Earth ( $\Omega_Y$ ), following Figure 3.1, may be defined as

$$\Omega_Y = -\frac{gm_l}{MY} \quad (3.17)$$

where  $g$  is the gravitational constant,  $m_l$  is the mass of the moon and  $MY$  is the distance from a point  $Y$  on the surface of the earth to  $M$ , the centre of the moon. From applying the cosine law to equation 3.16

$$MY^2 = R^2 + R_l^2 - 2RR_l \cos\phi \quad (3.18)$$

where  $R$  is the equatorial radius of the earth,  $R_l$  is the distance from the centre of the earth to the centre of the moon and  $\phi$  is the angle of latitude at which point  $Y$  lies on the surface of the earth. Substituting in 3.17, this gives

$$\Omega_Y = -\frac{gm_l}{R_l} \left\{ 1 - \frac{2R}{R_l} \cos\phi + \frac{R^2}{R_l^2} \right\}^{-\frac{1}{2}} \quad (3.19)$$

which may be rewritten

$$\Omega_Y = -\frac{1}{2} gm_l \frac{R^2}{R_l^3} (3\cos^2\phi - 1) \quad (3.20)$$

as the fourth and higher terms may be neglected because  $\frac{R}{R_l} \approx \frac{1}{60}$  and they therefore have little influence on the tide generating potential.

Munk and Cartwright (1966) expressed the gravitational potential ( $\Omega$ ) at the surface of the earth in complex spherical harmonics, which may be written (Pugh, 1987)

$$\Omega(\theta, \chi, t) = \sum_{i=0}^{\infty} \sum_{m=0}^{\infty} g[a_i^m(t)u_i^m(\theta, \chi) + b_i^m v_i^m(\theta, \chi)] \quad (3.21)$$

where  $\theta, \chi, t$  are north co-latitude ( $90^\circ - \text{latitude}$ ), east longitude and time variables, respectively and  $a_i^m$  and  $b_i^m$  are real and imaginary parts of a complex time-varying coefficient computed from lunar and solar motion and  $u$  and  $v$  are latitudinal and longitudinal velocities,  $i$  and  $m$  are the number of points at which calculations are made in the latitudinal and longitudinal directions, respectively. The tidal variations are expressed in terms of the weighted sum of past values of each spherical harmonic of the potential. The more detailed the result required, the more past values must be included in the analysis.

The method of response analysis leaves the physical characteristics of the ocean as a “black box” for further study (Pugh, 1987). However, harmonic analysis has the advantage of representing the individual tidal constituents in units of length and time which are useful for further analysis. The method of harmonic analysis is adopted in this study for this reason.

## **3.2. Tidal modelling**

### **3.2.1. Methods of tidal modelling**

Tidal models are used in order to predict or simulate the tidal regime of an area. Analysis of tide gauge records would indicate the most important tidal constituents at a point, but does not provide the dynamic methods of modelling and the length of recorded tidal observations limits its potential for assessing past or future tides. A physical model of the area under investigation would be possible, but may also exclude factors such as the rotation of the earth (Noye and Flather, 1990). Electrical analogue models have also been used (Ishiguro, 1972), but have the disadvantage of inflexibility in that application to a new region would probably require reconstruction. The most widely used method of tidal modelling is, therefore, mathematical.

Mathematical models can be considered as comprising two main types; analytical and numerical. An analytical solution provides the values of the desired unknown quantity at any location in a body. However, analytical solutions can be obtained only for certain simplified situations. It is generally not possible to specify a complex quantity completely accurately in mathematical terms. This is accommodated in tidal models by use of appropriate boundary conditions (discussed below) which permit inflow and outflow of water at different states of the tide to maintain an equilibrium condition. Analytical methods, using simplified equations and idealised bathymetry, provide an insight into the factors affecting the generation and propagation of tides in a particular area.

Numerical methods provide approximate, but acceptable, solutions at a number of discrete points in the body (Desai and Abel, 1972). Numerical methods are needed to obtain solutions for actual seas (Noye and Flather, 1990). Numerical modelling overcomes many of the difficulties with other methods mentioned above and, with the development of computers, has become the most widely used method of tidal modelling. The advantages of this method, with its ability to specify bathymetry in each grid rectangle and predict tidal movements over wide areas, allowing input of oceanic tide-generating effects at the

estuary scale, mean that it is the most suitable method for use in this study.

### **3.2.1.1. Criteria for consideration in the development of a numerical model**

Examination of a chart of the area to be modelled (Noye and Flather, 1990), together with a consideration of the problem to be solved, should determine the choice of the model to be used. Three-dimensional tidal models, in which the hydrodynamic equations are solved in two horizontal co-ordinates and the vertical (*i.e.* with depth) changes of these are modelled, are generally only used for tidal computations in deep sea areas, such as the Atlantic Ocean, where stratification is important in the water column (see, for example, Davies, 1983). In the area of the continental shelf, variations in water depth are relatively small and so vertical velocities are insufficient to warrant the extra computation of current variations with depth (Gunn and Yenigun, 1987). Two-dimensional models which employ depth-averaging are, therefore, more widely used from the scale of the continental shelf to that of an individual estuary and are used in this study. One-dimensional models, which have both depth- and lateral- averaging, are used for tidal rivers where there are only gradual changes in cross-section.

If the region to be studied is large, it may be necessary to take into account the curvature of the earth and use equations formulated in spherical polar, rather than Cartesian coordinates (Noye and Flather, 1990). This has been applied in a model of the north-west European continental shelf (Flather, 1976).

Grid size for the model is another consideration in the development of tidal models. A regular grid covering the area of the model is the simplest form, but where detailed information is required in one area, smaller grid widths may be introduced. This method was adopted by Garrett and Greenberg (1977), reducing grid sizes in a series of steps to obtain detailed tidal results for the Bay of Fundy, Canada. Interpolation is necessary from regions of low to high resolution to introduce tidal input to the finer resolution grid area from that generated in the coarse model grid at the open boundary of the finer model grid. There are two methods of dynamical connection of different grid sized models (Stephens,

1983). Different meshes can be dynamically connected by the coincidence of grid points along their common boundaries, but with no subsequent feedback to larger grid models. An alternative type of dynamical connection is that of dynamical patching with feedback, as used by Proctor (1981), into the coarser grid areas. The latter method is more difficult to program and does not add greatly to the accuracy of final results and so has not been used in this study. Use of a fine model grid in shallow water areas permits the resolution of tidal components with wavelengths of the size of the model grid which are smaller than those which can be resolved by a model with a larger grid area. It is also possible to use an irregular grid, but the advantages of flexibility to model boundaries and optimisation of the timestep for explicit models are offset by much increased programming complexity (Noye and Flather, 1990).

Open boundaries occur where the edge of the model joins another body of water; closed boundaries are solid boundaries which are land-water interfaces. Closed boundaries are modelled by assuming that the component of current flow normal to the boundary is zero, as water does not, in normal circumstances, cross coastlines.

The simplest method of modelling an open sea boundary uses specification of sea surface elevation, or the normal component of current flow, as a function of position and time (Noye and Flather, 1990). The radiation condition is more complicated and is used to avoid incorrect reflections at open boundaries. It takes the form of a specified relationship between surface elevation and currents. Input of tides is achieved by applying the formula for the speed of the tidal wave,  $(gh)^{\frac{1}{2}}$ , to the difference between the total elevation and current to be introduced (Flather, 1979). In this study, a radiation condition is used to link the models in a nested grid system (explained in Chapter 5.1) with resolution increasing down to the estuary scale, and the amplitudes and phases of the tidal constituents are converted into currents of varying magnitudes, introduced latitudinally and longitudinally along the boundaries of the models.

The initial state of the sea, in the form of a prescribed distribution of surface elevation

and components of currents, must also be specified for time-dependent problems (Noye and Flather, 1990). In many cases, and in this study, it is assumed that the sea is at rest initially, with no current flows or variations in elevation. From this “cold” start, the tidal solution is obtained by solving the equations with the appropriate forcing, for a time long enough for the influence of the initial state to be eliminated by either dissipation or radiation of energy across the open boundaries (Noye and Flather, 1990).

In summary, then, the information necessary for input to a numerical tidal model consists of the water depths relative to mean sea-level in the region covered by the model, tidal data for the open sea boundaries and tide-producing and propagating mechanisms within the model area. The appropriate form of the hydrodynamic equations and model grids depends on the nature of the problem to be solved.

### 3.2.1.2. Numerical modelling

Numerical models are based on the principles of Newton’s second Law of Motion (acceleration = force per unit mass) and continuity (*i.e.* the conservation of water volume within the tidal model). The hydrodynamic equations describe tidal movement. The hydrodynamic equations have been mentioned above but are summarised again here. The first hydrodynamic equation comes from the vertical equation of motion and represents changing hydrostatic pressure with depth. This varies due to changes of atmospheric pressure and the weight of water above any point in the water column, as is shown in the equation

$$P_{Z_d} = P_A - \rho g(z_d - \zeta) \tag{3.22}$$

where  $P_{Z_d}$  is the hydrostatic pressure at a point at depth  $z_d$  metres below the water surface,  $P_A$  is the atmospheric pressure on the water surface,  $\rho$  is water density,  $g$  is acceleration due to gravity and  $\zeta$  is the displacement of the water level from its mean value in metres (Pugh, 1987, p.89). This equation comes from the hydrostatic equation

$$\frac{\partial P}{\partial Z} = -\rho g \quad (3.23)$$

with  $P = P_A$  at  $Z = \zeta$  (the sea surface).

The continuity equation states that water is conserved. Since water density is assumed to be constant with depth, a volume of water is equivalent to its mass. In other words, as the total volume of water remains constant, a decrease in water level in one area will be compensated for by an increase elsewhere. The equation for this is expressed as

$$\frac{\partial \zeta}{\partial t} + \frac{\partial}{\partial x}(Du) + \frac{\partial}{\partial y}(Dv) = 0 \quad (3.24)$$

where  $t$  is time in hours and  $x$  and  $y$  are latitudinal and longitudinal distances, and  $u$  and  $v$  are the latitudinal and longitudinal velocities, respectively (Pugh, 1987, p.90).

Finally, the momentum equations are used latitudinally and longitudinally in the tidal calculations. These are, essentially, Newton's second law of motion expressed in the two directions, although the earth's rotation gives rise to additional acceleration in the form of the Coriolis force. The force is composed of tidal forces, pressure forces and shear forces (on the upper and lower surfaces) acting on the water (Pugh, 1987). The resulting equations may be written

$$\frac{\partial u}{\partial t} + v \frac{\partial u}{\partial y} + u \frac{\partial u}{\partial x} - f_c v = -g \left( \frac{\partial \zeta}{\partial x} + \frac{\partial \Omega}{\partial x} \right) + \frac{F_B}{\rho D} \quad (3.25)$$

$$\frac{\partial v}{\partial t} + u \frac{\partial v}{\partial x} + v \frac{\partial v}{\partial y} + f_c u = -g \left( \frac{\partial \zeta}{\partial y} + \frac{\partial \Omega}{\partial y} \right) + \frac{G_B}{\rho D} \quad (3.26)$$

where  $t$ ,  $u$ ,  $v$ ,  $x$ ,  $y$  and  $\rho$  are as defined above,  $f$  is the Coriolis parameter,  $\Omega$  is the gravitational potential of the equilibrium tide,  $F$  is stress in the  $x$  direction and  $G$  is stress in the  $y$  direction and the subscript  $B$  denotes bottom stress. Integrating the

momentum equations gives the flows in the latitudinal and longitudinal directions which cause the changes in the water level described by the continuity equation.

A large number of methods of numerical modelling have been developed. The most widely used fall broadly into the categories of finite element and finite difference methods.

### 3.2.1.2.1. Finite difference models

Finite difference methods in tidal modelling involve the rewriting of the hydrodynamic differential equations into finite difference form (Dronkers, 1974). For example, the simplest finite difference approximation to the equation

$$\frac{\partial^2 u}{\partial y^2} = \frac{\partial^2 u}{\partial x^2} \quad (3.27)$$

is

$$\frac{\frac{\partial u}{\partial x}(y+k) - 2\frac{\partial u}{\partial x}(y) + \frac{\partial u}{\partial x}(y-k)}{k^2} = \frac{\frac{\partial u}{\partial(x+j)}(y) - 2\frac{\partial u}{\partial x}(y) + \frac{\partial u}{\partial(x-j)}(y)}{j^2} \quad (3.28)$$

This is obtained by replacing the partial derivatives by finite difference quotients, using the increments  $j$  and  $k$  in the  $x$  and  $y$  directions respectively (Forsythe and Wasow, 1960). Beginning with the known solution at  $y = -k$ , values for the grid points can be calculated for  $y = 2k, 3k, \text{ etc.}$  Grid values for the next value of  $y$  are calculated as a difference from the current value of  $t$ . Derivatives at a point are approximated by difference quotients over a small interval, so that  $\frac{du}{dy}$  is replaced by  $\frac{\Delta u}{\Delta y}$  where  $\Delta y$  is small.

In application to tidal modelling, grid point tidal values are computed at a selected time interval. A requirement of the finite difference method is that the solution of the difference equations must converge to the solution of the differential equations when the size of the grid boxes approaches zero. Many examples of the use of finite difference schemes for the computation of the propagation of tidal waves can be found in the literature (see, for example, Brebbia and Connor, 1988; Noye and Flather, 1990).

The quality of the input data and complicated and time-consuming nature of the calculations required by the finite element method do not justify its use in the present



study. Finite difference methods generally give solutions that are either as accurate as the data warrant or as accurate as is necessary for the technical purposes for which the data are required (Smith, 1978). Finite difference numerical tidal models are, therefore, employed in this research.

Finite difference methods fall into the categories of implicit and explicit schemes. These are now discussed in turn.

#### **3.2.1.2.1.1. Implicit schemes**

Implicit methods couple new, unknown, values at grid points by a set of equations which must be solved simultaneously. Thus it is necessary to solve a subsystem for all components at once before a single one can be determined (Forsythe and Wasow, 1960). Thus, at first sight, implicit methods appear to involve a large amount of computational effort. However, they have the advantage that a longer timestep (time interval between calculations for individual grid points) may be used than with explicit methods, saving computational time. To counter this, though, there is a concomitant danger that low accuracy of the solution may result from use of timesteps which are too long in implicit schemes, giving results with a lower degree of accuracy. Examples of the use of semi-implicit schemes abound in the literature. Backhaus (1985), for instance, has developed a semi-implicit finite difference model for the North Sea area.

#### **3.2.1.2.1.2. Explicit schemes**

Explicit schemes are completely different with regard to numerical procedure and stability from implicit methods and much simpler to apply. With explicit methods the  $k$  th time approximation to the  $j$  th grid point component  $U_{k,j}$  of  $U_k$  can be determined without the necessity of simultaneously determining a group of other components of  $U_k$  (Forsythe and Wasow, 1960). Thus a new value at any given grid point is calculated only from the known values at other grid points, so only one equation is treated at any time (Ramming and Kowalik, 1980). Explicit schemes must satisfy the criteria for stability, examined below, in order to ensure valid and accurate solutions.

The explicit finite difference scheme is preferred in this study due to the potentially greater accuracy of the results obtained. The method used is almost identical to that of Flather (1976) and is elaborated below and in Chapter 5.

### 3.2.1.1.2.3. Criteria to be satisfied by numerical models

The difference equations contain (implicitly) a certain method of solution and so should satisfy a number of requirements which are essential, both for deriving a proper solution and for a sufficiently high degree of approximation (Ramming and Kowalik, 1980):

- (a) Consistency - if the grid width,  $h_w$ , and timestep,  $\Delta T$ , vanish, the difference equations should approach the differential equations. This is closely related to the degree of approximation.
- (b) Stability - if errors due to rounding off and truncation do not grow with time, the method is stable.
- (c) Convergence - if  $h_w$  and  $\Delta T$  vanish, the difference equations should not only approach the differential equations, but the solutions of the two sets of equations should also approach each other, or converge.

The “equivalence theorem” of Lax and Richtmyer (1956) states that consistency and stability are necessary and sufficient for convergence, if the correct method of introducing initial values to the model is used and there are no turbulent discontinuities (Ramming and Kowalik, 1980). In this case, a separate analysis of convergence is generally not necessary.

Explicit finite difference schemes must satisfy the consistency criterion in the formulation of the equations used. They must also satisfy the condition for numerical stability due to Courant *et al.* (1928)

$$2\Delta T < \frac{2h_{ws}}{\sqrt{2gh_{max}}} \quad (3.29)$$

where  $\Delta T$  and  $g$  are as defined above and  $h_{ws}$  is the smallest grid width (for a model with

variable grid sizes) and  $h_{max}$  is the maximum mean sea depth, or bathymetric value, in the model. The physical significance of equation 3.29 is that

$$\frac{h_{ws}}{\sqrt{gh_{max}}} \quad (3.30)$$

is the time taken for the fastest possible gravity wave to travel across a grid square. Thus the model timestep must take into account the width of the model grid and the water depth.

The application of the outline of tidal theory and modelling given in this chapter to the study carried out is explained in Chapter 5. Chapter 4 details the stratigraphic data available for the palaeogeographic reconstructions of the study areas. In Chapter 6 it is shown how the stratigraphic data are linked into the tidal models for palaeotidal study and results of the work are presented.

## CHAPTER 4

### PALAEOGEOGRAPHIC MAPS

Many methods have been used to reconstruct the shape of a land surface at a former time. For each of these, the minimum requirement is knowledge of the erosional and depositional history of an area (*i.e.* the sedimentary sequence), together with information concerning the age of the lithological units. The data available for The Wash Fenlands and Morecambe Bay, in terms of both the stratigraphic and the chronostratigraphic record, are now discussed, followed by factors taken into consideration when producing the palaeogeographic maps for the present study.

#### 4.1. Stratigraphic record

Details of the Holocene sediments in the field areas were collected with use of the scheme devised by Troels-Smith (1955) in a format similar to that of the Strat program (Everett and Shennan, 1987). By this means the nature, thickness and depth of each sedimentary layer in a borehole or section log is recorded. With the aid of grid references, sedimentary units may be correlated over large areas.

Stratigraphic records exist in a variety of forms. Most researchers note the depths and thicknesses of sediments of a given type together with descriptions of the sediments (*e.g.* Jennings and Smyth, 1982). However, Holocene stratigraphic data are not always recorded for the purpose of research into the area concerned. Many construction firms have recorded Holocene sediments whilst undertaking explorations for foundations and searching for material for road and building works. In most cases the main aim is to establish the nature of the underlying geology and so accurate records of the Holocene

sequences are often not kept (*e.g.* Mineral Assessment Reports, B.G.S.). Interpretations put on the data are a further problem. Some workers (*e.g.* Gresswell, 1958) note the presence of “inter-tidal marine deposits” in a description of clastic deposits of sand, silt or clay. It is not usually possible to determine the origin of a deposit in the field before laboratory work, so this brings into question the reliability and accuracy of the description provided.

The means of obtaining the stratigraphic sequence is also variable. Sections, such as those available along cleaned dyke sides, provide the best data as the lateral extent of sediments may be seen easily. Boreholes provide only point records of sediments and therefore run the risk of recording features which are of only very local significance, such as roddons (former river channels) in the Fenland, in place of the regional stratigraphic changes. This is shown clearly in Plate 4.1. The cleaned dyke section contains a roddon, giving an area of clastic sediments on either side of which the sediments have a much greater organic content at the same altitude. A borehole taken through the roddon would, therefore, be unrepresentative of the overall regional stratigraphy. Most stratigraphic records are, however, from boreholes as few sections are available. Shennan (1980) noted the sources of errors in recording stratigraphic data (see Table 4.1) and gave estimates of the magnitude of errors involved. At maximum, the figures suggest a possible error of 0.81 metres in identification of the altitude of stratigraphic boundaries, although Shennan (1980) suggests a figure of *circa* 0.30 metres.

#### **4.1.1. The Wash Fenlands**

Stratigraphic data for The Wash Fenlands have been collected from a number of sources with varying quality. The Mineral Assessment Reports by the British Geological Survey were essentially concerned with the pre-Quaternary geology of the Fenland and so do not provide very detailed data concerning the Holocene sequences. Stratigraphic records from scientific journals and data provided by colleagues at the University of Durham were also collected and these, together with a large database of over 700

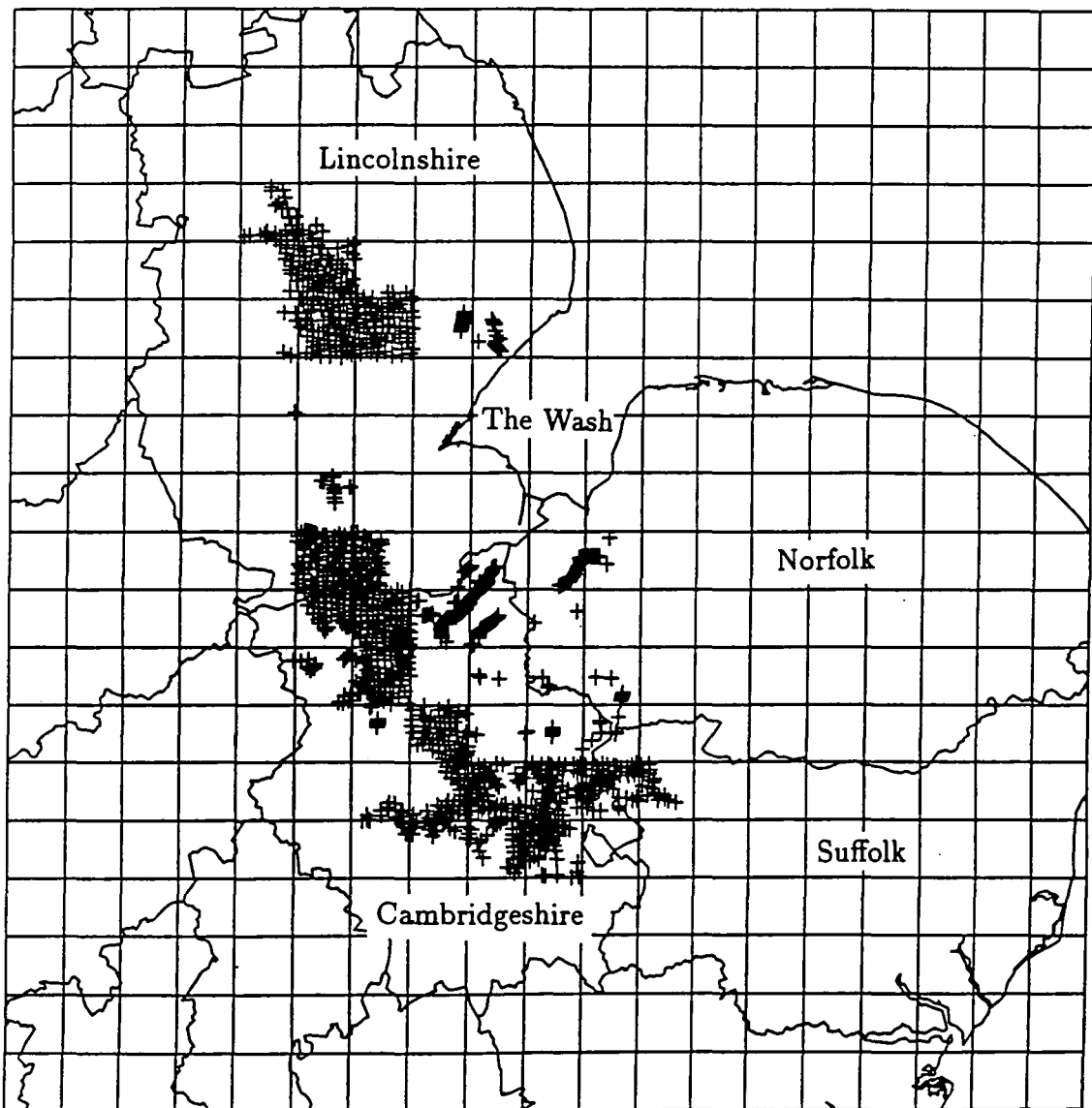


Plate 4.1. A former river channel (roddon) shown by the light -coloured silty material intruded through the darker peat in the cleaned dyke section at Morton Fen.

**Table 4.1. Errors affecting the measured altitude of stratigraphic boundaries, after Shennan (1980), from work in the Fenland.**

Type of error	Amount of error (metres)	Maximum error (metres)
Identification of boundary	$\pm 0.01$	-0.01
Measurement of depth - handcoring	$\pm 0.01$	
- commercial	$\pm 0.25$	-0.25
Compaction and extrusion of piston cores	-0.06	
Duits gouge	-0.20	-0.20
Angle of borehole	$\leq +0.04$	-0.04
Levelling to nearest benchmark	$\leq \pm 0.02$	-0.02
Accuracy of benchmark to O.D.	$\pm 0.15$	-0.15
Sampling density - boreholes (one per 180 x 30 metres)	$c.\pm 0.14$	-0.14
	Total	-0.81

Figure 4.1. Spatial Distribution of 2069 Borehole Records Showing Holocene Stratigraphy in The Wash Fenlands. The scale is shown by a 10 × 10 kilometre grid.





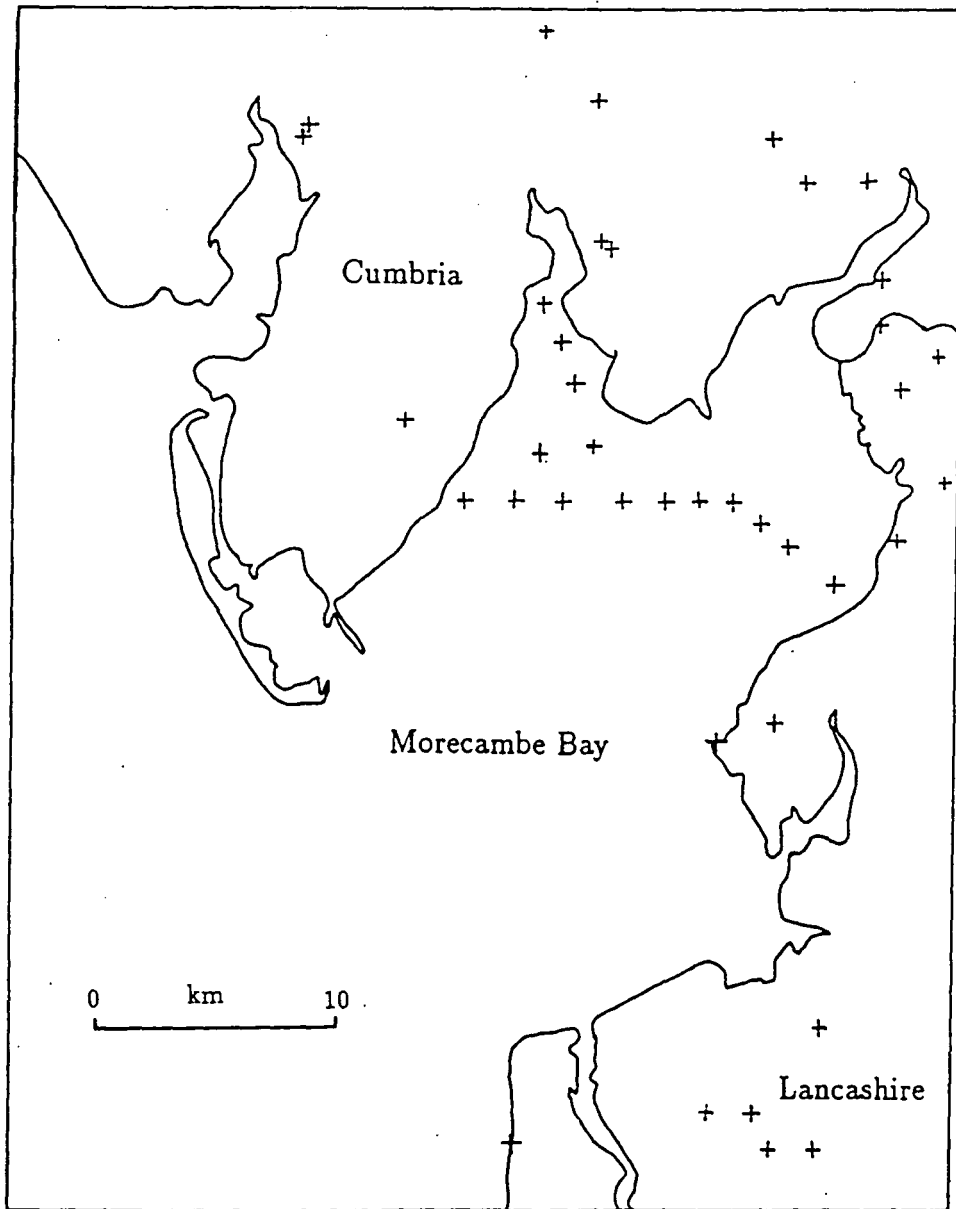


Figure 4.2. Spatial Distribution of Borehole Records Showing Holocene Stratigraphy in Morecambe Bay and surrounding areas.

borehole records from the Fenland project, form the data on which construction of the Fenland palaeogeographic maps has been based. The distribution of the boreholes used for stratigraphic information is shown in Figure 4.1. Reference was also made to Soil Survey Reports, especially Robson (1988). The sources used for stratigraphic records from the Fenland are given in Appendix 4.1.

It had been hoped to include stratigraphic data from the bottom of The Wash. The data available are given in Wingfield *et al.* (1978). Unfortunately, no cores of the stratigraphy were available and only surface sediments were collected. Geophysical traverses had been made across The Wash and, from these, a map of pre-Holocene rockhead contours had been constructed in the same Report. This provided a limit to the base of the Holocene sediments, although it is possible that erosion of sediments occurred when the sea transgressed the area in the post-Devensian sea-level rise.

#### **4.1.2. Morecambe Bay**

The amount of stratigraphic data for the Holocene sequences in the area of Morecambe Bay is considerably less than that for The Wash Fenlands, as discussed in Chapter 2.3.3. There are no Mineral Assessment Reports for this area. The data available have been collected from research papers, many of which are summarised in Tooley (1987), and colleagues at the University of Durham. The distribution of boreholes used for stratigraphic information is shown in Figure 4.2.

Offshore data in Morecambe Bay collected from the barrage feasibility study (Knight, 1977) have already been discussed in Chapter 2.3.2. This is included in the full database on which construction of the palaeogeographic maps has been based, sources for which are given in Appendix 4.2.

#### **4.2. Chronostratigraphic record**

Dating of the sediments in the stratigraphic sequence is necessary to obtain a time for their deposition. Dates of the same age are needed from as many sites within the field area

as possible over a wide area on a close enough spacing to enable extrapolation between the points with as high a probability of accuracy as possible. From the 1960s onwards radiocarbon dating has been applied to determine the age of sediments (*e.g.* Willis, 1961). Dating of the upper and lower contacts of a peat layer with other sediments provides an estimate of the minimum (for the upper contact) age of deposition of the sediment above and the maximum (for the lower contact) age of deposition of the sediment below.

The dates used in this study are all radiocarbon dates on peat. Techniques, such as thermoluminescence dating, for determining the age of clastic sediments have not been developed to the same degree of accuracy as radiocarbon dating and have not been used to date positions in the stratigraphic column in the current study.

Radiocarbon dates are given as a year plus or minus a number of years which represent one standard error in the date due to the precision of measurement in the laboratory (Kidson, 1982). In addition the accuracy of dates is affected by contamination of the sediment being dated by younger or older carbon, tending to reduce or increase the age of the resultant date on the peat. Furthermore, the assumption that levels of  $^{14}\text{C}$  have not varied over time is not true (de Vries, 1958; Suess, 1970). Corrections have to be made to the radiocarbon timescale for comparison with sidereal ages. For this reason, all  $^{14}\text{C}$  dates given in the text are expressed in radiocarbon years or are given with the equivalent radiocarbon age in brackets, converted using the formula of Klein *et al.* (1982).

The expense of radiocarbon dating reduces the number of assays made. In general, the stratigraphy of one borehole from a field area is taken as the best representative of the regional stratigraphic sequence. A core of sediment is then taken from this location for further analysis (*e.g.* particle size, pollen and diatom analysis) and, if the research budget permits, samples are taken from any peat layers present for dating. Thus the number of radiocarbon dates available is far less than the total amount of stratigraphic information for each of the field areas in the present study.

The altitudinal range from which material is collected for dating is a further impor-

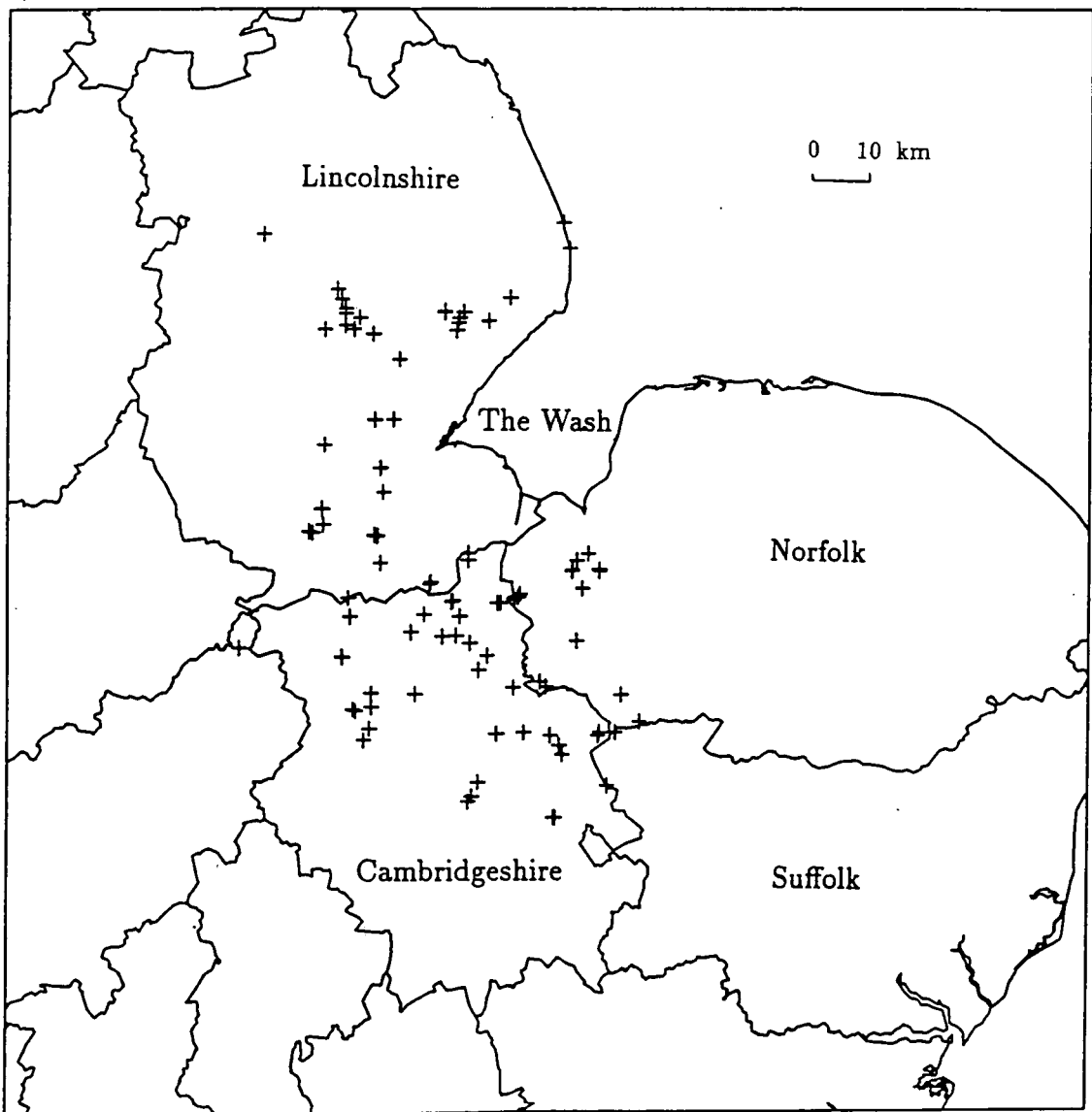
tant factor in determining the error of the radiocarbon date. Variations in the rapidity of sediment deposition mean that for a rapidly depositing sediment a date may be obtained to a higher degree of altitudinal accuracy than for a slowly depositing sediment. Post-depositional compaction of sediments in an area of slow deposition will increase the influence of older and younger material.

#### 4.2.1. The Wash Fenlands

The spatial distribution of radiocarbon dates from the Fenland is shown in Figure 4.3. It can be seen that dated sediments do not cover the whole of the Fenland area, but tend to be clustered in a few locations. This is largely due to two factors. Firstly, peat deposits are more widespread further from The Wash as they were only formed beyond the marine limit and surface peat layers, which formerly existed nearer to The Wash, have largely disappeared due to erosion by wind and peat cutting by man (Godwin, 1978). The second explanation for the spatial distribution of dated sediments is that research workers have concentrated their efforts on understanding the stratigraphy and environmental development of relatively small areas in detail. When combined with several similar studies, between which some stratigraphic evidence is available, this permits correlation between sites and consequently a good understanding of the environmental history of the whole area may be obtained (Shennan *et al.*, 1983). Sufficient stratigraphic information for correlation between sites is available in the Fenland for 3,000, 4,000 and 5,000 radiocarbon years before present. It is for these times that palaeogeographic maps of the area have been constructed although this was not the primary factor in determining at which times palaeogeographic reconstructions would be made for study of tidal changes, as is discussed below.

There are 271 radiocarbon dates available in the Fenland area. Details of these are given in Appendix 4.3 and Figure 4.5. The most recent radiocarbon date from the Fenland is 755 years B.P. and the oldest, 10,650 years B.P. Most dates are concentrated around the mean of 3,691 years B.P., with a standard deviation of 1,361 years. This was taken

Figure 4.3. Spatial Distribution of Radiocarbon Dates in The Wash Fenlands.



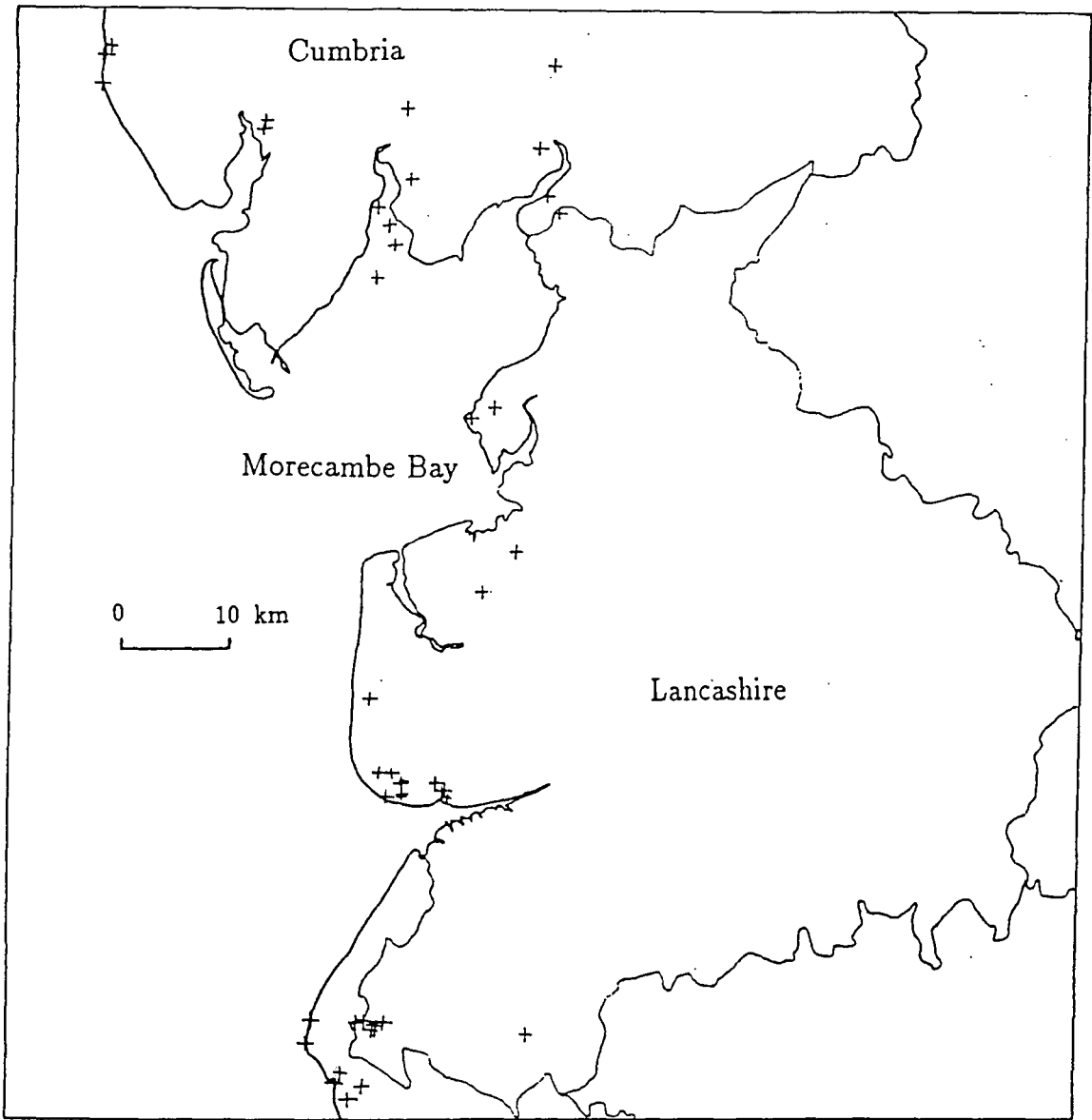


Figure 4.4. Spatial Distribution of Radiocarbon Dates in Morecambe Bay and surrounding areas.

**Figure 4.5. Histogram to Show the Temporal Distribution of Radiocarbon Dates from The Wash Fenlands.**

Years B.P.	No. of Observations	Observations
Midpoint	Count	
1000	3	**
2000	55	*****
3000	69	*****
4000	94	*****
5000	25	*****
6000	16	*****
7000	4	**
8000	3	**
9000	1	*
10000	0	
11000	1	*

Each \* represents 2 observations

Total of 271 radiocarbon dates

**Figure 4.6. Histogram to Show the Temporal Distribution of Radiocarbon Dates from Morecambe Bay and surrounding areas.**

Years B.P.	No. of	Observations
Midpoint	Count	
0	2	**
1000	3	***
2000	5	*****
3000	3	***
4000	8	*****
5000	18	*****
6000	18	*****
7000	11	*****
8000	8	*****
9000	7	*****

Each \* represents 1 observation

Total of 83 radiocarbon dates



into account when determining the times for which palaeogeographic maps of the area would be constructed as most information which could be used to obtain the former geography of the area was available within the period of  $3,691 \pm 1,361$  years B.P. A more important factor in this respect, though, was the effect of a change in shape of the coastline and sea depths and so this was the primary influence on the choice of palaeogeographic reconstructions used in the study.

#### **4.2.2. Morecambe Bay**

The spatial distribution of radiocarbon dates from the Morecambe Bay area is shown in Figure 4.4. There are 83 dates available in total and details of these are given in Appendix 4.4. Compared with the Fenland, there are far fewer dates available but, as noted in Chapter 2.3.3, the Morecambe Bay area is much smaller than that of the Wash Fenlands. In Morecambe Bay the dates are, in general, representative of marine limits in the estuaries which are separated by high land making stratigraphic correlation more difficult than in the Fenland.

The histogram in Figure 4.6 shows the temporal distribution of radiocarbon dates in the Holocene, though, as in the Fenland, these are not all related to sea-level indicators. The dates range from 170 to 9,360 years B.P. with a mean of 5,459 years B.P. and standard deviation of 2,138 years. They are, therefore, in general older than those available from the Fenland. This is also reflected in the fact that palaeogeographic reconstructions of Morecambe Bay have been made for 5,000 and 8,000 years B.P. as the shape of the Bay was considerably different from that of the present at those times giving an impetus for investigation of the tidal regimes.

#### **4.3. Construction of palaeogeographic maps**

Maps showing the former geography of an area have been constructed for many different purposes and hence by a number of methods. Much work on the former physical geography of north Germany has been carried out using stratigraphic records, especially by Barckhausen *et al.* (1977) and Barckhausen and Streif (1978). The sequence map has

been developed by these researchers. It represents the spatial extension of sedimentary sequences by classifying them into profile types which can then be represented by maps. This lithological system has to be linked with a chronostratigraphic system in order to obtain a clarification of the coastal development in terms of time and space. It has been used to produce geological sheets of Holocene sequences at scales of 1:25,000, such as that of Emden West (Barckhausen and Streif, 1978). This provides a three-dimensional picture of the sub-surface geology which is of use for scientific purposes and also provides information for construction of buildings and roads, for example.

Palaeogeographic maps may also be drawn using the simple method of marking out the contours of the former land surface and, where relevant, the coastline. This method has been used by Waller (in press) to draw palaeogeographic maps of The Wash Fenland during the Holocene. The information provided does not extend to the subsurface sedimentary sequence in this case and is therefore less useful for construction purposes.

For this study palaeogeographic information is required in sufficient detail to provide a coastal boundary in the tidal model at a resolution of approximately one square kilometre. This resolution was decided upon from consideration of the available stratigraphic and chronostratigraphic data and the possibility of obtaining information on local tidal changes during the Holocene from construction of palaeogeographic maps. The method used has therefore been similar to that of Waller (in press), although contours on the former land surface were not needed in the present case. From plots of the locations of sea-level index points and with reference to the dates of these and surrounding, undated, stratigraphy, the coastline has been drawn. This was done for times when there were judged to be stratigraphic and chronostratigraphic data available requiring a minimum of interpolation and extrapolation at the scale needed and the shape of inlets was different, both from that of the present and from other times during the Holocene giving added purpose to the study of the tidal regime at that time. Factors affecting the accuracy of sea-level reconstructions are discussed in Chapter 1.

Quaternary sediments, from the Quaternary Sediments U.K. (South) sheet (Woodland, 1977), were taken into account when drawing former coastlines, especially in the Morecambe Bay area where less Holocene stratigraphic data are available. The contours from latest edition metric 1:25,000 Ordnance Survey map sheets were also used to avoid interpolating or extrapolating the former coastline over areas of high land.

Detailed modifications to sea depth data were not possible from the stratigraphic data available, as discussed in Chapter 2.3.1 and Chapter 2.3.2. The only dated contacts available are from changes from marine to terrestrial conditions or *vice versa*. Sea depths for the times of palaeogeographic reconstruction have been obtained from Mörner's (1976) eustatic sea-level curve. However, as shown by Waller (in press), stratigraphic data provide information on the general locations of river channels prior to post-glacial inundation of the Fenland and sea depths were deepened locally to allow for these in the palaeogeographic reconstructions. For a given time of reconstruction, the tidal models used (see Chapter 5) have been run with the number of metres of sea depth reduced according to that read from the eustatic curve. For the two most detailed tidal models for both The Wash and Morecambe Bay, sea depths were further modified according to the isostatic curves drawn for the areas by Shennan (1987, 1989).

Indicators of eustatic sea-level and isostatic movement are generally only available on land. Modification of the offshore bathymetry from data obtained from land records is, therefore, potentially inaccurate. The influence of hydroisostasy and sediment movements, in particular, on sea depths is an unknown factor and no attempt has been made to take its influence into account in this thesis. The possible influence of factors not taken into account in this study in determining the altitude at which sea-level indicators are found is discussed in Chapter 7.

#### **4.3.1. The Wash Fenlands**

The present sea-level water depths for the EC3 model are shown in Figure 4.7. For the Fenland, the shape of the former coastline was reconstructed at 3,000, 4,000 and 5,000

years B.P., as shown in Figures 4.8, 4.9 and 4.10. The variations in extent of marine inundation in different parts of the Fenland justify the use of these three reconstructions, as do the adequacy of the stratigraphic and chronostratigraphic datasets. Sea-level in the tidal models is not lowered for the 3,000 and 4,000 years B.P. reconstructions, but is reduced by 2 metres to be representative for 5,000 years B.P., according to the eustatic curve of Mörner (1976), shown in Figure 4.11.

Variations in sea-level due to isostatic effects (Shennan, 1987, 1989) meant that the depths in the two most detailed models were further modified, after Shennan (1989, table 2), beyond the influence of a eustatic sea-level change. At 3,000 years B.P. sea-level east of the Norfolk coast was increased by two metres and further increased by another metre for the 4,000 and 5,000 years B.P. reconstructions to take the subsidence of the area over this time period into account. In the Wash area and to the north, sea-level was increased by three metres for 3,000 years B.P., four metres for 4,000 years B.P. and five metres for 5,000 years B.P.

#### **4.3.2. Morecambe Bay**

The present sea-level water depths for the LBM model are shown in Figure 4.12. A reconstruction of the coastline of Morecambe Bay was made for 5,000 years B.P., as shown in Figure 4.13, at which time the sea extended to its greatest distance up the river estuaries. Two further reconstructions were made for 8,000 years B.P., when sea-level was much lower than at present and covered a much smaller area of the Bay than it does today. These are shown in Figures 4.14 and 4.15.

From the eustatic sea-level curve of Mörner (1976), sea-level was lowered by two metres in the tidal models to represent the situation at 5,000 years B.P. For 8,000 years B.P. sea depths were reduced by 15 metres, in the tidal models, from the eustatic curve. These depths were further modified for isostatic effects after Shennan (1989). At 5,000 years B.P. sea-level west of south Lancashire in the tidal model was reduced by one metre. In the Morecambe Bay area sea-level was lowered by two metres, while to the north, in the

Water depths (m.)



Figure 4.8. EAST COAST 3 MODEL at 3,000 years B.P. Sea-Level

Water depths (m.)

95

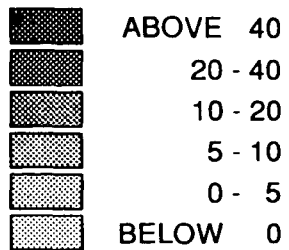


Figure 4.9. EAST COAST 3 MODEL at 4,000 years B.P. Sea-Level

Water depths (m.)

96

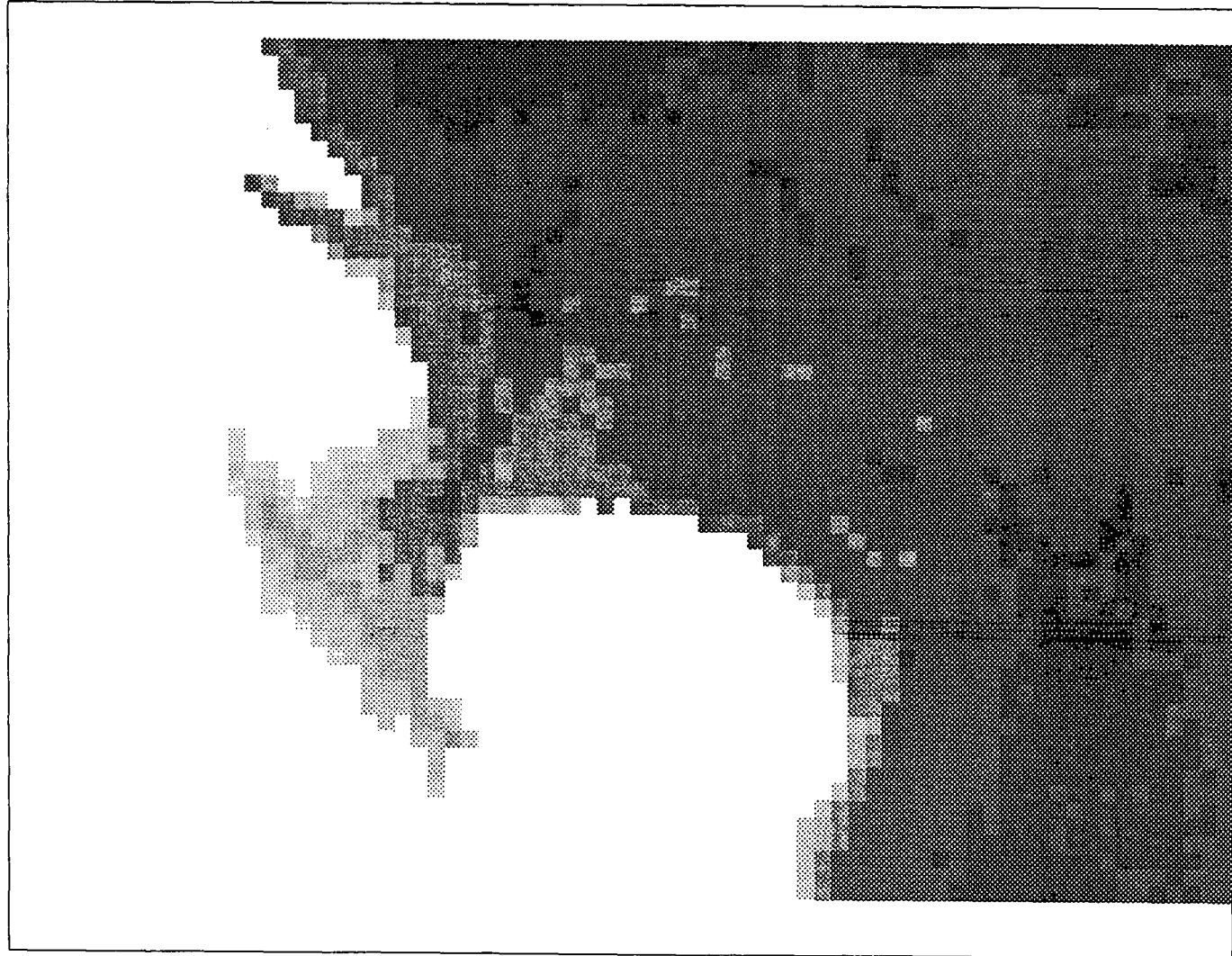
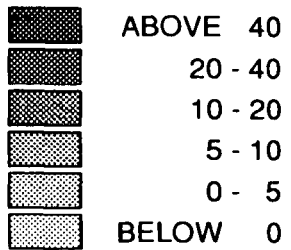
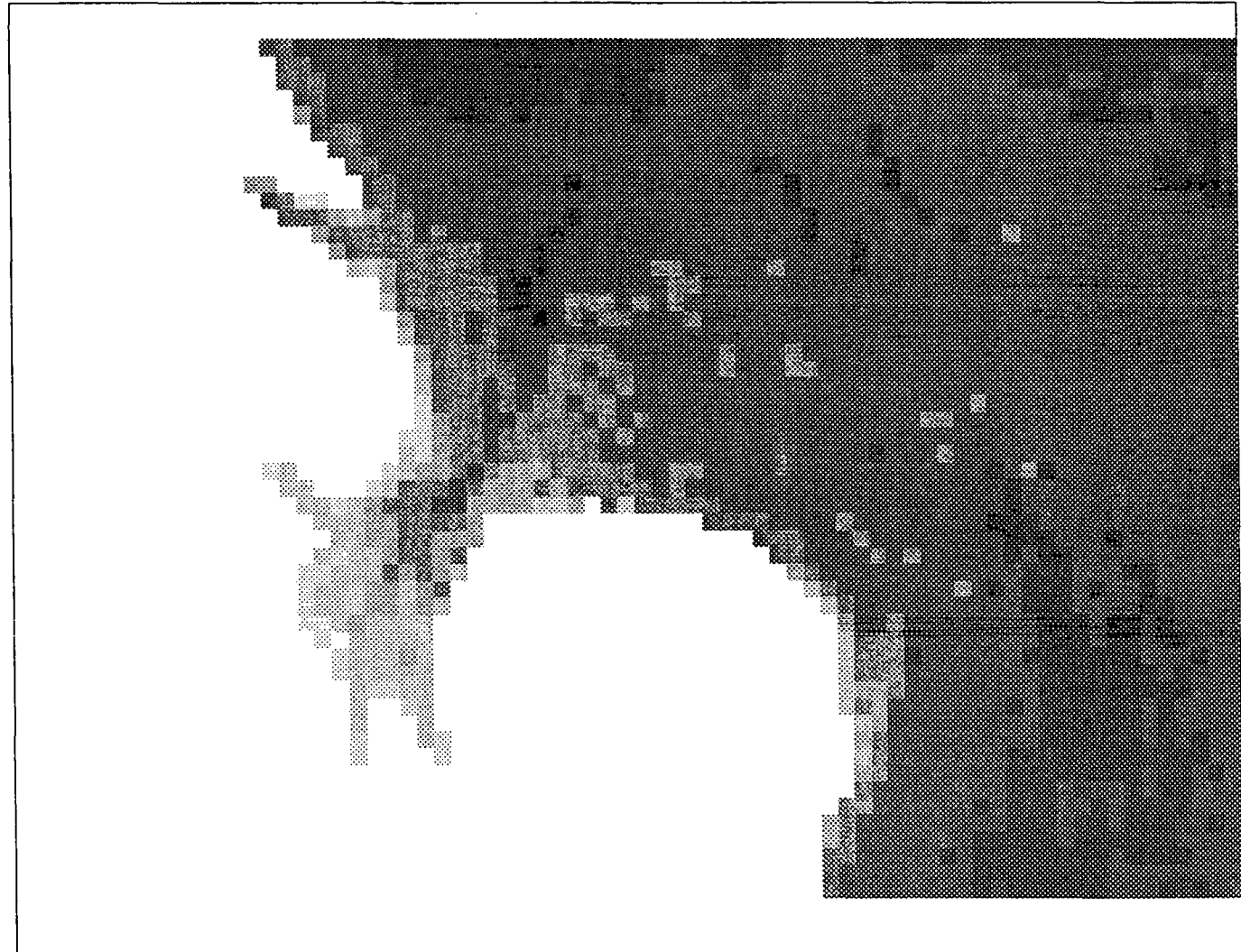
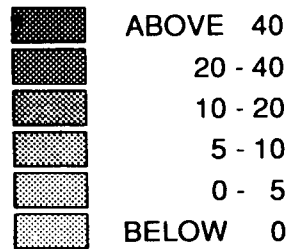


Figure 4.10. EAST COAST 3 MODEL at 5,000 years B.P. Sea-Level

Water depths (m.)

97





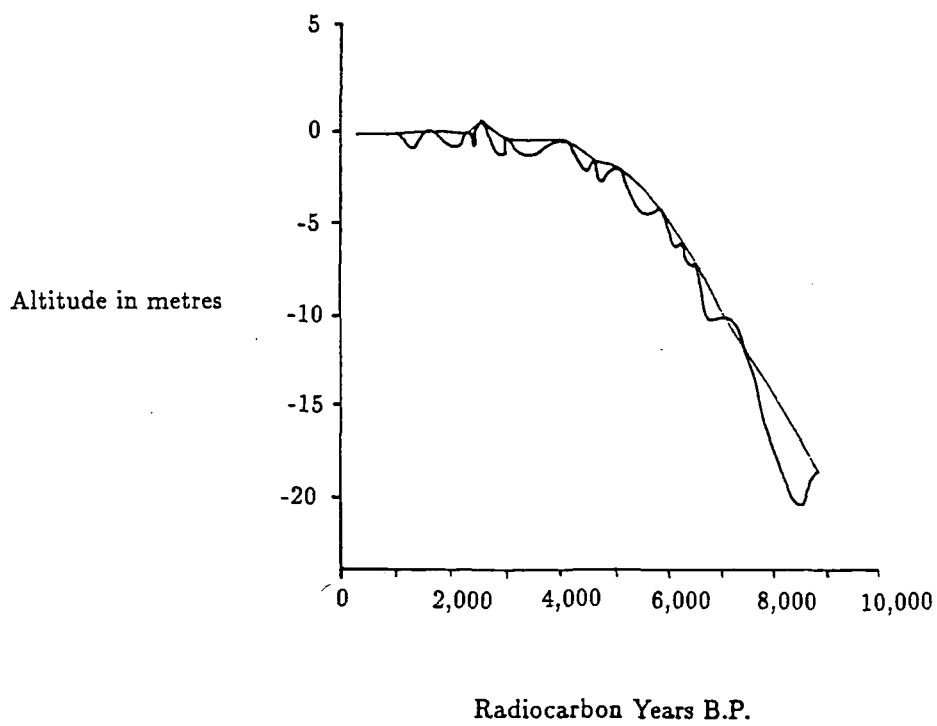
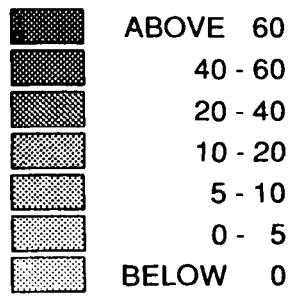


Figure 4.11. The Regional Eustatic Curve (of Mörner, 1984), with and without oscillations (after Shennan, 1989).

# LIVERPOOL BAY MODEL Present Sea-Level

## Water depths (m.)

66



## Water depths (m.)

100

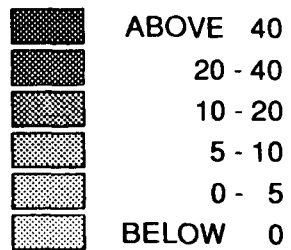
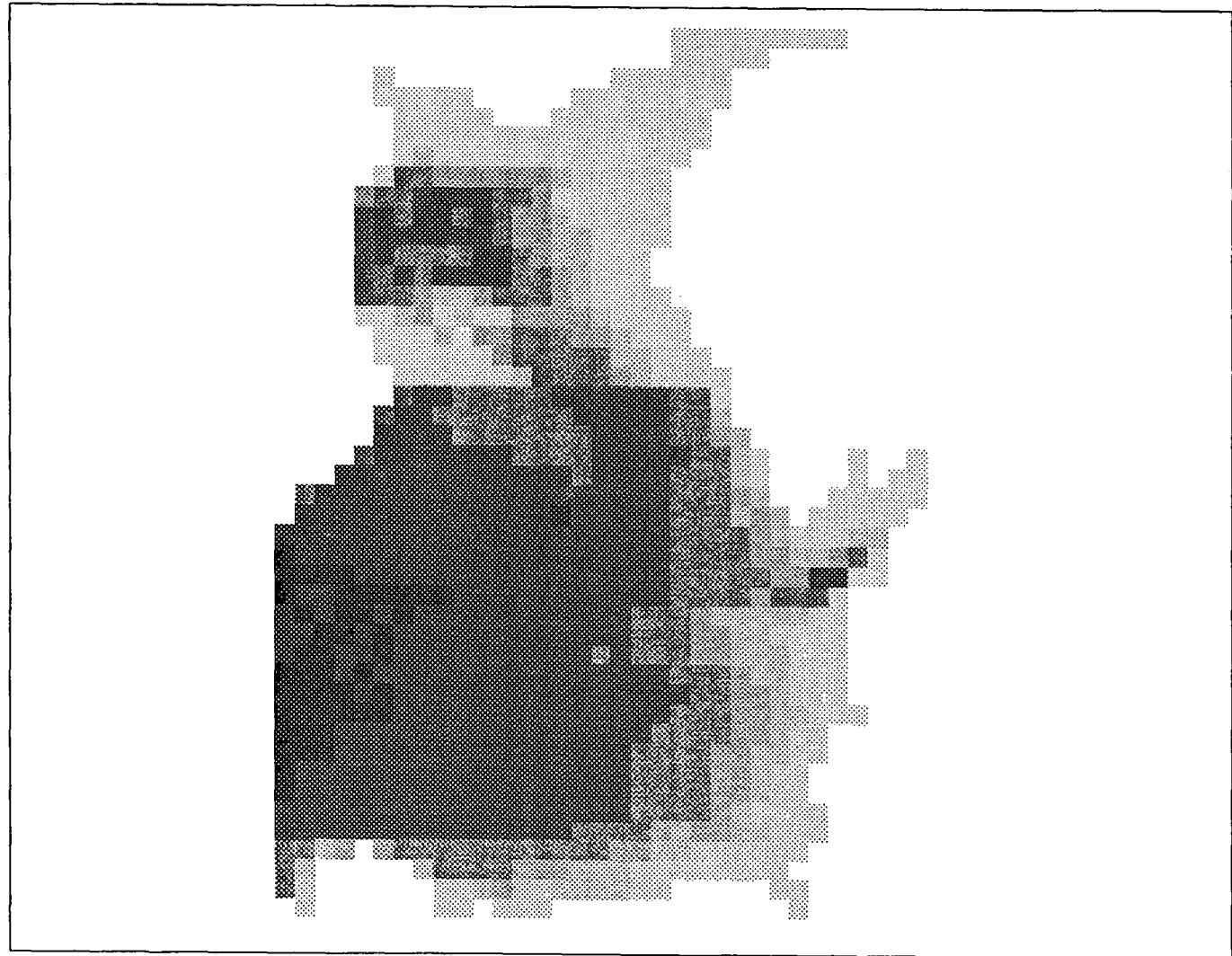


Figure 4.14.

# LIVERPOOL BAY MODEL 8,000 Years B.P. Palaeogeography

Higher Sea-Level  
Water depths (m.)

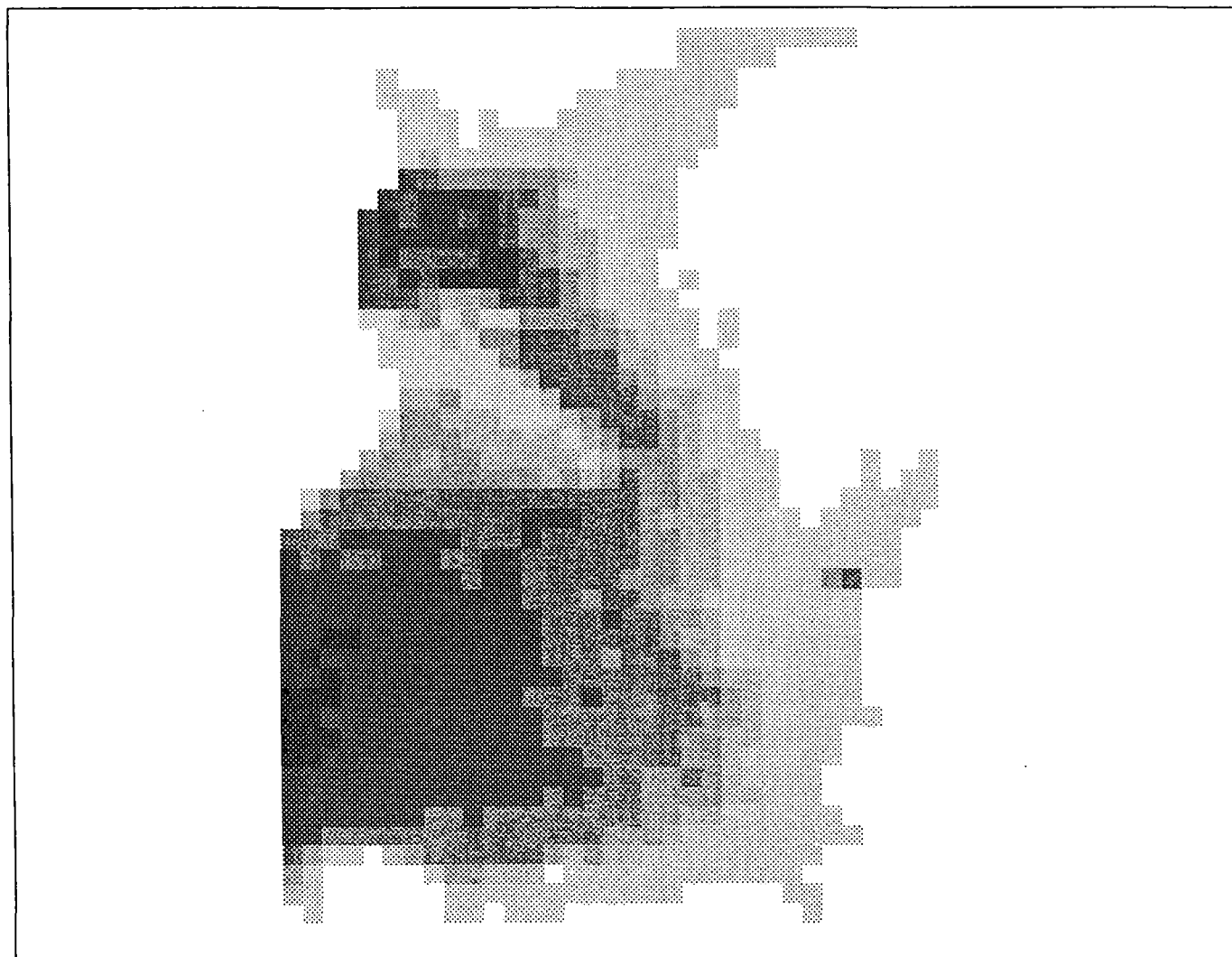


101

Figure 4.15.

# LIVERPOOL BAY MODEL 8,000 Years B.P. Palaeogeography

Lower Sea-Level  
Water depths (m.)



Solway Firth, it was lowered by a further five metres. For 8,000 years B.P. two different runs of the tidal models were used with different sea depths due to the variation in isostatic effects shown for this time period in Shennan (1989, Figure 8), Figure 4.11. A “maximum” sea-level run was carried out, with depths reduced by five metres off south Lancashire, two metres off north Lancashire, increased by eight metres around Morecambe Bay and lowered by fifteen metres in the Solway Firth area. For the “minimum” sea-level run, the depths were lowered by eight metres off Lancashire, ten metres around Morecambe Bay and eighteen metres in the Solway Firth.

The structure of the tidal models used for the field areas is described in Chapter 5. The method by which sea depths and coastline shapes are entered in the tidal models is also explained.

## CHAPTER 5

### TIDAL MODEL METHODOLOGY

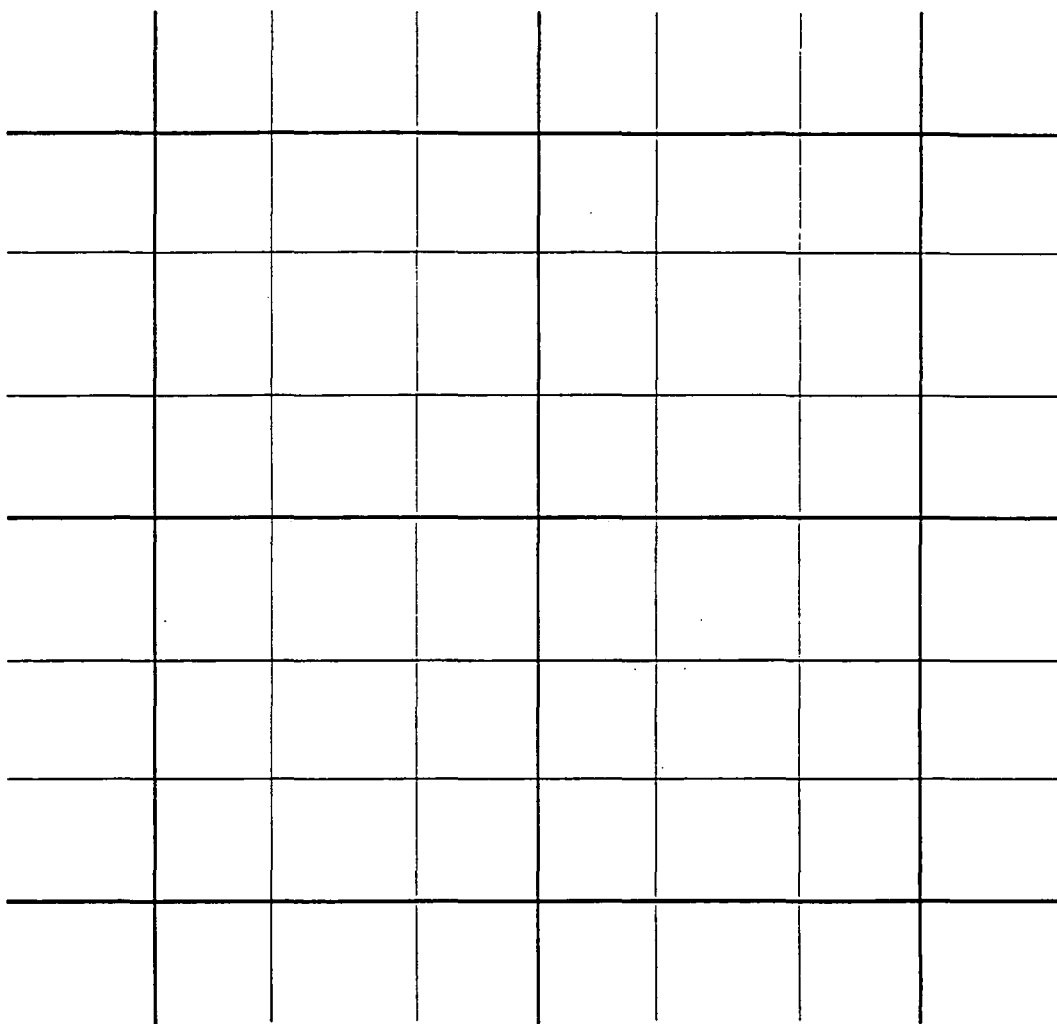
#### 5.1. Tidal models used

The tidal models used in the present study employ programs which were essentially written by Dr. Roger Flather of the Proudman Oceanographic Laboratory, Birkenhead, although some modifications to the basic programs have been made to facilitate running the models at lower sea-levels. The modifications are outlined in Chapter 6.1. The models employ the explicit finite difference scheme discussed in Chapter 3.

A series of models has been used to study the tides in The Wash and Morecambe Bay. The area covered for the intended study is required to be such that changes in sea-level may be reasonably assumed not to affect tidal variations at its boundary. This led to the use of a nested series of models from the north-east Atlantic ocean where there is little change in the ratio of mean sea-level to water depth. This point is discussed further in Chapter 6. The need to resolve the detail of tidal patterns in the Wash and Morecambe Bay so that changes in the tidal regime can be related to palaeogeographic data led to the choice of a system of “nested” models.

It was decided that the quantity and quality of palaeogeographic data available for reconstructions of The Wash and Morecambe Bay at times during the Holocene were insufficient to permit greater accuracy of tidal computations than that obtained from a grid size returning values for tidal calculations from an area of  $1/81^{\text{st}}$  of a degree of latitude and  $1/54^{\text{th}}$  of a degree of longitude. The choice of this grid size was also partly determined from the resolution of a set of bathymetric data available for the area of the

Figure 5.1. Diagram to show the increase in resolution from one model to the next model down the hierarchy.



———— Coarser resolution model grid

———— Finer resolution model grid

(9 values returned for every one of that of the coarser model)



north-east Atlantic Ocean, which were available on a resolution of a third of a degree of latitude and half of a degree of longitude. The lack of bathymetric data available to the required resolution of approximately one square kilometre over the area of this model was one factor which led to the decision to use more than one tidal model. Another factor was the enormous computing requirement which would have been necessary to make tidal calculations to the required resolution over the entire area of this model. This, together with the fact that data to this resolution were only required in Morecambe Bay and The Wash and no detailed palaeogeographic data were available beyond these areas, meant that the approach adopted was to run a series of tidal models in a nested hierarchy with increasing spatial resolution into The Wash and Morecambe Bay. Output from one model was interpolated and, where necessary, extrapolated as input along the boundary to the next, more detailed, model down the scale. The input data are discussed further in Chapter 5.2.

The nested hierarchical method of running tidal models has been used by a number of authors, including Garrett (1972), who ran tidal models of the area of the Bay of Fundy with a model with a finer grid in the inner part of the Bay. An alternative solution was used by Greenberg (1975) who employed one tidal model with variations in the size of the grid mesh in different parts of the model. This increases the amount and complexity of programming required for the model but has the advantage that any tidal generation that occurs in the area with finer grid spacing is allowed to flow out into and interact with the tidal waves generated in the coarser grid area of the model. The method employed in this study allows the fine grid solution to differ from that obtained from the coarse grid boundary, as discussed in Chapter 3.

The reasons for running each of the models separately were that, firstly, the amount of tidal generation below the scale of the north-west European continental shelf is relatively small (Pugh, 1987). Secondly, a considerably greater amount of effort would be required in programming tidal movements with several changes in grid size within one model. Thirdly, running the models separately facilitated the identification of errors within each

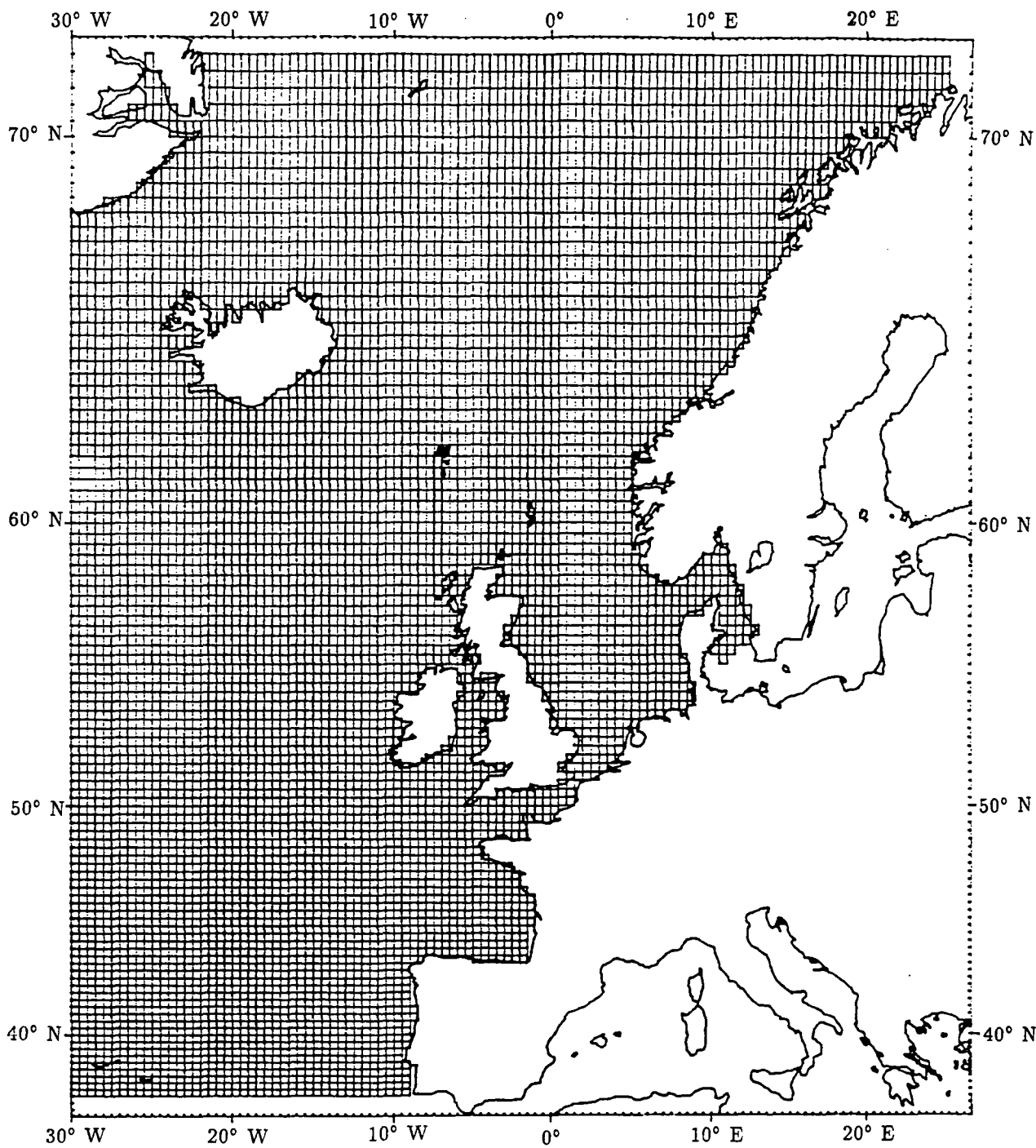


Figure 5.2. North-East Atlantic Model (NEA)

model and provided a means of comparison of tidal results to check the output of the models for present sea-level.

The increase of resolution at each stage in the model hierarchy was nine times that of the preceding model, so that where one tidal value was returned for an area in the coarser model, this was replaced by nine figures in the finer resolution model, as shown in Figure 5.1. This step of increase in resolution was chosen as it was considered to represent a good balance between the necessary increase in resolution and degree of interpolation required to keep consistency of model results. The method of interpolation used is described in Chapter 5.2.

#### **5.1.1. North-east Atlantic Model**

The north-east Atlantic model covers an area from 37° North to 71°40' North and 30° West to 25°30' East, with a grid resolution of a third of a degree latitude and half of a degree longitude, or approximately 30 × 30 kilometres, varying with latitude. The grid of this model is shown in Figure 5.2. The bathymetric data for this model were obtained from the Proudman Oceanographic Laboratory, Birkenhead.

#### **5.1.2. Models for The Wash**

Tidal input data were obtained from the north-east Atlantic model and interpolated as boundary data to the East Coast Model (ECM) by the method described in Chapter 5.2 below. The East Coast Model extends from 49°20' North to 55° North and 1°10' West to 4°40' East, with a grid resolution of one ninth of a degree latitude and one sixth of a degree longitude. The grid of this model is shown in Figure 5.3. The bathymetric data for this model were again obtained from the Proudman Oceanographic Laboratory.

The next model down the hierarchy from the East Coast Model is EC3. The extents of this model are from 52°8.89' North to 53°57.78' North and 0°13.3' West to 2°56.67' East, with a grid resolution of  $1/27^{\text{th}}$  of a degree latitude and  $1/18^{\text{th}}$  of a degree longitude. The setup and bathymetric data for this model were collected from Admiralty Charts no.s 105,

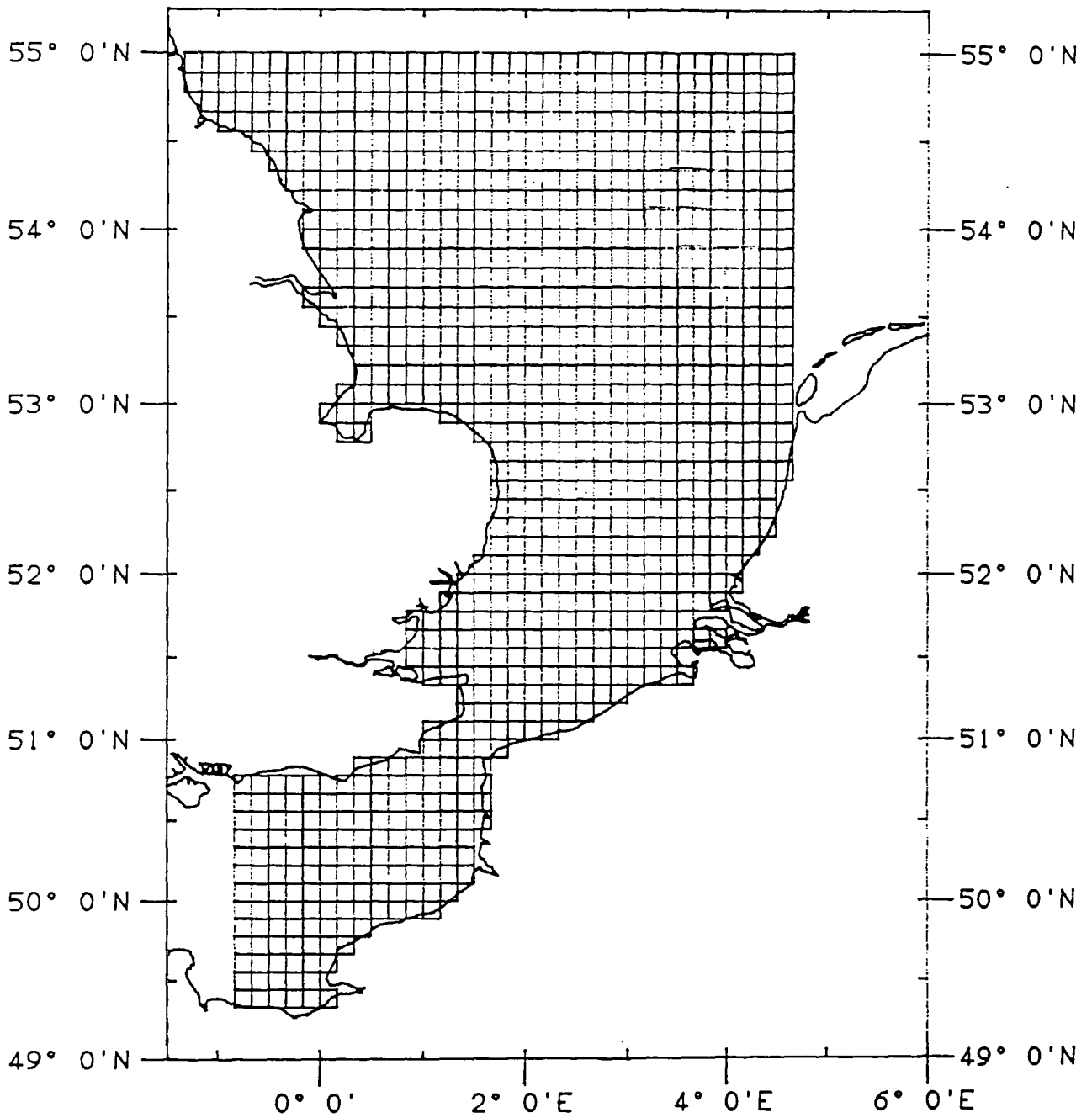


Figure 5.3. East Coast Model (ECM)

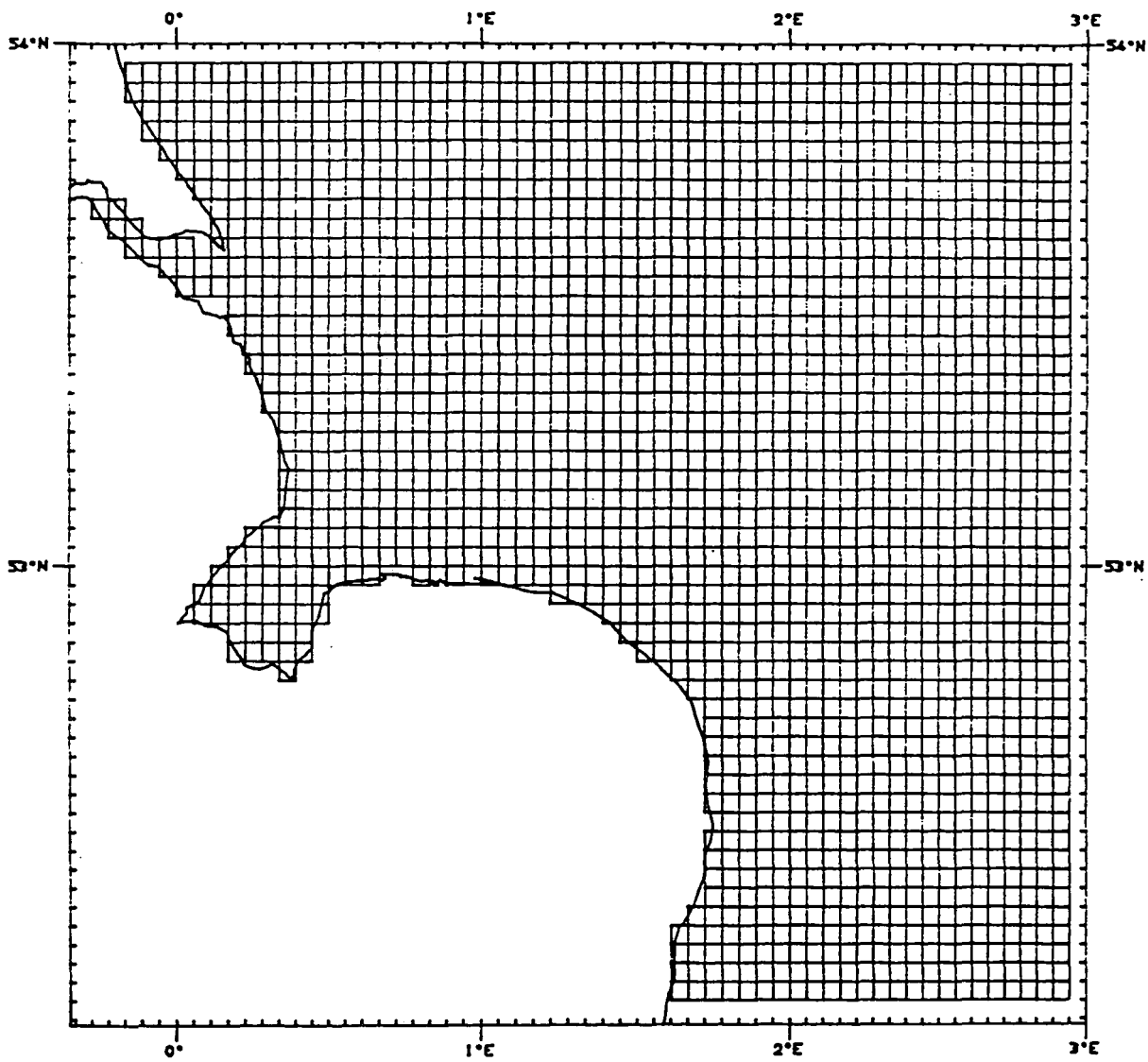


Figure 5.4. EC3 Model (EC3)

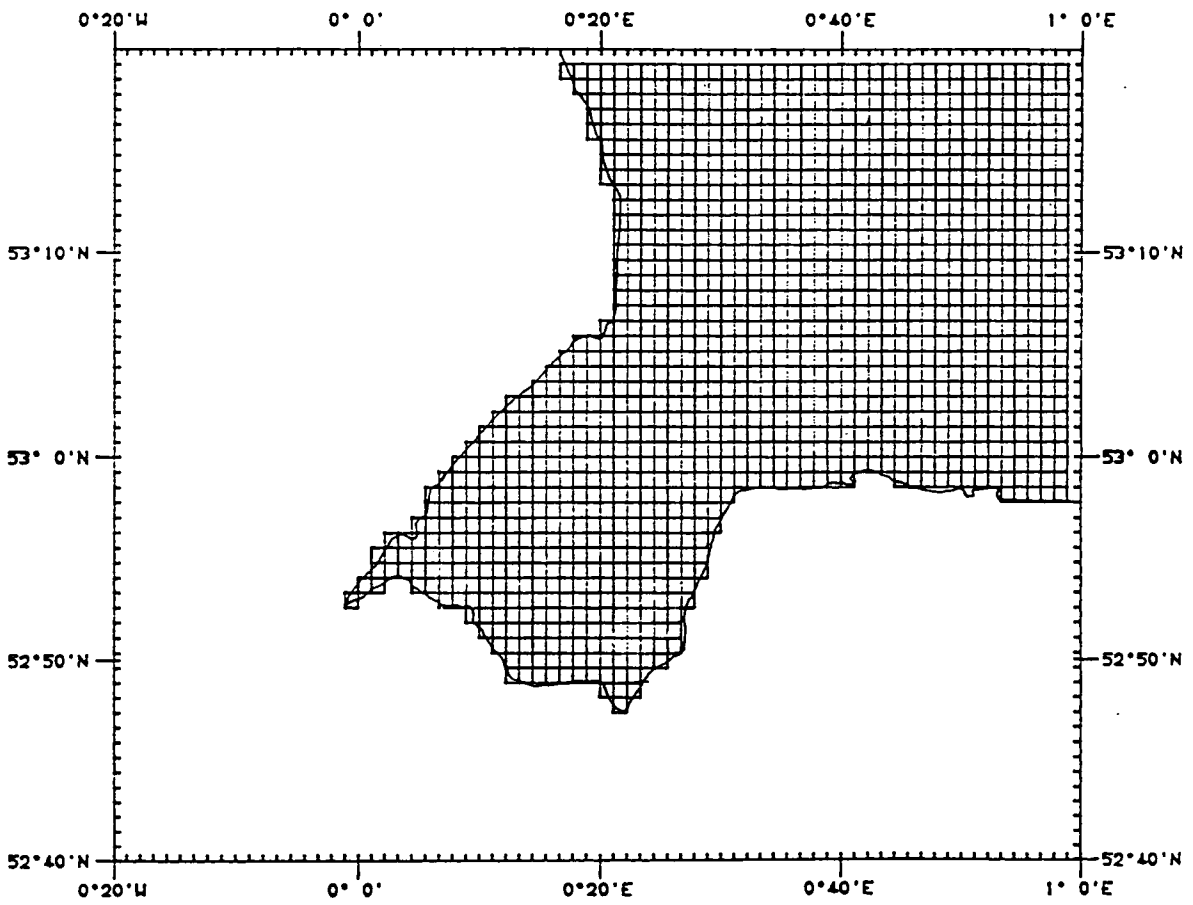


Figure 5.5. WASH Model

106, 107, 108, 109, 121, 1187, 1190, 1200, 1503, 1504 and 1543 by the methods described in Chapter 5.2. The grid of this model is shown in Figure 5.4.

To obtain the resolution required for the palaeotidal work, a further model, the WASH model, was developed to a grid resolution of  $1/81^{\text{st}}$  of a degree latitude and  $1/54^{\text{th}}$  of a degree longitude, extending from  $52^{\circ}47.4'$  North to  $53^{\circ}19.26'$  North and  $0^{\circ}1.1'$  West to  $0^{\circ}58.9'$  East. The data for this model were, again, obtained from Admiralty Charts (no. 108 and no. 1200). The grid of the WASH model is shown in Figure 5.5.

### **5.1.3. Models for Morecambe Bay**

Three models, of the same resolution as those for the Wash, were again run to obtain the required resolution for tidal results in Morecambe Bay. All the bathymetric data for these models were provided by the Proudman Oceanographic Laboratory. The West Coast Model (WCM), corresponding to the ECM for The Wash, covers the area from  $50^{\circ}$  North to  $56^{\circ}20'$  North and  $8^{\circ}$  West to  $3^{\circ}20'$  West, as shown in Figure 5.6. The Liverpool Bay Model (LBM), corresponding to the EC3 model for The Wash, covers the area from  $53^{\circ}13.3'$  North to  $54^{\circ}56.67'$  North and  $4^{\circ}36.67'$  West to  $2^{\circ}50'$  West, as shown in Figure 5.7. The Morecambe Bay Model (MBM), at the same resolution as the WASH model on the east coast of the U.K., extends from  $53^{\circ}48.89'$  North to  $54^{\circ}17.78'$  North and  $3^{\circ}30'$  West to  $2^{\circ}47.78'$  West, as shown in Figure 5.8.

## **5.2. Input data**

Input data to run the tidal model are organised by two programs in the scheme employed here. The first takes the bathymetric data and either determines from this where the tidal calculations are to be made or reads in this data too. The second program arranges the tidal input data.

### **5.2.1. Bathymetric data**

The bathymetric data for use as sea depths in the tidal models were mostly available from the Proudman Oceanographic Laboratory. For the EC3 and WASH models, however,

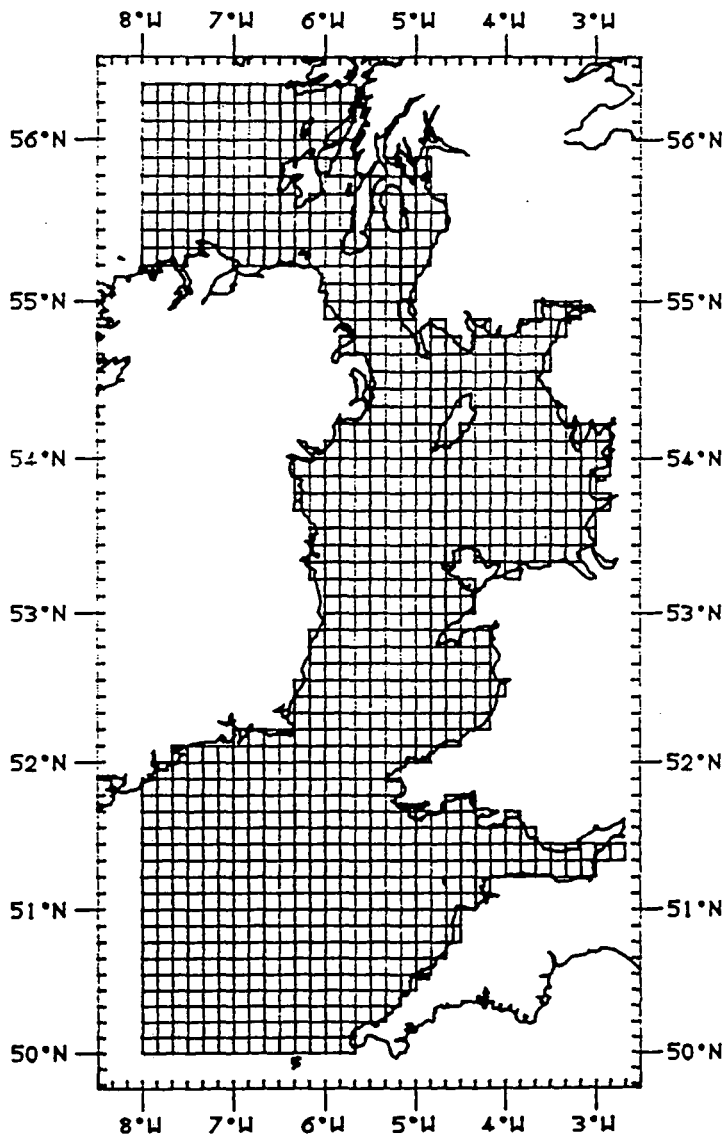


Figure 5.6. West Coast Model (WCM)



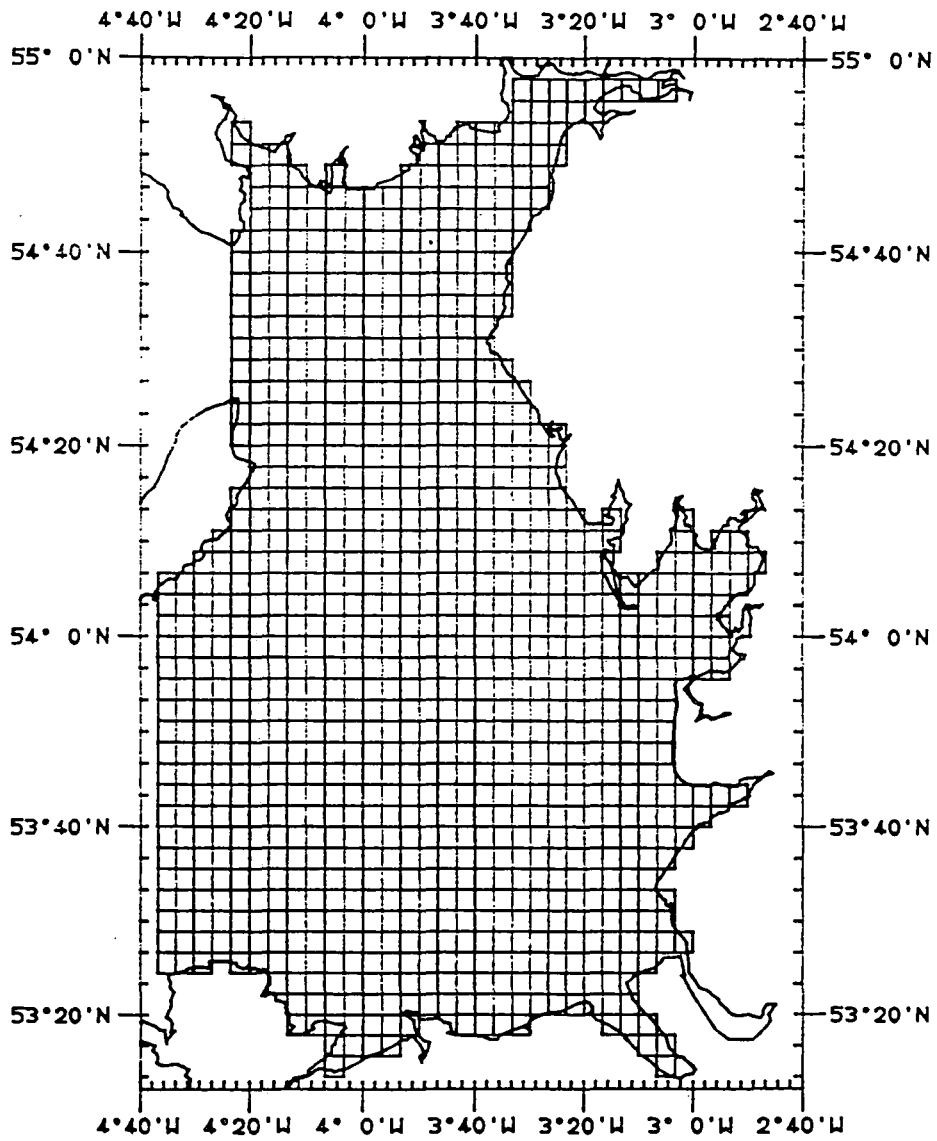


Figure 5.7. Liverpool Bay Model (LBM)

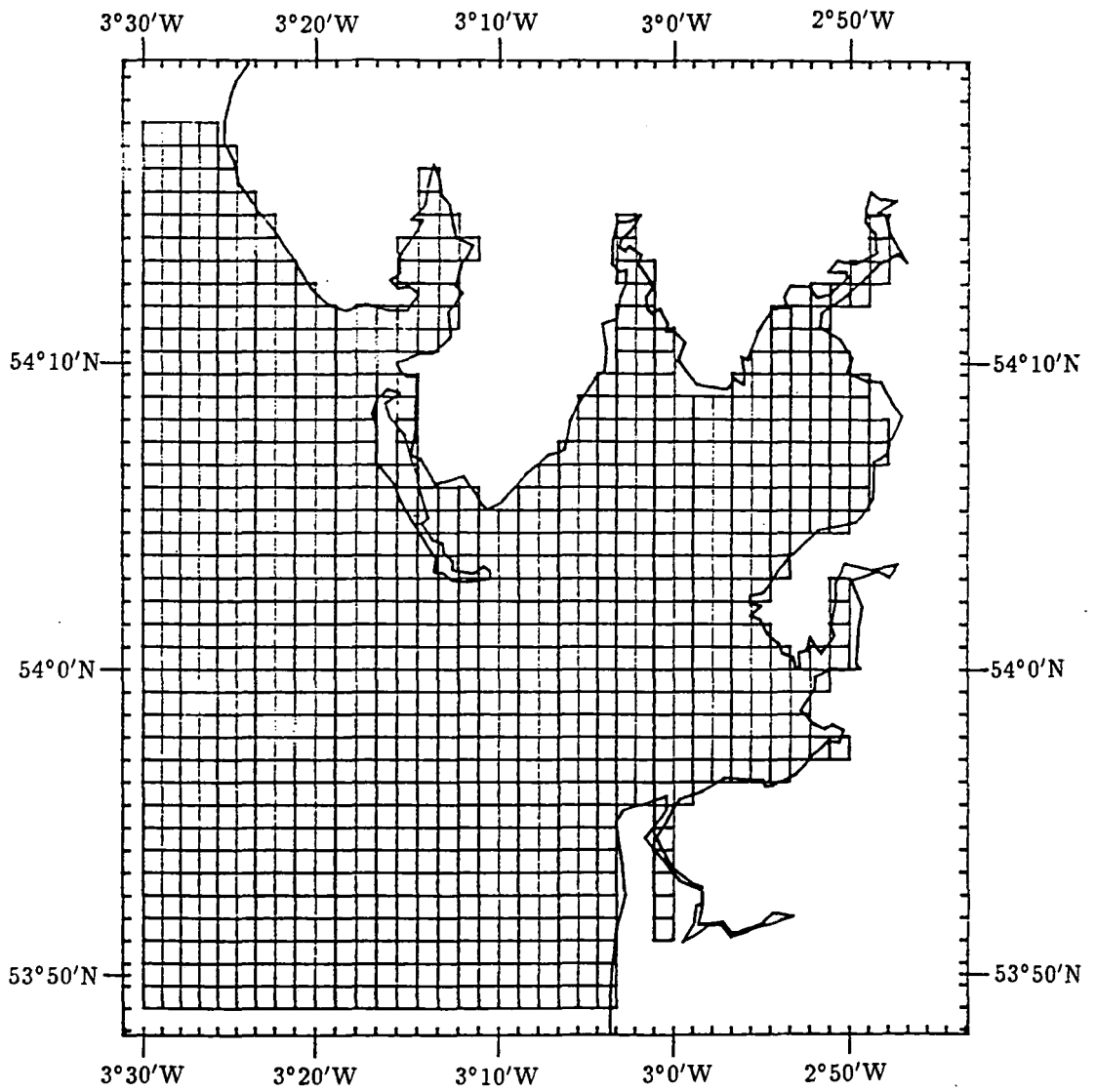


Figure 5.8. Morecambe Bay Model (MBM)

the data were collected from Admiralty Charts. The method used, in this case, was to overlay tracing paper on the chart with a grid drawn to the appropriate latitudinal / longitudinal scale required for the model. The mean value of the spot depths in each grid square was then taken as a representative value of the sea depth for that area. This method was modified in some nearshore areas in The Wash in order to resolve channel flow up rivers. In these areas, the very narrow nature of the channel meant that much of the grid rectangle comprised tidal flats, with altitudes above zero. In such cases the sea depth values from the channel were averaged and used as the depth value for the grid rectangle. The criterion used to determine whether a grid rectangle is “land” or “sea” is whether more or less than half of the area which it covers is “land” or “sea”, respectively. The same criterion was applied by the staff of the Proudman Oceanographic Laboratory in the extraction of their depth data.

Bathymetric data obtained from the Admiralty charts were relative to chart datum. These values were corrected to mean sea-level by adding the distance from the mean spring tide level (taken as half the mean spring range - the equivalent of the amplitudes of  $M_2$  together with  $S_2$ ) to mean tide level at Lowestoft and Immingham, the standard ports from the Admiralty Tide Tables (1990) in the area covered by the EC3 model.

From Table 5.1 it can be seen that the ratio of the mean spring tide level to mean tide level is approximately 1.5:1.0. A routine from the International Mathematics and Statistics Library (IMSL) was therefore used to interpolate results of ECM for values of  $(M_2 + S_2) \times 1.5$  over the area of the EC3 and Wash models at the appropriate resolution for each model. IMSL routine IQHSCV was used for this purpose. This routine provides smooth surface fitting for irregularly distributed data points and so overcomes the problem of interpolating results at irregular coastal boundaries in the tidal model. The interpolating function used is a fifth-degree polynomial in each triangle of a triangulation of the  $x - y$  projection of the surface. The interpolating function is continuous and has continuous first-order partial derivatives. The information required for use of the routine consists of the distance of points used for interpolation from the required location and the

**Table 5.1. Calculation of interpolation factor to apply to chart datum depths in order to obtain values for mean sea-level.**

<b>Standard Ports</b>	<b>Mean Spring Tide Level (<math>M_2 + S_2</math>)</b>	<b>Mean Tide Level (MTL)</b>	<b>Ratio (MTL/MSTL)</b>
Immingham	$(2.28 + 0.75) = 3.03$ metres	4.10 metres	$(4.10/3.03) = 1.35$
Lowestoft	$(0.70 + 0.21) = 0.91$ metres	1.50 metres	$(1.50/0.91) = 1.65$

values of the data points used. The output consists of a matrix of the interpolated values. The interpolated values of  $(M_2 + S_2) \times 1.5$  were then added to those at chart datum to give mean sea-level depths for use in the EC3 and WASH tidal models.

#### 5.2.1.1. Labels

Labels are used to indicate what calculations are to be carried out for each element. Elements are distinct from grid rectangles, as shown in Figure 5.9. Each element consists of one  $u$  (latitudinal) and one  $v$  (longitudinal) current value, together with a  $z$  value of sea surface elevation, whereas a grid rectangle has  $u$  and  $v$  currents flowing into and out of it. Where a  $z$  is at a point of dry land, a zero is put into the label. Where a value of a neighbouring  $z$  is zero, resulting in no current flow in one direction, a zero value is given to the appropriate  $u$  or  $v$  component. Where values are positive, “1”s are written into the label and the  $z$ ,  $u$  or  $v$  value is then used in the calculations of the model. Examples of resulting labels are shown in Figure 5.10.

The next step is definition of labels along the model boundaries and filling in with zero values for the land and parts of the grid outside the model boundaries. For an open sea boundary a value of “2”, rather than “1”, is used to indicate that a modification to the normal calculation must be made to allow for this fact. There is also a provision for spits, where there is a narrow section of land extending across the grid rectangle, but of insufficient width for the whole grid rectangle to be included as land. In these cases, no flow at a  $u$  or  $v$  point may be specified, with a zero value at the appropriate point in the label, as shown in Figure 5.11. Thus it is possible to establish, by this means, where the tidal calculations have to be made and to provide the bathymetric input data for the tidal model.

#### 5.2.2. Tidal input

Tidal calculations within the model area are made from the hydrodynamic equations described in Chapter 3 which are written in spherical polar coordinates in the model. However, as mentioned in Chapter 3.2.1.1, the tidal input is needed on the model boundary

Figure 5.9. Diagram to show the distinction between a grid box and an element

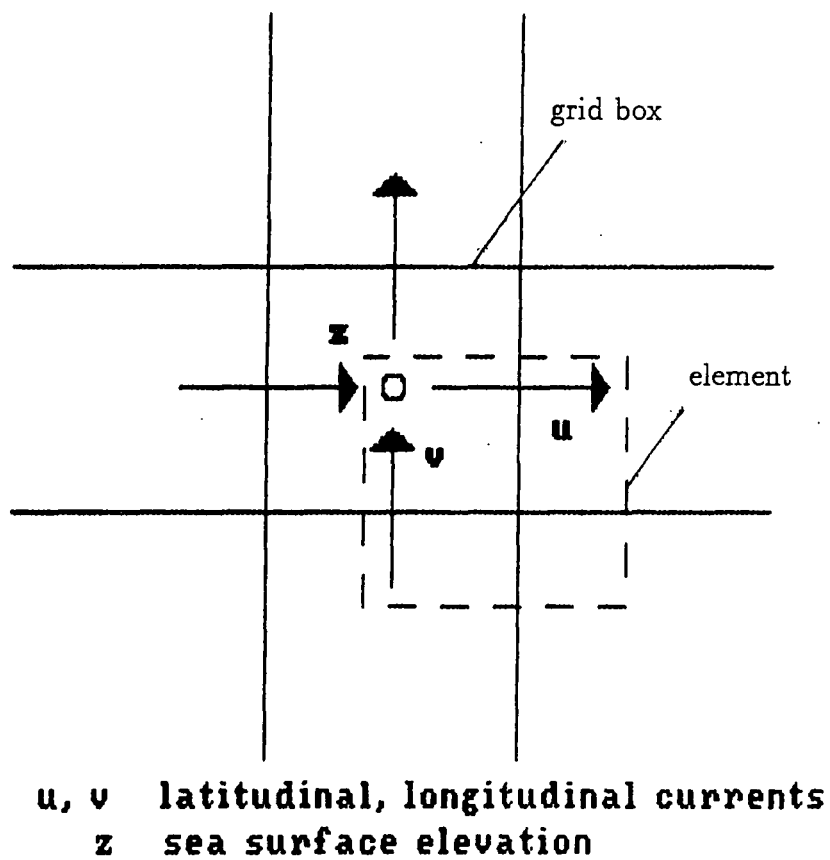
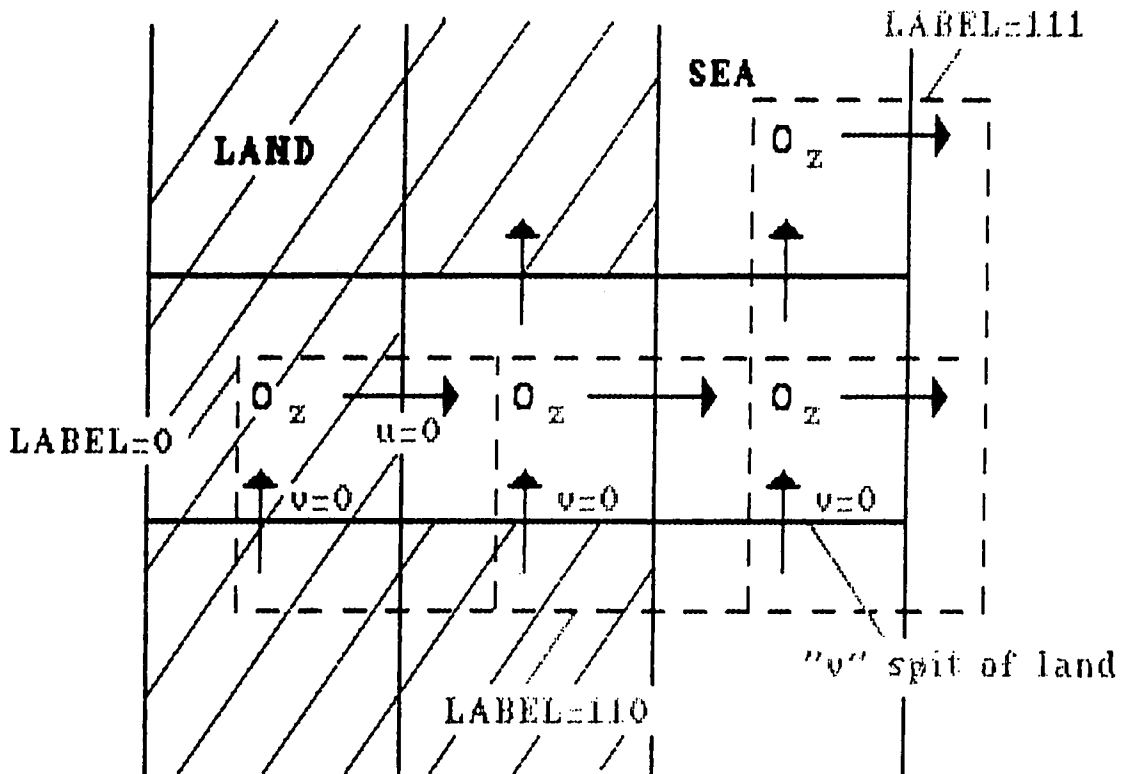


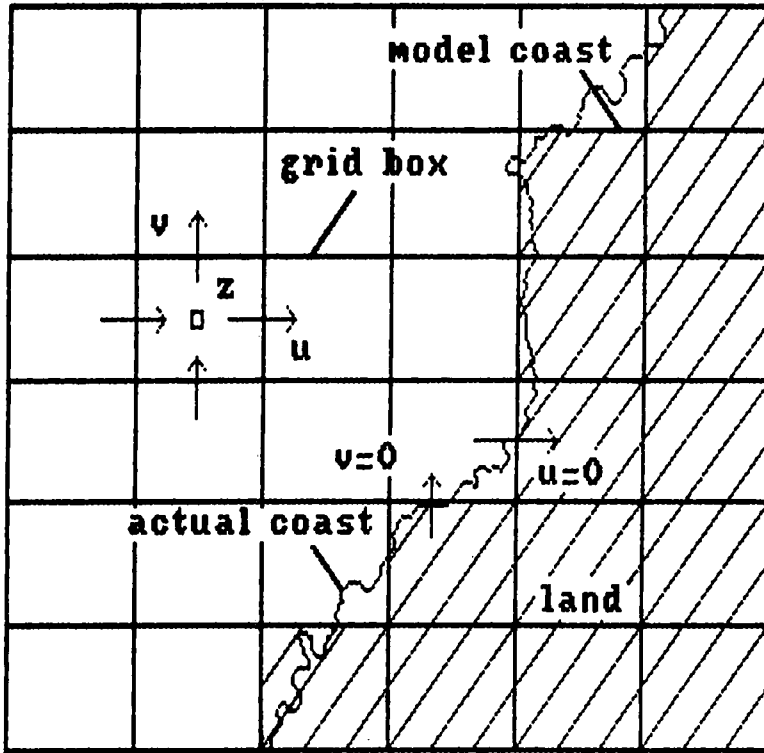
Figure 5.10. Examples of labels for various combinations of land and sea



**Label values for  $z$ ,  $u$  and  $v$  are given in that order.**

**$u$  and  $v$  label values are not calculated if  $z=0$ .**

Figure 5.11. Diagram to illustrate the conversion of real land and sea parameters into model format



**u, v** are latitudinal and longitudinal  
currents  
**z** is sea surface elevation



with open sea areas to provide the external tidal input from the oceans and to link together the series of tidal models. Tidal results from the next model up the scale are interpolated as boundary input to the more detailed model, although, in the case of the north-east Atlantic model, the tidal data for boundary input were provided by the Proudman Oceanographic Laboratory, Birkenhead.

For each tidal constituent used in the tidal models, the amplitude and phase values are read in from the grid rectangles of the less detailed model which correspond with the boundary of the tidal model for which input data is required. These are stored, for each constituent, in the form

$$H \cos c_g \quad (5.1)$$

$$H \sin c_g \quad (5.2)$$

where  $H$  is the tidal amplitude and  $c_g$  is the phase lag, equivalent to  $(\sigma t - g)$  from equation 3.12.

In a fuller development, the tidal input  $\hat{q}$ , defined as the sea surface elevation on the model boundary, given by  $\hat{\zeta}$ , is expressed in harmonic form as, for example,

$$\zeta = \sum_{e=1}^k f_e H_e \cos(\sigma_e t + n_e - c_e - g_e) \quad (5.3)$$

where  $\sigma_e$  is the speed and  $c_e$  is the phase of the corresponding Equilibrium constituent at Greenwich at time  $t = 0$  and  $f_e$ ,  $n_e$  are nodal factors which may be modified to allow for the 18.61 year variation in amplitude and phase of the constituent. The values of  $c_e$ ,  $f_e$  and  $n_e$  are computed for  $M_2$  and  $S_2$  with the input of the Equilibrium Tide in the north-east Atlantic model only.

The method of interpolation used to obtain the tidal boundary input is that of weighted averages. Examples of calculations are given in Figure 5.12.

Figure 5.12. Examples of calculations used to obtain the tidal input on an open boundary from a smaller resolution model

		1			2	
		a	b	c	d	
		e	f	g	h	
		i	j	k	l	
		3			4	

Examples of model boundary interpolation

a:  $(3 \times \textcircled{1})/3$

b:  $((2 \times \textcircled{1}) + 1 \times \textcircled{2})/3$

c:  $((1 \times \textcircled{1}) + 2 \times \textcircled{2})/3$

d:  $(3 \times \textcircled{2})/3$

e:  $((6 \times \textcircled{1}) + (3 \times \textcircled{3}))/9$

f:  $((4 \times \textcircled{1}) + (2 \times \textcircled{2}) + (2 \times \textcircled{3}) + (1 \times \textcircled{4}))/9$

g:  $((4 \times \textcircled{2}) + (2 \times \textcircled{1}) + (2 \times \textcircled{4}) + (1 \times \textcircled{3}))/9$

h:  $((6 \times \textcircled{2}) + (3 \times \textcircled{4}))/9$

i:  $((6 \times \textcircled{3}) + (3 \times \textcircled{1}))/9$

j:  $((4 \times \textcircled{3}) + (2 \times \textcircled{1}) + (2 \times \textcircled{4}) + (1 \times \textcircled{2}))/9$

k:  $((4 \times \textcircled{4}) + (2 \times \textcircled{2}) + (2 \times \textcircled{3}) + (1 \times \textcircled{1}))/9$

l:  $((6 \times \textcircled{4}) + (3 \times \textcircled{2}))/9$

(Coarser resolution model grid labelled 1-4)

### 5.3. Model program

The area of the north-east Atlantic Ocean extends from 37° North to 71°40' North, so the curvature of the earth and variation with latitude of the Coriolis acceleration are taken into account by using spherical coordinates (Flather, 1976). It is assumed that bottom stress is related to depth-mean current by the vector equation

$$\tau_b = k\rho\mathbf{q}|\mathbf{q}| \quad (5.4)$$

where  $\tau_b$  is the bottom stress,  $k$  is a constant,  $\rho$  is the water density and  $\mathbf{q}$  is the current vector. The equilibrium tide was only included in the north-east Atlantic model and is therefore excluded here. In this two-dimensional model, the equations of continuity and depth-mean motion are therefore written as

$$\frac{\partial\zeta}{\partial t} + \frac{1}{R\cos\phi} \left\{ \frac{\partial}{\partial\chi}(Du) + \frac{\partial}{\partial\phi}(Dv\cos\phi) \right\} = 0 \quad (5.5)$$

$$\begin{aligned} \frac{\partial u}{\partial t} + \frac{u}{R\cos\phi} \frac{\partial u}{\partial\chi} + \frac{v}{R\cos\phi} \frac{\partial}{\partial\phi}(u\cos\phi) - 2\omega\sin\phi v \\ = \frac{g}{R\cos\phi} \frac{\partial\zeta}{\partial\chi} + \frac{su(u^2 + v^2)^{1/2}}{D} \end{aligned} \quad (5.6)$$

$$\begin{aligned} \frac{\partial v}{\partial t} + \frac{u}{R\cos\phi} \frac{\partial v}{\partial\chi} + \frac{v}{R} \frac{\partial v}{\partial\phi} + \frac{u^2 \tan\phi}{R} + 2\omega\sin\phi u \\ = \frac{g}{R} \frac{\partial\zeta}{\partial\phi} + \frac{sv(u^2 + v^2)^{1/2}}{D} \end{aligned} \quad (5.7)$$

where  $\chi$  is east-longitude and  $\phi$  is latitude,  $t$  is time,  $\zeta$  is the elevation of the sea surface above the mean value and  $u_q$  and  $v_q$  are components of the depth mean current in the directions of increasing  $\chi$  and  $\phi$ , respectively,  $D$  is total water depth ( $h + \zeta$ ),  $h$  is the

undisturbed depth of water,  $R$  is the mean radius of the earth assumed spherical,  $\omega$  is the angular speed of the earth's rotation,  $s$  is a coefficient of bottom friction and  $g$  is the acceleration of the earth's gravity.

The hydrodynamic equations and equation of continuity are solved by means of finite difference techniques. The grid consists of a rectangular array of  $m$  rows and  $i$  columns. Elements, each consisting of a  $\zeta$ -point (or  $z$ -point), a  $u$ -point and a  $v$ -point are numbered consecutively

$$j = 1, \dots, i, i + 1, \dots, 2i, \dots, (m - 1)i + 1, \dots, mi$$

counting by element from left to right along each row and moving down row by row. Discrete values of the variables at grid points are denoted by subscripts. The basic tidal equations are written in finite difference form as (Proctor and Flather, 1983)

Equation of continuity:

$$\frac{\zeta_j^{t+\Delta t} - \zeta_j^t}{\Delta t} + \frac{1}{R \cos \phi_j} \left\{ \frac{d_j^t u_j^t - d_{j-1}^t u_{j-1}^t}{\Delta \chi} + \frac{k_{j-i}^t v_{j-i}^t \cos \phi - k_j^t v_j^t \cos \phi}{\Delta \phi} \right\} = 0 \quad (5.8)$$

U-equation of motion:

$$\begin{aligned} & \frac{u_j^{t+\Delta t} - u_j^t}{\Delta t} + \frac{1}{R \cos \phi} \frac{1}{2} \left( \frac{u_{j+1}^{t^2} - u_{j-1}^{t^2}}{2 \Delta \chi} \right) - 2 \omega \sin \phi \tilde{v}_j^t \\ & + \frac{1}{2R} \left\{ \frac{(v_{j-i}^t + v_{j-i+1}^t)(u_{j-i}^t - u_j^t)}{2 \Delta \phi} + \frac{(v_j^t + v_{j+1}^t)(u_j^t - u_{j+i}^t)}{2 \Delta \phi} \right\} \\ & = \frac{g}{R \cos \phi} \left\{ \frac{\zeta_{j+i}^{t+\Delta t} - \zeta_j^{t+\Delta t}}{\Delta \chi} \right\} - \frac{s u_j^{t+\Delta t} (u_j^{t^2} + \tilde{v}_j^{t^2})^{\frac{1}{2}}}{d_j^t} \end{aligned} \quad (5.9)$$

V-equation of motion:

$$\frac{v_j^{t+\Delta t} - v_j^t}{\Delta t} + \frac{1}{2R} \left( \frac{v_{j-i}^{t^2} - v_{j+i}^{t^2}}{2 \Delta \phi} \right) + 2 \omega \sin \phi \tilde{u}_j^{t+\Delta t}$$

$$\begin{aligned}
& + \frac{1}{R \cos \phi} \frac{1}{2} \left\{ \frac{(u_j^t + u_{j+i}^t)(v_{j+1}^t - v_j^t)}{2 \Delta \chi} + \frac{(u_{j-1}^t + u_{j+n-1}^t)(v_j^t - v_{j-1}^t)}{2 \Delta \chi} \right\} \\
& = \frac{g}{R} \left\{ \frac{\zeta_j^{t+\Delta t} - \zeta_{j+i}^{t+\Delta t}}{\Delta \phi} \right\} - \frac{sv_j^{t+\Delta t} (\tilde{u}_j^t + v_j^t)^{\frac{1}{2}}}{e_i^t} \quad (5.10)
\end{aligned}$$

where  $\frac{v}{R \cos \phi} \frac{\partial}{\partial \phi} (u \cos \phi)$  is approximated by  $\frac{v}{R} \frac{\partial u}{\partial \phi}$  in the U-equation (5.9) and the term  $\frac{u^2}{R} \tan \phi$  is ignored in the V-equation (5.10).  $u_j^t$  and  $v_j^t$  are the latitudinal and longitudinal components of the depth-mean current at  $u$ - or  $v$ -point  $j$  at time  $t$ ,  $\tilde{v}_j^t = \frac{1}{4}[v_j^t + v_{j+1}^t + v_{j-i+1}^t + v_{j-i}^t]$  and  $\tilde{u}_j^t$  is represented in the same way, replacing each  $v$  in the equation above with a  $u$ .  $\Delta t$  is the timestep,  $\zeta_j$  is the sea-surface elevation above the undisturbed water depth  $h_j$  at  $\zeta$ -point  $j$ ,  $s$  is the friction coefficient and  $d_j^t = \frac{1}{2}[h_j + \zeta_j^t + h_{j+1} + \zeta_{j+1}^t]$  and  $k_j^t = \frac{1}{2}[h_j + \zeta_j^t + h_{j+i} + \zeta_{j+i}^t]$ .

The model provided by Dr. Roger Flather of the Proudman Oceanographic Laboratory has two possible means of tidal calculations along the open boundary. The first is an elevation-specified condition in which the amplitude and phase of each tidal constituent are input along the boundary. The boundary elevation is thus specified as a function of position and time by the equation

$$\zeta = \hat{\zeta}(s', t) = H \cos(\sigma t - g) \quad (5.11)$$

where  $\zeta$  is the sea surface elevation,  $s'$  and  $t$  are elements of space and time,  $H$  is tidal amplitude,  $g$  is the gravitational constant and  $\sigma$  is the angular frequency. The second method is a radiation condition which prescribes a relationship between elevation and current at the boundary. The radiation condition used is written as

$$\mathbf{q} = \hat{\mathbf{q}} + \frac{c}{h}(\zeta - \hat{\zeta}) \quad (5.12)$$

(where  $c = (gh)^{1/2}$  and  $\hat{\mathbf{q}}$ ,  $\hat{\zeta}$  describe the tidal input, as  $\mathbf{q}$  represents the component of depth-mean current normal to the boundary,  $\hat{\mathbf{q}}$  is the depth-mean current,  $c$  is the speed

of progression of the tidal wave,  $h$  is the water depth,  $g$ , the gravitational constant,  $(\zeta - \hat{\zeta})$  represents the difference of the computed sea surface elevation from the prescribed tidal input) seeks to prevent the artificial reflection from the open boundary of disturbances generated within the model by making them propagate out, locally, as free progressive waves (Proctor and Flather, 1983).

At a coastline the boundary condition is set to

$$\mathbf{q} = 0 \tag{5.13}$$

where  $\mathbf{q} = 0$  is the component of depth-mean current along the outward-directed normal to the boundary.

The bottom friction parameter is set at 0.0025 in the present model. The value of 0.0025 used in the present study is similar to that found from observations by Taylor (1919), as discussed in Chapter 3.1.2. This factor may have changed during the Holocene with shallower water levels, as is discussed in Chapter 6.

Two factors in the model input data were changed between the north-east Atlantic model and the more detailed coastal models. In the north-east Atlantic model the Equilibrium tide is included in tidal calculations because of its influence on tide generation in the oceans. There is, however, little effect from the Equilibrium tide on the continental shelf (Pugh, 1987). Horizontal eddy viscosity was used in the north-east Atlantic model, but excluded from the shallower water models. It was employed in the north-east Atlantic model to smooth out grid-scale oscillations at the shelf break.

A further parameter altered between models is the timestep which, as explained in Chapter 3, must satisfy the equation

$$\Delta T < \frac{\Delta S}{\sqrt{2gh_{max}}} \tag{5.14}$$

where  $\Delta T$  is the timestep in seconds,  $\Delta S$  is the grid width,  $g$  is acceleration due to gravity and  $h_{max}$  is the maximum water depth in the model. This is varied between models due to the control of water depth. The timesteps used in calculations for each of the models are given in Table 5.2.

Tidal calculations in areas of the models which dry out, such as tidal flats, are dependent on the depth difference between neighbouring grid rectangles for the tidal calculation to be employed. Flather and Hubbert (1990) have reviewed and extended the methods of modelling areas that dry out.

The method used in the current model (Flather and Heaps, 1975) requires definition of a critical depth for drying (1.0 metre used in this study) and a critical elevation difference (0.1 metres here) chosen so as to prevent the drying and flooding of a grid rectangle at alternate timesteps. The critical depth for drying is needed to prevent problems with the calculation of surface and bottom terms in the momentum equations in which the total water depth is in the denominator.

Flather and Hubbert (1990) divided the drying procedures used in numerical models into two types. The first are those useful in embayments with large, shallow and relatively flat areas, separated by deep channels and creeks. The entire bay area may be water-covered at high tide, but as levels fall the shallow areas are exposed and ultimately the flow is confined to the deeper channels. A variety of methods have been used in this case to determine when a grid rectangle becomes wet or dry. Most methods use a condition of zero normal flow,  $\mathbf{q} = 0$ , on the coastal boundary, which is constrained to follow the sides of grid rectangles and thus moves in discrete steps. This is a simple scheme and is used in the present model, but may have the disadvantage of generating “noise” where compromises have to be made for the movement of the land-water interface in steps of discrete grid rectangles.

Flather and Hubbert’s (1990) second group of drying processes comprise nearshore regions characterised by relatively uniform shelving bathymetry. Sielecki and Wurtele

**Table 5.2. Timesteps used for the Tidal Models**

<b>Tidal Model</b>	<b>Timestep (seconds)</b>
North-east Atlantic Model	72.00000
West Coast Model	60.00000
East Coast Model	186.30900
Liverpool Bay Model	60.00000
East Coast 3 Model	93.15451
Morecambe Bay Model	10.00000
Wash Model	20.00000



(1970) used a technique involving linear extrapolation of total water depth and momentum for use in the continuity equation at each grid rectangle containing the land-water interface. Lynch and Gray (1980) used a different method, with the finite element technique, involving deformation of the grid. At the land-water interface, the velocity of a fluid particle is equal to the velocity with which the interface moves. This may cause large additional amounts of computation. Johns *et al.* (1982) used a similar method with the finite difference technique.

The second group of drying processes represent the physical process of inundation and drying much more satisfactorily than the first group, but tend to be much more complex and difficult to apply in areas with large tidal flats and creek systems (Flather and Hubbert, 1990), such as The Wash and Morecambe Bay. The first method described above is therefore used in the present tidal model.

#### 5.4. Harmonic analysis

Harmonic analysis of the tidal data was carried out from the model results. This was done in order to obtain the amplitude and phase of each tidal constituent for use as boundary input to the next model down the hierarchy.

Harmonic analysis is carried out using the Gauss-Seidel method. The elevation and current data obtained from the model program is set up in the form of elements of a matrix. The series of simultaneous equations thus obtained are solved over time for the frequency of each tidal constituent required. The equation thus takes the form

$$E \times \Delta T^{-1} = HO \quad (5.15)$$

where  $E$  is a matrix consisting of the values of elements predicted from the model,  $HO$  is a matrix consisting of the values of amplitude and phase of the required harmonic constituents and  $\Delta T$  is the timestep used in the tidal model.

#### 5.4.1. Constituents used

Tidal constituents were chosen to obtain an estimate of the level of mean high water of spring tides for each grid rectangle. The level of mean high water of spring tides is required as it is the altitude recorded by most sea-level indicators, as discussed in Chapter 1. Doodson and Warburg (1941) provided a basic estimate of the level of mean high water of spring tides ( $z_0$ ) as

$$z_0 = M_2 + S_2 \quad (5.16)$$

neglecting shallow water constituents. Shallow water constituents were, however, considered to be important in the field areas, following the discussion in Doodson and Warburg (1941). Shallow water harmonics of  $M_2$  and  $S_2$  have therefore been included in the analysis from each model. The constituents used for input to the tidal models within the continental shelf are therefore  $M_2$ ,  $S_2$ ,  $2MS_2$  (or  $Meu_2$ ),  $M_4$ ,  $M_6$  and  $MS_4$ . It was noted in Chapter 3 that the even-order shallow water constituents tend to have a greater effect on tidal amplitudes than the odd-order constituents. The constituents chosen were used following Doodson and Warburg (1941).

The method of obtaining a value for mean high water of spring tides at each grid element was to take the maximum value from a 15 day run of the tidal model, covering a spring-neap tidal cycle. This also covered a long enough time span for  $M_2$  and  $S_2$  to be analysed independently (see discussion in Chapter 3.1.6.1.), so that input on the open boundary to the next model down the hierarchy for each constituent could be obtained. This did not provide a mean value for the altitude of high water of spring tides, but longer runs of each model were not possible in the time available with the existing computing resources. An estimate of the maximum error in obtaining a mean value for the high water of spring tides was taken as half of the difference between the figure for Mean High Water of Spring tides (MHWS) and that for Mean High Water of Neap tides (MHWN) from the Admiralty Tide Tables (1990) (see Table 5.3). This method assumes, by taking

**Table 5.3. Mean High Water Altitudes for The Wash and Morecambe Bay (from Admiralty Tide Tables, 1990)**

Mean High Water of Spring Tides MHWS

Mean High Water of Neap Tides MHWN

Tidal heights are given in metres relative to Chart Datum.

<b>Location</b>	<b>MHWS</b>	<b>MHWN</b>	<b>Difference (MHWS - MHWN)</b>
<b>The Wash</b>			
Hunstanton	7.4	5.6	1.8
West Stones	7.0	5.4	1.6
King's Lynn	6.8	5.0	1.8
Wisbech Cut	7.0	5.1	1.9
Lawyers Sluice	7.0	5.2	1.8
Tab's Head	7.5	5.6	1.9
Boston	6.8	4.8	2.0
Skegness	6.9	5.3	1.6
Inner Dowsing Light Tower	6.4	5.1	1.3
<b>Morecambe Bay</b>			
Barrow (Ramsden Dock)	9.1	7.1	2.0
Hawes Point	9.2	7.1	2.1
Ulverston	9.3	7.3	2.0
Arnside	9.8	7.6	2.2
Morecambe	9.5	7.4	2.1
Heysham	9.4	7.4	2.0

the midpoint between MHWS and MHWN, that the variation in range of the spring tides is equal to that of the neap tides. For The Wash, the MHWS - MHWN tidal height differences vary from 2.00 metres at Boston to 1.60 metres at West Stones and 1.30 metres at the Inner Dowsing, beyond the mouth of The Wash, giving a maximum error in the estimation of MHWS of between 0.65 and 1.00 metres. For Morecambe Bay, differences vary from 2.20 metres at Arnside to 2.00 metres at Barrow, Heysham and Ulverston, giving a maximum error in the estimate of MHWS of 1.00 to 1.10 metres. The accuracy of model results for present sea-level in comparison with figures for the mean high water of spring tides from the Admiralty Tide Tables (1990) is assessed in Chapter 6.

Abstraction of maximum water levels was preferred to calculation of the level of mean high water of spring tides from the equation provided by Doodson and Warburg (1941) (Eqn. 5.37 above) due to the distortion to the tidal wave in shallow water areas created by the drying out of shallow water areas model calculations. If an area were to dry out at any state of the tide, calculation of the harmonic terms could only be based on the part of the tidal curve for the time during which the sea inundated the area and the constituents would therefore have amplitudes which are lower than in reality. This reduction of the amplitude of tidal constituents would result in an incorrect model prediction value for the mean high water of spring tides wherever drying out occurs during a tidal cycle. In presentation of the model results in Chapter 6, the terms “maximum tidal altitudes” or “maximum tidal heights” are employed when discussing the model results used as equivalents to the mean spring high tide levels.

Model results, based on the aims of the study outlined in Chapter 1, are presented and analysed in Chapter 6. The results are considered relative to the contribution of factors not studied in this thesis in determining the altitudinal variation of sea-level index points within each embayment in Chapter 7 and the conclusions are presented in Chapter 8.

## CHAPTER 6

### TIDAL CHANGES WITHIN THE WASH AND MORECAMBE BAY

#### 6.1. Procedure adopted to obtain results

Seven tidal models, described in Chapter 5, were used to obtain tidal simulations. Each of these used essentially the same FORTRAN 77 programs, outlined below. For each model, two programs were run prior to the tidal simulation program. The first of these consists of reading in sea depth data for the model run and the location of any spits, the number of grid rectangles per degree latitude and longitude and the latitudinal and longitudinal locations of the model boundaries. The labels for each grid rectangle (described in Chapter 5.2.1.1) may be either read in as part of the dataset or calculated from the bathymetric data to determine whether '1's or '0's should be assigned to the  $z$ ,  $u$  and  $v$  values. The location of the edge of the model grid is calculated and when this is reached appropriate labels for open boundaries are assigned, as described in Chapter 5.2.1.1. These data are stored in binary format for use in the tidal model.

The second program used to set up data for the tidal model consists of reading tidal input on the model open boundaries into binary format. The tidal data is read in and stored in the form of  $H \cos c_g$  and  $H \sin c_g$  (see Chapter 5.2.2) for each of the non-zero  $z$ ,  $u$  and  $v$  label positions on the open boundaries of the tidal models for each tidal constituent. Data for each tidal constituent is also needed; *viz.* the speed of the constituent, coefficients for the nodal factors  $f$  and  $n$  (described in Chapter 5.2.2) and coefficients for the phase of the equilibrium tide at Greenwich at the start time ( $t = 0$ ) of the model run. The equilibrium tide is only used in the North-east Atlantic model as explained in Chapter

## 5.2.

The tidal model program uses the bathymetric data to calculate tidal heights for each grid rectangle based on the open boundary tidal input and resolution of the equations of continuity and momentum within the model grid area. The equations on which the FORTRAN 77 program is based together with other variables used in the model are explained in Chapter 5.3. The timestep (interval between tidal calculations) for each model was set according to the bathymetric values to comply with equation 3.23 to relate the size of the grid spacing and water depth to the timestep used to ensure stability of the numerical solution. Table 5.2 gives the timesteps used in each tidal model. A series of parameters and counters are used to determine the number of timesteps in the model run. The number of timesteps was set to allow for a length of 15 days' model run to cover the 14.77 days needed for the separation of  $M_2$  and  $S_2$  in harmonic analysis, described in Chapter 3.1.6.1.

Modification to the basic tidal model program obtained from Dr. Roger Flather of the Proudman Oceanographic Laboratory was made to facilitate running the tidal models at lower sea-levels. Calculations of tidal heights based on the tidal generation within the model area were made for each grid rectangle prior to the addition of the tidal influence from the open boundary of the model. This was done to avoid the effect within the model of zero tidal heights due to drying on the open boundary at some stages of the tide at lower sea-levels. The consequent lack of tidal propagation would give zero water depth values while tidal generation within the model area alone might result in inundation of the grid rectangles concerned. This overcame the problem of inclusion of a zero current value for the element where a non-zero value had been specified in the labels in the setup data.

The model program obtained from the Proudman Oceanographic Laboratory was further modified to write out the maximum tidal height recorded in each grid rectangle over the length of the model run. The maximum values were used as a surrogate for mean

high water of spring tides values, as explained in Chapter 5.4.1.

In order to obtain tidal open boundary input for each of the six tidal constituents ( $M_2$ ,  $S_2$ ,  $Meu_2$ ,  $M_4$ ,  $M_6$  and  $MS_4$ ) down the model hierarchy, harmonic analysis was carried out on the results of all except the WASH and MBM models. The model results are written out in the form of equation 5.36 to give the computed tidal amplitude ( $H$ ) and phase speed ( $c_g$ ) for each of the elevation ( $z$ ) and latitudinal ( $u$ ) and longitudinal ( $v$ ) currents. The harmonic analysis results are then converted into  $H \cos c_g$  and  $H \sin c_g$  results by multiplying the tidal amplitude by the cosine and sine of the phase speed value for each tidal constituent for each  $z$ ,  $u$  and  $v$  value.

The harmonic analysis results are used as tidal boundary input to the next model down the hierarchy using a weighted interpolation method on the principle of least squares, illustrated in Figure 5.12. Input of the constituents to each model gives the best potential of predicting mean high water of spring tides heights, following Doodson and Warburg (1941). In the case of the North-east Atlantic model, however, open boundary tidal input in deep water was only available from the Proudman Oceanographic Laboratory for the semi-diurnal constituents,  $M_2$  and  $S_2$ . The remaining four constituents were analysed from the results of the north-east Atlantic model for input on the boundaries of the WCM and ECM models on the continental shelf. The interpolation method used for obtaining values on the open boundaries of the models is the simplest available and takes into account variations in the tidal values related to their distance from the required grid rectangle, so allowing for non-linearity in tidal values in neighbouring grid rectangles. The interpolation shown in Figure 5.12 was at the same scale for each model down the hierarchy as the increase in resolution from one model to the next was always nine-fold. The interpolation method was modified in coastal areas to avoid use of areas which dried out in the tidal cycle and had distorted harmonic analysis results as a consequence of the flattening of the sine and cosine waves fitted to the tidal model results in the harmonic analysis method. To allow for non-use of grid rectangles which dried out, heavier positive weighting values were given to grid rectangle results in the immediate neighbourhood of

the required point than those shown in Figure 5.12 and negative weighting was applied to more results from distant grid rectangles.

The tidal model program, together with the programs for setting up the bathymetry and tidal input data and the harmonic analysis program, may be viewed on application to Dr. Roger Flather, Proudman Oceanographic Laboratory, Birkenhead.

## **6.2. Limitations of the analysis**

Limitations of the analysis of model results fall into two categories; those resulting from assumptions made with the model parameter changes at lower sea-levels and the accuracy of reconstructing the former palaeogeographies of the areas from the geological information available. The accuracy of model parameters used is discussed here, while factors affecting the accuracy of the sedimentary record from which the palaeogeographic reconstructions are derived are the subject of Chapter 7.

### **6.2.1. Ocean/ shelf boundary tidal changes**

A nested series of models was run in order to obtain input to the bay models from the Atlantic Ocean. This was carried out in order to avoid changes to tidal amplitudes in the embayments caused by inaccuracy in assessing the open boundary tidal input at the continental shelf edge. Tidal input from the ocean was considered to be important in the study as a result of the different predominant mechanisms involved in tidal amplitude generation on the continental shelf compared with those of the open ocean. Much larger tidal amplitudes are found on the continental shelf than those in the open ocean due to the different mechanisms involved in tidal generation in each area. The tide on the continental shelf is driven by co-oscillation with the ocean tide.

No modifications were made to the open boundary tidal input supplied by the Proudman Oceanographic Laboratory for the NEA model for changes of sea-level. This is justified by the argument that the shape of the ocean basins and alterations to astronomical variables, which affect the gravitational forcing potential of the tide, are assumed not



to have changed significantly during the Holocene. Furthermore, other external factors affecting the ocean tide, such as the influence of other shelf tides and interaction of the tide with changing oceanographic and climatic patterns, which are not easily quantifiable are likely to have been small, as argued by Austin (1991).

In a test of the effect of shelf changes on the ocean tide, Austin (1991) compared his results for lower sea-level simulations using a model of the continental shelf for those of the present author from the NEA model. He found that use of the NEA model tidal boundary input for a reduced sea depth simulation of 15 metres resulted in elevations of the  $M_2$  tide 5% lower at coasts than using the model covering the continental shelf alone.

### **6.2.2. Sea bed friction**

The bottom friction parameter used in the tidal models is maintained as  $s = 0.0025$  in all model simulations. Pingree and Griffiths (1979) found that the value of  $s$  used for the continental shelf area caused overestimation of local  $M_2$  amplitudes in shallow water areas, such as coastal embayments. This suggests that tidal amplitudes may have been lower than model simulations indicate during the early Holocene in particular when there were extensive areas of shallow seas. Austin (1991) also points out that the underwater topography immediately following glacial scouring and deposition may have imposed a different effective bed roughness than that of the present day. It was noted in Chapter 2 that much offshore sedimentation during the Holocene has consisted of redistribution of pre-existing deposits, largely controlled by bathymetry (Caston, 1979). Both these factors suggest that slightly higher values of the bottom friction coefficient may be appropriate within the embayments, especially for lower sea-levels than present. However, as is shown in Chapter 6.4, heights of mean high water of spring tides are predicted with reasonable accuracy in both the Wash and Morecambe Bay for present sea-levels. The friction coefficient is at best a crude estimate (Taylor, 1919), as discussed in Chapter 5, and results from the tidal models are relatively insensitive to changes in this parameter (Flather, 1976).

### 6.2.3. Eustatic sea-level changes

Changes in eustatic sea-level made in the present study employ Mörner's (1976, 1980, 1984) eustatic curve which shows an oscillating rise in sea-level to approximately 5,000 years B.P. from which time sea-levels are shown as oscillating around present values. However, Shennan (1987, 1989) modified this in his assessment of isostatic changes during the Holocene to smooth out the oscillations, as shown in Figure 4.13. Debate continues in the literature (*cf.* Kidson, 1982) on whether the Holocene sea-level rise has occurred in a series of oscillations or a smooth increase in sea depths to approximately present levels at 5,000 years B.P. Mörner's eustatic curve includes data from Scandinavia which is shown, even at the present day, to be subject to neotectonic movements along faults (*cf.* Anundsen, 1985) associated with the large amount of isostatic uplift recovery from the last glacial. This casts doubt on whether the oscillations in Mörner's curve are the result of real eustatic sea-level change or more local sea-level change factors. Mörner's curve is used in this study as a best estimate of eustatic sea-level changes during the Holocene. A further incentive in employment of Mörner's eustatic sea-level estimations was the use of these by Shennan (1987, 1989) in his work on isostatic movements in Britain during the Holocene. The results of Shennan's work are employed to modify sea depths in the palaeogeographic reconstructions of the embayments in order to include an estimate of sea-level change as a result of isostatic movements. Shennan (1987) estimated the error in the use of Mörner's eustatic curve as being of the order of  $\pm 2$  metres.

### 6.2.4. Isostatic bathymetry changes

Sea depth modifications are made in the palaeogeographic reconstructions of the Wash and Morecambe Bay for the response of the land to glacial unloading, following calculations by Shennan (1987, 1989). However, two factors are noted in the use of these calculations. Firstly, Shennan's analysis is based on the existing sea-level index point record and therefore contains errors related to the accuracy of these points in reflecting sea-level. Secondly, no account is made for hydroisostatic changes due to post-glacial

water loading effects on former land areas which would reduce the amount of any crustal rebound.

Results of Shennan's work (1987, 1989) are used as best estimates of isostatic movements during the Holocene in this study. Discussion continues in the literature concerning models of crustal response to ice/ water loading (*cf.* Mörner, 1987; Peltier, 1987) and without sufficient knowledge of rheological properties it is difficult to assess the accuracy of any proposed model.

Post-glacial isostatic movements cannot be neglected in reconstructions of former land/sea-level altitudes in Britain. Shennan's results (1989) show linear subsidence during the Holocene of approximately 1.0 metre per thousand years in the Fenland, compared with a eustatic sea-level change of about 2.0 metres over the last 5,000 years. Lack of data on neotectonic movements precludes any changes to model bathymetries as a result of this factor. This point is discussed further in Chapter 7.

#### **6.2.5. Sediment movements**

Offshore sediment variations are not studied directly in this thesis, although a test of the influence of sediment pattern changes within embayments is made, such as might occur with the movement of sand banks. The details of this modification to the present sea-level models are given in Chapter 6.4. Sediment movement during the Holocene has largely consisted of a redistribution of pre-existing sediments, as is discussed in Chapter 2, with infilling of 'deeps', such as the Lune Deep, Morecambe Bay. Linear sand banks have also been formed in the shallower waters of the North Sea and are associated with the action of currents. Austin (1991) suggested that the localised nature of the sediment changes may imply that their effects on tides may also be localised. The test carried out in Chapter 6.4 simulating sediment distribution changes within the embayments under study therefore provides a test of this suggestion.

### 6.3. Presentation of results

In this chapter, results of the tidal model runs are presented for The Wash and Morecambe Bay. Results of the NEA, WCM and ECM models are not presented as these were only run in order to obtain results for input to other models down the hierarchy allowing for changes to the tidal regime at different sea-levels at the continental shelf edge. A summary of the models used in producing the results examined in this thesis is given in Table 6.1. Due to the limited amount of time and computing resources available it has not been possible to analyse all the model runs intended. In place of analysing the WASH and MBM models (very expensive in terms of computing time and space) for robustness, sea depth changes and coastline changes results for the nine square kilometre (EC3 and LBM) models are compared with present sea-level run results. Results of the EC3 and LBM models for present sea-level and palaeogeographic coastlines with depth changes are compared with the finest (one square kilometre) WASH and MBM embayment model runs.

In assessing the accuracy of the model runs, it was recognised that whereas the models return one average value for the tide in each grid rectangle, tide gauge observations represent point samples within or adjacent to the model grid rectangle. Emphasis is placed on the overall distribution of comparisons between model predictions and observations although the only means of checking results is at point locations. The point locations chosen for use in the analysis of results are, in the main, at the coastline or on or near positions of a former simulated coastline position in a given model, especially in the WASH and MBM models. The points have been chosen so as to provide a comparison with the sea-level index point data (discussed in Chapter 6.9.1 and 6.9.2), which provide evidence of the location and altitude of the coastline around the embayments during the Holocene. The same points are used in all the statistical analyses and representations of the model simulations in histograms, scatter plots and diagrams of the descriptive statistics of the model simulations. Statistical techniques applied to the model results in this chapter are not designed for spatial data, but are used as best estimates of accuracy, although

**Table 6.1. Table to Summarise the Characteristics of each Tidal Model employed.**

<b>Model Name in full</b>	<b>Short Name used in the text</b>	<b>Latitudinal Extent</b>	<b>Longitudinal Extent</b>	<b>Approximate Grid Resolution (km)</b>
North-east Atlantic Model	NEA	37° North - 71°40.00' North	30° West - 25°30.00' East	30 × 30
East Coast Model	ECM	49°20.00' North - 55° North	1°10.00' West - 4°40.00' East	9 × 9
East Coast 3 Model	EC3	52°8.89' North - 53°57.78' North	0°13.30' West - 2°56.67' East	3 × 3
WASH Model	WASH	52°47.40' North - 53°19.26' North	0°1.10' West - 0°58.90' East	1 × 1
West Coast Model	WCM	50° North - 56°20.00' North	8° West - 3°20.00' West	9 × 9
Liverpool Bay Model	LBM	53°13.30' North - 54°56.67' North	4°36.67' West - 2°50.00' West	3 × 3
Morecambe Bay Model	MBM	53°48.89' North - 54°17.78' North	3°30.00' West - 2°47.78' West	1 × 1

it is recognised that spatial changes due to a factor not examined here may influence the results. Alterations to tidal altitudes using different model sea-levels and coastlines may occur due to a variable not included in the analysis. Description of model results, presented in diagrammatic form in the figures in Volume 2 of this thesis (with the original data for all simulations in Appendix 6.3, presented on diskette), is followed by comparisons of changes to tidal altitudes within and between model simulations. A summary of the model simulations carried out is given in Table 6.2.

Model results are referred to mean sea-level as zero. However, sea-level index point altitudes are given relative to Ordnance Datum. To facilitate comparison of results, Table 6.3 gives the differences between Ordnance Datum and mean sea-level, taken from the Admiralty Tide Tables (1990). It is common to express results in tidal studies relative to mean sea-level from the tidal models and this procedure is adopted here. It can be seen from Table 6.3 that values for Ordnance Datum (defined as the average value of mean sea-level at Newlyn, Cornwall, from 1915 to 1921) do not differ greatly from those for mean sea-level in The Wash and Morecambe Bay, reaching a maximum for mean sea-level of 0.36 metres above O.D. at Skegness, in the area of The Wash, and 0.21 metres above O.D. at Barrow, Morecambe Bay. Due to relative sea-level rise, O.D. is now about 0.2 metres below mean sea-level at Newlyn (Admiralty Tide Tables, 1990). When this figure is subtracted from results in Table 6.3, the differences between sea-level index point altitudes (related to O.D.) and mean sea-level are minimal, with a maximum difference of 0.16 metre at Skegness. The error involved in making the assumption of O.D. equal to mean sea-level is minimal in the light of the errors in model predictions of maximum tidal heights shown below.

In the next section, the ability of the tidal models to simulate observed tidal heights at the present day is assessed. After this the series of tests carried out on the tidal models is described, outlining the reasoning behind the use of each test, presenting the results of each for The Wash and Morecambe Bay and assessing their usefulness in terms of the study of tidal component to sea-level changes within the embayments during the Holocene.

**Table 6.2. Table to show Model Simulations Carried Out (indicated by ‘Yes’).**

Model Name	Present Sea-Level [0]	Modification 1 (spit)	Modification 2 (depth changes)
NEA	Yes	-	-
ECM	Yes	-	-
EC3	Yes	Yes	Yes
WASH	Yes	-	-
WCM	Yes	-	-
LBM	Yes	Yes	Yes
MBM	Yes	-	-

Model Name	Reduced Sea Depth Simulations (metres reduction compared with present sea-level)			
	[2]	[5]	[10]	[15]
NEA	Yes	Yes	Yes	Yes
ECM	Yes	Yes	Yes	Yes
EC3	Yes	Yes	Yes	Yes
WASH	-	-	-	-
WCM	Yes	Yes	Yes	Yes
LBM	Yes	Yes	Yes	Yes
MBM	-	-	-	-

Model Name	Palaeocoastline Simulations			
	3,000 Years B.P.	4,000 Years B.P.	5,000 Years B.P.	8,000 Years B.P.
NEA	-	-	-	-
ECM	-	-	-	-
EC3	Yes	Yes	Yes	-
WASH	-	-	-	-
WCM	-	-	-	-
LBM	-	-	Yes	Yes
MBM	-	-	-	-

Model Name	Palaeogeographic Reconstructions				
	3,000 Years B.P.	4,000 Years B.P.	5,000 Years B.P.	8,000 Years B.P. (higher sea-level)	8,000 Years B.P. (lower sea-level)
NEA	-	-	-	-	-
ECM	-	-	-	-	-
EC3	Yes	Yes	Yes	-	-
WASH	Yes	Yes	Yes	-	-
WCM	-	-	-	-	-
LBM	-	-	Yes	Yes	Yes
MBM	-	-	Yes	Yes	Yes

**Table 6.3. Altitude of Mean Sea-Level (MSL) relative to Ordnance Datum (OD) in metres (from Admiralty Tide Tables, 1990)**

<b>Location</b>	<b>Difference (MSL - OD)</b>
<b>The Wash</b>	
Skegness	0.36
Tabbs Head	0.12
Hunstanton	0.05
Cromer	0.22
<b>Morecambe Bay</b>	
Barrow	0.21
Hawes Point	0.19
Heysham	0.20



## 6.4. Accuracy of model results

Results for present sea-levels for EC3, WASH, LBM and MBM models are presented to compare the tidal model computations with tide gauge observations to show the accuracy of prediction of tidal heights by the models used. Bathymetric data for LBM and MBM for present sea-levels were obtained from the Proudman Oceanographic Laboratory. The bathymetry and labels used in running the EC3 and WASH models compiled for this research (as described in Chapter 5.1.2 Chapter and 5.2.1) are given in Appendix 6.1. The tidal input data for all six constituents for each model for present sea-level runs is given in Appendix 6.2. Tidal input for EC3 and LBM models was obtained from the ECM and WCM models, respectively and results from the EC3 and LBM models were, in turn, used to provide the tidal input for the WASH and MBM models. Tidal model results are obtained for present day maximum sea-levels during a 15 day model run after the influence of the initial state of the model had been removed by running the model for 7 days prior to the 15 day period.

### 6.4.1. The Wash

The EC3 model (in Figure 6.1) shows highest maximum tidal altitudes in the western half of the Wash bay and Humber estuary of over 3.5 metres. A pattern of steadily decreasing heights towards the amphidromic point in the southern North Sea off Lowestoft, where maximum heights are below 0.5 metre, is shown outside the mouth of the bay. Figures from the model at tide gauge locations, given in Table 6.5 and located in Figure 6.2, show the increasing maximum tidal heights into the Wash from values of 3.296 metres at Gibraltar Point and 3.414 metres at Hunstanton to a maximum of 3.844 metres at Tabs Head. The histogram of EC3 model results for present sea-level (Figure 6.3) in conjunction with Figure 6.1 shows that results for maximum tidal heights are below these values over much of the model area outside the Wash.

Descriptive statistics for the EC3 model, given in Table 6.6 and illustrated in Figure 6.4, give a mean value for maximum sea-levels of 2.132 metres above mean sea-level, with

**Table 6.4.a. Accuracy of Model Results Compared with Observations in metres (from Admiralty Tide Tables, 1990)**

Location	MHWS (ATT)	Model Predictions		Difference (computed - observed)	
		EC3	WASH	EC3	WASH
<b>The Wash</b>					
Bull Sand Fort	2.87	3.14	-	0.17	-
Inner Dowsing	2.60	2.89	3.15	0.29	0.55
Skegness	2.79	3.17	3.30	0.38	0.51
Tab's Head	3.68	3.84	4.00	0.20	0.32
West Stones	3.20	3.37	3.96	0.17	0.76
Hunstanton	3.60	3.41	3.71	-0.19	0.11
Cromer	3.23	2.39	-	-0.84	-

MHWS Mean High Water of Spring Tides

ATT Admiralty Tide Tables

**Table 6.4.b. Accuracy of Model Results Compared with Observations in metres (from Admiralty Tide Tables, 1990)**

Location	MHWS (ATT)	Model Predictions		Difference (computed - observed)	
		LBM	MBM	LBM	MBM
<b>Morecambe Bay</b>					
Workington	3.78	3.56	-	-0.22	-
Barrow	4.14	3.97	4.19	-0.17	-0.05
Hawes Point	4.31	3.92	4.15	-0.39	-0.16
Heysham	4.30	4.02	4.39	-0.28	0.09
Fleetwood	4.22	3.82	4.18	-0.40	-0.04
Formby	3.85	3.60	-	-0.25	-
New Brighton	4.16	3.70	-	-0.46	-
Llandudno	3.37	3.20	-	-0.17	-

MHWS Mean High Water of Spring Tides

ATT Admiralty Tide Tables

**Table 6.5. EC3 Model Maximum Sea-Levels (Metres)**

<b>Location</b>	<b>M1</b>	<b>M2</b>	<b>0</b>	<b>-2</b>	<b>-5</b>	<b>-10</b>	<b>-15</b>	<b>1a</b>	<b>1b</b>	<b>2a</b>	<b>2b</b>	<b>3a</b>	<b>3b</b>
Rough Gas Field	2.429	2.425	2.433	2.418	2.454	2.290	2.196	2.431	2.422	2.429	2.404	2.426	2.412
North Star Rig	1.485	1.481	1.485	1.489	1.474	1.383	1.380	1.476	1.481	1.479	1.469	1.473	1.501
Withernsea	2.693	2.691	2.699	2.685	2.721	2.507	0.000	2.707	2.702	2.703	2.689	2.701	2.688
West Sole	2.121	2.114	2.124	2.112	2.127	1.950	1.943	2.109	2.093	2.108	2.046	2.105	2.099
Immingham	3.720	3.712	3.744	3.679	3.012	0.000	0.000	3.527	3.184	3.531	3.035	3.510	3.171
Easington	2.787	2.780	2.794	2.734	2.758	2.541	0.000	2.829	2.785	2.828	2.757	2.823	2.803
OSTG 236	2.080	2.073	2.083	2.077	2.082	1.907	1.834	2.067	2.046	2.054	1.983	2.062	2.058
Bull Sand Fort	3.120	3.114	3.137	2.945	2.753	2.864	0.000	3.068	2.934	3.068	2.880	3.063	2.948
Conoco	1.384	1.379	1.384	1.395	1.404	1.331	1.184	1.373	1.385	1.366	1.363	1.369	1.427
6ZW	1.444	1.436	1.442	1.456	1.484	1.401	1.173	1.421	1.445	1.404	1.405	1.415	1.485
8ZY	1.200	1.195	1.199	1.208	1.210	1.135	1.010	1.182	1.221	1.182	1.208	1.177	1.262
Inner Dowsing	2.834	2.855	2.887	2.813	2.791	2.448	2.349	2.847	2.738	2.826	2.603	2.843	2.774
Indefatigable	1.054	1.050	1.053	1.063	1.067	0.972	0.842	1.039	1.087	1.038	1.089	1.034	1.128
Station B81	1.358	1.348	1.356	1.374	1.411	1.334	1.121	1.336	1.362	1.320	1.322	1.330	1.420
Skegness	3.057	3.135	3.169	3.069	2.975	0.000	0.000	3.032	2.803	2.992	2.643	3.055	2.898
4ZQ	1.762	1.758	1.773	1.782	1.830	1.678	1.358	1.765	1.741	1.737	1.655	1.757	1.798
Shell - Esso	1.206	1.196	1.204	1.220	1.256	1.153	0.951	1.185	1.226	1.168	1.191	1.180	1.293
Gibraltar Point	3.130	3.261	3.296	3.216	3.092	0.000	0.000	2.993	2.700	2.983	2.488	3.034	2.842
Leman Bight	1.124	1.115	1.122	1.139	1.175	1.066	0.869	1.103	1.149	1.087	1.121	1.099	1.221
Tab's Head	3.643	3.806	3.844	3.793	0.000	0.000	0.000	2.877	2.590	2.945	2.263	3.112	2.855
Hunstanton	3.355	3.381	3.414	3.468	3.377	0.000	0.000	2.812	2.336	2.895	2.080	2.893	2.590
Cromer	2.285	2.296	2.319	2.294	2.327	1.972	0.000	2.288	2.219	2.239	2.068	2.278	2.270
Roaring Middle	3.412	3.547	3.580	3.656	3.577	2.992	0.000	2.852	2.419	2.983	2.126	2.973	2.684
West Stones	3.243	3.336	3.369	3.566	3.738	0.000	0.000	2.495	2.318	2.966	1.992	2.667	2.568
Caister	1.083	1.087	1.095	1.087	1.133	1.057	0.000	0.000	0.000	1.063	1.080	1.078	1.187
Gorleston	1.025	1.029	1.037	1.024	1.067	1.017	0.000	0.000	0.000	1.005	1.018	1.021	1.121
OSTG 276	0.417	0.425	0.431	0.415	0.410	0.366	0.304	0.416	0.421	0.402	0.397	0.417	0.466
WG	0.228	0.227	0.227	0.192	0.148	0.239	0.241	0.237	0.217	0.245	0.221	0.238	0.196

**Key**

- M1** Modification 1
- M2** Modification 2
- 0** Present Sea-Level
- 2** -2 Metres Sea-Level
- 5** -5 Metres Sea-Level
- 10** -10 Metres Sea-Level
- 15** -15 Metres Sea-Level
- 1a** 3,000 years B.P. coastline
- 1b** 3,000 years B.P. palaeogeography
- 2a** 4,000 years B.P. coastline
- 2b** 4,000 years B.P. palaeogeography
- 3a** 5,000 years B.P. coastline
- 3b** 5,000 years B.P. palaeogeography

The positions of the locations named in this Table are shown on the model grid in Figure 6.2.

**Table 6.6. Descriptive Statistics for EC3 Model Simulations.**

<b>Model Simulation</b>	<b>Mean</b>	<b>Median</b>	<b>Standard Deviation</b>	<b>Minimum</b>	<b>Maximum</b>	<b>Lower Quartile</b>	<b>Upper Quartile</b>
Modification 1	2.096	2.100	1.024	0.228	3.720	1.201	3.104
Modification 2	2.116	2.093	1.053	0.227	3.806	1.195	3.130
Present Sea-Level	2.132	2.103	1.065	0.227	3.844	1.200	3.161
-2 Metres	2.120	2.094	1.058	0.192	3.793	1.211	3.038
-5 Metres	1.959	1.956	1.032	0.000	3.738	1.184	2.783
-10 Metres	1.272	1.242	0.952	0.000	2.992	0.271	1.966
-15 Metres	0.670	0.272	0.776	0.000	2.349	0.000	1.181
3,000 years B.P. coastline	1.910	2.088	1.019	0.000	3.527	1.183	2.842
3,000 years B.P. palaeogeography	1.822	2.069	0.923	0.000	3.184	1.222	2.672
4,000 years B.P. coastline	2.002	2.081	0.930	0.245	3.531	1.171	2.932
4,000 years B.P. palaeogeography	1.807	1.987	0.750	0.221	3.035	1.195	2.467
5,000 years B.P. coastline	2.005	2.083	0.927	0.238	3.510	1.178	2.880
5,000 years B.P. palaeogeography	1.970	2.078	0.823	0.196	3.171	1.270	2.752

The locations of the points employed to obtain the statistics are shown in Figure 6.2.

The data used are given in Table 6.5.

a range from a minimum value of 0.227 metres to the maximum of 3.844 metres at Tabs Head. The standard deviation about the mean value is 1.065 metres, showing that the distribution does not record a strong concentration of tidal heights about the mean value but rather a spread of values over more than 2 metres of the approximately 2.6 metre range of the data. The spread of the distribution is also shown in the histogram in Figure 6.3, in which only one class (0.5 to 1.0 metres) is not represented, and by the smooth progression of increasing tidal heights from the amphidromic point off Lowestoft into the Wash embayment and Humber estuaries illustrated in Figure 6.1. The median value of 2.103 metres is close to the mean value and suggests that the distribution is close to normal around the mean value, as is shown by the histogram. This is also suggested by the upper and lower quartile values (Table 6.6) which differ from the mean by approximately the standard deviation value of 1.065 metres.

The accuracy of EC3 model results is shown in comparison with tide gauge observations for the mean high water of spring tides from the Admiralty Tide Tables (1990). The maximum difference shown is 0.84 metre underprediction of the model results at Cromer, but differences in the Wash area are within 0.2 metre. The pattern of change of mean high water spring tides values within the EC3 model, compared with values from the Admiralty Tide Tables, shows that the mean high water of spring tides results are well reproduced by the model. The results of both tidal observations and predictions by the model show maximum height values for the mean high water of spring tides near Tabs Head, with decreases in height towards the outer part of the Wash bay area.

The WASH model (Figure 6.5) reproduces the pattern of increase in mean high water of spring tides heights shown by EC3, but with greater detail in the variations shown. Model predictions rise to 4.0 metres at Tabs Head, giving a slightly greater overestimate of the mean high water spring tide height here than from the EC3 model. The pattern of higher tidal predictions using the WASH model compared with EC3 results is shown throughout the results. Comparison results from the locations given in Table 6.7 and Figure 6.6, as for EC3 shows a maximum difference of 0.76 metre overprediction of tidal

**Table 6.7. WASH Model Maximum Sea-Levels (Metres)**

<b>Location</b>	<b>0</b>	<b>1</b>	<b>2</b>	<b>3</b>
Inner Dowsing	3.153	2.814	3.007	2.840
Skegness	3.301	2.960	3.152	3.000
Gibraltar Point	3.471	2.923	3.239	3.010
Burnham (Overy Staithe)	3.139	2.659	2.919	2.686
Wells	3.111	2.646	2.894	2.674
Tabbs Head	3.999	2.586	3.274	2.973
Hunstanton	3.711	2.671	3.205	2.799
Roaring Middle	3.871	2.720	3.320	2.896
West Stones	3.962	2.571	3.327	2.732
Point 1	0.000	2.374	2.788	3.114
Point 2	0.000	2.263	2.822	2.748
Point 3	0.000	2.514	3.262	2.673
Point 4	0.000	2.279	0.000	2.830
Point 5	0.000	2.483	2.947	2.564

**Key**

- 0** Present Sea-Level
- 1** 3,000 years B.P. palaeogeography
- 2** 4,000 years B.P. palaeogeography
- 3** 5,000 years B.P. palaeogeography

The positions of the locations named in this Table are shown on the model grid in Figure 6.6.

**Table 6.8. Descriptive Statistics for WASH Model Simulations.**

<b>Model Simulation</b>	<b>Mean</b>	<b>Median</b>	<b>Standard Deviation</b>	<b>Minimum</b>	<b>Maximum</b>	<b>Lower Quartile</b>	<b>Upper Quartile</b>
Present Sea-Level*	3.524	3.471	0.368	3.111	3.999	3.146	3.916
Present Sea-Level	2.266	3.146	1.776	0.000	3.999	0.000	3.751
3,000 years B.P. palaeogeography	2.605	2.616	0.214	2.263	2.960	2.456	2.744
4,000 years B.P. palaeogeography	2.868	3.079	0.847	0.000	3.327	2.876	3.265
5,000 years B.P. palaeogeography	2.824	2.815	0.158	2.564	3.114	2.683	2.978

The locations from which data have been used to obtain the results presented above are shown in Figure 6.6.

The data are given in Table 6.7.

\* Present Sea-Level data omitting points 1 to 5 in Table 6.8.



heights at West Stones. WASH model results in the outer part of the bay at Hunstanton are, however, closer to observations (with an overprediction of 0.11 metre).

Statistical analysis gives a mean value of 3.524 metres (Table 6.8 and Figure 6.7), omitting the five points inland from the present sea-level coastline, which is, again, slightly higher than that for the EC3 model. The median, at 3.471 metres, also shows that the tidal heights in the Wash embayment are, on average, higher than those from the EC3 model, where a greater spread in values is observed. The minimum value of 3.111 metres, maximum of 3.999 metres and standard deviation of 0.368 metres illustrate the concentration of present sea-level maximum tidal heights in the Wash at between 3 and 4 metres above mean sea-level. The bimodality of the data, between the generally high values of maximum tidal heights in the Wash and the five 'dry' points, is clearly seen in the histogram in Figure 6.8.

In summary, maximum tidal heights of over 3 metres are recorded in the Wash embayment, with lower tidal heights seaward from the mouth of the Wash. Observations of mean high water of spring tides compared with maximum tidal altitudes obtained from running the tidal models over a spring-neap cycle of 15 days show that the model results have a maximum error of 0.84 metre at Cromer in the EC3 model and 0.76 metre at West Stones in the WASH model. There is a greater tendency towards overprediction of mean high water of spring tides values in the WASH model compared with the EC3 model. The reasons for this are not known, but may be related to the location of tide gauges used for comparisons with regard to depths used in the model bathymetric data. The results suggest that in the Wash a maximum error of  $\pm 0.80$  metres should be allowed for with EC3 model results and the same figure for the WASH model results.

#### **6.4.2. Morecambe Bay**

The LBM model shows (Figure 6.9) an increase in maximum tidal altitudes into the inner (especially the north-eastern) part of Morecambe Bay and the Solway Firth, rising to altitudes of over 4.5 metres, as shown in Table 6.9. A steady decrease of maximum

**Table 6.9. LBM Model Maximum Elevations (Metres)**

<b>Location</b>	<b>M1</b>	<b>M2</b>	<b>0</b>	<b>-2</b>	<b>-5</b>	<b>-10</b>	<b>-15</b>	<b>1a</b>	<b>1b</b>	<b>2a</b>	<b>2b</b>	<b>2c</b>
Creetown	3.102	3.266	3.279	3.575	0.000	0.000	0.000	3.218	0.000	3.368	0.000	0.000
35 Irish Sea	3.194	3.348	3.349	3.281	3.002	1.822	3.026	3.253	3.319	3.401	2.989	2.562
Workington	3.385	3.565	3.558	3.481	3.205	2.071	2.707	3.451	3.517	3.606	0.000	0.000
Ramsay	2.958	3.052	3.051	2.954	2.773	2.011	2.691	2.997	2.970	3.080	2.728	0.000
34 Irish Sea	3.433	3.305	3.305	3.263	2.985	2.219	3.003	3.276	3.262	3.304	3.195	3.014
Lowsy Point	3.680	3.574	3.577	3.515	0.000	0.000	0.000	3.552	0.000	0.000	0.000	0.000
Douglas	2.835	2.781	2.778	2.726	2.460	2.014	2.363	2.761	2.744	2.793	2.568	2.473
Barrow	4.058	3.986	3.972	0.000	0.000	0.000	0.000	0.000	0.000	0.000	0.000	0.000
Hawes Point	4.022	3.928	3.924	3.958	0.000	0.000	0.000	3.946	0.000	0.000	0.000	0.000
Morecambe	4.251	4.163	4.155	3.910	3.685	0.000	0.000	4.055	0.000	3.942	0.000	0.000
Halfway Shoals	3.765	3.677	3.675	3.582	3.322	2.684	0.000	2.730	2.724	3.626	3.598	0.000
Heysham	4.105	4.066	4.022	3.834	3.412	0.000	0.000	2.992	2.974	0.000	0.000	0.000
Wyre Light	3.965	3.880	3.877	3.738	3.396	2.756	3.890	3.779	3.738	3.760	3.768	0.000
Glasson Docks	4.094	4.040	4.011	3.834	3.327	0.000	0.000	4.196	0.000	0.000	0.000	0.000
Fleetwood	3.912	3.817	3.822	3.703	3.376	2.942	3.741	0.000	0.000	3.711	3.728	0.000
Std. Irish Sea	2.940	2.852	2.847	2.784	2.520	2.119	2.502	2.807	2.800	2.838	2.667	2.636
10 Irish Sea	3.311	3.224	3.221	3.169	2.909	2.355	2.900	3.222	3.200	3.203	3.104	3.071
Formby	3.696	3.599	3.600	3.553	3.295	2.618	0.000	3.660	3.636	0.000	0.000	0.000
Queens Channel	3.642	3.542	3.535	3.514	3.230	2.663	0.000	3.605	3.547	3.446	0.000	0.000
OSTG	3.687	3.581	3.578	3.541	3.273	2.633	0.000	3.627	3.577	3.467	0.000	0.000
New Brighton	3.840	3.676	3.702	3.683	3.414	2.596	0.000	3.699	3.750	0.000	0.000	0.000
Wylfa Head	2.486	2.401	2.402	2.346	2.188	1.821	2.324	2.373	2.361	2.429	2.382	2.456
Amlwch	2.811	2.725	2.724	2.688	2.435	2.032	2.520	2.686	2.660	2.727	2.614	2.582
Hilbre Island	3.696	3.643	3.635	3.509	0.000	0.000	0.000	3.654	3.704	0.000	0.000	0.000
Llandudno	3.302	3.196	3.195	3.249	2.920	2.387	2.938	3.200	3.200	3.167	3.108	0.000
Beaumaris	3.213	3.107	3.092	3.355	0.000	0.000	0.000	3.128	3.389	0.000	0.000	0.000

**Key**

- M1** Modification 1
- M2** Modification 2
- 0** Present Sea-Level
- 2** -2 Metres Sea-Level
- 5** -5 Metres Sea-Level
- 10** -10 Metres Sea-Level
- 15** -15 Metres Sea-Level
- 1a** 5,000 years B.P. coastline
- 1b** 5,000 years B.P. palaeogeography
- 2a** 8,000 years B.P. coastline
- 2b** 8,000 years B.P. palaeogeography higher sea-level
- 2c** 8,000 years B.P. palaeogeography lower sea-level

The positions of the locations named in this Table are shown on the model grid in Figure 6.10.

**Table 6.10. Descriptive Statistics for LBM Model Simulations.**

<b>Model Simulation</b>	<b>Mean</b>	<b>Median</b>	<b>Standard Deviation</b>	<b>Minimum</b>	<b>Maximum</b>	<b>Lower Quartile</b>	<b>Upper Quartile</b>
Modification 1	3.515	3.661	0.472	2.486	4.251	3.171	3.925
Modification 2	3.461	3.570	0.455	2.401	4.163	3.173	3.833
Present Sea-Level	3.457	3.568	0.451	2.402	4.155	3.169	3.836
-2 Metres	3.259	3.511	0.780	0.000	3.958	3.115	3.688
-5 Metres	2.351	2.952	1.359	0.000	3.685	1.641	3.323
-10 Metres	1.529	2.023	1.168	0.000	2.942	0.000	2.601
-15 Metres	1.331	0.000	1.503	0.000	3.890	0.000	2.755
5,000 years B.P. coastline	3.072	3.237	1.010	0.000	4.196	2.795	3.655
5,000 years B.P. palaeogeography	2.349	2.972	1.497	0.000	3.750	0.000	3.524
8,000 years B.P. coastline	2.149	2.959	1.628	0.000	3.942	0.000	3.451
8,000 years B.P. palaeogeography	1.402	0.000	1.575	0.000	3.768	0.000	3.018
higher sea-level							
8,000 years B.P. palaeogeography	0.723	0.000	1.221	0.000	3.071	0.000	2.460
lower sea-level							

The locations from which the data are taken to obtain these statistics are shown in Figure 6.10.

The data are given in Table 6.9.

tidal altitudes reached into the Irish Sea from those areas is also shown, with maximum tidal altitudes in the south-western part of the model of under 2.0 metres. In Morecambe Bay itself, a decline in maximum tidal heights from the north-east to the south-west is shown of about 1.0 metre. Model results give a prediction of mean high water of spring tides at Morecambe, in the east of the bay, of 4.155 metres, declining to 3.822 metres at Fleetwood near the south-west entrance to the bay.

The histogram (Figure 6.11) shows a peak in the data from Table 6.9 at between 3.5 and 4.0 metres. This coincides well with the mean value of 3.457 metres (Table 6.10 and Figure 6.12) and the median of 3.568 metres. The standard deviation value of under 0.5 metre also shows that there is a strong concentration of maximum tidal height values around 3.5 metres in the model. The range of the maximum tidal heights is from a minimum of 2.402 metres to a maximum of 4.155 metres, but the lower and upper quartile values are between 3 and 4 metres.

The MBM model (Figure 6.13) shows a similar pattern to that of LBM, but with greater detail of changes. Model results for maximum tidal altitudes (given in Table 6.11 and Figure 6.14) are shown as above 4.5 metres in the northern and extreme eastern parts of the bay, decreasing to values of between 4.0 and 4.25 metres across the entrance to the bay. The range in maximum tidal heights within the MBM model area is from 3.745 metres to 4.973 metres (Table 6.12 and Figure 6.15). Thus the results from the MBM model show maximum tidal heights which are higher and less widely spread (standard deviation 0.333 metre) than those from the LBM model. The histogram (Figure 6.16) also illustrates the peaked distribution.

Maximum differences in tidal height predictions between the LBM and MBM models occur at Fleetwood at the entrance to the bay, with heights of 4.18 metres predicted from MBM and 3.82 metres from LBM. This is also reflected in the difference in comparison of predicted and observed tidal heights between the models.

Within Morecambe Bay, the LBM model shows maximum differences of 0.40 metres'

**Table 6.11. MBM Model Maximum Sea-Levels (Metres)**

<b>Location</b>	<b>0</b>	<b>1</b>	<b>2</b>	<b>3</b>
Lowsy Point	3.885	0.000	0.000	0.000
Barrow	4.186	0.000	0.000	0.000
Morecambe	4.478	0.000	0.000	0.000
Hawes Point	4.148	0.000	0.000	0.000
Halfway Shoals	3.982	0.000	0.000	0.000
Heysham	4.353	0.000	0.000	0.000
Glasson Docks	4.507	0.000	0.000	0.000
Wyre Light	4.162	3.917	3.704	0.000
Fleetwood	4.176	0.000	0.000	0.000
Point 1	4.973	0.000	0.000	0.000
Point 2	4.710	0.000	0.000	0.000
Point 3	4.202	0.000	0.000	0.000
Point 4	3.956	3.751	3.557	0.000
Point 5	3.745	3.522	3.399	0.000

**Key**

- 0** Present Sea-Level
- 1** 5,000 years B.P. palaeogeography
- 2** 8,000 years B.P. palaeogeography higher sea-level
- 3** 8,000 years B.P. palaeogeography lower sea-level

The positions of the locations named in this Table are shown on the model grid in Figure 6.14.

**Table 6.12. Descriptive Statistics for MBM Model Simulations.**

<b>Model Simulation</b>	<b>Mean</b>	<b>Median</b>	<b>Standard Deviation</b>	<b>Minimum</b>	<b>Maximum</b>	<b>Lower Quartile</b>	<b>Upper Quartile</b>
Present Sea-Level	4.247	4.181	0.333	3.745	4.973	3.976	4.485
5,000 years B.P. palaeogeography	0.799	0.000	1.590	0.000	3.917	0.000	0.880
8,000 years B.P. palaeogeography higher sea-level	0.761	0.000	1.514	0.000	3.704	0.000	0.850
8,000 years B.P. palaeogeography lower sea-level	0.000	0.000	0.000	0.000	0.000	0.000	0.000

The locations from which the data have been taken to obtain these statistics are shown in Figure 6.14.

The original data are presented in Table 6.11.

underprediction of the mean high water of spring tides heights at Fleetwood. Results beyond Morecambe Bay reach a maximum error of 0.46 metres at New Brighton with LBM. MBM model results are much closer to observations, reaching a maximum difference of 0.16 metres underprediction at Hawes Point. These results suggest that errors of  $\pm 0.5$  metres should be allowed in results from LBM, but only  $\pm 0.20$  metres for MBM due to the much better tidal height predictions from this model.

#### **6.4.3. Comparison of The Wash and Morecambe Bay**

Maximum tidal heights are greater (at maximums of over 4.5 metres) in Morecambe Bay than the Wash (where they reach over 3.5 metres) by about one metre. The pattern of variation of tidal heights is similar in both bays with higher maximum tidal heights found in the inner areas than at the mouth of the bay. The extent of this change is, again, greater in Morecambe Bay than the Wash, varying by up to a metre in the former and 0.5 metre in the latter.

Model results show differences from observations of up to about  $\pm 0.8$  metre in the EC3 and WASH models. This error is reduced to within 0.5 metre of observations for LBM and 0.2 metre for MBM. The better predictions for the west coast may be due to better quality bathymetric representations in the models than was available for the east coast area.

The magnitude of the error in maximum tidal altitudes in the Wash is of a similar order to the variation in range of present day maximum tidal height variations within the bay, whereas results for Morecambe Bay have an error term of at most (for LBM) half of the difference in maximum tidal heights within the bay. This suggests that a greater reliance may be placed on the accuracy of different model simulations used in the case of Morecambe Bay than for those of the Wash.

#### **6.5. Robustness of the tidal models**

An assessment of the sensitivity of model results to local bathymetry and coastline

changes within the model area was made by altering present sea-level depth data and labels in the EC3 and LBM models. These tests were carried out to determine the extent of the influence on tidal patterns of local changes within the model compared with those introduced by altering depths or coastline shapes over the whole model area.

The first modification (Mod. 1) comprised a test of the influence of an alteration to tidal input to the embayments as a result of coastline shape changes. To enter this into the tidal models a spit was introduced by making the appropriate changes to labels outlined in Chapter 5.2.1.1. The spit in the Wash was run westward from Hunstanton at approximately  $52^{\circ}58'N$  to a position in the middle of the Wash at  $0^{\circ}18'E$ . A similar modification was made for application to Morecambe Bay by extending a spit from Cumbria at approximately latitude  $54^{\circ}18'N$  towards the Isle of Man, ending at  $4^{\circ}0'W$ . The locations of the spits are shown by the black lines on the diagrams of maximum tidal altitudes for Mod. 1.

The choice of a modification comprising a spit running westwards from Hunstanton in The Wash was influenced by the possibility of a former morainic barrier across part of the mouth of The Wash, following Godwin's (1978) suggestion (see Chapter 2.3.1). Barriers are, however, best developed in microtidal regimes (Hayes, 1975) and the extent of the influence of the presence of a barrier in lowering the tidal range to contribute to its self-perpetuation led to the examination of the hypothesis that considerably lower tidal heights than at present would be found in the inner part of The Wash with the barrier in place.

For Morecambe Bay, a spit was run westwards from Cumbria towards the Isle of Man in an attempt to simulate a reduction of tidal input to Morecambe Bay from the north which would have occurred as a consequence of the post-glacial uplift of areas near the former centres of ice accumulation. It is recognised that an uplifted area would not take the form of a spit of land extending from the current coast but would probably have consisted of a much greater extent of dry land in the area of the spit and to the north



of it. The modification was made in the form of a spit for compatibility with the similar modification made to The Wash.

The second modification (Mod. 2) to the present day tidal models consisted of depth changes within the embayments. Depths were altered in the tidal models by swapping the model depths in the bathymetric setup data on one side of an imaginary line running down the middle of each bay from centre of its mouth with those depths on the other side of the line. By this means, the order of magnitude of depth changes was maintained, but the location of deep and shallow areas within the bays was altered. This modification provides a test within The Wash and Morecambe Bay of the effect of the accuracy of knowledge of sea depths. The accuracy of knowledge of past offshore sea depths is limited due to the lack of availability of dated sediment sequences from such areas. This, in turn, is due to both the lack of available techniques for obtaining the required information and the current movement of sea bed sediments within the shallow embayments. Results of this modification permit some assessment of the magnitude and spatial extent of error in tidal model results for former sea-levels employing sea depths based on only eustatic and isostatic sea depth alterations.

### **6.5.1. Modification 1 - Introduction of a spit**

#### **6.5.1.1. The Wash**

Results of the EC3 model including the introduction of a spit across part of the mouth of the Wash (Mod. 1 above) show (Figure 6.17) highest tidal altitudes (above 3.5 metres) in the inner part of The Wash, between Tabs Head and West Stones, comprising approximately one quarter of the area of The Wash. However, the area of maximum tidal altitudes above 3.5 metres is not as great as for the present day simulation in which maximum tidal altitudes over the whole of the western part of the Wash are above 3.5 metres. Figure 6.18 shows that the spit has lowered maximum tidal heights on the northern shore of the Wash in particular. There is also a slight lowering of maximum tidal altitudes in the North Sea beyond the mouth of the Wash compared with the present situation, shown by

comparison of the present day tidal simulation results with those of the spit modification.

The histogram for the EC3 Mod. 1 simulation (Figure 6.19) shows very little difference from that for present sea-level. The descriptive statistics (Table 6.6 and Figure 6.4) are comparable in value with those for the present sea-level model simulation. There is a slight decrease in the range of maximum tidal height values within the Wash for the Mod. 1 simulation. The minimum value is raised by 0.001 metre and the maximum lowered by 0.124 metre. However, this maximum value is not found at the same location in each simulation, so that there is a maximum difference of 0.201 metres between the two simulations at Tabs Head in the inner Wash, with a mean of 0.036 metres over all the EC3 model observations. Both the upper and lower quartiles are very slightly (0.057 and 0.001 metre) higher than for present sea-level. The median value (2.100 metres) again nearly coincides with that of the mean. Differences are greater in the Wash, as would be expected from the location of the spit, with the minimum difference here being 0.059 metres at Hunstanton. The scatter plot (Figure 6.20) shows the tendency for the higher maximum tidal heights to be reduced, compared with the present sea-level situation, whereas those locations with lower maximum tidal heights (outside the Wash, as shown in Figure 6.17) are almost identical to the present day situation.

#### **6.5.1.2. Morecambe Bay**

The introduction of a spit from Cumbria towards the Isle of Man to the north of Morecambe Bay in the LBM model shows an increase in maximum tidal altitudes reached in the inner part of Morecambe Bay (Figure 6.21 and Figure 6.22) especially in the north-east corner, compared with an unmodified simulation of present day conditions. There is a five-fold increase in the area of maximum tidal altitudes over 4.5 metres in the area of the Kent and Leven estuaries. In general over the model area, tidal altitudes show an increase south of the spit and a decrease to the north. The area of higher maximum tidal altitudes extends further west in the case of the Mod. 1 results than for the present sea-level results south of the spit, whereas to the north, the area of lower tidal altitudes

increase extends further west than with the unmodified simulation.

A comparison of the maximum tidal altitudes reached, using the data in Table 6.9 at tide gauge stations, gives a range of differences from present sea-level results of -0.138 to 0.177 metres, with increases of the order of 0.10 metre in Morecambe Bay (at Barrow and Morecambe, for example). The locations of maximum and minimum highest tidal altitudes, however, change between the models. Table 6.10 shows that the minimum value for the dataset is raised by 0.084 metre from the present sea-level simulation to the Mod. 1 simulation, while the maximum value is also raised, by 0.096 metre. These slight increases in maximum tidal altitude values are reflected in the upper and lower quartile results which are, again, slightly greater for Mod. 1 than for the present sea-level situation. The mean difference over the whole of the model area is -0.058 metres (Table 6.10). The median value is 0.146 metre greater than that of the mean for Mod. 1 results (Table 6.10). The difference between the mean and median results has increased slightly (less than 0.05 metre) over the results for the present sea-level simulation, but there is still very little difference between the two values. The greatest differences are immediately south of the spit in the Irish Sea. A slightly greater spread of much of the data is shown by the higher standard deviation value for Mod. 1, at 0.472 metres, compared with the value for the present day simulation (Table 6.10). However, the histogram (Figure 6.23) shows overall that there is very little difference in the distribution of the maximum tidal height values from the present day situation, shown in Figure 6.11. A scatter plot of present sea-level results against those of Mod. 1 (Figure 6.24) shows the greater spread of the data, with some points having higher maximum tidal heights and others lower maximum tidal heights than at the present day.

## **6.5.2. Modification 2 - Depth changes within the embayments**

### **6.5.2.1. The Wash**

The pattern of maximum tidal altitudes in the Wash in the EC3 model following depth changes is very similar to that for the present day simulation (Figures 6.25 and

6.26). Only slight decreases in tidal altitudes reached in the Wash are apparent in a few areas from comparison of the diagrammatic results of this simulation compared with that for the present day. Comparison of results from the tide gauge stations throughout the EC3 model given in Table 6.5, shows differences of between 0.000 and 0.038 metres compared with present sea-level results. The maximum difference is, as with Mod. 1, at Tabs Head in the inner part of the Wash. Maximum tidal altitudes are typically reduced by over 0.03 metre at stations in the Wash, compared with the mean reduction of 0.016 metre throughout the model (Table 6.6), showing that the influence of depth changes is mainly within the bay. Taking the results for maximum tidal altitudes at the locations in Table 6.5 as a whole, Table 6.6 shows that the median, standard deviation, minimum, maximum and upper and lower quartile values all fall slightly compared with the present sea-level simulation, but by less than 0.04 metre. The histogram (Figure 6.27) shows an almost identical spread of the data to that for the present sea-level. Figure 6.20 shows virtually no change from present sea-level results in a scatter plot of the data. Therefore the effect of changing the bathymetry within the Wash embayment has been to give a very slight lowering (less than 0.04 metre) of maximum tidal heights but with a similar pattern to that for the present day.

#### **6.5.2.2. Morecambe Bay**

The diagrammatic results of LBM with depth changes in Morecambe Bay show only very minor changes (Figures 6.28 and 6.29) compared with the present day simulation. The maximum tidal altitudes are slightly increased (with two squares shaded as having tidal altitudes of over 4.5 metres) in the north-east corner of the Bay and slightly reduced (to just below 4.0 metres) at the northern entrance to the Bay near Hawes Point. A comparison of the tide gauge station results in Table 6.9 for the present sea-level run compared with that for Mod. 2 shows a very slight overall increase in maximum tidal altitudes for Mod. 2, with a mean value of 0.004 metre. Table 6.10, taking the results for all the locations in Table 6.9 together, illustrates the very minor differences between the two simulations in the descriptive statistics results. In general the maximum tidal

altitudes increase for Mod. 2 in Morecambe Bay by only less than 0.01 metre (Table 6.10), although the maximum figure for the whole model (0.044 metre) is recorded at Heysham (Table 6.9). The histogram (Figure 6.30) also shows that the spread of the data is almost identical to that for the present sea-level (Figure 6.11), as does the scatter plot (Figure 6.24).

### 6.5.3. Comparison of results

The differences in comparison with the results for an unmodified simulation of present day maximum tidal heights show that the greatest changes to tidal heights occur in the immediate neighbourhood of the modifications carried out. With all the modifications, except for the spit extending across the Irish Sea some distance north of Morecambe Bay, this has resulted in maximum changes to the tidal heights within the embayments under study. The amount of change in tidal heights for Mod. 1 throughout the EC3 and LBM models corresponds closely between the models, reaching a maximum of *circa* 0.2 metre in both models and averaging only a few centimetres. The direction of change of tidal heights within the embayments is, however, different with heights increased with the introduction of the spit for Morecambe Bay but decreased in the Wash. This can probably best be explained by the location of the spits with regard to the direction of tidal wave propagation in both areas, although detailed examination of this factor is beyond the scope of the present study.

In the case of the Wash, the spit created a barrier which gave lower than present maximum tidal heights in the Wash, but tidal heights were not lowered anywhere near the extent of becoming meso- or micro-tidal in the Wash behind the barrier and the spit had even less of an influence on the tidal heights in the North Sea beyond the Wash. There is, in any case, little geological evidence of a morainic barrier across the Wash during the Holocene (Shennan, 1986a). The higher than present maximum tidal heights reached in Morecambe Bay and to the south of the spit in the Irish Sea, however, suggest a possibility that higher tidal ranges may have been seen in this part of the Irish Sea when the area

to the north was land and the only opening to the sea was to the south. This hypothesis is tested more rigorously, employing palaeogeographic reconstructions of Morecambe Bay for the early Holocene, below.

Modification 2, in which sea depths were altered within the embayments, showed smaller changes to maximum tidal heights in both embayments than occurred as a result of the introduction of the spits. Average changes for the EC3 and LBM models were *circa* two centimetres, reaching maximum figures of around four centimetres in the inner parts of the bays. The directions of change in tidal heights compared with those for the present day simulation again differed between the two bays, decreasing in the Wash with the modification, but increasing in the inner part of Morecambe Bay. This may be attributed to the exact location of depth changes in relation to movement of the tidal wave, whose amplitude is reduced by dissipation of tidal energy in extensive shallow water areas. The order of magnitude of the maximum tidal height changes is similar in both embayments which suggests that this may be taken as a guide to the error due to inexact knowledge of the palaeobathymetries of the embayments in the palaeogeographic reconstructions below in which sea depths are altered according to eustatic and isostatic sea-level changes.

The differences recorded between the modified model simulations and that for the present day are measured in terms of centimetres. In this respect they are so low that they fall within the figures for accuracy of the computed present day tidal model results compared with observations at the tide gauge stations. This suggests that use of the tidal models for palaeogeographic reconstructions of the Wash and Morecambe Bay may provide results from which the magnitude of overall maximum tidal height changes can be assessed with a good degree of reliability even in the absence of detailed knowledge of former sea depths within the embayments. However, the alterations to the pattern of tidal height changes as a consequence of the modifications suggest that the pattern of changes to tidal heights within the embayments may be less easy to simulate without detailed knowledge of the palaeocoastline and palaeobathymetry of an area.

## 6.6. Reduced sea depth simulations

A first estimate of tidal changes resulting from sea depth changes was made by making uniform subtractions of 2, 5, 10 and 15 metres to the bathymetry of the tidal models at the present day. These are referred to in the text below as [2], [5], [10] and [15] for simplicity, with the present sea-level simulation designated as [0]. The sea depth reductions correspond to sea-level altitudes at 5,000, 6,500, 7,700 and approximately 8,000 years B.P. from Mörner's (1976, 1980, 1984) eustatic curve. The depth reductions were chosen to reflect the development of the present tidal regime during the Holocene sea-level rise.

Tidal changes were studied from an analysis of sea depth reductions to present day tidal models by Franken (1987) and Austin (1988, 1991). However, the present study differs in two respects from those of Franken and Austin. The model area used by Franken and Austin was the whole of the north-west European continental shelf, at resolutions of approximately  $30 \times 30$  kilometres and  $8 \times 9$  kilometres, respectively. In this study, tidal input from reduced sea-levels over the scale of the north-east Atlantic is applied at the scale of individual coastal embayments with model grid resolutions of approximately  $3 \times 3$  kilometres. Furthermore the studies by Franken and Austin consisted of examinations of the change of one tidal constituent,  $M_2$ , whereas the present study incorporates six constituents in order to assess changes to the height of mean high water of spring tides. The importance of shelf edge boundary conditions was discussed in Chapter 6.2.1. Austin (1991) noted overestimates of 5% near the coast in amplitudes of the  $M_2$  tide with the continental shelf model compared with results obtained by the present author from the north-east Atlantic model with sea depths reduced by 15 metres. Results such as these suggest that the methods applied in this thesis provide a more realistic simulation of tides at lower sea-levels than has previously been attempted. The local effects in embayments are also illustrated at the scale employed in the present study, whereas this has previously been recognised as an unresolved problem (Austin, 1991).

Sea depth reduction simulations were carried out by making uniform depth reductions to the bathymetries used as input to the tidal model. No changes were made to the labels in the tidal models so that tidal inundation might still occur up to the present coastline if high enough tide levels were attained during the model run.

### 6.6.1. The Wash

Results of the EC3 model between present sea-level [0] and simulation of a sea-level reduced by 2 metres [2] (Figures 6.31 and 6.32) show an increase in the area of maximum tidal altitudes above 3.5 metres in the Wash, extending over two-thirds of the area of the Bay compared with only the western half of the Bay from the [0] results. The magnitude of tidal changes is not great, however. Over much of the model area tidal altitude changes are less than  $\pm 0.10$  metres. In the Wash, the increase in maximum tidal altitudes is most marked (at over 0.20 metres) in the south, near King's Lynn, and decreases northwards, with the mouth of the Bay in the east and an area near Tabs Head in the west showing slight decreases of maximum tidal altitudes (of less than approximately 0.10 metres).

An examination of the figures of change at tide gauge stations listed in Table 6.5 shows that mean maximum tidal heights are lower (2.120 compared with 2.132 metres) in the EC3 model with sea-levels reduced by 2 metres (Table 6.6). Results in the Wash show reductions of typically *circa* 0.05 metre, but an increase of 0.203 metres at West Stones in the south-western corner for [2] compared with [0]. Values for all the descriptive statistics are lower for [2] than [0], but by not more than 0.051 metre (Table 6.6). The mean and median values are within 0.04 metre, the standard deviation is reduced in [2] to 1.058 metre, compared with 1.065 metre for [0], showing a very slightly reduced spread around the mean value for much of the maximum tidal altitudes results. The minimum and maximum values are also reduced slightly, showing a general tendency for lower maximum tidal heights with the reduction of 2 metres to sea depths. Figure 6.33 shows an almost identical spread of the data to that for present sea-level. The count for the 2.5 to 3.0 metre class has, however, increased by one at the expense of the 3.0 to 3.5



metre class, showing a reduction in maximum tidal heights reached for the [2] simulation compared with the [0] simulation. The scatter plot (Figure 6.34) shows a more varied pattern of change of maximum tidal altitudes for locations with maximum tidal heights over 2.5 metres for both [0] and [2] simulations. There is a tendency for values just over 2.5 metres for [0] to be reduced slightly with the [2] simulation, while those over 3.0 metres are, in some cases (as at West Stones), increased.

Between present sea-level and the simulation of a sea-level reduction of 5 metres [5] an increase in the area of maximum tidal altitudes reached above 0.20 metres is again found in the southern part of the Wash (Figures 6.35 and 6.36). In the central and northern parts of the Bay, however, maximum tidal altitudes are reduced by amounts ranging from 0.0 to 0.3 metres. The magnitude of changes shown by throughout most of the EC3 model area is again within 0.10 metre, as with the comparison between [0] and [2]. Maximum tidal altitudes remain above 3.5 metres in the inner (western) half of the Wash bay. The tide gauge station results give mean values of maximum tidal altitudes approximately 0.2 metre lower compared with present sea-level results for EC3 (Table 6.6). The median value remains close to that of the mean. West Stones is the only station in the Wash to show an increase in maximum tidal altitudes, at 3.738 metres for [5] compared with 3.369 metres for [0] and 3.566 metres for [2]. Gibraltar Point shows a tendency in the opposite direction, with maximum tidal altitudes of 3.092 for [5] compared with 3.296 for [0]. Figure 6.37 shows that the greatest differences (of over 0.5 metre) between the [2] and [5] simulations occur in the Humber estuary. The changes in the Wash itself are generally within  $\pm 0.25$  metre.

The reduction in maximum tidal altitudes is typically of the order of less than 0.05 metre within the Wash for [5] compared with [0] (Table 6.6). However, the minimum value of 0.0 metres in the descriptive statistics shows that drying out occurs as Tabs Head has become dry land as a result of the reduction in sea depths (Table 6.5). The maximum value of the highest tidal heights reached in the Wash is reduced by over 0.1 metre for [5] compared with [0], and by over 0.05 metre from [2] (Table 6.6). A reduction by 0.033

metre in the standard deviation from [0] to [5] indicates less spread in height of most of the maximum tidal altitudes within the model area. Values of both the upper and lower quartiles are reduced compared with both [0] and [2] simulations, especially that of the upper quartile, again indicating that most of the values of maximum tidal heights are not spread over so large a range of values. The histogram (Figure 6.38) shows fewer counts in the higher maximum tidal altitude classes (such as 3.5 to 4.0 metres) and more in the 2.5 to 3.0 metre and 0.0 to 0.5 metre classes. Figure 6.34 shows that the scatter of values at the locations in Table 6.5 for [5] compared with [0] have the greatest differences above 3.0 metres, where both increases and decreases in maximum tidal altitudes are shown at [5] compared with the [0] results.

The simulation of a sea-level reduction of 10 metres [10] shows that the coastal area of the present Wash bay is dry land and the southern part of the mouth of the bay has also been extended northwards due to an increase in the land area north of Hunstanton (Figures 6.39 and 6.40). Maximum tidal altitudes are reduced by well over a metre for [10] compared with [0] in much of the Wash and surrounding parts of the northern Norfolk and east Lincolnshire coasts (Table 6.6). The magnitude of maximum tidal height changes decreases considerably in to the North Sea, where tidal reductions are generally of the order of less than 0.2 metres. In the EC3 model mean maximum tidal altitudes for tide gauge stations at [10] are 1.272 metres, representing a reduction of *circa* 0.85 metre compared with the present. However, this figure is not representative of the actual change in tidal altitudes as a number of the tide gauge stations record zero values due to locations inland of the [10] coast. Roaring Middle is the only station left in the sea in the Wash. The changes recorded at this station showed a slight increase in maximum tidal heights for [2] compared with [0] (figures of 3.656 and 3.580 metres, respectively), but then decreased to 3.577 at [5] and 2.992 metres at [10], giving an overall decrease compared with [0] of *circa* 0.6 metres at [10]. Figure 6.41 shows that in part of the Wash there is a decrease in the maximum tidal altitudes from [5] to [10] of over 0.5 metre, with the amount of decrease in maximum tidal altitudes lessening into the North Sea. The

westward movement of the amphidromic point off Lowestoft is shown by the increase in maximum tidal altitudes in this area between the [5] and [10] simulations.

The histogram for [10] (Figure 6.42), using data from Table 6.5, shows a considerable change from that for [5]. The two classes above 3.0 metres now have no counts, whilst those below 2.0 metres register an increase. Indeed, the highest recorded maximum tidal altitude (Table 6.6) is now 2.992 metres. The upper quartile value of 1.966 metres represents a fall of over a metre from the [0] value and of over 0.8 metre from the [5] value. The lower quartile has decreased by nearly a metre from the [0] value and the reduced spread in tidal heights reached is further reflected in the drop in the standard deviation to below 1.0 metre. The scatter plot (Figure 6.34) shows a pattern of increased reductions of maximum tidal altitudes for those locations which had the higher values for [0].

There is only a narrow channel left down the central part of the Wash with the 15 metre sea-level reduction simulation [15] (Figures 6.43 and 6.44). Maximum tidal altitudes are considerably reduced, by the order of 1.25 metres compared with present sea-level results in the vicinity of the Wash. Changes of up to 0.5 metre in maximum tidal altitudes are found in the North Sea area. No tide gauge station results are available in the Wash for comparison of maximum tidal altitudes due to their inland locations as a result of the lowering of sea-level. Figure 6.45 shows reductions in parts of the Wash embayment of over 0.75 metre in maximum tidal altitudes from [10] to [15], larger reductions than were shown from [5] to [10]. Table 6.6, which includes data from the now inland tide gauges, gives a mean value of 0.670 metres for maximum tidal altitudes in the EC3 model at [15]. This represents a reduction of approximately 1.5 metres from the [0] value and 0.6 metre from the [10] value. The median is now 0.4 metre below the mean value (Table 6.6), indicating that most of the data are now in the 0.0 to 0.5 metre class (Figure 6.46), below the mean value, due to the drying out of large parts of the original model area. The highest maximum tidal altitude from Table 6.5 is now 2.349 metres. The standard deviation, 0.776 metres, shows a reduction of approximately 0.3 metre in the spread of most of the data around the mean value compared with [0]. The upper quartile for the

dataset is reduced to 1.181 metres and the lower quartile (at 0.0 metres) reflects the fact that most of the locations used in the analysis have now dried out. The scatter plot (Figure 6.34) emphasises the large number of tide gauge locations which have dried out and the considerable reduction of [10] maximum tidal altitudes compared with those for [0], which is accentuated for the stations which recorded the higher maximum tidal altitudes in [0].

Discussed in terms of the tidal development of the area during the Holocene, results from the [0] to [2] simulation show changes of within 0.10 metre in maximum tidal altitudes attained, with increases of slightly greater than this amount in the Wash. Comparisons from the simulations of [2] to [5] show differences within 0.1 metre for much of the EC3 model area. However, an increase of over 0.2 metres in maximum tidal altitudes from [2] to [5] in the southern Wash is shown, contrasting with the decrease in maximum tidal altitudes of 0.1 to 0.2 metres in the central and northern part of the Wash. From [5] to [10] there is a decrease of maximum tidal altitudes over most of the EC3 model area by up to 0.25 metre. This is accentuated in the vicinity of the Wash to 0.5 metre, with some decreases of even greater amounts in the central Wash. Between [10] and [15] the overall model differences in maximum tidal altitudes are again up to 0.25 metre, but within the Wash minimum differences are over 0.50 metre and rise to over 0.75 metre in the inner, western, part of the Wash. Analysis of variance results (Table 6.13) show greater variation between the results for the [0], [2] and [5] simulations and transformed results from the [10] and [15] simulation results than within model tidal altitudes.

In summary the results show a general decrease in maximum tidal altitudes with lower sea-level simulations, but this pattern is more complicated in the Wash bay. The amphidromic point off Lowestoft in the North Sea is seen to move westward with the reduction in sea depths. This was also noted by Franken (1987) and Austin (1988, 1991). The magnitude of tidal range remains similar in all simulations, but is based on significantly lower values for [10] and [15]. The pattern of change to maximum tidal altitudes is more complicated within the Wash, with increases of maximum tidal altitudes at [2] compared with [0] and extended to increase in maximum tidal altitudes at [5] in the south-

**Table 6.13. EC3 Model: Analysis of Variance Results From Data in Table 6.5.**

**Model Simulations:** Present Sea-Level, -2, -5, -10 and -15 Metres Sea-Levels

Mean value for [0] simulation = 2.132 m.      Mean value for [2] simulation = 2.120 m.

Mean value for [5] simulation = 1.959 m.      Mean value for [10] simulation = 1.272 m.

Mean value for [15] simulation = 0.670 m.

F = 11.98      Degrees of freedom = 4, 23      Critical F value for 0.05 probability = 2.80

A significant difference is shown in the maximum tidal altitudes between the simulations.

**Model Simulations:** Present Sea-Level, 3,000, 4,000 and 5,000 Years B.P. Coastlines

Mean value for [0] simulation = 2.132 m.      Mean value for [3c] simulation = 1.910 m.

Mean value for [4c] simulation = 2.002 m.      Mean value for [5c] simulation = 2.005 m.

F = 0.24      Degrees of freedom = 3, 24      Critical F value for 0.05 probability = 3.01

No significant difference is shown in the maximum tidal altitudes between the simulations.

**Model Simulations:** Present Sea-Level, 3,000, 4,000 and 5,000 Years B.P. Palaeogeographic Reconstructions

Mean value for [0] simulation = 2.132 m.      Mean value for [3p] simulation = 1.822 m.

Mean value for [4p] simulation = 1.807 m.      Mean value for [5p] simulation = 1.970 m.

F = 0.80      Degrees of freedom = 3, 24      Critical F value for 0.05 probability = 3.01

No significant difference is shown in the maximum tidal altitudes between the simulations.

**Model Simulations:** 3,000, 4,000 and 5,000 Years B.P. Palaeogeographic Reconstructions

Mean value for [3p] simulation = 1.822 m.      Mean value for [4p] simulation = 1.807 m.

Mean value for [5p] simulation = 1.970 m.

F = 0.33      Degrees of freedom = 2, 25      Critical F value for 0.05 probability = 3.38

No significant difference is shown in the maximum tidal altitudes between the simulations.

m. represents metres

ern Wash, but decreases in tidal heights in the northern part of the Wash, as described above. Comparison of [10] and [15] with [0] shows that maximum tidal altitudes are lowered throughout the Wash, but the greatest change to tidal variations within the bay is between the [0], [2] and [5] simulations.

### 6.6.2. Morecambe Bay

Results of the LBM model for [2] (Figure 6.47) show reductions in maximum tidal altitudes reached compared with the present sea-level tidal model results. Drying out of some coastal areas occurs in the Solway Firth and Morecambe Bay and in the estuaries to the south. The difference diagram, [0] minus [2] simulation (Figure 6.48), shows that most changes to maximum tidal heights reached represent a lowering of within 0.25 metre of current tidal maximum altitudes, although around Arnside and Morecambe in the north-eastern part of Morecambe Bay differences are greater than these values. At Hawes Point on the northern entrance to Morecambe Bay maximum tidal altitudes are slightly increased for [2] over the [0] simulation. Maximum tidal altitudes reached are also increased in the [2] simulation along the north Wales coast.

The tide gauge data in Table 6.9 show that the mean maximum tidal altitudes reached in the LBM model are lower for [2] than [0] by *circa* 0.2 metre at 3.259 compared with 3.457 (Table 6.10), respectively, although this may be influenced by the zero value resulting from the inland location of Barrow at [2]. In Morecambe Bay, the reduction of maximum tidal altitudes is typically 0.2 metre, for example 4.155 at [0] to 3.910 at [2] at Morecambe, with greater reductions in the north-eastern part of the bay. The median value, like the mean, is reduced with the [2] simulation compared with [0]. However, the difference between the mean and median values is increased for the [2] simulation, showing the influence of the 0.0 metre value for Barrow in reducing the mean value of maximum tidal heights for [2]. This is also shown by the histogram in Figure 6.49, in which most of the observations are grouped in the 3.5 to 4.0 metre class. The 0.0 metre value has also influenced the standard deviation, which has increased from 0.451 metres for [0] to 0.780 metres for [2].

There is a reduction of approximately 0.2 metres in the maximum values of highest tidal heights, shown in Table 6.10, from [0] to [2]. The zero value at Barrow has reduced the minimum figure by 2.402 metres from that of the [0] simulation and so extended the range of the data from under 2 metres to nearly 4 metres. The upper and lower quartile values are both reduced from the [0] figures, indicating the general lowering of maximum tidal heights for the [2] simulation. The scatter plot in Figure 6.50 shows that at some locations, the [2] simulation has resulted in an increase in maximum tidal altitudes, compared with [0], especially for Creetown and Beaumaris at the northern and southern extremes of the model, but in general there has been a reduction of maximum tidal altitudes with the lowering of mean sea-level by two metres.

Comparison of present sea-level results [0] with those for a simulated lowering of sea-level by 5 metres [5] (Figures 6.51 and 6.52) show greater tidal changes than for [2]. In much of the LBM model, maximum tidal altitudes are reduced by between 0.25 and 0.50 metre compared with present sea-level results. There are modifications to this in coastal areas, with increased reductions (of up to over 0.75 metre) in Morecambe Bay and the Solway Firth and smaller reductions (of the order of 0.0 to 0.25 metre) along the north Wales coast in particular. Maximum tidal altitudes reached in the north-eastern part of Morecambe Bay are between 3.5 and 4.0 metres, compared with results of up to over 4.5 metre reached at present sea-level. The reductions in tidal altitudes are greatest in the inner (eastern) part of Morecambe Bay. Tide gauge station results from Table 6.9 indicate reductions of the order of 0.3 metre (3.414 compared with 3.702 metres at New Brighton, for example) for LBM but are greater within Morecambe Bay, for example 3.412 compared with 4.022 metres at Morecambe and in the north-eastern part of the bay. Comparison between the [2] and [5] results (Figure 6.53) show the greatest changes at Glasson Docks in Morecambe Bay, where maximum tidal altitudes are reduced from 3.834 metres for [2] to 3.327 metres for [5] (Table 6.9).

The descriptive statistics (Table 6.10) show a reduction in the mean value of maximum tidal altitudes attained of 1.106 metres from the [0] to [5] results. The decrease in the

median value is not so great (at 0.616 metres) between the two simulations, showing that the mean value is influenced by the drying out of coastal areas as sea-level is lowered in the tidal model. This is clearly shown by the bimodality of the histogram in Figure 6.54. The influence of the areas that have 0.0 metre sea-levels as a consequence of their position inland from the coast at [5] is also reflected in the increase in the standard deviation from its values for [0] and [2] to 1.359 metres. The general lowering of tidal heights is indicated by the reduction of the maximum value for highest tidal altitudes by 0.470 metre from [0] to [5] and the associated reduction of both the upper and lower quartile values from [0] to [5] (Table 6.10). However, the lower quartile's substantial reduction (of *circa* 1.5 metres) between [0] and [5] must be largely attributed to the number of tide gauges which are dry land at [5]. The scatter plot of reduced sea depth simulations against present sea-level results (Figure 6.50) indicates a general lowering of maximum tidal altitudes compared with both [0] and [2] at [5]. The scatter plot also shows that this lowering is increased for some of the originally higher (approximately 4 metre) maximum tidal altitudes, which are those found in Morecambe Bay itself.

Comparison of present sea-level results with those for a simulated lowering of sea-level by 10 metres [10] (Figures 6.55 and 6.56) show reduced maximum tidal altitudes compared with [0], especially in a line running from the Isle of Man to Cumbria, approximately in the same location as that of the spit introduced as Mod. 1 in Chapter 6.4.1. Maximum tidal altitudes are increased by over a metre compared with present sea-level results to the north of this line, reaching a maximum of over 1.75 metres difference on the southern Scottish coast. In Morecambe Bay the differences in maximum tidal altitudes are between 0.75 and 1.25 metre. However, the highest tidal altitudes reached in the model are still in the north-eastern part of Morecambe Bay. Drying of the bay at this sea-level means that most tide gauge stations are inland, but results for Halfway Shoals in the northern entrance to the bay show a considerably greater reduction of maximum tidal altitudes at this sea-level compared with other simulations. At Halfway Shoals the difference compared with present sea-level results is almost 1.0 metre (2.684 metres for [10] and 3.675 metres



for [0]). Between the [5] and [10] simulations, Figure 6.57 shows reductions in maximum tidal altitudes of over a metre in the northern part of the model and general reductions of between 0.5 and 1.0 metre over the model as a whole. The difference between the [5] and [10] simulations at Halfway Shoals, Morecambe Bay, is 0.638 metre (Table 6.9).

The histogram for the LBM [10] simulation (Figure 6.58) shows even stronger bimodality in the data than that for [5], as more of the model area becomes dry land. The mean value (Table 6.10) for maximum tidal altitudes is now nearly two metres below that for [0]. The median value differs from that for the mean by almost 0.5 metre, so drawing attention to the bimodality of the data. The standard deviation value, although slightly lower than that for [5], remains at over a metre due to the large number of tide gauges which have dried out and consequently have zero values for maximum tidal altitudes although those which remain in the sea have maximum tidal altitude values of up to 2.942 metres (Table 6.10). The upper quartile value of 2.601 metres is also due to the concentration of maximum tidal altitude values between 2.0 and 3.0 metres (Figure 6.58). The lower quartile value of 0.0 metres is explained by the large number of tide gauges which have dried out at [10]. The scatter plot (in Figure 6.50) shows that all the tide gauge locations have much lower maximum tidal altitudes for [10] than [0], especially for those locations in which maximum tidal altitudes for the [0] simulation were around 3.5 metres.

By contrast with the increasing amounts of reduction in the maximum tidal altitudes noted with lower sea-levels above, maximum tidal altitudes are reduced from [0] for [15] (Figures 6.59 and 6.60) by between only 0.25 and 0.50 metre over much of the model in line for those of the [5] simulation compared with [0]. In Morecambe Bay this change is even more marked with maximum tidal altitudes recorded within  $\pm 0.25$  metre of those of [0]. Greater reductions than 0.75 metre are, however, present at the mouth of the Solway Firth in the north-eastern corner of the LBM model. The Wyre Light near the southern entrance to Morecambe Bay is the only tide gauge station in the vicinity of Morecambe Bay not inland with the [15] simulation. The reverse in the trend of maximum tidal altitudes is noted here, with a very slight increase in the maximum tidal altitudes reached

compared with those for present sea-level, with figures of 3.890 metres at [15] compared with 3.877 metres for [0] at Wyre Light. Between [10] and [15] (Figure 6.61), maximum tidal altitudes are increased by as much as 1.204 metres at 35 Irish Sea in the north of the model. In general there is an increase in maximum tidal heights from [10] to [15] of between 0.5 and 1.0 metres. In the entrance to Morecambe Bay, the Wyre Light shows a change from 2.756 metres ([10]) to 3.890 metres ([15]).

More than half the tide gauge stations in Table 6.9 are dry land with the [15] simulation, giving a median value of 0.0 metres. This is clearly shown in the histogram (Figure 6.62) and acts as a bias on the statistics (Table 6.10). The mean maximum tidal altitude value has fallen by almost 0.2 metre from the [10] simulation as a consequence of the drying out of the tide gauge stations. The maximum recorded value (from Table 6.9) for the maximum tidal altitude in the model has risen by nearly a metre from that for the [10] simulation to 3.890 metres. The standard deviation has, as a consequence of the increase in altitude of maximum tidal heights attained, increased from its value for the [10] simulation to 1.503 metres. Figure 6.50 shows that maximum tidal altitudes from the [15] simulation are in line with those from the [5] simulation, although for higher tidal altitudes (above 3.8 metres maximum tidal altitudes with the [0] simulation), the [15] results exceed the heights reached by the [2] simulation where the tide gauge stations have not been taken inland from the coast at [15] with the reduction in sea depths.

Diagrams of differences between successive reduced sea depth simulations best show the alterations in the sequence of maximum tidal heights at lower sea-levels. For the [2] simulation, subtracting results for [5] shows an overall decrease in the maximum tidal altitudes in LBM at the lower sea-level of between 0.20 and 0.30 metre. For the centre of Morecambe Bay this difference is increased to between 0.30 and 0.40 metre, as is also found along the north Wales coast. Differences in the north-eastern part of Morecambe Bay are only of the order of 0.20 metre.

For comparisons of [5] and [10] results, the differences are greater than between the

[2] and [5] simulations. There is also a much greater range of differences in the case of comparisons from [5] to [10] results than from [2] to [5] differences. Maximum reductions from [5] to [10] are greater than 1.25 metres in the northern part of the LBM model, but decrease south-westwards to figures of below 0.25 metre. In Morecambe Bay, reductions in tidal altitudes are of the order of 0.75 metre from [5] to [10].

Between [10] and [15], differences in maximum tidal altitudes reached in the LBM model are in the opposite sense from those of previous sea-level reductions. Maximum tidal altitudes increase with the reduction in sea-level from [10] to [15]. Areas where this occurs to over 1.25 metres are present in the north of the LBM model. The smallest increases in tidal altitudes occur in the southwestern part of the model. In Morecambe Bay, there is an increase of maximum tidal altitudes of the order of a metre in the central part of the Bay and slightly greater increases in the coastal areas around the edge of the Bay. Analysis of variance results (Table 6.14) show greater differences in tidal heights between the [0], [2], [5], [10] and [15] simulations than within these simulations.

There is an overall reduction in maximum tidal heights reached with lower sea-level simulations, but the trend is not linear and reverses with the lowest sea-level simulation, [15], for which an overall increase in maximum heights is noted in the LBM model. In Morecambe Bay, changes are not uniform over the area of the bay and also vary in magnitude with each simulation. There is a tendency for greater changes in maximum tidal altitudes to occur with the [10] and [15] simulations, for which the present coastal areas of Morecambe Bay are inland, but, as with the Wash, the variation within Morecambe Bay in the degree of change to maximum tidal altitudes is greatest between [0], [2] and [5]. The magnitude of tidal range variations within the model remains similar for all simulations, but the base tidal heights on which changes occur are the main cause of change in tidal heights, as for the Wash. This is shown in the results from the analysis of variance.

**Table 6.14. LBM Model: Analysis of Variance Results From Data in Table 6.9.**

**Model Simulations:** Present Sea-Level, -2, -5, -10 and -15 Metres Sea-Levels

Mean value for [0] simulation = 3.457 m.      Mean value for [2] simulation = 3.259 m.

Mean value for [5] simulation = 2.351 m.      Mean value for [10] simulation = 1.529 m.

Mean value for [15] simulation = 1.331 m.

F = 19.45      Degrees of freedom = 4, 21      Critical F value for 0.05 probability = 2.84

A significant difference is shown in the maximum tidal altitudes between the simulations.

**Model Simulations:** Present Sea-Level, 5,000 and 8,000 Years B.P. Coastlines

Mean value for [0] simulation = 3.457 m.      Mean value for [5c] simulation = 3.072 m.

Mean value for [8c] simulation = 2.149 m.

F = 9.11      Degrees of freedom = 2, 23      Critical F value for 0.05 probability = 3.42

A significant difference is shown in the maximum tidal altitudes between the simulations.

**Model Simulations:** Present Sea-Level, 5,000 Years B.P. and 8,000 Years B.P. Higher and Lower Sea-Level Palaeogeographic Reconstructions

Mean value for [0] simulation = 3.457 m.      Mean value for [5p] simulation = 2.349 m.

Mean value for [8ph] simulation = 1.402 m.      Mean value for [8pl] simulation = 0.723 m.

F = 22.87      Degrees of freedom = 3, 22      Critical F value for 0.05 probability = 3.05

A significant difference is shown in the maximum tidal altitudes between the simulations.

**Model Simulations:** 5,000 Years B.P. and 8,000 Years B.P. Higher and Lower Sea- Level Palaeogeographic Reconstructions

Mean value for [5p] simulation = 2.349 m.      Mean value for [8ph] simulation = 1.402 m.

Mean value for [8pl] simulation = 0.723 m.

F = 8.38      Degrees of freedom = 2, 23      Critical F value for 0.05 probability = 3.42

A significant difference is shown in the maximum tidal altitudes between the simulations.

m. represent metres

### 6.6.3. Comparison of The Wash and Morecambe Bay

An overall decrease in the maximum tidal altitudes reached is shown for reduced sea depth simulations in the Wash and Morecambe Bay. However, in the LBM model maximum tidal altitudes are shown to increase for [15] compared with results from [10]. Furthermore, there are variations in the overall trend towards reduced tidal altitudes within the Wash and Morecambe Bay, shown by the increase in maximum tidal altitudes in the southern Wash and decrease in maximum tidal altitudes at the same time in the central and northern parts of the bay from [0] to [2], for example. This illustrates that a simple linear model of decreasing maximum tidal altitudes with lower eustatic sea-levels cannot be used within the embayments, emphasising the importance of the study of tidal variations within such local coastal areas for different sea-levels. The variations in maximum tidal altitudes are accentuated within the Wash and Morecambe Bay compared with other areas offshore in the models, showing the greater importance of local changes to coastline and bathymetry compared with the effect of sea depth reductions on offshore areas with more uniform bathymetry than is found in the coastal zone.

Eustatic sea-level change is the major factor in determining changes in the land/ sea interface altitudes. The relative importance of the tidal factor in comparison with this eustatic change is shown by the magnitude of variations of maximum sea-level altitude changes with the reduced sea depth simulations. In the Wash, using results from the EC3 model, there is a decrease by *circa* 0.6 metre at Roaring Middle from [0] to [10] showing a 6% change in tidal heights compared with the overall eustatic sea-level change. For Morecambe Bay, Halfway Shoals and the Wyre Light show decreases of *circa* 1.0 metre from [0] to [10], giving a 10% change in tidal heights with a eustatic fall of sea-level of 10 metres. The maximum magnitude of changes to tidal heights at lower sea-levels is therefore greater in Morecambe Bay than the Wash. The present altitude of current maximum tidal heights is higher in Morecambe Bay than in the Wash, so that there is a greater potential for absolute tidal levels to decrease in Morecambe Bay than in the Wash. Analysis of variance results show that the variation of maximum tidal altitudes between

the results of EC3 and LBM at lower sea-levels converges towards similar tidal ranges in each model.

## **6.7. Coastline modifications**

Following the test carried out above, which used sea depth changes as a means of assessing tidal changes during the Holocene in the Wash and Morecambe Bay, the coastline in the study areas was modified to reflect the changes in shape to the bays during the Holocene. The same principle as in the previous section was used in order to determine which palaeogeographic reconstructions to use in the Wash and Morecambe Bay. Palaeogeographic reconstructions of the coastline were entered into the tidal models for times when each Bay took on a shape distinctly different in its development following post-glacial inundation in the early Holocene from that of its present shape. Thus the coastline shape is separated as a factor for study alone permitting the influence of the shape of the land/ sea boundary on the tidal regime to be studied and comparison with the tidal changes consequent on sea depth reductions studied in Chapter 6.5 above to be made.

Construction of the palaeogeographic coastline of The Wash and Morecambe Bay comprised establishing the shape of the former coastline. The shape of the former coastlines was drawn using the stratigraphic data to link dated sea-level index points as described in Chapter 4.3. The former coastline shapes of the embayments were entered into the tidal models (EC3 for the Wash Fenland area and LBM for the Morecambe Bay area) by appropriate changes to the labels in the setup data. Sea depths were left at zero water depth values for areas beyond the present coastline in the former coastline simulations.

### **6.7.1. The Wash**

The simulations of the shape of the Wash at 3,000, 4,000 and 5,000 years B.P. all show a considerable increase on the current area of tidal inundation of the bay, as discussed in Chapter 2. The palaeocoastline simulation at 3,000 years B.P. [3c] simulation for EC3 (Figure 6.63) shows that the area of highest maximum tidal altitudes reached occurs in

the area of Skegness and Gibraltar Point, with maximum tidal altitudes decreasing southwards into the Wash towards Roaring Middle and eastwards into the North Sea from here. Maximum tidal heights in the southern Wash are between 1.5 and 2.0 metres and in the west, between 2.0 and 2.5 metres, whilst in the present Wash bay area, maximum tidal heights are over 2.5 metres.

The descriptive statistics in Table 6.6 show a mean value from tide gauge locations for maximum tidal altitudes with the [3c] simulation of 1.910 metres. The median value is only slightly higher, at just over two metres and the histogram in Figure 6.64 shows a spread of the tide gauge maximum tidal altitude values across most of the classes. This is also indicated by the standard deviation of just over 1.0 metre and the lower and upper quartiles, which show a fairly even distribution of the data between the minimum value of 0.0 and the maximum of 3.527 metres.

Results from the EC3 model show maximum tidal altitudes reached with the 4,000 years B.P. coastline [4c] (Figure 6.65) are over 3.0 metres along the northern shore of the present Wash bay area and extending southwards to Roaring Middle. Maximum tidal altitudes decrease in all directions away from this area, giving altitudes of over 2.0 metres along the former northern shore of the bay and declining to just over 1.0 metre in the south of the former bay area.

Figure 6.66 shows that the tide gauges record maximum tidal altitudes in most of the classes of the histogram, but with large counts (10 and 9, respectively) recorded in the 1.0 to 1.5 metre and 2.5 to 3.0 metre classes. The mean value of just over 2 metres (Table 6.6) is close to that for the median, which, in conjunction with the evidence of the histogram, indicates a fairly even spread of the data around the mean value. The standard deviation is just under a metre and the upper and lower quartile results indicate that the maximum tidal altitudes reached at the tide gauge locations are generally well spread between the minimum of 0.245 metres and the maximum of 3.531 metres, although it is noted that the upper and lower quartile results fall within the classes shown to have the largest counts

on the histogram.

The 5,000 years B.P. coastline [5c] in the Wash for the EC3 model (Figure 6.67) again shows a situation of maximum tidal altitudes over 3.0 metres along the northern and central parts of the Wash and along the Lincolnshire coast to just north of Skegness. Tidal altitudes decrease to maximum values of over 1.5 metre in the south of the former bay area, but are not reduced below 2.0 metres in the north-western part of the area.

The descriptive statistics for the [5c] simulation (Table 6.6) show that the mean and median values for the maximum tidal heights are almost coincident at just over 2 metres so that the mean value almost represents the mid-point of the dataset when the maximum tidal altitudes values are placed in rank order. The standard deviation is just under a metre, as with the [3c] and [4c] simulations. Like the [3c] and [4c] simulations, the lower and upper quartile values, in conjunction with the minimum value (of 0.238 metres) and maximum value (of 3.510 metres) suggest that the maximum tidal altitudes reached at the tide gauge stations are generally well spread over the dataset, although a gap in the 0.5 to 1.0 metre class is shown on the histogram (Figure 6.68) with a count of ten in the neighbouring 1.0 to 1.5 metre class.

To illustrate the general trends to maximum tidal changes with the palaeocoastline simulations, results for the EC3 model are compared for present sea-level with each of the palaeocoastline simulations and between each of these simulations. The broad changes which occur are more clearly visible at this scale than with use of the finer WASH model grid.

Subtracting results for [3c] from the [0] simulation (Figure 6.69) shows a pattern of increasing differences (from about 0.5 metre) into the Wash, reaching a maximum of above 1.0 metre near Tabs Head. Tide gauge stations give results of 2.877 metres for [3c] compared with 3.844 metres for [0] at Tabs Head but only 2.993 metres for [3c] compared with 3.296 [0] at Gibraltar Point. This illustrates the reduction in maximum tidal altitudes into the Wash with the [3c] simulation compared with that for the present day. The



situation for [0] minus [4c] (Figure 6.70) shows a similar pattern, with differences of 0.5 metre common in the Wash, rising to over 0.75 metre near Tabs Head where a slightly higher maximum tidal altitude of 3.112 metres is recorded. This is repeated for the [0] minus [5c] situation (Figure 6.71), but the differences are not so great, averaging between 0.25 and 0.5 metre in the central part of the Wash, but rising again towards Tabs Head though again the difference here is less than for [3c] or [4c] with a maximum tidal altitude of 3.112 metres recorded. This pattern suggests that the general trend in the current Wash bay area with the palaeocoastline reconstructions has been for a similar pattern of tidal changes to be developed with each palaeocoastline simulation, with differences from the present sea-level situation decreasing further back in time. The descriptive statistics in Table 6.6 show little difference in mean values or the spread of the data between the palaeocoastline simulations. A scatter plot of the palaeocoastline simulations against present sea-level results (Figure 6.72) only shows significant differences from the present sea-level results where present sea-level maximum tidal altitudes are above 3.0 metres. Where this is the case, tide gauge data for the [3c] simulation are, almost without exception, reduced below 3.0 metre maximum tidal altitudes. This pattern also applies to the [4c] and [5c] simulations, but is slightly less marked in these cases.

The pattern of changes to maximum tidal altitudes is not as simple for comparisons between the palaeocoastline simulations as for the situation compared with the present day. Differences for the EC3 model for [3c] minus [4c] (Figure 6.73) show little change in the area of the present Wash bay, but up to over 0.75 metre higher maximum tidal altitudes were reached in the southern part of the current Fenland area, with larger differences also found in the north-west (up to about 0.5 metre). The situation from [4c] minus [5c] results (Figure 6.74) shows changes within 0.25 metre over much of the present area of the Wash bay, but decreases in maximum tidal altitudes of over 0.25 metre in the inner part of the former bay (the present Fenland area) for [5c]. This situation is reversed, however, near King's Lynn, where [5c] maximum tidal altitudes increase by over 0.75 metre compared with [4c]. Analysis of variance results (Table 6.13) show smaller variations within the bay

than between the different palaeocoastline simulations from comparisons of current tide gauge results.

In summary, maximum tidal altitudes are shown as similar to those of the present in the current Wash bay area, but in place of the increase in tidal altitudes into the inner bay, the coastline modifications result in a decrease in maximum tidal altitudes into the former Fenland area. Between the palaeocoastline reconstructions, the order of changes is relatively small (within 0.25 metre), but this pattern is modified locally in the south-eastern and north-western coastal areas which show decreases to maximum tidal heights of over 0.5 metre between the palaeocoastline simulations. The differences between present and palaeocoastline variations of maximum tidal heights within the Wash are less than the variations in tidal heights within the present day bay area.

### 6.7.2. Morecambe Bay

The coastline at 5,000 years B.P. [5c] in LBM shows maximum tidal altitudes (Figure 6.75) in the northern half of Morecambe Bay of over 4.0 metres, with values of between 3.5 and 4.0 metres in the outer (western) part of the bay. Maximum tidal altitudes decrease westwards to around 2.0 metres on the western edge of the model. There is a greater area of tidal inundation than for present sea-level in the bay at [5c].

The maximum and minimum values of the data, at 4.196 and 0.0 metres, with the upper and lower quartile range results and histogram (Figure 6.76) show that the data are concentrated between 2.5 and 4.0 metres with a tailing off to two counts of zero causing the difference of 2.795 metres between the minimum and lower quartile results. Figure 6.76, together with the descriptive statistics results in Table 6.10, shows a concentration of the maximum tidal altitudes for the LBM [5c] simulation between 2.5 and 4.0 metres. Both the mean and median fall in the 3.0 to 3.5 metre class. The standard deviation value of just over a metre reflects well this concentration in the distribution.

For [8c], LBM results show maximum tidal heights (Figure 6.77) above 4.0 metres only in the northernmost part of Morecambe Bay, but maximum tidal altitudes over

the remainder of the bay area are above 3.5 metres. There is a westwards decrease in maximum tidal altitudes to 2.0 metres on the western edge of the model. The coastline reconstruction for [8c] has resulted in a smaller area of tidal inundation than at present in the bay.

The [8c] simulation has a distinctly bimodal distribution (Figure 6.78) due to the inland location of a number of tide gauge stations. The mean value has therefore been reduced to 2.149 metres. The median value is above this, at 2.959 metres, but again does not reflect the concentration of the maximum tidal altitudes from tide gauge locations on the coast or further out to sea which record modal values in the 3.0 to 3.5 metre class (Figure 6.78). The standard deviation value, at 1.628 metres, reflects the wide spread of the tide gauge data from Table 6.9 between the minimum value of 0.0 and the maximum of 3.942 metres. This is also shown in the wide interquartile range of 3.451 metres.

Results of LBM are compared with [0] situation and between the two palaeocoastline simulations, as was done for EC3 in the Wash. Comparisons with the present-day situation for [5c] (Figure 6.79) show reductions of maximum tidal altitudes of up to 0.5 metre in the northern part of Morecambe Bay with a maximum change of 3.675 metres [0] to 2.730 metres [5c] at Halfway Shoals. There is a strong gradient of change into the northern part of Morecambe Bay, with much of Morecambe Bay showing reductions in maximum tidal heights typical of the changes in the Irish Sea of less than 0.1 metre such as the change from 3.877 metres [0] to 3.779 metres [5c] at the Wyre Light. Maximum tidal heights are reduced by up to 0.2 metre in the Solway Firth area, but the changes in Morecambe Bay are by far the greatest in the model area.

Compared with the present day situation, results for LBM of the 8,000 year coastline (Figure 6.80) show reductions of maximum tidal altitudes of up to 0.5 metre in the northern part of Morecambe Bay with a change from 4.155 metres [0] to 3.942 metres [8c] at Morecambe. The changes to tidal heights within Morecambe Bay are more extensive than for the present sea-level at [8c], with the whole of the eastern and southern

half of Morecambe Bay showing reductions of maximum tidal altitudes of at least 0.1 to 0.2 metre. The maximum tidal height reductions in the Irish Sea and the north-eastern part of Morecambe Bay are again less than 0.1 metre, as for the [0] minus [8c] situation, although in this case there are areas of less than 0.1 metre increase in maximum tidal heights in the western part of the LBM model and near the Wirral. The scatter plot in Figure 6.81 shows that in general there is a slight decrease in maximum tidal altitudes reached in the palaeocoastline simulations compared with that for the present day, but in two cases maximum tidal altitudes with both the [5c] and [8c] simulations are reduced by more than a metre.

Differences between the [5c] and [8c] model simulations (Figure 6.82) show that reductions in maximum tidal altitudes are greatest in the southern part of LBM, typically around 0.2 metre reduction from the [5c] situation at [8c], compared with increases in maximum tidal heights of the same order in the north of the model. Morecambe Bay reflects this pattern in miniature, with reductions in tidal altitudes of the same order as in the Irish Sea in the southern part of the bay and increases in the northern areas of both. Analysis of variance results (Table 6.14) show greater variation in tidal heights within the model than between results for the different palaeocoastline simulations.

In summary, maximum tidal altitudes are reduced compared with the present for both simulations. There is a greater area of maximum tidal altitudes above 4.0 metres in Morecambe Bay for [5c] than for [8c]. The overall change in maximum tidal altitudes is of the order of 0.1 to 0.2 metres between [0] and [5c] and [8c] simulations, but changes are up to 0.5 metre in the north-eastern parts of Morecambe Bay and also reach greater values than 0.1 to 0.2 metres in other embayments, such as the Solway Firth.

### **6.7.3. Comparison of The Wash and Morecambe Bay**

The range of maximum tidal altitudes reached in both bays with the palaeocoastline simulations remains similar to those of the present day. Differences are accentuated in the areas of highest maximum tidal heights in the present inner bay areas. In the case of

the Wash, where tidal inundation occurs over a considerably greater area than at present for [3c], [4c] and [5c], the pattern of tidal heights in the former bay differs from the [0] situation in which an increase in tidal heights further into the bay is evidenced. For each of [3c], [4c] and [5c] there is a decrease into the inner bay areas of maximum tidal altitudes. In Morecambe Bay, however, the inner bay area remains as with the present day situation. Changes in the coastline for [5c] and [8c] applied in this case do not increase or decrease the area of tidal inundation to the extent of the simulations carried out for the Wash.

Differences between the present day and palaeocoastline simulations for both the Wash and Morecambe Bay in the range of maximum tidal altitudes are less than the differences in the range within each embayment. The analysis of variance results do not take into account the tidal heights in the Fenland area in the Wash model which is inundated for [3c], [4c] and [5c]. In this area there are no tide gauge stations to provide comparative results. This part of the Wash does show significantly lower maximum tidal altitudes than are shown in the present Wash bay. Differences in maximum tidal altitudes are greater within both embayments than between the palaeocoastline reconstructions, but where there is a considerably greater area of inundation (shown in the Wash for [3c], [4c] and [5c]), the range in maximum tidal altitudes within the embayments increases considerably over that of the present day.

## **6.8. Palaeogeographic reconstructions**

A more realistic assessment of tidal variations during the Holocene may be made from combining the palaeocoastlines with bathymetric data for the former sea-level in question. Problems with obtaining such palaeo-sea depth data were noted in Chapter 2 above due to the lack of datable geological evidence for sea-levels from offshore locations, but an attempt is made here to simulate the palaeotidal regime of the Wash and Morecambe Bay using estimates of former sea depths from eustatic and isostatic land/ sea level changes modified within the embayments using the available stratigraphic data for the embayments during the Holocene.

In order to obtain the palaeogeography of the embayments, the same palaeocoastline reconstructions were used as in Chapter 6.7 above, but with modifications to sea depths within the areas of the EC3 and LBM models. Sea depth modifications were made using information from the stratigraphy to suggest the locations of river channels prior to marine inundation of the embayments. In these former channels, sea depths were increased compared with the surrounding areas. Elsewhere, water depths were estimated using isostatic land movements (after Shennan, 1987, 1989) to modify the altitude of the existing land surface. Beyond this, eustatic sea-levels were also added in to the changes in sea depths to give the palaeogeographic sea depths used. The resulting palaeogeographic sea depths were described in Chapter 4 and shown in Figures 4.8-4.10 and 4.13-4.15 for the EC3 and LBM models. The sea depth and label data for the palaeogeographic reconstructions of all the models is given in Appendix 6.1.

### 6.8.1. The Wash

Results for palaeogeographic simulations were obtained from both the EC3 and WASH models for this area. Results are presented first for the EC3 model and then for the WASH model. The differences between the results for the models at different resolutions are noted.

For the palaeogeographic reconstruction at 3,000 years B.P. [3p] with the EC3 model (Figure 6.83), maximum tidal heights in most of the Wash are between 2.5 and 3.0 metres, with areas of lower heights (by up to 0.5 metre) around the Hunstanton, King's Lynn, Roaring Middle area. The pattern of maximum tidal heights remains similar to that of the present day in the North Sea area. Differences show maximum tidal heights up to 1.5 metres lower in the southern half of the Wash area compared with present sea-level results (Figure 6.84), with a change from 3.844 to 2.590 metres at Tabs Head, for example. The corresponding differences are less in the northern part of the Wash, generally within 0.5 metre of present sea-level results, as illustrated by the change from 3.296 for [0] to 2.700 metres for [3p] at Gibraltar Point.

Descriptive statistics (Table 6.6) give a mean value for maximum tidal altitudes from the data in Table 6.5 of 1.822 metres for the EC3 model with the [3p] simulation. The median is slightly higher at 2.069 metres and the 0.0 metres minimum value, maximum of 3.184 metres and the histogram (Figure 6.85) show that the mean and median results have been influenced by the four tide gauge stations which are inland from the coast for this simulation. The upper and lower quartile results (2.672 metres and 1.222 metres) give a better indication of the distribution of the data for tide gauge stations reached by the sea with the [3p] simulation. The scatter plot (Figure 6.86) shows a general decline in maximum tidal altitudes, especially where these were above 2.5 metres for the [0] simulation where reductions are of a metre or more. There is, however, a tendency for some of the highest maximum tidal altitudes (above 3.5 metres for the present sea-level simulation) to show smaller reductions in maximum tidal altitudes than the maximum tidal altitudes which were between 2.5 and 3.5 metres for the [0] simulation.

The WASH model results (Figure 6.87) show a much greater range of changes than is apparent from the EC3 model. There is a range of approximately 1.0 metre in maximum tidal heights within the Wash for [3p], with maximum tidal heights of over 3.0 metres in the south of the former embayment and in the northern half of the present Wash bay area, with a figure of 2.923 metres for maximum tidal altitudes at Gibraltar Point, for example, compared with 3.471 metres for the present day. In the central part of the current Fenland area, however, maximum tidal altitudes are shown to be typically of the order of 2.0 metres. Compared with the present day simulation (Figure 6.88) maximum tidal altitudes are shown to decrease in the present Wash embayment area by over a metre. For example, the decrease in maximum tidal altitudes from [0] to [3p] at West Stones is 1.389 metres and that at Roaring Middle is 1.151 metres.

The [3p] simulation shows mean maximum tidal altitudes of 2.605 metres, close to the median value of 2.616 metres. The histogram (Figure 6.89) shows that all the locations record maximum tidal altitudes in two class, namely 2.0 to 2.5 metres and 2.5 to 3.0 metres above mean sea-level. The minimum and maximum values within these classes are 2.263

and 2.960 metres. This lack of spread in the data is mirrored in the standard deviation of 0.214 metres and upper and lower quartile values of 2.744 metres and 2.456 metres, respectively. The scatter plot (Figure 6.90) shows that the maximum tidal altitudes recorded in the Wash for [3p] fall well below those from the [0] simulation and that this trend increases for higher maximum tidal altitudes (above 3.5 metres in the [0] simulation).

The increased detail of the palaeogeographic simulation for the WASH model highlights the maximum tidal altitude changes. Whereas the broad pattern for both EC3 and WASH shows decreasing maximum tidal altitudes into the current Fenland area, only the WASH model shows the modification of this towards increased tidal altitudes in the south of the former embayment and the lowering of tidal altitudes in the central Fenland area, together with decreases of over a metre in maximum tidal altitudes at [3p] compared with the [0] simulation in the area of the present embayment.

Results of the 4,000 years B.P. [4p] palaeogeographic simulation for EC3 (Figure 6.91) show maximum tidal altitudes between 2.0 and 2.5 metres in the greater part of the bay area, but increases above these figures are shown in the southernmost and northwesternmost parts of the former Fenland area. Comparisons with present sea-level results show the greatest differences in the inner half of the embayment, with [0] simulation results over 1.5 metre higher than results from [4p]. Taking comparison for Tabs Head in the western Wash and Gibraltar Point on the northern coastline, results for [0] compared with [4p] (Figure 6.92) show changes from 3.844 to 2.263 and from 3.296 to 2.488 metres, respectively, illustrating the magnitude of changes. Changes from [3p] to [4p] (Figure 6.93) show decreases in maximum tidal altitudes of approximately 0.3 metre in the present Wash embayment with smaller changes (less than 0.1 metre) beyond the mouth of the Wash in the North Sea. The scatter plot (Figure 6.86) shows that a much greater reduction in maximum tidal altitudes is recorded between the [0] and [4p] simulations than between the [0] and [3p] simulations, with the decrease in maximum tidal altitudes from [0] again substantially increased where [0] maximum tidal altitudes are over 3.0 metres.



The highest maximum tidal altitude recorded in Table 6.5 is just over 3.0 metres for the [4p] simulation. The minimum is 0.221 metres, but the lower and upper quartile values (1.195 metres and 2.467 metres) reflect the spread of most of the data, as shown in the histogram in Figure 6.94. The standard deviation at 0.750 metres around the mean of 1.807 metres also indicates that most of the maximum tidal altitudes for the [4p] simulation fall between 1.0 and just over 2.5 metres.

The Wash model for [4p] (Figure 6.95) shows a very complicated pattern of maximum tidal altitudes and some drying out of areas in the Fenland. The presence of these 'islands' may be indicative of the poor estimate of the bathymetry for the Wash at this time in that the depths used in the tidal model were insufficient for tidal inundation of these areas. No geological evidence is available, however, to test this suggestion. Maximum tidal altitudes in the present Wash bay area are about 3.25 metres, considerably (greater than 0.75 metre) higher than those shown for the EC3 model at this time. The palaeogeographic reconstruction shows marine inundation of a number of embayments in the present Fenland area in the Wash model. The pattern of maximum tidal heights reached in these Fenland bays is complicated, with increases in tidal altitudes (of 0.25 metre or more) occurring towards the western end of some of these, but no increases of maximum tidal altitudes occurring in others. Overall, there is a variation in the maximum tidal altitudes reached of approximately 1.0 metre within the Wash embayment as shown at 4,000 years B.P.

Compared with the present sea-level maximum tidal altitudes, results for the WASH model for [4p] (Figure 6.96) indicate reductions of over 0.5 metre in the present Wash embayment area, but smaller reductions (only 0.1 or 0.2 metre) beyond the mouth of the Wash. The magnitude and spatial variation of the maximum tidal altitudes shown in the results of the WASH model are considerably greater than that for the EC3 model. Maximum tidal altitudes in the present Wash area are higher at [4p] than those recorded for [3p] (Figure 6.97), with increases from 2.923 metres at [3p] to 3.239 metres at [4p] at Gibraltar Point, for example, and corresponding figures of 2.586 and 3.274 metres at Tabs Head.

The histogram (Figure 6.98) shows that maximum tidal altitudes are concentrated between 2.5 and 3.5 metres for locations not inland of the coastline at [4p]. The mean value is approximately 0.2 metre below that for the median as a consequence of the influence of drying out at one location for the [4p] reconstruction. Highest maximum tidal altitudes are, however, 0.367 metres higher for [4p] than [3p]. The standard deviation is influenced by the inland location of one point used in the analysis, but the upper and lower quartiles (3.265 and 2.876 metres) provide a better reflection of the distribution of maximum tidal altitudes for [4p]. The scatter plot (Figure 6.90) shows a reduction in maximum tidal altitudes compared with present, but by a lower amount than that for the [3p] simulation, in contrast with the EC3 model [4p] results which suggested that maximum tidal altitudes were reduced further at [4p] than [3p].

The 5,000 years B.P. palaeogeography results [5p] for the EC3 model (Figure 6.99) show maximum tidal altitudes of 2.5 to 3.0 metres in the Wash, with again little change to the tidal patterns of the North Sea. Maximum tidal altitudes are within the range of 2.5 to 3.0 metres over most of the area of the former Wash embayment, increasing to just over 3.0 metres in the southernmost parts of the current Fenland area. Comparison of results for Tabs Head and Gibraltar Point with present sea-level results (Figure 6.100) shows reductions from 3.844 to 2.855 and from 3.296 to 2.842 metres, respectively, indicating the order of the reductions to be approximately a metre in the inner Wash area and 0.5 metre by the mouth of the Wash.

The difference between the [4p] and [5p] simulations (Figure 6.101) shows that maximum tidal altitudes are slightly higher for [5p] than [4p] across the model area, with maximum differences in the Tabs Head and Roaring Middle areas of the inner part of the present Wash embayment. This is also clearly seen from the scatter plot (Figure 6.86) in which [5p] maximum tidal altitudes are shown as higher than those for [3p]. The scatter plot does, however, show the same general trend with decreases of up to about a metre from present sea-level maximum tidal altitudes for [5p] where present sea-levels recorded maximum tidal altitudes above 3.0 metres. The mean value for maximum tidal altitudes

from the [5p] simulation is (Table 6.6) 1.970 metres, close to the median value. The data range from 0.196 metres to 3.171 metres, but are concentrated within the upper and lower quartile range from 2.752 to 1.270 metres, as is shown by the histogram (Figure 6.102).

Results for [5p] of the WASH model (Figure 6.103) show a more complicated pattern than for EC3 as with the other palaeocoastline simulations. In general, maximum tidal altitudes recorded are less than for [4p], but slightly greater than with [3p]. WASH model results for [5p] are higher in the outer bay and lower in the inner part of the present bay than recorded for [5p] with the EC3 model. Results at Tabs Head and Gibraltar Point with WASH for [5p] are 2.674 and 3.010 metres for maximum tidal altitudes for the WASH at [5p], for example.

Compared with the present sea-level simulation, the [5p] results (Figure 6.104) show decreases of maximum tidal altitudes which increase further into the present Wash embayment, reaching 1.230 metres at West Stones. Between the [4p] and [5p] simulations, Figure 6.105 shows that decreases of about 0.5 metre occur in maximum tidal altitudes in the southern part of the present Wash embayment, although these differences are only about 0.2 metre at the northern entrance to the Wash.

The histogram for the WASH model [5p] simulation (Figure 6.106) shows that maximum tidal altitudes are concentrated around the mean value of 2.824 metres, with maximum and minimum values of 3.114 and 2.564 metres (Table 6.8). The standard deviation of 0.158 metre and the upper and lower quartiles suggest that most of the maximum tidal altitudes are very close to the mean value indeed.

### 6.8.2. Morecambe Bay

The LBM model shows an east to west decrease in maximum tidal altitudes for the 5,000 years B.P. palaeogeographic simulation [5p] (Figure 6.107), as is also shown for the present day. Maximum tidal heights reached are not so great, however, for the [5p] simulation as for [0] (Figure 6.108), with heights reaching maximum values of 3.5 metres in the eastern part of the model, approximately 1.0 metre lower than present sea-level

results for Morecambe Bay. The lack of tidal inundation in Morecambe Bay over as great an area is indicated by the sea-level index point data which record the former coastline as surrounding a greater area of sea than for the present day situation. This may be attributed to poor representation of bathymetry due to lack of knowledge of exact sea depth values for 5,000 years B.P. Tide gauge station results show a reduction from 4.022 to 2.974 metres at Heysham, but only a change from 3.877 to 3.738 metres at the Wyre Light at the entrance to the bay. Figure 6.109 shows that the scatter plot of [5p] results against those for the [0] simulation indicate lower maximum tidal altitudes for [5p] than [0], but with a large variation in the amount of the lowering.

Statistical results (Table 6.10) show that mean maximum tidal altitudes are 2.349 metres, below the median value of 2.972 metres. This difference is explained by the histogram (Figure 6.110) which shows that a large number of tide gauge locations (seven) are inland from the coast at [5p]. There is a large spread in non-zero maximum tidal altitudes recorded, which reach a maximum of 3.750 metres at New Brighton.

Figure 6.111 shows that Morecambe Bay is largely dry in the MBM model [5p] simulation. There is, however, a very large increase in maximum tidal altitudes just south of Morecambe Bay along the Lancashire coast, where maximum tidal altitudes in an embayment formed at this sea-level are over 12 metres in one location and above 5 metres in others. It appears that resonance (discussed in Chapter 3) may be important here in causing such large tidal heights. Much of Morecambe Bay itself, however, is dry with the [5p] simulation. The Wyre Light is not dry, though, and a reduction of maximum tidal altitudes from 4.162 [0] to 3.828 metres [5p] is recorded here. This decrease clearly shows the higher altitudes of the finer grid model results as present sea-level results for LBM are only tens of centimetres higher than the [5p] result at the Wyre Light for MBM.

Comparison of results for [5p] with [0] (Figure 6.112) indicates a general reduction of about 0.2 metre in maximum tidal heights in the Irish Sea. However, extensive areas of the inner part of the bay are dry land and where drying out has not occurred maximum

tidal altitudes are, in general, reduced by the order of at least 0.5 metre in the Bay at [5p]. The scatter plot (Figure 6.113) shows that the three locations which are not dry (Table 6.11) have maximum tidal altitudes reduced by about 0.5 metre from those for [0]. The histogram (Figure 6.114) shows that the locations which are not dry all have maximum tidal altitudes within the 3.5 to 4.0 metre class. In view of the bias to the descriptive statistics resulting from the drying out of so much of the model, the maximum tidal altitudes shown by the histogram must be taken as a best estimate of the heights reached over the model area as a whole.

The 8,000 year B.P. palaeogeographic reconstructions were made using two sets of sea depth data due to the uncertainty of error in sea-level index point altitudinal data at this time noted by Shennan (1987). The details of the sea depths used in these are given in Chapter 4 and shown as used in the tidal models in Appendix 6.1.

LBM model results for the higher sea-level at 8,000 years B.P. [8ph] (Figure 6.115) show maximum tidal altitudes over 3.5 metres in the area of Morecambe Bay, with the pattern of maximum tidal altitudes decreasing westwards, as for present sea-level. The greater part of the current area of Morecambe Bay is dry land at this sea-level, but results at the Wyre Light show a decrease from 3.877 to 3.768 metres in maximum tidal altitudes from [0] to [8ph]. Figure 6.116 shows that maximum tidal altitudes are generally reduced by between 0.1 and 0.2 metre from [0] to [8ph]. The difference of the [8ph] simulation with that for [5p] is shown (Figure 6.117) to vary considerably around the model. There is virtually no difference in the maximum tidal altitudes for [5p] to [8ph] at the Wyre Light, whereas an increase of 0.874 metres is shown at Halfway Shoals. Slightly reduced maximum tidal altitudes between the two simulations are, however, evident over much of the model. The scatter plot in Figure 6.109 shows the general reduction in maximum tidal altitudes for [8ph] compared with [0] and [5p], but also considerable variation from place to place in the amount of the difference.

More than half of the stations used in the statistical analyses are inland from the

coast at [8ph], as Figure 6.118 illustrates. The remaining locations record maximum tidal altitudes varying from 2.0 to 4.0 metres, according to the histogram. The highest recorded maximum tidal altitude is 3.768 metres at the Wyre Light, in the entrance to Morecambe Bay.

MBM model results for [8ph] (Figure 6.119) give maximum tidal altitudes of about 3.7 metres in the inner part of the bay which is still subject to inundation at this sea-level, indicating reductions of the order of 0.75 metre compared with present sea-level results for the same area (Figure 6.120). Compared with the [5p] simulation, Figure 6.121 shows a general reduction of 0.2 metre in maximum tidal altitudes. The scatter plot (Figure 6.113) shows a reduction in maximum tidal altitudes for the [8ph] simulation beyond that for [5p] compared with [0] results.

Almost all the locations used in constructing the histogram for the MBM [8ph] simulation (Figure 6.122) are inland from the coastline at [8ph]. Those that remain have maximum tidal altitudes between 3.399 and 3.704 metres. In view of the large amount of drying out of the locations used to obtain the descriptive statistics the usefulness of these statistics is very limited, other than showing the highest recorded maximum tidal altitude.

The lower sea-level simulation at 8,000 years B.P. shows that only the mouth of the current Morecambe Bay is not dry land in the LBM model (Figure 6.123). The LBM model shows maximum tidal altitudes at the mouth of the current Morecambe Bay as over 3.5 metres, as with the simulation using the higher sea-level at 8,000 years B.P. There is a similar pattern of decrease westwards of maximum tidal altitudes in the Irish Sea as for [8ph], but lower maximum tidal heights are shown in the north of the model area, between the Scottish coast and the Isle of Man with the reduced sea-level in the model. Compared with the [0] simulation (Figure 6.124), reductions in maximum tidal altitudes increase from south to north in the model, reaching 0.632 metre at 35 Irish Sea. Differences with the [5p] simulation (Figure 6.125) reach 0.757 metre at the same location

and 0.427 metre in comparison with the [8ph] simulation (Figure 6.126). Figure 6.109 shows that maximum tidal altitudes for [8pl] vary widely in comparison with those for [0], but show reductions in maximum tidal altitudes in almost all cases.

The histogram (Figure 6.127) is a better indicator of the variation in maximum tidal altitudes for those tide gauge stations which are not inland from the coast at [8pl] than the descriptive statistics, which are strongly influenced by the zero maximum tidal altitudes recorded for the tide gauge stations that have dried out. The highest maximum tidal altitude recorded is 3.071 metres and the histogram shows that the remaining maximum tidal altitudes fall within the range of 2.0 to 3.5 metres on the histogram.

The whole of the MBM model is dry for the [8pl] sea-level, as is shown by the nd the scatter plot in Figure 6.113. This is also shown by the scatter plot in Figure 6.113.

### **6.8.3. Comparison of The Wash and Morecambe Bay**

Maximum tidal altitudes are reduced in the palaeogeographic model reconstructions compared with the present day results in the embayments. Comparisons by analysis of variance in the present area of the Wash bay using EC3 results show that the range in maximum tidal altitudes reached within this area does not differ significantly compared with the changes for the palaeogeographic reconstructions (Tables 6.13 and 6.15). The diagrammatic results suggest that it is the pattern of maximum tidal altitudes within the embayments which shows the most change from the present day situation. An overall decrease of about 0.5 metre in maximum tidal altitudes in the present Wash bay is noted by comparison with the present day situation. In the inundated Fenland area, the maximum tidal altitudes reached vary to a greater extent in more local patterns than is shown by the present day results in the Wash bay. The difference between the [5p] results for the EC3 model and the [5p] results from the WASH model suggests that local coastline and bathymetric changes may be very important in obtaining accurate results as the greater detail of the WASH model shows, in this instance, that the scale of the simulation can influence the results.

**Table 6.15. WASH Model: Analysis of Variance Results From Data in Table 6.7.**

**Model Simulations:** Present Sea-Level, 3,000, 4,000 and 5,000 Years B.P. Palaeogeographic Reconstructions

Mean value for [0] simulation = 2.266 m.      Mean value for [3p] simulation = 2.605 m.

Mean value for [4p] simulation = 2.868 m.      Mean value for [5p] simulation = 2.824 m.

F = 1.08      Degrees of freedom = 3, 10      Critical F value for 0.05 probability = 3.71

No significant difference is shown between the maximum tidal altitudes in the simulations.

**Model Simulations:** 3,000, 4,000 and 5,000 Years B.P. Palaeogeographic Reconstructions

Mean value for the [3p] simulation = 2.605 m.      Mean value for the [4p] simulation = 2.868 m.

Mean value for the [5p] simulation = 2.824 m.

F = 1.77      Degrees of freedom = 2, 11      Critical F value for 0.05 probability = 3.98

No significant difference is shown between the maximum tidal altitudes in the simulations.

m. represents metres



**Table 6.16. MBM Model: Analysis of Variance Results From Data in Table 6.11.**

**Model Simulations:** Present Sea-Level, 5,000 Years B.P. and 8,000 Years B.P. Higher and Lower Sea-Level Palaeogeographic Reconstructions

Mean value for the [0] simulation = 4.247 m.      Mean value for the [5p] simulation = 0.799 m.

Mean value for the [8ph] simulation = 0.761 m.      Mean value for the [8pl] simulation = 0.000 m.

$F = 40.97$       Degrees of freedom = 3, 10      Critical F value for 0.05 probability = 3.71  
A significant difference is shown between the maximum tidal altitudes for the simulations.

**Model Simulations:** 5,000 Years B.P. and 8,000 Years B.P. Higher and Lower Sea-Level Palaeogeographic Reconstructions

Mean value for the [5p] simulation = 0.799 m.      Mean value for the [8ph] simulation = 0.761 m.

Mean value for the [8pl] simulation = 0.000 m.

$F = 1.06$       Degrees of freedom = 2, 11      Critical F value for 0.05 probability = 3.98  
No significant difference is shown between the maximum tidal altitudes for the simulations.

m. represents metres

The considerable drying out of Morecambe Bay using the palaeogeographic reconstructions makes use of tide gauge station analysis of variance on the changes within the bay compared with the present day situation difficult, however, this is presented together with analysis of variance between the palaeogeographic simulations excluding the present day simulation to give an indication of the changes between the simulations (Table 6.16). Table 6.14 gives the analysis of variance results for LBM. However, the general tendency is for reduced maximum tidal heights at earlier times in the Holocene. The increase in maximum tidal altitudes along the Lancashire coast south of Morecambe Bay at [5p] (to heights of over 12 metres in one location) shows, as with the [5p] simulation differences between the WASH and EC3 models that the scale of the simulation may play an important part in the results. The results from [5p] and [8ph] and [8pl] for Morecambe Bay suggest that considerably greater knowledge of the palaeobathymetry is needed for this area, as is discussed in more detail below.

## 6.9. Discussion

Austin (1991) noted six ways in which tidal model validation for the tidal regimes at former sea-levels may be attempted. He noted that results of changes to tides shown indicate much lower tidal changes compared with historical changes shown by tide gauges. Woodworth *et al.* (1990) presented data showing trends of similar magnitude for changes of mean tide and mean sea-levels for some European tide gauges. However, the absolute magnitude of the tide gauge trends, measured in centimetres, is lower than some of the changes in maximum tidal heights found in this study. Results presented in this Chapter concur with those of Austin (1991) in noting tidal changes of lower orders of magnitude compared with mean sea-level changes.

Historical changes to tidal patterns at different sea-levels occur on different temporal and spatial scales from those studied in this thesis which extend over thousands of years and tens of kilometres in the changes in spatial extent of marine inundation. The other major category of evidence indicative of palaeotidal heights which may be used to validate

model results is that of sedimentary evidence.

Use of sedimentary evidence in palaeotidal work was discussed in Chapter 1. Such data may be used to derive direct indications of former tidal heights or indications of other aspects of tidal changes. Coarse grained sandy material is indicative of higher current speeds than clay and silt deposits, whilst changes to the faunal and floral populations of nearshore areas occur with different salinity levels and lengths of tidal inundation, for example. In this thesis, examination of tidal changes is confined to the alterations in mean high water of spring tides, taken as equivalent to the maximum tidal altitudes derived from the tidal models of the Wash and Morecambe Bay run for a fifteen day period. Testing of model results is therefore undertaken by comparison with the altitude of sea-level indicators of mean high water of spring tides.

### **6.9.1. The Wash**

The age/altitude graphs of Shennan (1987, 1989) show a decrease in altitude for older sea-level index points in the Wash Fenland. Shennan accounted for this trend by post-glacial isostatic subsidence of the area. However, in detail there are variations in the altitude of sea-level index points within the Fenland for any given time, which may partly reflect tidal changes within the local area.

In the Wash Fenlands at  $3,000 \pm 200$  years B.P. (taken as the standard error for radiocarbon dates, following Shennan (1989)), dated index points (from Appendix 4.3) vary by almost three metres from depths of  $-1.93$  metres O.D. (date reference Q2599) to  $+0.95$  metres O.D. (date reference HV8644). For  $4,000 \pm 200$  years B.P. the range is from  $-4.15$  metres O.D. at Welland Wash for an assay from Cambridge University (referenced as WW4C) to  $-0.12$  metres O.D. (date reference Q2565), showing an increase to four metres in the altitudinal range of the sea-level index points at this time. At  $5,000 \pm 200$  years B.P., dated points vary from  $-5.83$  metres O.D. (date reference IGS121) to  $-3.04$  metres O.D. (date reference Q580). The number of dates available at different times varies as was shown in Figure 4.5 and discussed in Chapter 4.

Results from the palaeotidal simulations for reduced sea depths, coastline changes and palaeogeographies of the area corresponding to 3,000, 4,000 and 5,000 years B.P. may be compared with the pattern of sea-level index point altitudes at those times to assess the quality of reproduction of maximum tidal height changes shown by the models. The number of sea-level index points available is insufficient for comparisons of within-bay tidal changes for earlier periods in the Holocene.

Higher altitudes of sea-level index points (such as that at Chapel Point on the east Lincolnshire coast, date reference Q844) occur in the north of the Fenland area at about 3,000 years B.P., with lower altitudes in the western part of the area at Morten Fen (date reference Q2599, for example). Southern Fenland results, such as that at Welney Wash (date reference Q2820), are also low. For the period  $4,000 \pm 200$  years B.P., sea-level index point altitudes are again higher in the north, such as that at Chapel Point (date reference Q685) compared with the southern and western Fenland results, those of Wood Fen, Ely, and Adventurers' Land (date references Q544 and SRR1589) being cases in point. Around 5,000 years B.P., the Spalding results (*e.g.* date references IGS119 and IGS121) show lower altitudes in Lincolnshire than are found in Cambridgeshire to the south (at Shippea Hill, date reference Q581, for example).

The present sea-level variations in the Wash show increases in maximum tidal altitudes into the inner part of the bay near Tabs Head. Reduced sea-levels of two metres showed decreases of less than 0.10 metre in maximum tidal altitudes in the north and west of the present bay area, but increases of the order of 0.20 metre in the south. These results are within the error band of  $\pm 0.80$  metre established for the accuracy of the tidal models at the present day, but the tendency of higher maximum tidal altitudes in the north of the Wash area which they show is reflected in the sea-level index point altitudinal variations in the Fenland.

Palaeocoastline simulations show greater absolute changes in maximum tidal heights within the Wash than the simulated reduction of sea-level lowered by two metres from

the present level. The general pattern of maximum tidal height changes again accords well with the areas of higher and lower sea-level index points around the Fenland, but the tendency for differences of the tidal regime to decrease, compared with the present day situation, further back in time does not concur with the changes in sea-level index point altitudes which decrease at a greater rate earlier in the Holocene. Sediment compaction, affecting the altitude of sea-level index points, may be an influence in this pattern. It should be noted again, though, that the tidal altitude changes of less than 1.0 metre for the palaeocoastline simulations compared with the present day situation are within the model error assessment figures.

Palaeogeographic simulations show a complicated pattern of variation of maximum tidal altitudes within the Wash Fenland, making comparisons with sea-level index point altitude changes more difficult. The series of embayments shown for 4,000 years B.P., some with changes of maximum tidal altitudes locally of 0.5 metre, is a particular problem. The overall tendency is, however, for higher maximum tidal altitudes in the north of the former Fenland and the lowest results in the west, reflecting the spatial variation in the altitudinal distribution of the sea-level index points. For many parts of the present Wash bay the tidal changes shown with the palaeogeographic reconstructions are still within the error band of  $\pm 0.80$  metres for the accuracy of the present sea-level maximum tidal height patterns.

### **6.9.2. Morecambe Bay**

Shennan's (1987, 1989) graphs show an exponential increase in the altitude of sea-level index points for Morecambe Bay towards the early Holocene, the trend of which is accounted for by post-glacial isostatic uplift of the area. The variations on this trend may reflect neotectonic movements, tidal changes or other factors (Tooley, 1987). The contribution of tidal variations is assessed below.

Within 200 years of 5,000 years B.P., sea-level index points vary from around +5.0 metres O.D. (*e.g.* date reference HV3460) in the north-east of the bay with lower altitudes

south of the Morecambe Bay area (such as date reference HV3845). The altitudinal differences within the bay itself are difficult to assess due to the lack of dated sea-level index points for the area. At  $8,000 \pm 200$  years B.P., sea-level index point altitudes are around  $-11.0$  to  $-16.0$  metres O.D. (*e.g.* date reference HV3362) at sites currently offshore within the bay. However, the curve for post-glacial isostatic recovery of the area drawn by Shennan (1989) implies that sea-level index point altitudes should be up to over 20 metres higher than shown. Two palaeogeographic reconstructions for the area were made to allow for both possibilities in the tidal modelling experiments. The paucity of dates makes altitudinal variations within the bay difficult to assess from the geological data.

Sea depth reduction tidal simulations for two and fifteen metres lower sea-levels than present may be compared with the sea-level index point altitudes for 5,000 and 8,000 years B.P., respectively. Maximum tidal altitudes shown from model results are lower than present for 5,000 years B.P., whereas sea-level index points suggest that tidal heights should be increased compared with present values at this time. For the sea-level reduction of fifteen metres, almost the entire bay area is dry land, so that again tidal inundation does not occur so far into the bay area as the sea-level index points imply should be the case.

Palaeocoastline simulations for 5,000 and 8,000 years B.P. also fall short of inundation of areas shown to have been on the coast by sea-level index points. Maximum tidal altitudes are reduced for both simulations, whereas an increase in the height of the highest tides should have occurred according to geological information at 5,000 years B.P. Changes in the bathymetry not reproduced in these model simulations are a possible cause of the lack of correspondence with sea-level index point altitudes. However, palaeogeographic simulations incorporating sea depth changes for 5,000 and 8,000 years B.P. similarly show smaller areas of inundation than suggested from the geological record. A considerably improved knowledge of the detail of palaeogeographic changes to Morecambe Bay, especially with regard to depth changes within the bay may provide tidal simulations correspond-

ing more closely with the sea-level index point record. Variables such as neotectonic movements, suggested by Tooley (1978, 1987), may play an important role in this respect.

### **6.9.3. Comparison of The Wash and Morecambe Bay**

An attempt at validation of model results for tidal changes during the Holocene suggests that neither sea depth reductions nor former coastline shapes used individually in model simulations for tides are sufficient to give an accurate assessment of the magnitude and pattern of change to tidal regimes within the bays studied. Similarly, an attempt at tidal simulations using palaeogeographic data for coastline and bathymetry changes highlights the low quantity of the palaeogeographic data available for such work.

The overall pattern of maximum tidal heights reached shown in the geological record is reflected in the results for modelling of the Wash. An assessment of the magnitude of tidal changes is limited by the errors in the accuracy both of tidal model maximum tidal height predictions (of within 0.80 metre) and of the altitude of sea-level index points (discussed in Chapter 1). Results for Morecambe Bay show maximum areas of tidal inundation which are less than those indicated by sea-level index points and a considerably more detailed knowledge of the palaeogeography of this area should be attained to aid in overcoming this problem.

The factors affecting the accuracy of palaeogeographic reconstructions of the embayments and their possible contribution to the variations in sea-level index point altitudes within the local areas of the Wash Fenlands and Morecambe Bay are discussed in Chapter 7. An assessment of the conclusions from the model results with respect to the aims of the study is presented in Chapter 8, together with suggestions for further research.

## CHAPTER 7

### NEOTECTONICS AND SEDIMENT COMPACTION

#### 7.1. Neotectonic movements

Shennan (1987) states that controlling factors on the sea-level record at the estuary/bay scale may be illustrated by assessing the differences between local sea-level curves and the proposed regional eustatic curve (Mörner, 1980). In this study an examination has been made of the effect of tidal changes at different sea-levels on the altitudinal variation of sea-level index points within the Wash Fenland and Morecambe Bay. In Chapter 1 a brief outline was given of other factors affecting the variation within a local area of sea-level index point altitude. These factors are considered in more detail here and their relevance to the field areas examined in the thesis is considered.

Neotectonic movements, or recent earth movements, other than those of isostatic origin, are one variable in the local sea-level change equation. There are no major fault lines running through the area of The Wash, although minor faulting running northeast - southwest and northwest - southeast is shown on the British Geological Survey solid geology sheets for Spurn and East Anglia (1985 and 1985). Greensmith and Tucker (1980) recorded evidence of differential subsidence on the Essex coast to the south of the Fenland area. However, no evidence of fault movements has been recorded in the literature for the Wash Fenlands during the Holocene marine inundations and the scale of isostatic movements (at one metre per thousand years) suggest that these land movements have had little influence on the sea-level record of the Wash Fenland area. Sediment compaction, discussed below, may have been of greater importance.



In Morecambe Bay considerable differences were shown between the location of sea-level index points from the stratigraphic record and the areas reached by tidal inundation from the model simulations for former sea-levels. Tooley (1978, 1987) proposed that neotectonic movements had occurred in the bay. Figure 7.1 shows the distribution of faults in the area of Morecambe Bay. There are three major fault lines running across parts of the bay from directions of between north-south and northwest-southeast. Morecambe Bay lies much nearer to former centres of ice accumulation in the north of England and Scotland than the Fenland and has therefore undergone considerably more isostatic recovery (Shennan, 1987, 1989). It is possible that these isostatic movements may have reactivated the faults during the Holocene so that the current relationship of sea-level index points to Ordnance Datum may reflect these movements in addition to sea-level change. Ringrose (1987) identified stress patterns in the area which contribute further evidence to support this suggestion.

Neotectonic movements associated with post-glacial isostatic recovery have been identified in Scotland (Sissons, 1972; Sissons and Cornish, 1982) during reconstruction of the history of sea-level change. Studies in Scandinavia (*e.g.* Anundsen, 1985) have also identified this phenomenon, but very little work has been carried out in Britain on recent neotectonic movements (Davenport and Ringrose, 1985), probably due to the fact that the scale of current movements is generally very small (measured in terms of millimetres per annum at maximum) and that the potential for these movements is especially low in densely populated areas.

Neotectonic movements may have caused some of the altitudinal variation of sea-level index points at the bay scale, possibly in association with isostatic recovery, especially in an area where isostatic recovery has been measured at the rate of several metres per thousand years, as in Morecambe Bay. Rapid rates of isostatic movements may have reactivated old fault lines in such areas. This is a topic which deserves more attention in interpretation of the sea-level record near former centres of ice accumulation.

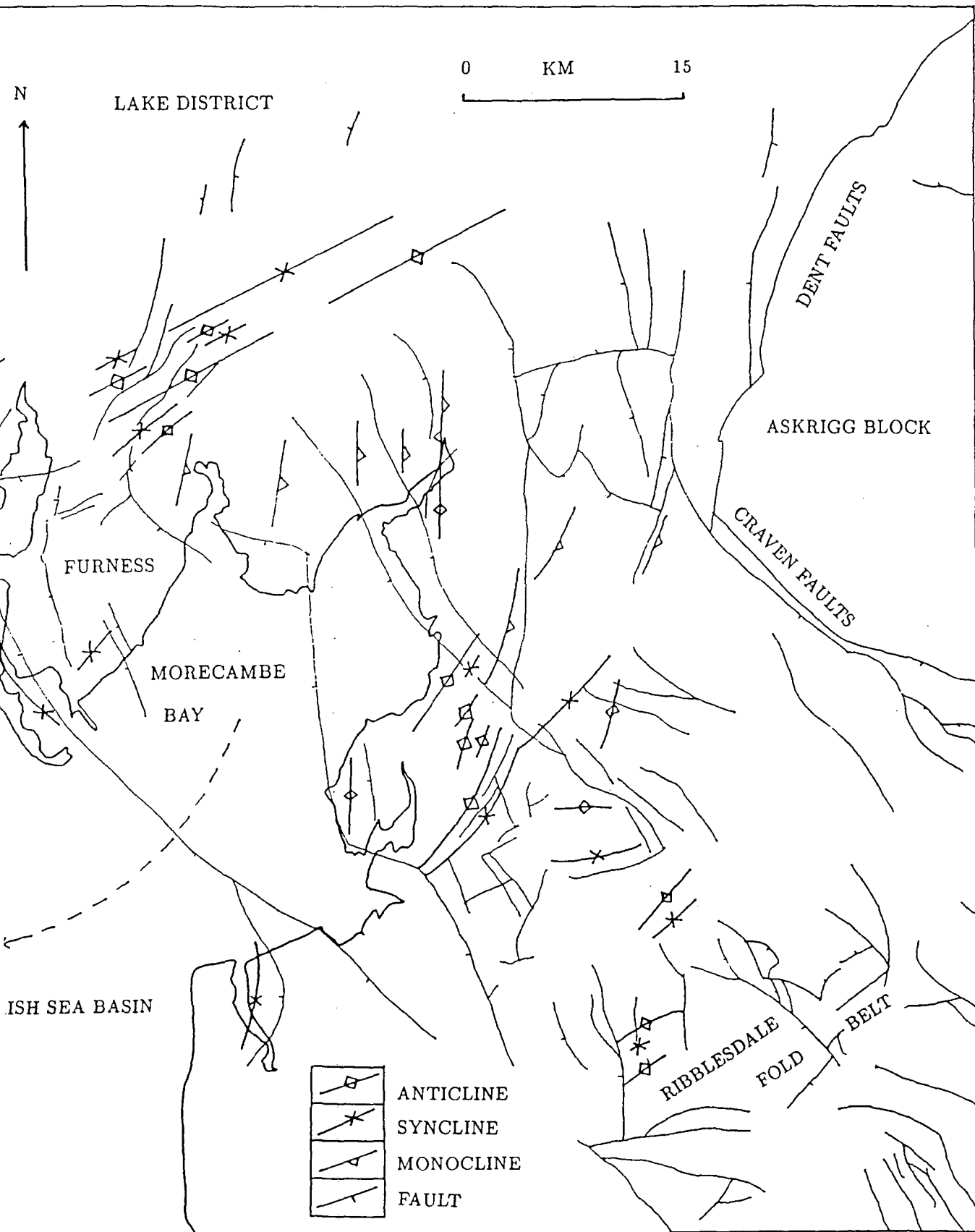


Figure 7.1. The Structural Setting of Morecambe Bay (after Patrick, 1987).

## 7.2. Sediment compaction

The importance of sediment compaction to sea-level studies, particularly its effect on the altitude and age of sea-level index points, was outlined briefly in Chapter 1. A further examination is made here of the influence of the reduction in volume of a sediment resulting from a lessening of the pore space in terms of its spatial and temporal, lateral and vertical, variation. This factor has a potential influence on the accuracy of construction of palaeogeographic maps used in the study and analysis of the altitudinal and age variation of the sea-level index points.

The factors contributing to the altitudinal and temporal effects of sediment compaction in an area may be divided into four main elements:

- (a) the nature and thickness of the sediments involved
- (b) the length of time since deposition and erosional/ depositional cycles which have occurred during this period
- (c) the nature and depth of former and existing overlying sediments
- (d) variations in local drainage over time, which may have caused changes to the nature of the sediments.

Coarse-grained sediments, such as sand, suffer least compaction, whereas organic and fine-grained sediments, especially peats, clays and silts, are most affected. Compaction, therefore, has implications for sediments based on the sea-level history of an area. Clays and silts are deposited in quiet water environments, such as salt marshes, whereas sand is found in areas where currents are stronger, generally further offshore. Peat growth may occur in association with stagnant water, landward of salt marshes. Therefore an area with a sea-level history of marine inundation in some depth of water may be characterised by a sandy stratigraphic sequence which is unlikely to undergo much compaction. By contrast, an area which has a history of being on the landward edge of a salt marsh, with a large amount of peat growth, may be compacted to a very small fraction of its original thickness. Altitudinal variations of sea-level index points may be related to the sequence

of sea-level change in this way.

Stratigraphic records suggest that the southern Fenland and areas not currently subject to inundation in Morecambe Bay were locations of quiet water sedimentation, characterised by deposition of intercalated peat and silt/clay sequences. These areas may thus have undergone more compaction than the northern Fenland, for example, where a greater proportion of the sediments are sands. The absolute altitudinal variation caused will be greater for thicker beds, given the same relative amount of compaction throughout. Streif (1979) points out that compaction may lead to a significant change in the altitudinal range of sediments as a compaction value of 50% for a peat bed would give a reduction in thickness of a two metre bed, at the time of deposition, to one metre following compaction.

Compaction occurs through three main mechanisms:

- (a) settlement of the sediment under its own weight (autocompaction)
- (b) desiccation by prolonged surface exposure (such as may occur with a fall of sea-level) leading to overconsolidation, which will affect sediments to greater depths with an increase in the length of exposure (Greensmith and Tucker, 1971)
- (c) deposition of a burden of overlying sediments.

Compaction does not occur at an even rate through time and variations in the rates of erosion and deposition (and therefore sediment load) may complicate the picture. The palaeogeographic maps show that different parts of the field areas were subject to inundation at different times. Compaction of sediments underlying those under examination will lower the altitude of the overlying sediments (Van de Plassche, 1980). At the site of the former Whittlesey Mere in the Fenland a peat layer is shown to vary in altitude depending on the nature of the sediments above or below it in the stratigraphic sequence (Godwin and Vishnu-Mittre, 1975, figure 22).

### 7.3. Other factors

No account has been taken in this study of sediment movement patterns which may have caused local depth variations and therefore within-estuary apparent sea-level change, such as that recorded in Chezzetcook Inlet, Nova Scotia, by Carter *et al.* (1990). This emphasises the need for detailed examination of potential sea-level index points in terms of their lithology, stratigraphic context and micro- and macro- faunal assemblages. More detailed study of this variable might allow local depth and coastal changes to be taken into account in the tidal models and so give a more realistic simulation of former tidal patterns. There is, however, no evidence of more than a few metres of sediment deposition in either the Wash or Morecambe Bay during the Holocene and so factors such as sedimento-isostasy are not considered to have influenced the altitude of sea-level index points in either bay.

Tidal studies may be of more use to sea-level change researchers than simply assessing the relevance of tidal height changes to altitudinal variations of sea-level index points within embayments. Preece *et al.* (1990) used a tidal model of the English Channel to test possible palaeobathymetries based on evidence of stratified seas from the present eastern Solent area. This approach may be more difficult to apply at the local scale in estuarine embayments where changes in salinity and stratification occur on the scale of tidal cycles.

A wide range of factors influence the pattern and nature of the sea-level record. The accuracy of sea-level index points was examined in Chapter 1. Geoidal changes are not considered to be of significance for the time and space scales in this study (Shennan, 1987). Similarly, other aspects of the sea-level change equation are not relevant to consideration of the causes of altitudinal variation of sea-level index points within embayments over the last few thousand years.

## CHAPTER 8

### CONCLUSIONS

“The value of palaeotidal work lies in aiding the precise evaluation on meso-macrotidal coasts of the relationship between a sea-level indicator’s height and a former sea-level position” (Devoy, 1987, p.22). The most reliable sea-level indicators occur in sediments from the uppermost portion of the tidal range (Scott and Greenberg, 1983), where changes in tidal amplitude over time will have the greatest effect, variably distorting the ‘true’ sea-level record and the reconstruction of sea-level movements derived from these sea-level index points (Devoy, 1987). “The application of numerical studies of tidal amplitude is essential, therefore, in aiding quantification of this distortion and obtaining a more accurate prediction of future changes in coastal position” (Devoy, 1987, p.23). This thesis has contributed towards understanding of tidal changes in association with the sea-level change record, as is summarised below.

#### **8.1. The magnitude of tidal variations within embayments**

Maximum tidal variations within the two macro-tidal embayments studied changed within 0.5 metre for the Wash, but by over 0.8 metre in the case of Morecambe Bay, for maximum tidal heights reached in the course of a spring-neap cycle at present sea-level simulated by numerical modelling. The finer resolution estuary models enlarged these differences and for Morecambe Bay showed higher degrees of correspondence with observational data. However, in general the pattern of tidal height variations agrees well with the observational data obtained from Admiralty Tide Tables (1990). Sea-level index point altitudinal variations, however, show greater variations for former times than the

currently recorded tidal differences within the embayments, varying by the order of metres.

### **8.2. The effect of the coastline shape of an embayment have on tidal variations**

For the Wash three palaeocoastline simulations were carried out. These all recorded less difference in tidal variations within the present bay area than for the present day, although greater changes were shown over the current Fenland area between the simulations. The same was true for Morecambe Bay, except for the simulation for 8,000 years B.P., when much of the bay was dry. When sea depth changes were introduced in addition to coastal shape changes, noticeable alterations were evident to the tidal heights reached within the embayments.

### **8.3. The effect of the sea-bed morphology on tidal variations**

Reductions of sea depths in the tidal models showed considerable alterations to the altitudinal range of maximum tidal heights reached within the embayments for sea level reductions of more than 5 metres. Full palaeogeographic reconstructions of the Wash and Morecambe Bay used eustatic sea-level reductions of at most 2 metres, except for the 8,000 year B.P. reconstruction of Morecambe Bay for which a eustatic sea-level of 15 metres below present was used. Therefore the tidal changes in the embayments were less than for all except the lower sea-level only simulations and were of much lower orders of magnitude than changes to mean sea-level.

### **8.4. The contribution of neotectonics and sediment compaction to the altitudinal variations of sea-level index points within the chosen embayments**

Neotectonic movements during the post-glacial period are a possible cause of altitudinal variations of sea-level index point heights within Morecambe Bay, which is located near a former centre of ice accumulation and has therefore undergone tens of metres of isostatic movement. This area is also characterised by faults in the basement geology, which may have been reactivated by isostatic movement. Neotectonic movements offer a possible explanation for the wide difference between the predicted tidal inundation in the

Bay at 8,000 years B.P. from the sea-level index point record and the situation produced by tidal model simulation in this study. In the Wash Fenlands, however, little isostatic movement has taken place and there are no major fault systems in the basement geology which are likely to have been reactivated by the minor isostatic recovery which occurred in the post-glacial period.

Sediment compaction is a phenomenon which, potentially, has a considerable effect on the sea-level record. It is variable in its effect within an embayment and assessment of the extent of its influence cannot easily be made without very detailed knowledge of the palaeogeographic history of an area.

Both neotectonic movements and sediment compaction remain as 'unknown' factors in the sea-level change equations of the Wash and Morecambe Bay. To these must be added the effect of sediment movements within the bays and other local changes which may have affected the palaeogeography of the embayments.

### **8.5. The implications of the results of this study for a rise of sea-level**

Simulation of the former maximum tidal heights reached in The Wash and Morecambe Bay has shown that tidal altitudes vary with changing sea-levels and so this must be taken into account in any assessment of a sea-level rise. In general the results showed that lower tidal heights were found with lower sea-levels in broad embayments, but this was modified by changes in the coastline shapes particularly those noted by the formation of embayments within the Fenland area at 4,000 years B.P., necessitating assessment to be made of this factor in a simulation of tidal conditions with a sea-level rise. Furthermore, the scale differences noted between the 5,000 years B.P. palaeogeographic simulations for the Wash between the EC3 and WASH models, giving higher tidal altitudes in the latter than for the 3,000 and 4,000 years B.P. simulations with the reverse situation for the EC3 simulations, suggests that the scale of modelling may have an important influence on the results. This is shown to be especially important locally with the apparent resonance effect in the MBM model 5,000 years B.P. palaeogeographic simulation leading to maximum



tidal altitudes of over 12 metres in an embayment created with this sea-level along the Lancashire coast. The LBM model does not show this embayment in the same way due to the scale of modelling.

### **8.6. Recommendations for further research**

A number of recommendations for the course of future research into sea-level change and tidal changes in particular may be made from the results of this study. These essentially fall into the categories of tightening up on the assumptions made in the research by improving the database (especially palaeogeographic data) and adding more factors in to the tidal simulations with higher resolution models, such as assessment of the change in tidal and other currents at different sea-levels (and so permitting study of sediment movement patterns). Tidal analysis *per se* may also be carried out as a study of the importance of different tidal constituents at different sea-levels in an area. When sufficiently good data are available for a wide area, the tidal factor may then be eliminated as an 'unknown' from the regional sea-level picture, permitting correspondence of sea-level histories between areas to be made. Possible sea-level rise scenarios may also be simulated for assessment of consequent tidal changes. Sea-level index points have been used in this study to represent approximately the altitude of mean high water of spring tides. However, this neglects variations in sea-level heights as a result of meteorological influences. Sea-level altitudes may be temporarily increased as a result of storm activity and the combined effect of an increase in the incidence of storminess and tidal height changes is a further area of potential for study.

### **8.7. Conclusions of the research with regard to sea-level change studies**

The statements by Devoy (1987, p.22) that

“Within a confined coastal environment local tidal range may differ considerably from that at the open coast. In a funnel-shaped estuary tidal amplification often rises landward, due to confinement of the tidal wave as it progresses up-estuary (the ‘estuary effect’, Fairbridge, 1961). Conversely a reduction in tidal range takes place when the tidal wave,

after passing through a confined coastal inlet, enters a flanking basin with a large storage capacity ('flood-basin effect', Van Veen, 1950). Dissipation of tidal energy due to water/bed interface friction also results in a decrease in tidal amplitude (Allen *et al.*, 1980)."

are justified by the results presented in this thesis. Therefore, where a good palaeogeographic reconstruction of an area is possible, the former tidal patterns may be simulated to assess the contribution of tidal changes to the overall and within-embayment sea-level change record.

## REFERENCES

- Admiralty (1990) *Admiralty Tide Tables; European Waters including the Mediterranean Sea*. Volume I. Taunton: H.M.S.O.
- Allen, G.P., Salomon, J.C., Bassoullet, P., du Penhoat, Y. and C. de Grandpré (1980) Effects of tides on mixing and suspended sediment transport in macrotidal estuaries. *Sedimentary Geology*, **26**, 69-90.
- Anon. (1972) *Annual Report for 1971*. London, Institute of Geological Sciences, Natural Environment Research Council.
- Anundsen, K. (1985) Changes in shore-level and ice-front positions in Late Weichsel and Holocene, southern Norway. *Norsk geografisk Tidsskrift*, **39**, 205-225.
- Ashmead, P. (1974) The caves and karst of the Morecambe Bay area. In Waltham, A.C.(ed.), *The Limestone and Caves of North-West England*. Newton Abbot: David and Charles.
- Austin, R.M. (1988) *The Paleotidal Regime on the North-West European Shelf*. Unpublished M.Sc. thesis, University College of North Wales, Bangor.
- Austin, R.M. (1991) Modelling Holocene tides on the North-West European continental shelf. *Terra Nova*, **3**, 276-288.
- Backhaus, J. (1985) A three-dimensional model for the simulation of shelf sea dynamics. *Deutsche Hydrographische Zeitschrift*, **38**, 165-187.
- Barckhausen, J., Preuss, H. and Streif, H. (1977) Ein lithologisches Ordnungsprinzip für das Küstenholozän und seine Darstellung in Form von Profiltypen. *Geologisches Jahrbuch*, **A44**, 45-77.
- Barckhausen, J. and Streif, H. (1978) *Erläuterungen zu Blatt Emden West nr.2608, 1:25,000*. Hannover: Niedersächsisches Landesamt für Bodenforschung, 80pp.

- Baden-Powell, D.F.W. (1934) On the marine gravels at March, Cambridgeshire. *Geographical Magazine*, **71**, 193-219.
- Behre, K.E., Menke, B. and Streif, H. (1979) The Quaternary geological development of the German part of the North Sea. In Oele, E., Schüttenhelm, R.T.E. and Wiggers, A.J. (eds.), *The Quaternary History of the North Sea*. Acta Univ. Ups. Symp. Univ. Ups. Annum Quingentesimum Celebrantis 2, 85-113, Uppsala.
- Bott, M.H.P. (1978) Deep structure. In Moseley, F. (ed.), *The Geology of the Lake District*, Yorkshire Geological Society, Occasional Publication no.3, 25-40.
- Boulton, G.S. (1990) (ed.) The Late Cenozoic Ice Age. *Transactions of the Royal Society of Edinburgh*, **C 18(4)**.
- Bradley, R.S. (1985) *Quaternary Paleoclimatology*. London: George Allen & Unwin, 472pp.
- Brebbia, C.A. and Connor, J.J. (1976) *Finite Element Techniques for Fluid Flow*. London: Newnes-Butterworths. 307pp.
- Brettschneider, G. (1967) *Anwendung des hydrodynamischnumerischen Verfahrens zur Ermittlung der  $M_2$ -Mitschwingungszeit der Nordsee*, Mitteilungen Institut Meereskunde Universität Hamburg nr. 7.
- Bridgland, D.R., Davey, N.D.W. and Keen, D.H. (1991) Northam Pit, Eye, near Peterborough. In Lewis, S.G., Whiteman, C.A. and Bridgland, D.R. (eds.) *Central East Anglia and the Fen Basin Field Guide*. Quaternary Research Association, London, 173-183.
- Bristow, C.R. and Cox, F.C. (1973) The Gipping Till: a reappraisal of East Anglian glacial stratigraphy. *Journal of the Geological Society of London*, **129**, 1-37.
- Broadhurst, F.M. (1985) The geological evolution of north-west England. In Johnson, R.H. (ed.) *The Geomorphology of north-west England*. Manchester: Manchester University Press, pp.24-36.

- Burton, R.G.O. and West, R.G. (1991) Mepal Fen, Cambridgeshire. In Lewis, S.G., Whiteman, C.A. and Bridgland, D.R. (eds.), *Central East Anglia and the Fen Basin*, Field Guide, Quaternary Research Association. London: Quaternary Research Association, pp.123-126.
- Carter, R.W.G., Orford, J.D. and Jennings, S.C. (1990) The recent transgressive evolution of a paraglacial estuary as a consequence of coastal barrier breakdown: Lower Chezzetcook Inlet, Nova Scotia, Canada. *Journal of Coastal Research Special Issue no. 9, 2*, 564-590.
- Caston, V.N.D. (1979) A new isopachyte map of the Quaternary of the North Sea. In Oele, E., Schüttenhelm, R.T.E. and Wiggers, A.J. (eds.), *The Quaternary History of the North Sea*, Acta Universitatis Upsaliensis Symposia Universitatis Upsaliensis Annum Quingentesimum Celebrantis: 2, Uppsala, 23-28.
- Castleden, R. (1980) The Second and Third Terraces of the River Nene. *Mercian Geologist*, **8**, 29-46.
- Catt, J.A. (1977) *Yorkshire and Lincolnshire*. Guidebook for excursion C7 (ed. D.Q. Bowen), 10th INQUA Congress, 1977. Norwich: Geoabstracts.
- Chatwin, C.P. (1961) *British Regional Geology - East Anglia and Adjoining Areas*. London: HMSO.
- Churchill, D.M. (1970) Post Neolithic to Romano-British sedimentation in the southern Fenlands of Cambridgeshire and Norfolk. In Phillips, C.W. (ed.), *The Fenland in Roman Times*, Royal Geographical Society Research Series no.5, London: William Clowes and Sons Ltd., 132-146.
- Clarke, R.H. (1973) Cainozoic subsidence in the North Sea. *Earth and Planetary Science Letters*, **18**, 329-332.
- Coope, G.R. (1974) Climatic fluctuations in north-west England since the last Interglacial indicated by fossil assemblages of Coleoptera. In Wright, A.E. and Moseley, F. (eds.),

- Ice Ages: Ancient and Modern*. Liverpool: Seel House Press, pp.153-168.
- Coope, G.R. and Pennington, W. (1977) The Windermere interstadial of the late Devensian. *Philosophical Transactions of the Royal Society of London*, **B 280**, 337-339.
- Courant, R., Friedrichs, K.O. and Lewy, H. (1928) Über die partiellen Differenzgleichungen der mathematischen Physik. *Mathematischen Annalen*, **100**, 32-74.
- Dansgaard, W., Johnsen, S.J., Clausen, H.B. and Langway, C.C. (1971) Climatic record revealed by the Camp Century ice core. In *Late Cenozoic Ice Ages*. New Haven, Connecticut: Yale University Press, pp. 37-56.
- Davenport, C.A. and Ringrose, P.S. (1985) Fault activity and palaeoseismicity during Quaternary time in Scotland - preliminary studies. In *Earthquake Engineering in Britain*. London: Thomas Telford, pp. 143-155.
- Davey, N.D.W. (1991) A Review of the Pleistocene Geology of the Peterborough District. In Lewis, S.G., Whiteman, C.A. and Bridgland, D.R. (eds.) *Central East Anglia and the Fen Basin Field Guide*. Quaternary Research Association, London, 150-162.
- Davies, A.M. (1983) Comparison of computed and observed residual currents during JONSDAP '76. In Johns, B. (ed.), *Physical Oceanography of Coastal and Shelf Seas*, Elsevier Oceanography Series 35, Amsterdam: Elsevier, pp. 357-386.
- Davies, J.L. (1964) A morphogenetic approach to world shorelines, *Zeitschrift für Geomorphologie*, **8**, 127-142.
- Desai, C.S. and Abel, J.F. (1972) *Introduction to the Finite Element Method: A numerical method for engineering analysis*. London: Van Nostrand Reinhold Company. 477pp.
- Devoy, R.J.N. (1982) Analysis of the geological evidence of Holocene sea-level movements in south-east England. *Proceedings of the Geologists' Association*, **93**, 65-90.
- Devoy, R.J.N. (1987) Introduction: First principles and the scope of sea surface studies. In Devoy, R.J.N. (ed.), *Sea Surface Studies: A global view*, Beckenham, Kent: Croom Helm, pp.1-30.

- Dickinson, W. (1973) The development of the raised bog complex near Rusland in the Furness district of north Lancashire. *Journal of Ecology*, **61**, 871-886.
- Dobson, M.R. (1977a) The geological structure of the Irish Sea. In Kidson, C. and Tooley, M.J. (eds.), *The Quaternary History of the Irish Sea*, Geological Journal Special Issue no.7, Liverpool: Seel House Press, 27-54.
- Dobson, M.R. (1977b) The history of the Irish Sea basins. In Kidson, C. and Tooley, M.J. (eds.), *The Quaternary History of the Irish Sea*, Geological Journal Special Issue no.7, Liverpool: Seel House Press, 93-98.
- Doodson, A.T. (1921) The harmonic development of the tide-generating potential. *Proceedings of the Royal Society*, **A 100**, 305-329.
- Doodson, A.T. and Warburg, H.D. (1941) *Admiralty Manual of Tides*. London: H.M.S.O., 270pp.
- Dronkers, J.J. (1974) Tidal theory and computations. In Chow, V.T. (ed.), *Advances in Hydrosciences*, vol. 10, New York: Academic Press, 418pp.
- Eden, R. A., Holmes, R. and Fannin, N.G.T. (1978) Quaternary deposits of the central North Sea 6. Depositional environment of offshore Quaternary deposits of the continental shelf around Scotland. *Institute of Geological Sciences Report*, **77/15**.
- Eisma, D. (1981) Supply and deposition of suspended matter in the North Sea., In Nio, S.-D., Schüttenhelm, R.T.E. and van Weering, T.C.E. (eds.), *Holocene Marine Sedimentation in the North Sea Basin*, Special Publication of the International Association of Sedimentologists no.5, Oxford: Blackwell Scientific Publications, 415-428.
- Eisma, D., Jansen, J.H.F. and van Weering, T.C.E. (1979) Sea-floor morphology and recent sediment movement in the North Sea. In Oele, E., Schüttenhelm, R.T.E. and Wiggers, A.J. (eds.), *The Quaternary History of the North Sea*, Acta Universitatis Upsaliensis Symposia Universitatis Upsaliensis Annum Quingentesimum Celebrantis: 2, Uppsala, 217-231.

- Evans, R. and Mostyn, E.J. (1979) *Stratigraphy and soils of a Fenland gas pipeline*. Cambridge: Ministry of Agriculture, Fisheries and Food, A.D.A.S. Land Service.
- Everett, R. and Shennan, I. (1987) *Strat: A computer program for Quaternary Stratigraphic Data display and management*. Department of Geography, University of Durham, Occasional Publications (New Series) No. 20.
- Eyles, N. and McCabe, A.M. (1989) The Late Devensian (<22,000 B.P.) Irish Sea Basin: The Sedimentary Record of a Collapsed Ice Sheet Margin. *Quaternary Science Reviews*, **8**, 307-351.
- Fairbridge, R.W. (1961) Eustatic changes in sea-level. *Physics and Chemistry of the Earth*, **5**, 99-185.
- Firth, C.R. and Haggart, B.A. (1989) Loch Lomond Stadial and Flandrian Shorelines in the inner Moray Firth area, Scotland. *Journal of Quaternary Science*, **4**, 37-50.
- Flather, R.A. (1976) A tidal model of the north-west European continental shelf. *Memoirs, Société Royale de Science de Liège, serie 6*, **10**, 141-164.
- Flather, R.A. (1979) Recent results from a storm surge prediction scheme for the North Sea. Pp.385-409 in Nihoul, J.C.J. (ed.), *Marine Forecasting, Proc. 10th International Liège Colloquium on Ocean Hydrodynamics 1978*. Amsterdam: Elsevier, 493pp.
- Flather, R.A. and Heaps, N.S. (1975) Tidal computations for Morecambe Bay, *Geophysical Journal of the Royal Astronomical Society* **42**, 489-517.
- Flather, R.A. and Hubbert, K.P. (1990) Tide and surge models for shallow water - Morecambe Bay revisited. Pp.135-166 in Davies, A.M. (ed.), *Modelling Marine Systems* volume 1, Boca Raton, Florida: CRC Press, 297pp.
- Flemming, N.C. (1982) Multiple regression analysis of earth movements and eustatic sea-level change in the United Kingdom in the past 9,000 years. *Proceedings of the Geologists' Association*, **93**, 113-125.
- Forsythe, G.E. and Wasow, W.R. (1960) *Finite-Difference Methods for Partial Differential*



- Equations*. London: J. Wiley and Sons. Applied Mathematics Series ed. Sokolnikoff, I.S. 444pp.
- Franken, A.F. (1987) *Rekonstruktie van het Paleo-Getijklimaat in de Noordzee*. Masters Thesis, Delft Hydraulics Laboratory, The Netherlands.
- Gale, S.J. (1981) The geomorphology of the Morecambe Bay karst and its implications for landscape chronology, *Zeitschrift für Geomorphologie*, **25**, 457-69.
- Gallois, R.W. (1979) Geological Investigations for the Wash Water Storage Scheme. *Institute of Geological Sciences Report*, **78/19**.
- Gallois, R.W. (1989) Geology of the country around Ely. *Memoirs of the British Geological Survey*, Sheet 173.
- Garrett, C.J.R. (1972) Tidal resonance in the Bay of Fundy and Gulf of Maine, *Nature*, **238**, 441-443.
- Garrett, C.J.R. (1984) Tides and tidal power in the Bay of Fundy, *Endeavour*, **8**, 58-64.
- Garrett, C.J.R. and Greenberg, D. (1977) Predicting changes in tidal regions: the open boundary problem, *Journal of Physical Oceanography*, **7**, 171-181.
- Gaunt, G.D., Bartley, D.D. and Harland, R. (1974) Two interglacial deposits proved in boreholes in the southern part of the Vale of York and their bearing on contemporaneous sea-levels. *Bulletin of the Geological Survey of Great Britain*, **48**, 1-24.
- Gibbard, P.L. and Turner, C. (1988) In defence of the Wolstonian stage, *Quaternary Newsletter*, **54**, 9-14.
- Godin, G. (1972) *The Analysis of Tides*. Liverpool: Liverpool University Press, 264pp.
- Godwin, H. (1940) Studies of the post-glacial history of British vegetation. III. Fenland pollen diagrams. IV. Post-glacial changes of relative land and sea-level in the English Fenland. *Philosophical Transactions of the Royal Society of London*, **B 230**, 239-303.

- Godwin, H. (1978) *Fenland: Its Ancient Past and Uncertain Future*. Cambridge: Cambridge University Press.
- Godwin, H. and Clifford, M.H. (1938) Studies of the post-glacial history of British vegetation. I. Origin and stratigraphy of the Fenland deposits near Woodwalton, Hunts. II. Origin and stratigraphy of deposits in southern Fenland. *Philosophical Transactions of the Royal Society of London*, **B 229**, 323-406.
- Godwin, H. and Vishnu-Mittre (1975) Studies of the post-glacial history of British vegetation. XVI. Flandrian deposits of the Fenland margin at Holme Fen and Whittlesey Mere., Hunts. *Philosophical Transactions of the Royal Society of London*, **B 270**, 561-604.
- Godwin, H. and Willis, E.H. (1959) Cambridge University radiocarbon measurements I. *American Journal of Science Radiocarbon Supplement*, **2**, 63-75.
- Greenberg, D.A. (1975) *Mathematical Studies of Tidal Behaviour in the Bay of Fundy*. Unpublished Ph.D. thesis, University of Liverpool.
- Greensmith, J.T. and Tucker, E.V. (1971) Overconsolidation in some fine-grained sediments: its nature, genesis and value in interpreting the history of certain English Quaternary deposits. *Geologie en Mijnbouw*, **50**, 743-748.
- Greensmith, J.T. and Tucker, E.V. (1973) Holocene transgressions and regressions on the Essex coast, outer Thames estuary. *Geologie en Mijnbouw*, **52**, 193-202.
- Greensmith, J.T. and Tucker, E.V. (1980) Evidence for differential subsidence on the Essex coast. *Proceedings of the Geologists' Association*, **91**, 169-175.
- Greensmith, J.T. and Tucker, E.V. (1986) Compaction and consolidation. In van de Plassche, O. (ed.), *Sea-Level Research: A Manual for the Collection and Evaluation of Data*. Norwich: Geo Books. 618pp.
- Gresswell, R.K. (1953) *Sandy Shores in South Lancashire, The Geomorphology of South-West Lancashire*. Liverpool: Liverpool University Press.

- Gresswell, R.K. (1957) Hillhouse coastal deposits in south Lancashire. *Liverpool and Manchester Geological Journal*, **2**, 60-78.
- Gresswell, R.K. (1958) The postglacial raised beach in Furness and Lyth, north Morecambe Bay. *Transactions of the Institute of British Geographers*, **25**, 79-103.
- Gunn, D.J. and Yenigun, O. (1987) A model for tidal motion and level in the Tay Estuary. *Proceedings of the Royal Society of Edinburgh*, **92B**, 257-273.
- Hageman, B.P. (1969) Development of the western part of the Netherlands during the Holocene. *Geologie en Mijnbouw*, **48**, 373-388.
- Hall, D. (1988) Survey results in the Cambridgeshire Fenland, *Antiquity*, **62**, 311-314.
- Hallam, S.J. (1970) Settlement round the Wash. In Phillips, C.W. (ed.), *The Fenland in Roman Times*, Royal Geographical Society Research Series no.5, London: William Clowes and Sons Ltd., 22-113.
- Hayes, M.O. (1975) Morphology of sand accumulation in estuaries: an introduction to the symposium. In Cronin, L.E. (ed.), *Estuarine Research vol. II. Geology and Engineering*, 2nd International estuarine research conference, Myrtle Beach, S.C., October 15-18, 1973, 3-22.
- Hibbert, F.A., Switsur, V.R. and West, R.G. (1971) Radiocarbon dating of Flandrian pollen zones at Red Moss, Lancashire. *Proceedings of the Royal Society of London*, **B 177**, 161-176.
- Holyoak, D.T. and Preece, R.C. (1985) Late Pleistocene interglacial deposits at Tattershall, Lincolnshire. *Philosophical Transactions of the Royal Society of London*, **B 311**, 193-236.
- Horton, A., Keen, D.H. and Davey, N.D.W. (1991) Hicks no.1 Brickyard, Fletton, Peterborough. In Lewis, S.G., Whiteman, C.A. and Bridgland, D.R. (eds.) *Central East Anglia and the Fen Basin Field Guide*. Quaternary Research Association, London, 163-171.

- Houghton, J.T., Jenkins, G.J. and Ephraums, J.J. (1990) (eds.) *Climatic Change - The IPCC scientific assessment*. Cambridge: Cambridge University Press. 365pp.
- Howarth, M.J. (1982) Tidal currents of the continental shelf. In Stride, A.H. (ed.), *Off-shore Tidal Sands - Processes and Deposits*. London: Chapman and Hall, 222pp.
- Huddart, D. (1971) A relative glacial chronology from the tills of the Cumberland lowland. *Proceedings of the Cumbrian Geological Society*, **3**, 21-32.
- Huddart, D., Tooley, M.J. and Carter, P.A. (1977) The coasts of northwest England. In Kidson, C. and Tooley, M.J. (eds.), *The Quaternary History of the Irish Sea*, Liverpool: Seel House Press, 119-154.
- Hull, E. (1864) The geology of the country around Oldham, including Manchester and its suburbs. *Memoirs of the British Geological Survey*, Sheet 88SW. London: Longman.
- Huntley, B. (1990) European vegetation history: palaeovegetation maps from pollen data - 13,000 yr B.P. to present, *Journal of Quaternary Science*, **5**, 103-122.
- Huthnance, J.M. (1973) Tidal current asymmetries over the Norfolk Sandbanks. *Estuarine and Coastal Marine Science*, **1**, 89-99.
- Ishiguro, S. (1972) Electrical analogues in oceanography, *Oceanography and Marine Biology: An Annual Review*, **10**, 27-96.
- Jardine, W.G. (1975) The determination of former sea-levels in areas of large tidal range. In Suggate, R.P. and Cresswell, M.M. (eds.) *Quaternary Studies: Selected papers from the 9th INQUA Congress, Christchurch, New Zealand*. Wellington, 163-168.
- Jardine, W.G. (1986) Determination of altitude. In van de Plassche, O. (ed.), *Sea-Level Research: A Manual for the Collection and Evaluation of Data*. Norwich: Geo Books, 618pp.
- Jelgersma, S. (1961) Holocene Sea-Level Changes in the Netherlands. *Mededelingen van de Geologische Stichting Serie C VI no.7*, Maastricht: Uitgevers-Maastchappij.
- Jelgersma, S. (1966) Sea-level changes during the last 10,000 years. In Sawyer, J.S. (ed.),

- Proceedings of the International Symposium on World Climate 8,000 to 0 B.C. held at Imperial College, London, 18-19 April, 1966*, Royal Meteorological Society of London, 54-69.
- Jelgersma, S. (1979) Sea-level changes in the North Sea basin. In Oele, E., Schüttenhelm, R.T.E. and Wiggers, A.J. (eds.), *The Quaternary History of the North Sea*. Acta Universitatis Upsaliensis Symposia Universitatis Upsaliensis Annum Quingentesimum Celebrantis:2, 233-248. Uppsala.
- Jennings, S. and Smyth, C. (1982) A preliminary interpretation of coastal deposits from East Sussex. *Quaternary Newsletter*, **37**, 12-19.
- Johns, B., Dube, S.K., Sinha, P.C., Mohanty, U.C. and Rao, A.D. (1982) The simulation of a continuously deforming lateral boundary in problems involving the shallow water equations. *Computers and Fluids*, **10**, 105-116.
- Johnson, R.H. (1985) The geomorphology of the regions around Manchester: an introductory review. In Johnson, R.H. (ed.), *The Geomorphology of north-west England*. Manchester: Manchester University Press, pp.1-23.
- Johnson, R.H., Tallis, J.H. and Pearson, M. (1972) A temporary section through late Devensian sediments at Green Lane, Dalton-in-Furness, Lancashire. *New Phytologist*, **71**, 533-544.
- Kendall, W.B. (1881) Interglacial deposits of west Cumberland and north Lancashire. *Quarterly Journal of the Geological Society of London*, **37**, 29-39.
- Kendall, W.B. (1990) Submerged peat mosses, forest remains and post-glacial deposits in Barrow Harbour. *Transactions of the Barrow Naturalists Field Club*, **3**, 55-63.
- Kent, P.E. (1975) The tectonic development of Great Britain and surrounding seas. In Woodland, A.W. (ed.), *Petroleum and the Continental Shelf of north-west Europe. Volume 1. Geology*. Barking: Applied Science Publishers Ltd., pp.3-28.
- Kidson, C. (1982) Sea-level changes in the Holocene. *Quaternary Science Reviews*, **1**,

121-151.

- Kidson, C. and Heyworth, A. (1979) Sea Level. *Proceedings of the International Symposium on Coastal Evolution in the Quaternary, September 1978, Sao Paulo, Brazil.* Sao Paulo, pp. 1-28.
- King, C.A.M. (1976) *The Geomorphology of the British Isles - Northern England.* London: Methuen.
- Klein, J., Lerman, J.C., Damon, P.E. and Ralph, E.K. (1982) Calibration of radiocarbon dates: tables based on the consensus data of the Workshop on Calibrating and Radiocarbon Time Scale. *Radiocarbon*, **24**, 103-150.
- Knight, D.J. (1977) Morecambe Bay feasibility study - sub-surface investigations, *Quarterly Journal of Engineering Geology*, **10**, 303-19.
- Kukla, G.J. (1975) Loess stratigraphy of central Europe. In Butzer, K.W. and Isaac, G.L. (eds.), *After the Australopithecines*, The Hague: Mouton, pp. 99-188.
- Lange, W. and Menke, B. (1967) Beiträge zur frühpostglazialen erd- und vegetationsgeschichtlichen Entwicklung in Eidergebiet, insbesondere zur Flussgeschichte und zur Genese des sogenannten Basistorfs, *Meyniana*, **17**, 29-44.
- Lax, P.D. and Richtmyer, R.D. (1956) Survey of the stability of linear finite difference equations. *Communications on Pure and Applied Mathematics*, **9**, 267-293.
- Lees, B.J. (1980) Quaternary sedimentation in the Sizewell - Dunwich Banks area, Suffolk. *Bulletin of the Geological Society of Norfolk*, **32**, 1-35.
- Lees, B.J. (1981) Sediment transport measurements in the Sizewell - Dunwich Banks area, East Anglia, U.K.. In Nio, S.-D., Schüttenhelm, R.T.E. and van Weering, T.C.E. (eds.), *Holocene Marine Sedimentation in the North Sea Basin*, Special Publication of the International Association of Sedimentologists no.5, Oxford: Blackwell Scientific Publications.
- Leatherman, S.P. (1987) Beach and shoreface response to sea-level rise: Ocean City,

- Maryland, U.S.A.. *Progress in Oceanography*, **18**, 139-149.
- Lynch, D.R. and Gray, W.G. (1980) Finite element simulation of flow in deforming regions. *Journal of Computational Physics*, **6**, 219-236.
- McIntyre, A., Ruddiman, W.F. and Jantzen, R.B. (1972) Southward penetrations of the North Atlantic polar front: faunal and floral evidence of large-scale surface water mass movements over the last 250,000 years. *Deep Sea Research*, **19**, 61-77.
- Maddock, L. and Pingree, R.D. (1978) Numerical simulation of the Portland Tidal Eddies. *Estuarine and Coastal Marine Science*, **6**, 353-363.
- Mangerud, J., Andersen, S.T., Berglund, B.E. and Donner, J.J. (1974) Quaternary stratigraphy of Norden, a proposal for terminology and classification. *Boreas*, **3**, 109-127.
- Mardell, G.T. and Pingree, R.D. (1981) Half-wave rectification of tidal vorticity near headlands as determined from current meter measurements. *Oceanologica Acta*, **4**, 63-68.
- Mitchell, G.F., Penny, L.F., Shotton, F.W. and West, R.G. (1973) *A Correlation of Quaternary Deposits in the British Isles*. Geological Society of London Special Report no. 4.
- Monk, A. (1976) *Site Investigation Report for British Gas Corporation Southern Feeder Gas Line (River Nene to B1165 section)*. A. Monk & Co. Ltd., Padgate, Warrington. SI 1452/DJ/MEB.
- Mörner, N.A. (1972) World climate during the last 130,000 years. In *24th International Geological Congress Proceedings, Section 12*, pp. 72-79.
- Mörner, N.A. (1976) Eustatic changes during the last 8,000 years in view of radiocarbon calibration and new information from the Kattegatt region and other north-western European coastal areas, *Palaeogeography, Palaeoclimatology and Palaeoecology*, **19**, 63-85.
- Mörner, N.A. (1980) The northwest European 'sea-level laboratory' and regional Holocene

- eustasy. *Palaeogeography, Palaeoclimatology and Palaeoecology*, **29**, 281-300.
- Mörner, N.A. (1984) Geoidal topography: origin and time consistency. *Marine Geophysical Researches*, **7**, 205-208.
- Mörner, N.A. (1987) Models of global sea-level changes. In Tooley, M.J. and Shennan, I. (eds.), *Sea-Level Changes*. Oxford: Blackwell, pp. 332-355.
- Moseley, F. (1972) A tectonic history of northwest England. *Journal of the Geological Society of London*, **128**, 561-598.
- Moseley, F. (1978) The geology of the English Lake District: An introductory review. In Moseley, F. (ed.) *The Geology of the Lake District*, Yorkshire Geological Society, Occasional Publication no. 3, 1-16.
- Munk, W.H. and Cartwright, D.E. (1966) Tidal spectroscopy and prediction. *Philosophical Transactions of the Royal Society of London*, **A 259**, 533-581.
- Naylor, D. and Mounteney, S.N. (1975) *Geology of the north-west European continental shelf. Volume 1*. London: Dudley. 162pp.
- Noye, B.J. and Flather, R.A. (1990) *Hydrodynamical - numerical modelling of tides and storm surges*, (unpublished manuscript), Proudman Oceanographic Laboratory.
- Oldfield, F. (1960a) Late Quaternary changes in climate, vegetation and sea-level in Lowland Lonsdale. *Transactions of the Institute of British Geographers*, **28**, 99-117.
- Oldfield, F. (1960b) Studies in the post-glacial history of British vegetation: Lowland Lonsdale. *New Phytologist*, **59**, 192-217.
- Oldfield, F. (1963) Pollen analysis and man's role in the ecological history of the south-east Lake District. *Geografiskar Annaler*, **14**, 23-40.
- Oldfield, F. and Statham, D.C. (1963) Pollen analytical data from Urswick Tarn and Ellerside Moss, north Lancashire. *New Phytologist*, **62**, 53-66.
- Pantin, H.M. (1977) Quaternary sediments of the northern Irish Sea. In Kidson, C.



- and Tooley, M.J. (eds.), *The Quaternary History of the Irish Sea*, Geological Journal Special Issue no.7, Liverpool: Seel House Press, 27-54.
- Pantin, H.M. (1978) Quaternary sediments from the north-east Irish Sea: Isle of Man to Cumbria. *Bulletin of the British Geological Survey*, **64**, 44pp.
- Patrick, C.K. (1987) Solid geology, structure and mineralisation. In Robinson, N.A. and Pringle, A.W. (ed.), *Morecambe Bay: An Assessment of Present Ecological Knowledge*. Lancaster University, pp.14-24.
- Pegrum, R.M., Rees, G. and Naylor, D. (1975) *Geology of the north-west European continental shelf. Volume 2. The North Sea*. London: Dudley.
- Peltier, W.R. (1987) Mechanisms of relative sea-level change and the geophysical responses to ice-water loading. In Devoy, R.J.N. (ed.), *Sea Surface Studies: A Global View*. London: Croom Helm, pp.57-94.
- Penck, A. and Brückner, E. (1909) *Die Alpen im Eiszeitalter*. Leipzig: Tauchnitz.
- Pennington, W. (1978) Quaternary geology. In Moseley, F. (ed.), *The Geology of the Lake District*, Yorkshire Geological Society Occasional Publication no.3, 207-225.
- Perrin, R.M.S., Rose, J. and Davies, H. (1979) The distribution, variations and origins of pre-Devensian tills in eastern England. *Philosophical Transactions of the Royal Society of London*, **B 287**, 535-570.
- Pingree, R.D. (1978) The formation of the shambles and other banks by tidal stirring of the seas. *Journal of the Marine Biological Association of the U.K.*, **58**, 211-226.
- Pingree, R.D. and Griffiths, D.K. (1979) Sand transport paths around the British Isles resulting from M<sub>2</sub> and M<sub>4</sub> tidal interactions, *Journal of the Marine Biological Association of the U.K.*, **59**, 497-513.
- Pingree, R.D. and Maddock, L. (1977a) Tidal residuals in the English Channel. *Journal of the Marine Biological Association of the U.K.*, **57**, 339-354.

- Pingree, R.D. and Maddock, L. (1977b) Tidal eddies and coastal discharge. *Journal of the Marine Biological Association of the U.K.*, **57**, 869-875.
- Pingree, R.D. and Maddock, L. (1979a) The tidal physics of headland flows and offshore tidal bank formation. *Marine Geology*, **32**, 269-289.
- Pingree, R.D. and Maddock, L. (1979b) Tidal flow around an island with a regularly sloping bottom topography. *Journal of the Marine Biological Association of the U.K.*, **59**, 699-710.
- Plassche, O. van de (1977) *A Manual for sample collection and evaluation of sea-level data*, (draft manuscript, unfinished), Amsterdam: Free University.
- Plassche, O. van de (1979) Sea-level research in the province of south-Holland, Netherlands. *Proceedings of the 78th International Symposium on Coastal Evolution in the Quaternary*. Brazil: Sao Paulo, 534-551.
- Plassche, O. van de (1980) Compaction and other sources of error in obtaining sea-level data: some results and consequences. *Eiszeitalter und Gegenwart*, **39**, 171-181.
- Plassche, O. van de (1986) *Sea-Level Research: A Manual for the Collection and Evaluation of Data*, Norwich: Geo Books, 618pp.
- Polyakov, Ye.V. (1986) Calculation of the tidal evolution of the earth-moon system based on a numerical model of tides in the paleocean. *Izvestiya, Atmospheric and Ocean Physics*, **22**, 383-388.
- Potter, T.W. (1981) The Roman occupation of the Fenland. *Brittania*, **12**, 79-126.
- Preece, R.C., Scourse, J.D., Houghton, S.C., Knudsen, K.L. and Penney, D.N. (1990) The Pleistocene sea-level and neotectonic history of the eastern Solent, southern England. *Philosophical Transactions of the Royal Society of London*, **B 328**, 425-477.
- Proctor, R. (1981) Mathematical modelling of tidal power schemes in the Bristol Channel. *Second International Symposium on Wave and Tidal Energy, Cambridge, England, 23-25 September, 1981*.

- Proctor, R. and Carter, L. (1989) Tidal and sedimentary response to the Late Quaternary closure and opening of Cook Strait, New Zealand: results from numerical modeling. *Paleoceanography*, **4**, 167-180.
- Proctor, R. and Flather, R.A. (1983) Routine storm surge forecasting using numerical models: procedures and computer programs for use on the CDC CYBER 205E at the British Meteorological Office. *Institute of Oceanographic Sciences Report No. 167*, 171pp.
- Provost, C. Le (1986) On the use of finite element methods for ocean modelling. In O'Brien, J.J. (ed.) *Advanced Physical Oceanographic Numerical Modelling*. Dordrecht: D. Reidel Publishing Company.
- Pugh, D.T. (1987) *Tides, Surges and Mean Sea-Level: A handbook for engineers and scientists*. Chichester: Wiley. 472pp.
- Rahmian, M. (1988) *The Hydrodynamics of Waves and Tides, with applications*. Southampton: Computational Mechanics Publications.
- Ramming, H.G. and Kowalik, Z. (1980) *Numerical Modelling of Marine Hydrodynamics - Applications to Dynamic Physical Processes*. Amsterdam: Elsevier.
- Reade, T.M. (1902) Glacial and post-glacial features of the lower valley of the River Lune and its estuary. *Proceedings of the Liverpool Geological Society*, **9**, 163-193.
- Reid, R.O. and Bodine, B.R. (1968) Numerical model for storm surges in Galveston Bay. *Journal of the Waterways and Harbours Division, Proceedings of the American Society of Civil Engineers*, **94**, No. WW1, 35-57.
- Ringrose, P.S. (1987) *Fault Activity and Palaeoseismicity in Scotland during Quaternary Time*. Unpublished Ph.D. thesis. University of Strathclyde.
- Robinson, A.H.W. (1968) The submerged glacial landscape off the Lincolnshire coast. *Transactions of the Institute of British Geographers*, **44**, 119-132.
- Robinson, I.S. (1983) Tidally induced residual flows. In Johns, B. (ed.), *Physical Oceanog-*

- raphy of Coastal and Shelf Seas*. Amsterdam: Elsevier, pp.321-356.
- Robson, J.D. (1988) *Soils in Lincolnshire IV*. Soils Survey of England and Wales.
- Roep, Th.B., Beets, D.J. and Ruegg, G.H.J. (1975) Wave-built structures in the sub-recent barriers of the Netherlands. *Proceedings of the Ninth International Congress of Sedimentology*, **6**, 141-146. Nice: International Association of Sedimentologists.
- Roep, Th.B. and Beets, D.J. (1988) Sea-level rise and paleotidal levels from sedimentary structures in the coastal barriers in the western Netherlands since 5600 B.P. *Geologie en Mijnbouw*, **67**, 53-60.
- Rose, J. (1987) Status of the Wolstonian glaciation in the British Quaternary. *Quaternary Newsletter*, **53**, 1-9.
- Salway, P. (1970) The Roman Fenland. In Phillips, C.W. (ed.), *The Fenland in Roman Times*, Royal Geographical Society Research Series no.5, London: William Clowes and Sons Ltd., pp.1-21.
- Scott, D.B. and Greenberg, D.A. (1983) Relative sea-level rise and tidal development in the Fundy tidal system. *Canadian Journal of Earth Science*, **20**, 1554-1564.
- Seale, R.S. (1975) *Soils of the Ely district*. Memoirs of the Soil Survey of England and Wales.
- de Serra, J.F.C. (1799) On a submarine forest from the east of England. *Philosophical Transactions of the Royal Society of London*, **89**, 479-484.
- Shackleton, N.J. and Opdyke, N.D. (1973) Oxygen isotope and palaeomagnetic stratigraphy of Equatorial Pacific core V28-238: oxygen isotope temperatures and ice volumes on a  $10^5$  year and  $10^6$  year scale. *Quaternary Research*, **3**, 39-55.
- Shackleton, N.J. and Opdyke, N.D. (1976) Oxygen isotope and palaeomagnetic stratigraphy of Equatorial Pacific core V28-239, Late Pliocene to Latest Pleistocene. In Cline, R.M. and Hays, J.D. (eds.), *Investigation of late Quaternary paleoceanography and palaeoclimatology*, Memoirs of the Geological Society of America, **145**, 449-464.

- Shackleton, N.J. and Opdyke, N.D. (1977) Oxygen isotope and palaeomagnetic evidence for early northern hemisphere glaciation. *Nature*, **270**, 216-219.
- Shennan, I. (1980) *Flandrian sea-level changes in the Fenland*. Unpublished Ph.D. thesis, University of Durham.
- Shennan, I. (1981) The nature, extent and timing of marine deposits in the English Fenland during the Flandrian Age. *Striae*, **14**, 177-81.
- Shennan, I. (1982) Interpretation of Flandrian sea-level data from the Fenland, England. *Proceedings of the Geologists' Association*, **93**, 53-63.
- Shennan, I. (1983) Flandrian and Late Devensian sea-level changes and crustal movements in England and Wales. In Smith, D.E. and Dawson, A.G. (eds.) *Shorelines and Isostasy*. Institute of British Geographers Special Publication no. 16, pp.255-283.
- Shennan, I. (1986a) Flandrian sea-level changes in the Fenland. II: Tendencies of sea-level movement, altitudinal changes, and local and regional factors. *Journal of Quaternary Science*, **1**, 155-179.
- Shennan, I. (1986b) Flandrian sea-level changes in the Fenland. I: The geographical setting and evidence of relative sea-level changes. *Journal of Quaternary Science*, **1**, 119-154.
- Shennan, I. (1987) Holocene sea-level changes in the North Sea. In Tooley, M.J. and Shennan, I. (eds.), *Sea-Level Changes*. Oxford: Blackwell.
- Shennan, I. (1989) Holocene crustal movements and sea-level changes in Great Britain. *Journal of Quaternary Science*, **4**, 77-89.
- Shennan, I., Tooley, M.J., Davis, M.J. and Haggart, B.A. (1983) Analysis and interpretation of Holocene sea-level data. *Nature*, **302**, 404-406.
- Shotton, F.W. (1986) Glaciations in the United Kingdom. *Quaternary Science Reviews*, **5**, 293-297.

- Sielecki, A. and Wurtele, M.G. (1970) The numerical integration of the non-linear shallow-water equations with sloping boundaries. *Journal of Computational Physics*, **6**, 219-236.
- Sissons, J.B. (1972) Dislocation and non-uniform uplift of raised shorelines in the western part of the Forth valley. *Transactions, Institute of British Geographers*, **55**, 145-159.
- Sissons, J.B. and Cornish, R. (1982) Differential glacioisostatic uplift of crustal blocks at Glen Roy, Scotland. *Quaternary Research*, **18**, 268-288.
- Skertchly, S.B.J. (1877) *The Geology of Fenland*. Memoirs of the British Geological Survey.
- Smith, A.G. (1959) The mires of south-western Westmorland: stratigraphy and pollen analysis. *New Phytologist*, **58**, 105-127.
- Smith, A.G. (1970) The stratigraphy of the northern Fenland. In Phillips, C.W. (ed.), *The Fenland in Roman Times*, Royal Geographical Society Research Series no.5, 147-164.
- Smith, A.G., Pearson, G.W. and Pilcher, J.R. (1971) Belfast Radiocarbon Dates IV. *Radiocarbon*, **13**, 450-467.
- Smith, G.D. (1978) *Numerical Solution of Partial Differential Equations: Finite Difference Methods*. Oxford: Clarendon Press. 304pp.
- Smith, M.V. (1985) The compressibility of sediments and its importance on Flandrian Fenland deposits. *Boreas*, **14**, 1-18.
- Smith, R.A. (1967) The deglaciation of south-west Cumberland: A re-appraisal of some features in the Eskdale and Bootle areas. *Proceedings of the Cumbrian Geological Society*, **2**, 76-83.
- Smith, R.A. (1977) The glacial landforms and deposits of the Corney and Bootle areas. *Proceedings of the Cumbrian Geological Society*, **3**, 260-264.

- Stephens, C.V. (1983) *Hydrodynamic Modelling Developments for the West Coast of the British Isles*. Unpublished Ph.D. thesis, University of Liverpool.
- Stoker, M.S., Long, D. and Fyfe, J.A. (1985) *A revised Quaternary stratigraphy for the central North Sea*. *Report of the British Geological Survey*, **17/2**, 35pp.
- Strang, G. and Fix, G.J. (1973) *An Analysis of the Finite Element Method*. Englewood Cliffs, New Jersey: Prentice-Hall, 306pp.
- Straw, A. (1963) The Quaternary evolution of the lower and middle Trent. *East Midlands Geographer*, **3**, 171-89.
- Straw, A. (1983) Pre-Devensian glaciation of Lincolnshire (eastern England) and adjacent areas. *Quaternary Science Reviews*, **2**, 239-260.
- Straw, A. and Clayton, K.M. (1979) *The Geomorphology of the British Isles - Eastern and Central England*. London: Methuen.
- Streif, H. (1978) A new method for the representation of sedimentary sequences in coastal regions. *Proceedings of the 16th Coastal Engineering Conference, American Society of Civil Engineers, Hamburg, West Germany, 28th August to 1st September, 1978*.
- Streif, H. (1979) Cyclic formation of coastal deposits and their indications of vertical sea-level changes. *Oceanis*, **5**, 303-306.
- Suess, H.E. (1970) Bristlecone pine calibration of the radiocarbon time-scale 5200 B.C. to the present. In Olsson, U. (ed.), *Radiocarbon Variation and Absolute Chronology*. New York: Wiley, pp. 595-605.
- Swinnerton, H.H. (1931) The post-glacial deposits of the Lincolnshire coasts. *Quarterly Journal of the Geological Society of London*, **87**, 360-375.
- Swinnerton, H.H. and Kent, P.E. (1976) *The Geological Evolution of Lincolnshire*. Lincoln: Lincolnshire Naturalists Union.
- Taylor, G.I. (1919) Tidal friction in the Irish Sea. *Philosophical Transactions of the Royal Society of London*, **A 220**, 1-93.

- Tooley, M.J. (1974) Sea-level changes during the last 9,000 years in north-west England. *Geographical Journal*, **140**, 18-42.
- Tooley, M.J. (1978) *Sea-Level Changes in North-West England During the Flandrian Stage*. Oxford: Clarendon Press, 232pp.
- Tooley, M.J. (1979) Sea-level changes during the Flandrian stage and the implications for coastal development. *Proceedings of the International Symposium on Coastal Evolution in the Quaternary, September 1978, Sao Paulo, Brazil*. Sao Paulo. pp. 552-572.
- Tooley, M.J. (1980) Solway Lowlands, shores of Morecambe Bay and south-western Lancashire. In Jardine, W.G. (ed.), *Western Scotland and North-Western England Field Guide*. Glasgow: INQUA Subcommittee on shorelines of northwestern Europe.
- Tooley, M.J. (1985) Sea-level changes and coastal morphology in north-west England. In Johnson, R.H. (ed.) *The Geomorphology of north-west England*. Manchester: Manchester University Press, pp. 94-121.
- Tooley, M.J. (1987) Quaternary history. In Robinson, N.A. and Pringle, A.W. (eds.), *Morecambe Bay: An Assessment of Present Ecological Knowledge*. Lancaster: Lancaster University, pp.25-50.
- Troels-Smith, J. (1955) Karakterisering af løse jordarter. *Danmarks Geologiske Undersøgelse*, **4**, 1-73.
- Van Veen, J. (1950) Eb- en Vloedschaar Systemen in de Nederlandse Getijwateren. *Tijdschrift Koninklijk Nederlands*, **67**, 303-325.
- Veenstra, H.J. (1971) Sediments of the southern North Sea. *Report of the Institute of Geological Sciences*, **70**(15), 9-23.
- Ventris, P.A. (1986) The Nar Valley. In West, R.G. and Whiteman, C.A. (eds.), *The Nar Valley and North Norfolk, Field Guide*. Quaternary Research Association, Coventry, 6-55.
- de Vries, H.L. (1958) Variation in concentration of radiocarbon with time and location on



- earth. *Proceedings, Konenlijk Nederlands Akademie Wetterschaft*, **B 61**, 94-102.
- Vincent, P.J. (1985) Quaternary geomorphology of the southern Lake District and Morecambe Bay area. In Johnson, R.H. (ed.), *The Geomorphology of north-west England*. Manchester: Manchester University Press, pp.159-177.
- Vincent, P.J. and Lee, M.P. (1981) Some observations on the loess around Morecambe Bay, north-west England. *Proceedings of the Yorkshire Geological Society*, **43**, 281-94.
- Waller, M. (1988) The Fenland Project's environmental programme. *Antiquity*, **62**, 336-343.
- Waller, M. (in press) *Fenland Project: Environmental Survey, Flandrian Environmental Change in the Fenland*, East Anglia Archaeology Monograph.
- West, R.G. (1972) Relative land - sea-level changes in south-eastern England during the Pleistocene. *Philosophical Transactions of the Royal Society of London*, **A 272**, 87-98.
- West, R.G. (1980) *The Pre-Glacial Pleistocene of the Norfolk and Suffolk Coasts*. Cambridge: Cambridge University Press.
- West, R.G. (1991a) Somersham, Cambridgeshire. In Lewis, S.G., Whiteman, C.A. and Bridgland, D.R. (eds.), *Central East Anglia and the Fen Basin*, Field Guide, Quaternary Research Association. London: Quaternary Research Association, pp. 120-122.
- West, R.G. (1991b) On the origin of Grunty Fen and other landforms in southern Fenland, Cambridgeshire. *Geological Magazine*, **128**, 257-262.
- Wheeler, W.H. (1868) *History of the Fens of South Lincolnshire*. London: Simpkin, Marshall & Co.
- Whittington, R.J. (1977) A late-glacial drainage pattern in the Kish Bank area and post-glacial sediments in the Central Irish Sea. In Kidson, C. and Tooley, M.J. (eds.), *The Quaternary History of the Irish Sea*. Liverpool: Seel House Press, pp. 55-68.

- Willis, E.H. (1961) Marine transgression in the English Fenlands. *Annals of the New York Academy of Science*, **95**, 368-376.
- Wilmot, R.D. and Collins, M.B. (1981) Contemporary fluvial sediment supply to the Wash. In Nio, S.-D., Schüttenhelm, R.T.E. and van Weering, T.C.E. (eds.), *Holocene Marine Sedimentation in the North Sea Basin*. Special Publication of the International Association of Sedimentologists no.5, Oxford: Blackwell Scientific Publications.
- Wingfield, R.T.R., Evans, C.D.R., Deegan, S.E. and Floyd, R. (1978) Geological and Geophysical Survey of the Wash. *Institute of Geological Sciences Report*, **78**(18).
- Woodland, A.W. (1977) *Quaternary Map of the United Kingdom South 1:625,000*. Southampton: I.G.S.
- Woodworth, P.L., Shaw, S.M. and Blackman, D.L. (1990) Secular trends in mean tidal range around the British Isles and along the adjacent European coastline. *Geophysical Journal International*, **104**, 593-609.
- Ziegler, P.A. and Louwerens, C.J. (1979) Tectonics of the North Sea. In Oele, E., Schüttenhelm, R.T.E. and Wiggers, A.J. (eds.), *The Quaternary History of the North Sea*, Acta Universitatis Upsaliensis Symposia Universitatis Upsaliensis Annum Quingentesimum Celebrantis: 2, 7-22. Uppsala.

## Admiralty Chart References

- 105. Cromer Knoll and the Outer Banks. (1988)
- 106. Cromer to Smith's Knoll. (1988)
- 107. Approaches to the River Humber. (1988)
- 108. Approaches to The Wash. (1988)
- 109. Entrance to the River Humber, Hull to Goole and Gainsborough. (1988)
- 121. Flamborough Head to Withernsea. (1988)
- 1187. Outer Silver Pit. (1988)
- 1190. Flamborough Head to Blakeney Point. (1981)
- 1200. The Wash Ports. (1987)
- 1503. Outer Dowsing to Smith's Knoll including Indefatigable Banks. (1988)
- 1504. Cromer to Orford Ness. (1988)
- 1505. Netherlands Gas Fields. (1988)
- 1543. Winterton Ness to Orford Ness. (1988)

#### **Appendix 4.1. Stratigraphic data sources for The Wash Fenlands**

Dr. D. Donoghue, Durham University, personal communication

Evans and Mostyn (1979)

Gallois (1979)

Gallois (1989)

Godwin (1940)

Godwin and Clifford (1938)

Godwin and Vishnu-Mittre (1975)

Godwin and Willis (1959)

Monk (1976)

Robson (1988)

Shennan (1980)

Shennan (1986a)

Smith (1970)

Waller (1980)

Dr. M. Waller, English Heritage Fenland Project, personal communication

Willis (1961)

Wingfield *et al.* (1978)

Mineral Assessment Reports, British Geological Survey, numbers 53, 54, 60, 73, 80, 93, 94, 96, 100, 108, 110, 123, 124, 128, 130.

## **Appendix 4.2. Stratigraphic data sources for Morecambe Bay**

Dickinson (1973)

Gresswell (1957)

Gresswell (1958)

Knight (1977)

Oldfield (1960a)

Oldfield (1960b)

Oldfield (1963)

Smith (1959)

Tooley (1974)

Tooley (1978)

Dr. M. Tooley, Durham University, personal communication

Dr. Y. Zong, Durham University, personal communication

### Appendix 4.3. Wash Fenland radiocarbon dates

#### Key

<b>Grid ref.</b>	Ordnance Survey map reference
<b>Lab. code</b>	Date reference (laboratory code)
<b>Date</b>	Radiocarbon age (years before present)
<b>Error</b>	Standard error of radiocarbon date (years)
<b>Altitude</b>	Altitude of material dated relative to Ordnance Datum in metres

Grid ref.	Lab. code	Date	Error	Altitude	Place Name
55260	29400	Q823	1212	154	0.40 Welney Wash
57000	28700	Q713	1464	154	2.43 Hockwold, Norfolk
52470	33090	IGS78A	1555	100	-3.00 Spalding, Lincolnshire
52478	33096	IGS78B	1615	100	-3.00 Spalding, Lincolnshire
53567	30182	SRR1588	1845	50	-0.67 Adventurers' Land 4
52417	31914	IGS124	1875	100	0.90 Spalding, Lincolnshire
56295	31327	IGS126	1875	100	0.00 Setch, Norfolk
56100	31600	Q549	1875	110	0.00 Saddlebow, Norfolk
52478	33096	IGS77	1915	100	-3.00 Spalding, Lincolnshire
55260	29400	Q820	1940	130	0.40 Welney Wash
55260	29400	Q819	1970	100	0.20 Welney Wash
56100	31600	Q550	2070	110	-0.02 Saddlebow, Norfolk
51953	30524	SRR1767	2220	50	0.00 Werrington
55260	29400	Q829	2227	90	0.40 Welney Wash
50410	37137	Q1163	2253	80	0.00 Washingborough Fen
54016	31608	SRR1755	2270	50	-0.37 Park Farm
56100	31600	Q806	2275	100	-0.12 Saddlebow, Norfolk
56100	31600	Q807	2377	100	-0.23 Saddlebow, Norfolk
55740	36880	Q81	2455	110	0.00 Ingoldmells, Lincolnshire
56100	31600	Q805	2495	110	0.00 Saddlebow, Norfolk
53875	30525	SRR1759	2510	50	0.10 Plash Farm
51500	35500	HAR3362	2540	100	2.50 Walcott Common
51920	30845	WW5	2550	60	1.50 Welland Wash 5
54790	29300	Q2113	2555	45	0.00 Manea
50000	30000	Q310	2560	110	0.00 Fordy Trackway
52411	31908	HV10808	2595	60	1.45 Cowbit Wash
51232	31997	HV9266	2625	65	1.26 Bourne Fen, Lincolnshire
55630	37325	Q687	2630	110	0.40 Chapel Point, Lincolnshire
55630	37325	Q688	2630	110	-2.74 Chapel Point, Lincolnshire
51296	31976	HV9264	2635	100	0.93 Bourne Fen, Lincolnshire
50000	30000	BM722	2677	123	0.00 Burwell Fen
51232	31997	HV9267	2780	70	1.06 Bourne Fen, Lincolnshire

Grid	Ref.	Lab. Code	Date	Error	Altitude	Place Name
55630	37325	Q844	2815	100	0.12	Chapel Point, Lincolnshire
51232	31997	HV8644	2970	65	0.95	Bourne Fen, Lincolnshire
51500	33500	HAR1749	3010	80	0.52	Horbling Fen, Lincolnshire
53024	30260	SRR1756	3050	50	-0.47	Park Farm
54340	29850	Q531	3065	110	0.28	Flaggrass, March
53810	30198	SRR1764	3080	200	0.00	Guyhirn Washes
56295	31327	IGS127	3215	100	-1.00	Setch, Norfolk
53344	31084	SRR1758	3250	50	0.00	Gedney Hill
52300	28600	Q546	3260	110	-1.25	Ugg Mere, Huntingdonshire
56000	31000	Q547	3305	120	0.00	Magdalene Bend, Norfolk
55630	37325	Q686	3340	110	0.02	Chapel Point, Lincolnshire
50000	30000	BM1469	3340	45	0.00	Lowes Farm, Norfolk
51953	30524	SRR1768	3390	40	0.00	Werrington
52050	28900	Q403	3400	120	-2.45	Holme Fen
51296	31976	HV9265	3415	45	0.10	Bourne Fen, Lincolnshire
52050	28900	Q404	3415	120	-2.45	Holme Fen
52200	28400	Q545	3415	110	0.00	Woodwalton Fen
51232	31997	HV9268	3430	60	0.63	Bourne Fen, Lincolnshire
51232	31997	HV8646	3435	65	0.95	Bourne Fen, Lincolnshire
51812	29844	IGS58	3475	100	-0.90	Peterborough
51232	31997	HV8645	3485	75	0.76	Bourne Fen, Lincolnshire
52368	31923	IGS117	3570	100	-1.95	Spalding, Lincolnshire
51232	31997	HV8648	3580	90	0.21	Bourne Fen, Lincolnshire
51232	31997	HV8647	3595	325	0.91	Bourne Fen, Lincolnshire
52000	35500	HAR149	3620	130	0.00	Woodhall Spa, Lincolnshire
51500	33500	HAR1750	3750	70	0.05	Horbling Fen, Lincolnshire
51860	35570	HAR148	3770	130	-1.25	Woodhall Spa, Lincolnshire
50000	30000	BM1443	3850	60	0.00	Lowes Farm, Norfolk
52474	31445	WW4B	3860	80	-4.05	Welland Wash 4
56100	31600	Q489	3905	120	-0.73	Saddlebow, Norfolk
56100	31600	Q490	3915	120	-0.70	Saddlebow, Norfolk
55630	37325	Q685	3943	100	-1.82	Chapel Point, Lincolnshire
51720	36190	IGS109	3945	100	-1.45	Woodhall Spa, Lincolnshire
51860	35570	HAR189	3950	120	-1.25	Woodhall Spa, Lincolnshire
51790	36020	IGS111	3980	100	-0.90	Woodhall Spa, Lincolnshire
56440	27600	BIRM1	4001	66	0.00	Isleham, Cambridgeshire
52474	31445	WW4C	4030	80	-4.15	Welland Wash 4
54200	29600	Q532	4055	110	-0.45	Flaggrass, March
51860	35850	HAR147	4080	130	-0.90	Woodhall Spa, Lincolnshire
55900	30100	Q264	4085	110	-1.50	Denver Sluice
51860	35850	HAR151	4116	130	-0.90	Woodhall Spa, Lincolnshire
51860	35770	IGS112	4130	100	-1.25	Woodhall Spa, Lincolnshire
51720	36190	IGS110	4155	100	-1.70	Woodhall Spa, Lincolnshire
51720	36190	HAR150	4162	130	-1.45	Woodhall Spa, Lincolnshire
53567	30182	SRR1589	4180	75	-4.06	Adventurers' Land 4
52050	28900	Q405	4190	130	-3.15	Holme Fen

Grid	Ref.	Lab. Code	Date	Error	Altitude	Place Name
55600	28300	Q544	4195	110	-1.50	Wood Fen, Ely
50000	30000	BM1525	4200	220	0.00	Burwell Fen
56440	27600	BIRM12	4201	60	0.00	Isleham, Cambridgeshire
50000	30000	Q1039	4204	60	0.00	Mildenhall Fen
51720	36190	HAR192	4210	110	-1.70	Woodhall Spa, Lincolnshire
56300	31300	Q2448	4210	65	0.00	Wormegay
53024	30260	SRR1766	4310	140	0.00	South Farm
53810	30198	SRR1765	4340	60	0.00	Guyhirn Washes
53100	29200	Q474	4345	110	-0.27	Glass Moor, Ramsey
55530	27040	Q129	4380	140	0.00	Wicken Fen
55900	30100	Q263	4390	120	-1.50	Denver Sluice
52368	31923	IGS118	4445	100	-2.52	Spalding, Lincolnshire
51823	29827	IGS57	4460	105	-1.30	Peterborough
53370	31113	SRR1762	4460	80	0.00	Sycamore Farm
55650	28140	Q589	4495	120	0.00	Queen Adelaide, Ely
53567	30182	SRR1590	4500	50	-4.27	Adventurers' Land 4
53875	30525	SRR1760	4520	70	-4.13	Plash Farm
52100	35700	BIRM447	4570	150	0.00	Tattershall
55530	27040	Q130	4605	110	0.00	Wicken Fen
55900	31480	Q31	4690	120	-5.70	Wiggenhall
56280	28470	Q499	4695	120	-3.20	Shippea Hill, Cambridgeshire
56280	28470	Q580	4800	120	-3.04	Shippea Hill, Cambridgeshire
56280	28470	Q525/6	4870	120	-3.50	Shippea Hill, Cambridgeshire
52368	31923	IGS119	4890	100	-5.09	Spalding, Lincolnshire
52370	31932	IGS64	4950	100	-3.70	Spalding, Lincolnshire
56280	28470	Q527/8	4950	120	-3.50	Shippea Hill, Cambridgeshire
52050	28900	Q406	4958	130	-3.85	Holme Fen
52474	31445	WW4D	5000	70	-4.65	Welland Wash 4
52411	31908	HV10016	5075	50	-5.18	Cowbit Wash
56280	28470	Q581	5130	120	-3.05	Shippea Hill, Cambridgeshire
52474	31445	WW4A	5140	60	-4.95	Welland Wash 4
52427	31919	IGS121	5175	100	-5.83	Spalding, Lincolnshire
56280	28470	Q583	5295	120	-3.50	Shippea Hill, Cambridgeshire
56280	28470	Q582	5310	120	-3.35	Shippea Hill, Cambridgeshire
56280	28470	Q585	5330	120	-3.70	Shippea Hill, Cambridgeshire
52411	31908	HV10017	5435	70	-5.81	Cowbit Wash
56295	31327	IGS128	5440	100	-3.70	Setch, Norfolk
56280	28470	Q584	5465	120	-3.65	Shippea Hill, Cambridgeshire
52411	31908	HV10806	5570	70	-5.92	Cowbit Wash
53567	30182	HV9261	5580	70	-7.99	Adventurers' Land 2
52427	31919	IGS122	5600	100	-6.23	Spalding, Lincolnshire
52368	31923	IGS120	5665	100	-5.60	Spalding, Lincolnshire
52411	31908	HV10807	5675	115	-6.02	Cowbit Wash
53567	30182	HV10817	5840	90	-6.92	Adventurers' Land 4
52427	31919	IGS123	5905	100	-6.49	Spalding, Lincolnshire
53370	31113	SRR1763	6010	200	0.00	Sycamore Farm



Grid	Ref.	Lab. Code	Date	Error	Altitude	Place Name
52427	31919	IGS123	5905	100	-6.49	Spalding, Lincolnshire
53370	31113	SRR1763	6010	200	0.00	Sycamore Farm
53875	30525	SRR1761	6080	60	-8.45	Plash Farm
52527	32675	IGS76	6220	120	-7.06	Spalding, Lincolnshire
52527	32675	IGS75	6240	120	-8.46	Spalding, Lincolnshire
53567	30182	HV9262	6275	125	-8.05	Adventurers' Land 2
53567	30182	HV9263	6415	185	-8.12	Adventurers' Land 2
53567	30182	HV10011	6575	95	-7.87	Adventurers' Land 4
52010	28930	Q1296	6600	120	-5.00	Holme Fen
56280	28470	Q586	6695	150	-3.90	Shippea Hill, Cambridgeshire
52010	28930	Q1297	6794	120	-5.00	Holme Fen
56280	28470	Q587	7610	150	-4.00	Shippea Hill, Cambridgeshire
54010	31487	SRR1757	7690	400	-9.12	Elm Tree Farm
56280	28470	Q588	8620	160	-4.30	Shippea Hill, Cambridgeshire

The remaining dates are given in Waller (in press).

#### Appendix 4.4. Radiocarbon dates from the Morecambe Bay area

##### Key

<b>Grid ref.</b>	Ordnance Survey grid reference
<b>Lab. code</b>	Date reference (laboratory code)
<b>Date</b>	Radiocarbon date (years before present)
<b>Error</b>	Standard error of radiocarbon date (years)
<b>Altitude</b>	Altitude of material dated relative to Ordnance Datum in metres

Grid ref.	Lab. code	Date	Error	Altitude	Place Name
32722	39284	BIRM1013	3980	70	1.82 Mockbeggar Wharf
33936	45989	BIRM139	9195	155	-16.37 Heysham, Lancashire
33933	45988	BIRM140	8925	200	-16.04 Heysham, Lancashire
33932	45990	BIRM141	9270	200	-17.60 Heysham, Lancashire
34100	46400	GU664	7544	306	0.00 Morecambe, Lancashire
33000	40400	GU666	4351	46	0.00 Alt-mouth, Lancashire
33441	48627	HAR3709	7750	100	-0.39 Rusland
32700	40858	HV0000	170	65	2.53 Formby Foreshore
33304	40787	HV12537	7015	90	-0.20 New Cut, Lancashire
33260	40762	HV12539	6840	85	0.99 New Cut, Lancashire
33260	40762	HV12540	6870	235	0.52 New Cut, Lancashire
32950	40290	HV2679	4545	90	3.14 Alt-mouth, Lancashire
33202	40838	HV2680A	6750	175	0.15 Downholland, Lancashire
33202	40838	HV2681	4325	345	0.30 Downholland, Lancashire
33202	40838	HV2682	4600	430	1.06 Downholland, Lancashire
33202	40838	HV2683	5565	205	1.27 Downholland, Lancashire
33202	40838	HV2684	4045	395	1.86 Downholland, Lancashire
34884	37614	HV2685	5250	385	1.29 Helsby Marsh, Lancashire
34884	37614	HV2686	5470	155	0.73 Helsby Marsh, Lancashire
33490	42858	HV2916	2270	65	4.22 Lytham, Lancashire
33490	42858	HV2917	3090	135	3.70 Lytham, Lancashire
33490	42858	HV2918	3150	150	3.50 Lytham, Lancashire
33471	42879	HV2919	4960	210	3.39 Lytham, Lancashire
34239	46083	HV2920	4190	150	4.49 Heysham, Lancashire
34160	44486	HV3052	4900	450	4.80 Lousanna, Lancashire
33350	47465	HV3356	8685	175	-15.48 Morecambe Bay
33202	40838	HV3357	4695	110	0.24 Downholland, Lancashire
33202	40838	HV3358	6050	65	1.06 Downholland, Lancashire
33220	47791	HV3360	7725	95	-15.84 Morecambe Bay
33293	47636	HV3361	8740	65	-16.54 Morecambe Bay
33208	47190	HV3362	7995	80	-11.16 Morecambe Bay
34672	47895	HV3460	5015	100	4.98 Arnside Moss, Lancashire

Grid	Ref.	Lab. Code	Date	Error	Altitude	Place Name
34672	47895	HV3461	1545	35	5.65	Arnside Moss, Lancashire
34486	46646	HV3462	8330	125	-16.03	Morecambe Bay
32205	48477	HV3840	4760	45	5.29	Duddon Estuary, Lancashire
32225	48520	HV3841	4960	50	4.06	Duddon Estuary, Lancashire
30768	48841	HV3842	2820	55	6.66	Annas Mouth, Cumbria
30795	49090	HV3843	7160	75	0.91	Bootle, Cumbria
33495	48024	HV3844	5435	105	3.72	Ellerside Moss, Lancashire
33309	42947	HV3845	5005	65	3.09	Lytham, Lancashire
33490	42858	HV3846	830	50	6.52	Lytham, Lancashire
33238	40839	HV3847	5615	45	1.59	Downholland, Lancashire
33212	43578	HV3933	4800	75	2.24	Peel, Lancashire
33212	43578	HV3934	6535	110	-0.83	Peel, Lancashire
33365	40819	HV3935	6760	95	-0.14	Downholland, Lancashire
33365	40819	HV3936	6980	55	-0.38	Downholland, Lancashire
33796	42863	HV4124	5945	50	0.88	Nancy's Bay, Lancashire
33796	42863	HV4125	7605	85	-2.33	Nancy's Bay, Lancashire
33796	42863	HV4126	6885	80	-1.17	Nancy's Bay, Lancashire
33796	42863	HV4127	6025	85	0.46	Nancy's Bay, Lancashire
33837	42799	HV4128	5775	85	1.93	Nancy's Bay, Lancashire
33837	42799	HV4129	5950	85	1.52	Nancy's Bay, Lancashire
33837	42799	HV4130	6245	115	1.13	Nancy's Bay, Lancashire
33837	42799	HV4131	6290	85	0.97	Nancy's Bay, Lancashire
33352	42747	HV4343	8390	105	-11.14	Starr Hills, Lancashire
33394	42946	HV4344	4895	95	2.87	Heyhouses Lane, Lancashire
33394	42946	HV4345	7820	60	-9.65	Heyhouses Lane, Lancashire
33394	42946	HV4346	8575	105	-9.75	Heyhouses Lane, Lancashire
34454	44837	HV4347	4830	140	2.95	Moss Farm, Lancashire
30310	38261	HV4348	4725	65	2.43	Rhyl
33309	42947	HV4417	805	70	5.63	Lytham, Lancashire
33127	40817	HV4705	4090	170	3.42	Downholland, Lancashire
33796	42863	HV4706	6950	175	-2.46	Nancy's Bay, Lancashire
33796	42863	HV4707	5880	180	-1.22	Nancy's Bay, Lancashire
33490	42775	HV4708	1370	85	4.60	Ansdell, Lancashire
32695	40642	HV4709	2335	120	5.08	Formby, Lancashire
34603	40715	HV4711	6195	80	0.00	Firwood Road, Lancashire
33482	42754	HV5215	1795	240	4.04	Ansdell, Lancashire
32700	40858	HV5219	390	55	0.00	Formby Foreshore, Lancashire
30824	49623	HV5221	9360	65	-0.77	Ravenglass, Cumbria
30838	49161	HV5227	6230	85	3.18	Williamsons, Lancashire
33837	42799	HV5294	6250	55	1.39	Nancy's Bay, Lancashire
32238	40839	HV8649	6050	80	2.12	Downholland, Lancashire
32238	40839	HV8650	6210	100	1.84	Downholland, Lancashire
32238	40839	HV8651	5985	195	1.88	Downholland, Lancashire
33873	42799	HV9260	2330	65	3.27	Nancy's Bay, Lancashire
34600	47500	Q256	5734	129	2.93	Silverdale Moss, Lancashire
34600	47500	Q260	6590	144	3.55	Silverdale Moss, Lancashire

<b>Grid</b>	<b>Ref.</b>	<b>Lab. Code</b>	<b>Date</b>	<b>Error</b>	<b>Altitude</b>	<b>Place Name</b>
34600	47500	Q261	5865	115	3.85	Silverdale Moss, Lancashire
32600	38900	Q620A	3695	110	3.05	Moreton, Cheshire
32600	38900	Q620B	3680	110	3.05	Moreton, Cheshire
34700	49000	Q85	5277	120	4.88	Helsington Moss, Westmorland

## Appendices 6.1 - 6.3: Data on Diskettes

### Appendix 6.1 Bathymetric and label data for model simulations

### Appendix 6.2 Tidal input for model simulations

### Appendix 6.3 Maximum sea-level elevations from model simulations

All data are presented in ASCII format on IBM 1.44 MB formatted diskettes. The contents of Appendices 6.1 and 6.2 are on diskette 1, whilst the Appendix 6.3 data are on diskette 2. Two copies of each diskette are provided. The programs, in which the data in Appendices 6.1 and 6.2 were employed and from which the data in Appendix 6.3 were obtained, were run on the Cray computers at the University of London Computer Centre using the FORTRAN 77 compilers available under the COS and UNICOS operating systems. The programs employed were essentially those of Dr. Roger Flather of the Proudman Oceanographic Laboratory, Birkenhead, as explained in Chapter 5.

### Appendix 6.1 Bathymetric and label data for model simulations

#### Contents

#### EC3 Model

File Name	Model Simulation
PRSET0.EC3	Present sea depths and labels
PRSETM1.EC3	Modification 1 depths and labels
PRSETM2.EC3	Modification 2 depths and labels
PRSET3P.EC3	3,000 years B.P. palaeogeography depths and labels
PRSET4P.EC3	4,000 years B.P. palaeogeography depths and labels
PRSET5P.EC3	5,000 years B.P. palaeogeography depths and labels

The present sea depths were employed for the -2, -5, -10 and -15 metre sea-level simulations and were read into the model with depths reduced by the amount required for the

simulation, namely 2, 5, 10 or 15 metres. For the palaeocoastline simulations, present sea depths were used in combination with the labels employed for the corresponding palaeogeographic simulation. For example, the 3,000 years B.P. coastline simulation employs present sea depths and the labels from the 3,000 years B.P. palaeogeographic simulation.

### **WASH Model**

<b>File Name</b>	<b>Model Simulation</b>
PRSET0.WAS	Present sea depths and labels
PRSET3P.WAS	3,000 years B.P. palaeogeography depths and labels
PRSET4P.WAS	4,000 years B.P. palaeogeography depths and labels
PRSET5P.WAS	5,000 years B.P. palaeogeography depths and labels

### **LBM Model**

<b>File Name</b>	<b>Model Simulation</b>
PRSET0.LBM	Present sea depths and labels
PRSETM1.LBM	Modification 1 sea depths and labels
PRSETM2.LBM	Modification 2 sea depths and labels
PRSET5P.LBM	5,000 years B.P. palaeogeography depths and labels
PRSET8PH.LBM	8,000 years B.P. palaeogeography higher sea-level depths and labels
PRSET8PL.LBM	8,000 years B.P. palaeogeography lower sea-level depths and labels

The present sea depths were employed for the -2, -5, -10 and -15 metre simulations and were read into the model with sea depths reduced by the amount required for the simulation, namely 2, 5, 10 or 15 metres. For the palaeocoastline simulations, present sea depths were used in combination with the labels employed for the corresponding palaeogeographic simulation, as with the EC3 model.

### **MBM Model**

<b>File Name</b>	<b>Model Simulation</b>
PRSET0.MBM	Present sea depths and labels
PRSET5P.MBM	5,000 years B.P. palaeogeography depths and labels
PRSET8PH.MBM	8,000 years B.P. palaeogeography higher sea-level

	depths and labels
PRSET8PL.MBM	8,000 years B.P. palaeogeography lower sea-level
	depths and labels

### **Format of the Data in the Files for Appendix 6.1**

In each file the format of the data is as follows:-

1. Header statement giving the model name and the simulation to which the sea depths apply.
2. Arrays of depth data in which the number in the first column refers to the row of the data on the model grid, numbered from north to south. The second and subsequent up to twenty columns give the depth values from west to east across the model grid. These arrays of depth data commence on the model western boundary and values east of the initial twenty columns of depth data are given in the same format in successive arrays beneath this. At the top of each of these arrays is a header statement giving the model name and the words "Depths in metres". Each array is ended by the number "1" in the initial column on the line immediately following the end of the depth data.
3. Following the depth data, the model labels are laid out arrays with identical format to the arrays of depth data. A header statement at the top of each array gives the model name and the word "Labels". The number in the first column refers to the row of the data on the model grid, numbered from north to south. The label data values are given in the second and subsequent up to twenty columns from west to east across the model grid, commencing at the model western boundary. Values east of the initial twenty columns of label data are given in the same format in successive arrays beneath this. Each array is ended by the number "1" in the initial column on the line immediately following the end of the label data, except the last array at the end of the file which has no indication of termination of the array.

## Appendix 6.2 Tidal input for model simulations

### Contents

#### EC3 Model

File Name	Model Simulation
PRTIN0.EC3	Present sea-level tidal input
PRTIN2.EC3	-2 metres sea-level tidal input
PRTIN5.EC3	-5 metres sea-level tidal input
PRTIN10.EC3	-10 metres sea-level tidal input
PRTIN15.EC3	-15 metres sea-level tidal input

The tidal input for Modifications 1 and 2 is the same as that for present sea-level. This is also the case for simulations of the 3,000 and 4,000 years B.P. coastlines and palaeogeography. The tidal inputs for the 5,000 years B.P. coastline and palaeogeographic simulations are the same as those for sea-level reduced by 2 metres.

#### WASH Model

File Name	Model Simulation
PRTIN0.WAS	Present sea-level tidal input
PRTIN3P.WAS	3,000 years B.P. palaeogeography tidal input
PRTIN4P.WAS	4,000 years B.P. palaeogeography tidal input
PRTIN5P.WAS	5,000 years B.P. palaeogeography tidal input

#### LBM Model

File Name	Model Simulation
PRTIN0.LBM	Present sea-level tidal input
PRTIN2.LBM	-2 metres sea-level tidal input
PRTIN5.LBM	-5 metres sea-level tidal input
PRTIN10.LBM	-10 metres sea-level tidal input
PRTIN15.LBM	-15 metres sea-level tidal input

The tidal input for Modifications 1 and 2 is the same as that for present sea-level. The 5,000 years B.P. coastline and palaeogeographic simulations employ the -2 metres sea-



level tidal input. The tidal input for the 8,000 years B.P. coastline and palaeogeographic simulations is the same as that for sea-level reduced by 15 metres from its present mean depth values.

### MBM Model

File Name	Model Simulation
PRTIN0.MBM	Present sea-level tidal input
PRTIN5P.MBM	5,000 years B.P. palaeogeography tidal input
PRTIN8P.MBM	8,000 years B.P. palaeogeography (higher and lower sea-levels) tidal input

### Format of the Data in the Files for Appendix 6.2

In each file the format of the data is as follows:-

1. Header statement giving the model name and the simulation to which the tidal input data apply.
2. Three numbers, representing in turn the number of open boundary  $z$ ,  $u$  and  $v$  points (see Chapter 5.2.2), are given on the next line of text.
3. The number of tidal constituents is given as an integer value on the next line. Chapter 5.4.1 explains that six constituents are used in each simulation, namely  $Meu_2$ ,  $M_2$ ,  $S_2$ ,  $M_4$ ,  $MS_4$  and  $M_6$ .
4. The next section is repeated in turn for each tidal constituent.
  - a. Firstly, the angular frequency of the constituent is given. This is followed on the next line by four numbers, representing the coefficients of nodal factor  $f_e$ , followed by the three coefficients of nodal factor  $n_e$  on the next line. The three integers on the line beneath this represent the coefficients for  $g_e$ , the phase angle of the equilibrium tide at time  $t = 0$ . These coefficients are ignored by the model program if the equilibrium tide is not employed in the tidal calculation. The equilibrium tide was only used in the north-east Atlantic model, as explained in Chapter 5.2.2.
  - b. Then come the amplitude and phase values, stored in the form  $H \cos c_g$  (see Chapter 5.2.2) for each of the open boundary  $z$  points, read in from west to east and north to south around the model boundary. These are written as eight numbers per line to the end

of the data. The corresponding amplitude and phase values stored in the form  $H\text{sinc}_g$  for the open boundary  $z$  points follow. The same procedure is then used for laying out the  $u$  and  $v$  point  $H\text{cos}c_g$  and  $H\text{sinc}_g$  values.

- c. The same procedure as laid out above is repeated for each tidal constituent commencing with the angular frequency of the constituent.

**Appendix 6.3 Maximum sea-level elevations from model simulations  
(approximately equivalent to mean high water of spring tides results  
in metres above mean sea-level)**

**Contents**

**EC3 Model**

<b>File Name</b>	<b>Model Simulation</b>
PRMAX0.EC3	Present sea-level
PRMAXM1.EC3	Modification 1
PRMAXM2.EC3	Modification 2
PRMAX2.EC3	-2 metre simulation
PRMAX5.EC3	-5 metre simulation
PRMAX10.EC3	-10 metre simulation
PRMAX15.EC3	-15 metre simulation
PRMAX3C.EC3	3,000 years B.P. coastline
PRMAX4C.EC3	4,000 years B.P. coastline
PRMAX5C.EC3	5,000 years B.P. coastline
PRMAX3P.EC3	3,000 years B.P. palaeogeography
PRMAX4P.EC3	4,000 years B.P. palaeogeography
PRMAX5P.EC3	5,000 years B.P. palaeogeography

**WASH Model**

<b>File Name</b>	<b>Model Simulation</b>
PRMAX0.WAS	Present sea-level
PRMAX3P.WAS	3,000 years B.P. palaeogeography
PRMAX4P.WAS	4,000 years B.P. palaeogeography
PRMAX5P.WAS	5,000 years B.P. palaeogeography

**LBM Model**

<b>File Name</b>	<b>Model Simulation</b>
PRMAX0.LBM	Present sea-level
PRMAXM1.LBM	Modification 1
PRMAXM2.LBM	Modification 2

PRMAX2.LBM	-2 metres sea-level
PRMAX5.LBM	-5 metres sea-level
PRMAX10.LBM	-10 metres sea-level
PRMAX15.LBM	-15 metres sea-level
PRMAX5C.LBM	5,000 years B.P. coastline
PRMAX8C.LBM	8,000 years B.P. coastline
PRMAX5P.LBM	5,000 years B.P. palaeogeography
PRMAX8PH.LBM	8,000 years B.P. palaeogeography - higher sea-level
PRMAX8PL.LBM	8,000 years B.P. palaeogeography - lower sea-level

### MBM Model

File Name	Model Simulation
PRMAX0.MBM	Present sea-level
PRMAX5P.MBM	5,000 years B.P. palaeogeography
PRMAX8PH.MBM	8,000 years B.P. palaeogeography - higher sea-level
PRMAX8PL.MBM	8,000 years B.P. palaeogeography - lower sea-level

### Format of the Data in the Files for Appendix 6.3

In each file the format of the data is as follows:-

1. Header statement giving the model name and simulation.
2. Statement saying "Maximum Elevations (metres)", or words to that effect.
3. Arrays of the data, laid out in similar format to the bathymetric data. The results are given with "\*" representing a land/dry value in a grid rectangle and the figures representing the maximum sea elevations in metres above this. The arrays are numbered across and down from north to south and west to east, with (1,1) representing the north-western most grid rectangle in the model. A line with grid numbers from west to east is followed by the array of data which commences in each case with an integer representing the grid row numbered from north to south and is followed by the model results. These are given typically with nineteen columns of data on each line. The end of each array is marked by a "0" in the first column. Each subsequent array is numbered across and down in similar fashion so that results for a particular model grid rectangle may be easily obtained. The last array in each file is not terminated with a "0".

